



**HAL**  
open science

# Biomarkers identification in spinocerebellar ataxias. Integrated functional evaluation of the cerebellum

Giulia Coarelli

► **To cite this version:**

Giulia Coarelli. Biomarkers identification in spinocerebellar ataxias. Integrated functional evaluation of the cerebellum. *Neurons and Cognition [q-bio.NC]*. Sorbonne Université, 2022. English. NNT : 2022SORUS430 . tel-04319574

**HAL Id: tel-04319574**

**<https://theses.hal.science/tel-04319574>**

Submitted on 3 Dec 2023

**HAL** is a multi-disciplinary open access archive for the deposit and dissemination of scientific research documents, whether they are published or not. The documents may come from teaching and research institutions in France or abroad, or from public or private research centers.

L'archive ouverte pluridisciplinaire **HAL**, est destinée au dépôt et à la diffusion de documents scientifiques de niveau recherche, publiés ou non, émanant des établissements d'enseignement et de recherche français ou étrangers, des laboratoires publics ou privés.

Sorbonne Université

Ecole doctorale Cerveau, Cognition, Comportement (ED3C)

Institut du Cerveau (ICM)

## **Identification de biomarqueurs dans les ataxies spinocérébelleuses**

*Evaluation multimodale du cervelet*

**Par Giulia Coarelli**

Thèse de doctorat en Neurosciences

Dirigée par le Pr. Alexandra Durr

Présentée et soutenue publiquement le 2 Décembre 2022

Devant un jury composé de :

<b>Pr. Catherine Lubetzki</b>	Présidente du Jury
<b>Pr. Andrea Nemeth</b>	Rapporteuse
<b>Dr. Caterina Mariotti</b>	Rapporteuse
<b>Pr. Thomas Klockgether</b>	Examineur
<b>Pr. Mathieu Anheim</b>	Examineur
<b>Pr. Alexandra Durr</b>	Directrice de thèse





Sorbonne Université

Ecole doctorale Cerveau, Cognition, Comportement (ED3C)

Paris Brain Institute (ICM)

## **Biomarkers identification in spinocerebellar ataxias**

*Integrated functional evaluation of the cerebellum*

**By Giulia Coarelli**

Thesis to obtain the degree of Docteur en Neurosciences

Supervisor: Pr. Alexandra Durr

Publicly presented on December 2nd, 2022

Jury members:

<b>Pr. Catherine Lubetzki</b>	President of the jury
<b>Pr. Andrea Nemeth</b>	Examiner
<b>Dr. Caterina Mariotti</b>	Examiner
<b>Pr. Thomas Klockgether</b>	External member
<b>Pr. Mathieu Anheim</b>	External member
<b>Pr. Alexandra Durr</b>	Supervisor



*A Simon, Livia et César*

## **Remerciements/ Acknowledgments**

I would like to thank all jury members for accepting to review and evaluate my thesis manuscript. In spite of your full agendas you all managed to rapidly find a spot for me and, for that, I am extremely grateful and honored.

Professor Nemeth, thank you for taking some of your time to bring your valuable expertise on my PhD manuscript.

Dr.ssa Mariotti, la ringrazio vivamente per aver accettato di partecipare alla discussione della mia tesi. Sono onorata che sia lei a valutare il lavoro svolto durante il mio dottorato, data la sua competenza nel campo della neurogenetica e l'eccellente livello di ricerca che riesce a svolgere, nonostante tutte le difficoltà del nostro caro Paese.

Professor Klockgether, thank you for agreeing to be part of my jury, it is an honor for me considering your competence in the ataxia field.

Professor Anheim, merci d'avoir accepté de faire partie de mon jury de thèse. Ce fut un plaisir de travailler avec vous dans l'étude ATRIL et dans la rédaction de notre review.

Professeure Lubetzki, merci d'avoir accepté de présider le jury et d'y apporter votre expertise clinique et scientifique.

Professeure Alexandra Durr, merci ! Merci de me transmettre ta passion dans ce travail, ton expertise clinique, ta créativité, ta positivité qui me manque parfois, ton énergie inépuisable (seizing every moment!). Je m'en souviens de notre première rencontre à Windsor où je te demandais si je pouvais venir à Paris pour un stage de six mois en 2015...depuis, j'apprends tous les jours de toi.

Professeur Alexis Brice, merci pour l'intérêt que vous montrez dans tous les projets. Vos observations et conseils sont toujours très pertinents, c'est un honneur de pouvoir travailler avec vous.

Professeur Charles Duyckaerts, merci de m'avoir appris à regarder un cerveau. Vous vous êtes toujours rendu disponible, et je garderai en mémoire ces nombreuses heures à compter les motoneurons du tronc cérébral. C'était un honneur de regarder les lames avec vous, tout en évoquant des sujets de culture latine et romaine.

Professeure Sophie Tezenas du Montcel, merci pour votre aide précieuse et votre approche très pédagogique dans tous les travaux que nous avons menés pendant ces années.

Professeure Sandrine Humbert, merci pour votre pensée innovante qui est d'inspiration dans le domaine des ataxies.

Merci au Docteur Lucette Lacomblez et au Docteur Anne-Louise Leutenegger pour m'avoir toujours apporté de riches suggestions et conseils lors des comités de thèse.

Pour réaliser ce travail de thèse, beaucoup de personnes ont été impliquées. Tout d'abord merci à nos attachées de recherche clinique : Elodie, Rania, Hortense, Mariana, Marie. Vous êtes toujours disponibles, réactives et souriantes. Vous supportez toujours mes demandes de la dernière minute, merci les filles ! Le bureau du premier étage est comme une deuxième maison. Merci à Sabrina d'être toujours à l'écoute, nous avons encore beaucoup de projets à réaliser. Merci à Emilien de trouver toujours le temps pour me sortir une petite p-value.

Un grand merci aux cliniciens avec qui j'ai la fortune de travailler et qui m'ont aidé dans la réalisation de ces essais cliniques : Anna, Claire, Pauline, Paulina, Perrine, Solveig, Elise, Lucie.

Merci au Professeur Fanny Mochel pour tous les enseignements pendant vos consultations et votre disponibilité.

Cette thèse est le produit de collaborations qui ont permis de réaliser ces différents projets. Merci à tous les centres hospitaliers impliqués dans l'essai thérapeutique ATRIL. Le projet CERMOI a été réalisé avec l'aide d'un grand nombre d'intervenants, que je remercie particulièrement : Bertrand Gaynard, Charlotte Dubec, Sabrina Sayah, Marco Nassisi, Isabelle Audo, Pierre Pouget, Pierre Daye, Sophie Pechoux, Peggy Gatignol, Stéphanie Borel, Emilie Dusclaux, Karim Dorgham, Lina Daghzen, Jean Charles Lamy, Marie Laure Welter, Clara Fischer, Marie Chupin, Jean François Mangin, Nadia Osman. Pour le projet BIOSCA, je remercie Fanny Mochel, Isaac Adanyeguh, Frederic Darios, et Karim Dorgham.

Merci à la Fondation pour la Recherche Médicale qui a financé mon poste en tant que doctorante.

Merci au CIC qui accueille nos essais cliniques, à la gentillesse et compétence de ses infirmières. Merci à Sylvie, Ludmila et Yassaman de la banque d'ADN, votre efficacité et rapidité est surprenante.

Un grand merci à tous les patients et à leurs familles qui ont participé à ces essais, avec l'espoir de pouvoir traiter un jour ces maladies rares...

Je voudrais également remercier le Professeur Carpentier et le Professeur Degos, avec qui j'ai passé mon clinicat en Neurologie, c'était un plaisir de travailler avec vous.

Merci au Docteur Delphine Heron et au Professeur Eric Le Guern de m'avoir accueilli dans votre service de Génétique.

Merci au Docteur Cecilia Marelli, qui m'a indiqué Alexandra et son équipe pour mon stage pendant mon Internat. Ça a été le meilleur choix !

Merci à tout le labo : Marie, je suis très contente que tu sois revenue dans l'équipe, ton aide est très précieuse ; merci à Giovanni, Claire-Sophie, Léna, Jean-Loup, j'attends toujours avec impatience nos réunions à la recherche d'un gène causal pour nos familles. Merci à Vincent et Radhia avec qui est un plaisir de travailler ensemble. Merci à Claire, je sais que je peux compter sur toi, c'est toujours intéressant de discuter avec toi, avec la promesse de le faire plus souvent.

Cambiamo registro, parliamo in Italiano, sicuramente più facile.

Grazie al Prof. Marco Salvetti che mi ha insegnato a fare un esame neurologico e a gestire un reparto, grazie al Prof. Giovanni Ristori e alla Dott.ssa Silvia Romano che mi hanno fatto appassionare alla Neurogenetica e dato la possibilità di venire in Francia.

Livia, quando torni? Te lo chiedo tutte le volte che ci sentiamo, lo sai. Grazie per essere un'amica su cui posso sempre contare, anche dall'altra parte dell'oceano. Spero che tornerai presto a Parigi, magari di nuovo all'ICM, sarebbe bello ritornare a lavorare insieme. Ma anche se non è l'ICM, basta che torni. Ci manchi tanto.

Grazie Marco per la tua disponibilità, anche ad intrattenere i bimbi, sai sempre mettermi di buonumore!

Grazie agli amici di sempre, quelli che mi hanno sempre supportato (e sopportato!): Sara, Alice, Carolina, Ilaria, Laura, Giulia, Valeria, Jessica, Ciocci, Elena, Nicole, Alberto, Marco, Daniele, Olmo.

Grazie alla mia famiglia, in particolare a mia madre sempre presente, dolce e amorevole, a mia nonna Orietta esempio di donna che mi ha saputo trasmettere grandi valori, alle zie Rossella e Paola pilastri della mia infanzia, a zio Luciano (l'unico che ci capirà qualcosa di questa tesi) per la sua lungimiranza e generosità. A papà.

Merci à l'Indonésie qui m'a fait rencontrer Simon, avec qui tout est plus facile et radieux. Simon, tu m'apprends à profiter de petites choses et à être heureuse. Avec toi, nous avons le meilleur projet du monde.

Grazie ai miei figli, Livia e César. Grazie a voi che mi rendete ogni giorno più felice.

Un énorme merci à tous,

Giulia

## TABLE OF CONTENTS

<b>RESUME</b> .....	<b>10</b>
<b>ABSTRACT</b> .....	<b>11</b>
<b>INTRODUCTION</b> .....	<b>12</b>
CHAPTER 1 – GENERAL INTRODUCTION OF THE INHERITED CEREBELLAR ATAXIAS .....	12
<i>The inherited cerebellar ataxias: an update</i> .....	15
CHAPTER 2 – SPINOCEREBELLAR ATAXIAS .....	30
<i>Autosomal dominant cerebellar ataxias: new genes and progress towards treatments</i> .....	33
CHAPTER 3: SCA BIOMARKERS STATE OF THE ART .....	71
<i>Recent advances in understanding dominant spinocerebellar ataxias from clinical and genetic points of view</i> .....	73
<i>Blood and CSF biomarkers in autosomal dominant cerebellar ataxias</i> .....	83
<b>OBJECTIVES</b> .....	<b>104</b>
<b>RESULTS</b> .....	<b>105</b>
CHAPTER 1: BIOSCA STUDY .....	105
<i>Plasma neurofilament light chain predicts cerebellar atrophy and clinical</i> .....	106
<i>progression in spinocerebellar ataxia</i> .....	106
CHAPTER 2: ATRIL STUDY.....	114
<i>Safety and efficacy of riluzole in spinocerebellar ataxia type 2 in France (ATRIL): a multicentre, randomised, double-blind, placebo-controlled trial</i> .....	116
CHAPTER 3: CERMOI STUDY .....	138
<i>Biomarkers in preataxic and early stage of SCA2 and SCA7</i> .....	138
INTRODUCTION .....	138
METHODS .....	139
RESULTS .....	146
DISCUSSION .....	174
<b>CONCLUSIONS AND PERSPECTIVES</b> .....	<b>185</b>
<b>REFERENCES</b> .....	<b>189</b>
<b>ANNEXES</b> .....	<b>198</b>
ANNEX 1 .....	198
<i>Motor neuron involvement threatens survival in spinocerebellar ataxia type 1</i> .....	198
ANNEX 2 .....	218
<i>List of publications during the PhD</i> .....	218

## **LIST OF ABBREVIATIONS**

ALS: Amyotrophic Lateral Sclerosis  
ASOs: Antisense Oligonucleotides  
BCVA: Best Corrected Visual Acuity  
CCAS: Cerebellar Cognitive Affective Syndrome  
CCFS: Composite Cerebellar Functional Score  
CSF: Cerebrospinal Fluid  
DTI: Diffusion Tensor Imaging  
ERG: Electroretinogram  
ETDRS: Early Treatment Diabetic Retinopathy Study charts  
FA-ADL: Friedreich's Ataxia Activities of Daily Living  
FACES Battery: Dynamic Emotional Recognition  
Ff-ERG: Full-field Electroretinography  
FSS: Fatigue Severity Scale  
HD: Huntington's Disease  
INAS: Inventory of Non-Ataxia Signs  
MBLF: Oral-Lingual-Facial Motility  
MRS: MR Spectroscopy  
NfL: Neurofilament light chain  
NIR-FAF: Near-infrared Fundus Autofluorescence  
ONL: Outer Nuclear Layer  
PHQ-9: Patient Health Questionnaire  
PM38: Raven's Progressive Matrices 1938  
PolyQ: Polyglutamine  
PROM-Ataxia: Patient-Reported Outcome Measure of  
Ataxia SARA: Scale for the Assessment and Rating of Ataxia  
SCA: Spinocerebellar Ataxia  
SCP: Superior Cerebellar Peduncle  
SD-OCT: Spectral-domain Optical Coherence Tomography  
SW-FAF: Short-wavelength Fundus Autofluorescence  
VEP: Visual Evoked Potential  
WES: Whole Exome Sequencing

## Résumé

Les ataxies spinocérébelleuses (SCAs) sont des maladies neurodégénératives rares à transmission autosomique dominante, caractérisées par une grande hétérogénéité clinique et génétique. Les formes les plus fréquentes de SCAs sont causées par des expansions de triplets CAG codant pour une expansion de polyglutamine (PolyQ) dans les protéines correspondantes. La maladie se déclare généralement au cours de la troisième ou de la quatrième décennie, mais le processus pathologique est déjà détecté par des changements tels que l'atrophie du cervelet et du pont. À ce jour, aucun traitement curatif n'est disponible pour les patients atteints d'une SCA, mais les thérapies géniques ont montré des résultats encourageants dans plusieurs modèles murins. Le premier essai clinique pour les patients SCA3 utilisant des oligonucléotides antisens a été initié début 2022 (NCT05160558). Les progrès réalisés dans le domaine thérapeutique rendent impérative l'identification de biomarqueurs fiables pour surveiller le traitement, détecter les patients dont la progression est plus rapide et prédire la conversion du stade préataxique au stade manifeste.

L'objectif de mon doctorat a été d'identifier des biomarqueurs biologiques, cliniques et d'imagerie dans les SCA à expansion de polyglutamine aux stades préataxique et ataxique. Pour atteindre cet objectif, j'ai étudié trois cohortes de SCA issues de trois études cliniques différentes. Dans la cohorte BIOSCA, comprenant 62 porteurs (17 SCA1, 13 SCA2, 19 SCA3 et 13 SCA7) et 19 témoins, nous avons exploré la progression des concentrations plasmatiques de neurofilaments sur deux ans et leurs corrélations avec les scores cliniques et la volumétrie par IRM cérébrale. Dans l'étude ATRIL, menée afin d'évaluer l'efficacité d'un traitement par riluzole chez une cohorte de 45 patients SCA2, nous avons exploré la progression clinique et radiologique sur un an. Enfin, dans l'étude CERMOI, nous avons eu recours à une évaluation multimodale pour identifier des biomarqueurs fiables et suivre l'évolution de la maladie sur un an chez 15 porteurs SCA2 et 15 porteurs SCA7 aux stades préataxique et ataxique précoce de la maladie. D'après les résultats de CERMOI, une stadification de SCA2 et de SCA7 a été proposée pour aider à concevoir les futurs essais cliniques.

Le développement de biomarqueurs valides et de conceptions innovantes d'essais cliniques destinés aux porteurs préataxiques sont les défis des prochaines années.

## Abstract

Spinocerebellar ataxias (SCAs) are rare autosomal dominant neurodegenerative disorders characterized by high heterogeneity regarding both their clinical manifestations and genetic background. The most frequent SCA subtypes are caused by heterozygous translated CAG repeat expansions encoding polyglutamine (PolyQ) stretches in the corresponding protein. Disease onset is typically observed in the third or fourth decades but pathological process can be detected at an early stage by changes such as cerebellar and pons atrophy. To date, curative treatments are not available for SCA patients but gene therapies reported encouraging results in several SCA mice models. The first clinical trial for SCA3 patients using antisense oligonucleotides began early 2022 (NCT05160558). The advances in the therapeutic field greatly increase the demand for novel and reliable biomarkers to efficiently monitor treatments, identify patients with more rapid progression, and predict the conversion from preataxic to manifest stage.

My PhD project revolved around the identification of biological, clinical, and imaging biomarkers in polyQ SCAs at preataxic and ataxic stages. To pursue this objective, I investigated three SCA cohorts issued from three different clinical studies. In the BIOSCA cohort, that included 62 SCA carriers (17 SCA1, 13 SCA2, 19 SCA3, and 13 SCA7) and 19 age-matched controls, we explored the progression of plasma neurofilament light chain concentrations over two years, as well as their correlations with clinical scores and brain MRI volumetry. With the ATRIL study, conducted to evaluate the safety and efficacy of riluzole treatment in 45 SCA2 patients, we explored the clinical and radiological progression over one year. Finally, in the CERMOI study, we leveraged a multimodal assessment to identify reliable biomarkers and track the disease progression over one year in 15 SCA2 and 15 SCA7 carriers, at preataxic and early ataxic stages of the disease. Based on CERMOI's results, a staging of SCA2 and SCA7 was proposed to help designing future clinical trials.

The development of precise outcome measures, valid biomarkers, and innovative clinical trial designs addressed to preataxic carriers will be the future challenges for the upcoming years.



# Introduction

## Chapter 1 – General introduction of the inherited cerebellar ataxias

Inherited cerebellar ataxias are a heterogeneous group of rare neurodegenerative disorders affecting the cerebellum and its afferent and efferent connections. Cerebellar ataxia, the disease hallmark, manifests as the lack of coordination of voluntary movements, gait impairment, poor balance, clumsiness, dysarthria, and eye movement incoordination.<sup>1</sup> It is often accompanied by additional non-cerebellar signs and symptoms. The extreme complexity characterizing the underlying phenotype is the direct consequence of the impairment of multiple systems such as the brainstem, the corticospinal tracts, the basal ganglia, the peripheral nervous system, and the retina, amongst others.<sup>2-5</sup> They can be inherited with autosomal dominant, autosomal recessive, as well as X-linked inheritance patterns. The prevalence for autosomal dominant forms is estimated at 2.7/100000 and for autosomal recessive at 3.3/100000.<sup>6</sup>

Historically, hereditary cerebellar ataxias have been classified according to their inheritance pattern, age at onset, and associated signs and symptoms (Figure 1).<sup>7</sup>

TABLE 1—CLASSIFICATION OF THE HEREDITARY ATAXIAS

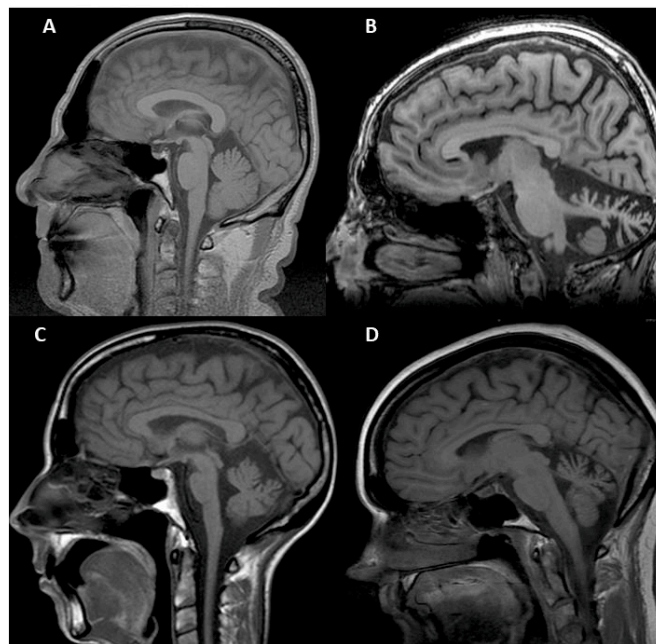
Type	Inheritance	Age of onset (decade)	% of index cases studied (total = 157)
<i>(I) Disorders with known metabolic or other cause</i>			
<i>(A) Metabolic disorders</i>			
<i>(i) Progressive, unremitting ataxia:</i>			
Abetalipoproteinaemia (Bassen-Kornzweig disease) <sup>16</sup>	AR	1st–2nd	NA
Hypobetalipoproteinaemia <sup>16</sup>	AR	2nd–4th	NA
Hexosaminidase deficiency <sup>17</sup>	AR	1st	NA
Glutamate dehydrogenase deficiency <sup>18</sup>	AR	2nd–6th	NA
Cholestanolosis <sup>19</sup>	AR	Ataxia 3rd–6th	NA
<i>(ii) Intermittent ataxia:</i>			
Pyruvate dehydrogenase deficiency <sup>20</sup>	AR	1st	NA
Hartnup disease <sup>21</sup>	AR	1st	NA
Intermittent branched chain ketoaciduria <sup>22</sup>	AR	1st	NA
Deficiencies of urea cycle enzymes (ornithine transcarbamylase deficiency*, citrullinaemia, argininaemia, argininosuccinicaciduria) <sup>23</sup>	AR/XLD*	1st	NA
<i>(B) Disorders characterised by defective DNA repair</i>			
Ataxia telangiectasia (Louis Bar syndrome) <sup>24</sup>	AR	1st	2.5
Xeroderma pigmentosum (de Sanctis-Cacchione syndrome) <sup>25</sup>	AR	1st–2nd	0
Cockayne syndrome <sup>26</sup>	AR	1st	0
<i>(II) Disorders of unknown aetiology</i>			
<i>(A) Early onset cerebellar ataxia (onset usually before 20 years)</i>			
Friedreich's ataxia <sup>1,2,27,28</sup>	AR	1st–2nd	67.5
Early onset cerebellar ataxia with retained tendon reflexes <sup>29</sup>	AR	1st–2nd	13.8
With hypogonadism±deafness and/or dementia <sup>30</sup>	AR	1st–3rd	0
With congenital deafness <sup>15,31</sup>	AR	Ataxia 2nd–3rd	1.27
With childhood deafness and mental retardation <sup>32</sup>	AR	1st	0
With pigmentary retinal degeneration±mental retardation/dementia/deafness <sup>33</sup>	AR	1st	1.9
With optic atrophy and mental retardation±deafness/spasticity (Behr's syndrome) <sup>15,34,35</sup>	AR	1st	0.64
Marinesco-Sjögren syndrome (with cataract and mental retardation) <sup>36</sup>	AR	1st	0
With myoclonus (Ramsay Hunt syndrome) <sup>15,37,38</sup>	AR/AD	1st–2nd	0.64
X-linked recessive spinocerebellar ataxia <sup>15,39,40</sup>	XLR	1st–2nd	1.27
Cerebellar ataxia with essential tremor <sup>41</sup>	AD	1st–3rd	1.27
<i>(B) Late onset cerebellar ataxia (onset usually after 20 years)</i>			
Cerebellar ataxia with optic atrophy/ophthalmoplegia/dementia/amyotrophy/extrapyramidal features (? includes Azorean ataxia) <sup>4,14,42</sup>	AD	3rd–5th	5.7
Cerebellar ataxia with pigmentary retinal degeneration±ophthalmoplegia and/or extrapyramidal features <sup>4,14,43</sup>	AD	Mid 2nd–4th	0.64
Pure cerebellar ataxia with later onset <sup>14,44</sup>	AD	6th–7th	0.64
Cerebellar ataxia with myoclonus and deafness <sup>14,45</sup>	AD	Ataxia 2nd–5th	0.64

AD=autosomal dominant; AR=autosomal recessive; XLD=X-linked dominant; and XLR=X-linked recessive. NA=not ascertained.

Figure 1. Classification of inherited cerebellar ataxias, after Harding A, *Lancet* 1983.<sup>7</sup>

However, following the identification of novel loci and genes, several novel forms of autosomal recessive<sup>8</sup> and dominant cerebellar ataxias<sup>9</sup> have been recognized, making this classification outdated. To date, a new nomenclature of autosomal recessive cerebellar ataxias has been proposed by the International Parkinson and Movement Disorder Society,<sup>10</sup> regrouping 62 entities with ataxia as the main feature, named with the ATX prefix followed by the gene name, and 30 entities with ataxia combined to another prominent movement disorder, named with a double prefix (e.g. ATX/HSP, combination of ataxia and spastic paraparesis). When focusing on autosomal dominant spinocerebellar ataxias (SCAs), 49 SCA forms and 39 genes have been described in the Online Mendelian Inheritance of Men (OMIM) database.

Acquired causes of cerebellar ataxia, such as autoimmune, infectious, vascular, paraneoplastic, vitamin or hormones deficiencies, should be ruled out before proceeding with any genetic analysis. Laboratory investigations and paraclinical evaluations are crucial to guide the clinician. Brain imaging is one of the essential exams to perform, usually revealing cerebellar atrophy with different degrees of severity, according to the genotype (Figure 2).



**Figure 2. Brain MRI findings in autosomal recessive and dominant ataxias.**

Sagittal T1 weighted brain MRI. A: Friedreich's ataxia, 59-year-old man, disease onset at age 46, SARA score 13.5/40. Spine atrophy and mild cerebellar atrophy. B: Ataxia-telangiectasia, 44-year-old man, disease onset at age 14, SARA score 23/40. Severe cerebellar atrophy. C: SCA3 (72 CAG repeats in *ATXN3*), 52-year-old woman, disease onset at age 40, SARA score 22/40. More pronounced brainstem and spine atrophy than cerebellar atrophy. D. SCA14/*PRKCG* (c.368G>A; p.Gly123Glu), 38-year-old woman, disease onset at age 31, SARA score 6/40. Marked cerebellar atrophy.

The clinical work-up is often limited to the most frequent forms, such as Friedreich's ataxia, Fragile X-associated tremor/ataxia syndrome (FXTAS), or polyglutamine spinocerebellar ataxias. The recent introduction of NGS techniques in everyday diagnostic process is a crucial support to identify the underlying genetic cause.<sup>11</sup>

In the review "The Inherited Cerebellar Ataxias: an update", accepted for publication in *Journal of Neurology* in September 2022, I provide an updated overview of the clinical, genetic, and diagnostic aspects of inherited cerebellar ataxias.<sup>12</sup>



# The inherited cerebellar ataxias: an update

Giulia Coarelli<sup>1</sup> · Thomas Wirth<sup>2,3,4</sup> · Christine Tranchant<sup>2,3,4</sup> · Michel Koenig<sup>5</sup> · Alexandra Durr<sup>1</sup> · Mathieu Anheim<sup>2,3,4</sup> 

Received: 1 July 2022 / Revised: 10 September 2022 / Accepted: 12 September 2022  
© The Author(s), under exclusive licence to Springer-Verlag GmbH Germany 2022

## Abstract

This narrative review aims at providing an update on the management of inherited cerebellar ataxias (ICAs), describing main clinical entities, genetic analysis strategies and recent therapeutic developments. Initial approach facing a patient with cerebellar ataxia requires family medical history, physical examination, exclusions of acquired causes and genetic analysis, including Next-Generation Sequencing (NGS). To guide diagnosis, several algorithms and a new genetic nomenclature for recessive cerebellar ataxias have been proposed. The challenge of NGS analysis is the identification of causative variant, trio analysis being usually the most appropriate option. Public genomic databases as well as pathogenicity prediction software facilitate the interpretation of NGS results. We also report on key clinical points for the diagnosis of the main ICAs, including Friedreich ataxia, CANVAS, polyglutamine spinocerebellar ataxias, Fragile X-associated tremor/ataxia syndrome. Rarer forms should not be neglected because of diagnostic biomarkers availability, disease-modifying treatments, or associated susceptibility to malignancy. Diagnostic difficulties arise from allelic and phenotypic heterogeneity as well as from the possibility for one gene to be associated with both dominant and recessive inheritance. To complicate the phenotype, cerebellar cognitive affective syndrome can be associated with some subtypes of cerebellar ataxia. Lastly, we describe new therapeutic leads: antisense oligonucleotides approach in polyglutamine SCAs and viral gene therapy in Friedreich ataxia. This review provides support for diagnosis, genetic counseling and therapeutic management of ICAs in clinical practice.

**Keywords** Cerebellar ataxia · Genetics · Next generation sequencing · Phenotype

## Introduction

Inherited cerebellar ataxias (ICAs) belong to a large group of rare and complex neurodegenerative diseases affecting the cerebellum, but also frequently the spinal cord and the peripheral nerves. ICAs are clinically dominated by progressive cerebellar syndrome, that may lead to significant disability [1]. Most patterns of inheritance have been described in ICAs. Over the past 25 years, and especially since the advent of the next-generation sequencing (NGS), there has been a tremendous improvement in this field with the description of more than 100 new entities, most of them being recessively inherited [2, 3]. In addition, up to 500 genes have been related to neurological disease whose clinical picture may include cerebellar ataxia [2, 3]. Taken together, the prevalence of ICA is close to 1:10 000, making them a common motive for outpatient referral to neurogenetics center [4]. Because of the recent and rapid progression in cerebellar ataxia knowledge, periodic reviews are required to provide up-to-date guidance for the diagnosis and management of

✉ Mathieu Anheim  
mathieu.anheim@chru-strasbourg.fr

<sup>1</sup> Institut du Cerveau-Paris Brain Institute (ICM), AP-HP, INSERM, CNRS, University Hospital Pitié-Salpêtrière, Sorbonne Université, Paris, France  
<sup>2</sup> Service de Neurologie, Département de Neurologie, Hôpitaux Universitaires de Strasbourg, Hôpital de Hautepierre, 1, Avenue Molière, 67098 Strasbourg Cedex, France  
<sup>3</sup> Institut de Génétique et de Biologie Moléculaire et Cellulaire (IGBMC), INSERM-U964/CNRS-UMR7104/Université de Strasbourg, Illkirch, France  
<sup>4</sup> Fédération de Médecine Translationnelle de Strasbourg (FMTS), Université de Strasbourg, Strasbourg, France  
<sup>5</sup> Institut Universitaire de Recherche Clinique, Laboratoire de Génétique de Maladies Rares EA7402, Laboratoire de Génétique Moléculaire, University Hospital, Université de Montpellier, Montpellier, France

this disorder. We consequently aimed at providing such an update on ICA literature by presenting the main clinical entities, proposing genetic analysis strategies and describing the present and future therapeutic perspectives.

## Initial approach to a patient with cerebellar ataxia

Cerebellar ataxia (CA) is usually diagnosed in a patient complaining gait and balance difficulties. Beside gait ataxia, neurological examination may reveal cerebellar dysarthria, dysmetria during nose–finger and heel–shin tests and hypotonia. Cerebellar eye signs are very frequent and can occur as the earliest clinical features suggesting the cerebellar

motor syndrome [5, 6] (Video 1–7). Facing such patients, many acquired causes of CA should be ruled out before considering any genetic analysis (Table 1). The family history should then be investigated in three generations at least (Fig. 1). It should be kept in mind that the lack of family history of CA is frequent in autosomal-recessive cerebellar ataxia (ARCA). The more reliable the clinical status of each member of the family and the higher number of subjects whose DNA may be collected, the more likely to establish the molecular diagnosis.

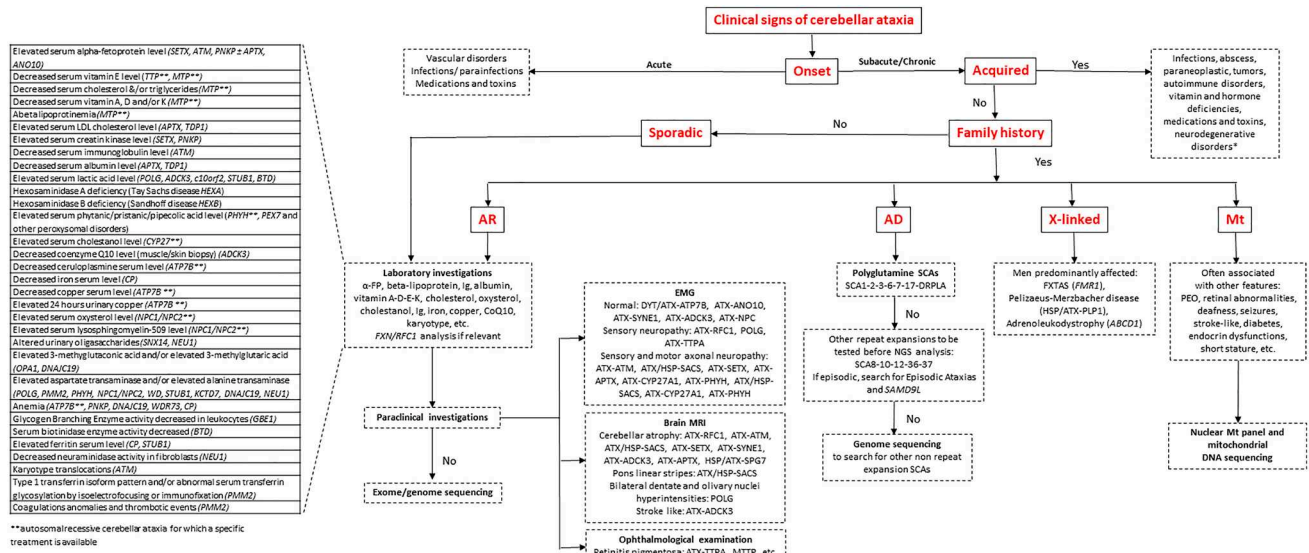
Most patients with ICA are referred to neurologist, pediatrician or geneticist due to insidious symptoms occurrence associated with slowly progressive worsening of gait imbalance on several months or years. Rarely, ICA is characterized by acute onset, especially when related to inborn error

**Table 1** Main causes of acquired cerebellar ataxia

Acute ataxias	Vascular disorders	Cerebellar ischemia Cerebellar hemorrhage
	Medications and toxins	<u>Antiepileptic drugs</u> (phenytoin, carbamazepine, oxcarbazepine, lacosamide, lamotrigine, zonisamide, rufinamide. With benzodiazepines, felbamate, phenobarbital and valproic acid in the setting of hyperammonemia) <u>Chemotherapy</u> (cytarabine, fluorouracil, capecitabine, hexamethylmelamine, procarbazine, vincristine, cisplatin and oxaliplatin) <u>Antiarrhythmic</u> (amiodarone, procainamide) <u>Antibiotics</u> (metronidazole, polymyxins) <u>Toxins and poisons</u> (alcohol, carbon tetrachloride, heavy metals, phencyclidine, toluene, pesticides) <u>Lithium</u>
	Infections	<u>Acute cerebellitis</u> (Epstein-Barr virus, varicella-zoster, herpes simplex virus 1, human herpesvirus 6, influenza A and B, mumps, coxsackie virus, rotavirus, echovirus, SARS-CoV2, enterovirus, hepatitis A, measles, parvovirus B19, typhoid fever, malaria) <u>Bacterial infection</u> ( <i>Mycoplasma pneumoniae</i> , <i>Listeria monocytogenes</i> , <i>Streptococcus pneumoniae</i> , <i>Neisseria meningitidis</i> , tuberculosis)
Subacute ataxias	Autoimmune disorders	Multiple sclerosis, ADEM, celiac disease/gluten ataxia, GAD antibody-associated ataxia, anti-NMDA receptor antibodies, anti-P/Q voltage-gated calcium channel antibodies, Homer-3 autoantibodies, contactin-associated protein-like 2 antibodies, anti-M-phase phosphoprotein-1 antibodies, Hashimoto thyroiditis/encephalopathy, histiocytosis X, anti-GQ1b antibody syndromes, Bickerstaff encephalitis, neurosarcooidosis, postinfectious cerebellitis, Behçet syndrome, polyarteritis nodosa, systemic lupus erythematosus, Sjögren syndrome Paraneoplastic cerebellar degeneration
	Infections	Lyme disease, Whipple disease, JC virus, HIV, syphilis, tuberculosis and Prion disease
	Structural causes	Primary or metastatic tumors Abscess Liver failure (hepatocerebral degeneration)
Chronic ataxias	Vitamin and hormone deficiencies	Deficiency in vitamin B1 (Wernicke encephalopathy), B12, E Hypothyroidism, Hypoparathyroidism
	Toxins	Alcohol, heavy metals, phencyclidine, toluene, solvents, pesticides
	Medications	Antiepileptic drugs, chemotherapy
	Infections	HIV, tuberculosis, syphilis, Lyme disease, Creutzfeldt–Jakob disease
	Autoimmune disorders	Progressive multiple sclerosis
	Neurodegenerative disorders	Multiple system atrophy, progressive supranuclear palsy
Other	Arnold–Chiari malformation, normal pressure hydrocephalus, superficial siderosis, psychogenic ataxia	

*ADEM* acute disseminated encephalomyelitis, *GAD* glutamic acid decarboxylase, *HIV* human immunodeficiency virus





**Fig. 1** Flowchart of the diagnostic process in cerebellar ataxias. This flowchart shows the steps in evaluating a patient with cerebellar ataxia based on clinical and family history, physical evaluation and paraclinical tests. First, the onset should be differentiated between acute and subacute/chronic; second, the acquired causes have to be ruled out by paraclinical investigations as neuroimaging, blood and cerebrospinal fluid exams; third, if family history is positive for inherited cerebellar ataxia, the clinician should determine the transmis-

sion pattern by pedigree in three generations at least. Sporadic forms should be explored as recessive ones especially in the case of early-onset (before the age of 40). The main laboratory investigations for the diagnosis of autosomal-recessive cerebellar ataxias are reported in the table on the left. \*For sporadic patients with unknown or censored family history, autosomal forms should be also considered. *AD* autosomal dominant, *AR* autosomal recessive, *α-FP* alpha-fetoprotein, *CoQ10* Coenzyme Q10, *Ig* Immunoglobulin, *Mt* mitochondrial

of metabolism, such as nonketotic hyperglycinemia, pyruvate dehydrogenase deficiency, or mitochondrial encephalomyopathy with lactic acidosis and stroke-like episodes (MELAS).

### An algorithm for investigations into a patient with suspected cerebellar ataxia

Several algorithms [7, 8] have been proposed to guide the diagnosis workup and the genetic analysis in ICA. To ask for the age at onset and to assess the speed of disease progression according to the current functional disability is the first major step (Fig. 1). Among the most frequent ARCA, an early AO (< 10 years) is usual suggestive of ATX–ATM (ataxia telangiectasia), ATX/HSP–SACS (ARSACS) and ATX–APT (AOA1) for instance while ATX–SETX (AOA2), ATX–SYNE1, ATX–ANO10 and POLG-related disease have an onset usually after 10 years of age. For ATX–FXN (Friedreich’s), the most frequent ARCA, age of onset generally falls in the first two decades. Regarding disease progression, patients affected with ATX–FXN, ATX–ATM, ATX–APT are confined to wheelchair faster (in less than 15 years) than those with ATX–SYNE1, ATX–ANO10 or ATX/HSP–SACS. In autosomal dominant CA (ADCA), age at onset is usually earlier

and disease progression slower in case of missense mutations (SCA5/*STPBN2*, SCA13/*KCNC3*, SCA14/*PRKCG*, SCA21/*TMEM240*, SCA28/*AFG3L2*) compared to SCAs due to CAG triplet repeat expansions (SCA3/*ATXN3*, SCA2/*ATXN2*, SCA1/*ATXN1*, SCA6/*CACNA1A*, SCA7/*ATXN7*, SCA17/*TBP*) whose age at onset is usually around 30 to 35 years but disease worsening faster. It should be pointed out that for SCA3 and SCA6, age of onset can be later as the sixth or seventh decade and for the latter the disease progression is the slowest among polyglutamine SCAs [9].

The collection of the clinical signs associated to CA is the second crucial step in the assessment (Table 2). When the formers are lacking, the following pure forms should be considered: SCA6/*CACNA1A*, SCA5/*STPBN2*, SCA11/*TTBK2*, SCA15–16/*ITPR1*, SCA22/*KCND3*, SCA 31/*BEAN*, SCA 41/*TRCP3*, ATX–SYNE1, ATX–ANO10.

### Laboratory investigations and brain imaging

Numerous biological markers presented in Fig. 1 have been associated with CA, mainly with ARCA. Of note, some of these diseases, which are summarized in Table 3, are accessible to specific disease-modifying treatments, and should be consequently systematically searched for.

**Table 2** List of diseases for which cerebellar ataxia is associated with other main clinical features

Clinical feature	Diseases
Chorea	ATX-ATM, ATX-APTX, ATX-SETX, ATX-MRE11A, ATX-OPA3 NBIA/DYT/PARK-CP XFE/ERCC4 SCA2/ATXN2 (large CAG expansion) SCA17/TBP, DRPLA/ATN1 (in the course of the disease) SCA48/STUB1
Myoclonus	ATX-ADCK3 MYC/ATX-GOSR2, MYC-SCARB2, MYC/ATX-KCTD7, MYC/ATX-NEU1 PRICKLE1 SCA2/ATXN2, DRPLA/ATN1 SCA13/KCNC3, SCA14/PRKCG, SCA19/KCND3, SCA21/TMEM240
Dystonia	ATX-ATM, ATX-APTX, ATX-SETX, ATX-NPC ATX/HSP-HEXA, ATX/HSP-HEXB, NBIA/DYT/PARK-PLA2G6 PNKP, MARS2 HSP/ATX/NBIA-FA2H DYT/ATX-ATP7B SCA2/ATXN2, SCA3/ATXN3, SCA17/TBP DYT/PARK/NBIA-PLA2G6 ATX-POLR3A/ATX-POLR3B
Parkinsonism	ATX-ATM, ATX-CYP27A1 POLG DYT/ATX-ATP7B NBIA/DYT/PARK-PLA2G6 Fragile X-associated tremor ataxia syndrome (FXTAS) SCA2/ATXN2, SCA3/ATXN3, SCA17/TBP DYT/PARK/NBIA-PLA2G6
Spastic paraplegia	ATX-CYP27A1, ATX/HSP-SACS, ATX/HSP-SPG7, ATX/HSP-POLR3A, ATX/HSP-CLCN2, HSP/ ATX/NBIA-FA2H MARS2, GBE1, MTPAP, ATX/HSP-DARS2, HSD17B4 DYT/PARK/NBIA-PLA2G6
Pyramidal signs	ATX-ANO10 SCA1/ATXN1, SCA3 /ATXN3, SCA7/ATXN7, SCA17/TBP SCA8/ATXN8, SCA10/ATXN10, SCA14/PRKCG, SCA15/ITPR1 SCA35/TGM6, SCA40/CCDC88C, SCA43/MME ATX-POLR3A/ATX-POLR3B
Oculomotor apraxia	ATX-ATM, ATX-APTX, ATX-SETX, ATX-MRE11 AOA4/PNKP
Strabismus or diplopia	ATX-SETX SCA3/ATXN3
Square wave jerks	ATX-FXN, POLG FXTAS SCA3/ATXN3
Hypometric, slow saccades	SCA2/ATXN2
Vertical supranuclear saccades palsy	ATX-NPC, ATX/HSP-SACS, ATX-STUB1
Intellectual deficiency	ATX-GRID2, ATX-L2HGDH, ATX-POLR3A, ATX-APTX ATX-KIAA0226, SCAR12/WWOX, ATX-SNX14, SCAR22/VWA3B, SCAR23/TDP2, MYC/ATX- KCTD7, ATX-PEX10, ATX/MYC-TPP1, ATX-SPTBN2, MARS2, ACO2, ATX-WDR73, MGR1, ATX-PMPKA, ATX-POLR3B, ATX-KCNJ10, SPAX4/MTPAP, OPA3, ATX-VLDLR, SCAR5/ WDR73, ATX-CA8, ATX-BTD, NBIA/DYT/PARK-PLA2G6, SCA13/KCNC3, SCA19-22/KCND3, SCA21/TMEM240
Cognitive decline	ATX-NPC, ATX-CYP27A1, ATX-ANO10, ATX/HSP-PNPLA6, ATX-ADCK3 NBIA/DYT/PARK-CP, MYC/ATX-KCTD7, GRM1, NBIA/DYT/PARK-PLA2G6 SCA2/ATXN2, SCA17/TBP, DRPLA/ATN1, SCA48/STUB1 FXTAS

**Table 3** Treatments available for inherited cerebellar ataxias

Disease	Treatment
ATX–TTP (Ataxia with vitamin E deficiency)	α-tocopherol (vitamin E)
ATX–CYP27A1 (Cerebrotendinous Xanthomatosis)	Chenodeoxycholic acid, ursodeoxycholic acid, cholic acid and taurocholic acid
ATX–PHYH (Refsum’s disease)	Diet with phytanic acid restriction, plasmapheresis for acute presentation
ATX–NPC1 (Niemann–Pick disease type C1)	Miglustat
ATX–ADCK3 (ARCA2/SCAR9)	Oral supplementation of coenzyme Q10
ATX–ATM (Ataxia–telangiectasia)	Avoid exposure to sun and radiations
ERCC4 (XFE progeroid syndrome)	
DYT/ATX–ATP7B (Wilson’s disease)	D-penicillamine, trientine, zinc acetate/sulfate and liver transplantation in acute forms
MTTP (Abetalipoproteinemia)	Fat-soluble vitamins (vitamin A, E, D, K) low-fat diet
PxMD–SLC2A1 (GLUT1 deficiency)	Ketogenic diet and triheptanoin
PxMD–KCNA1 (Episodic ataxia type 1)	Carbamazepine
PxMD–CACNA1A (Episodic ataxia type 2)	Acetazolamide 4-aminopyridine or baclofen (useful for downbeat nystagmus treatment)

Ophthalmological evaluation, including fundus and optical tomography coherence, might be helpful to identify peculiar ocular characteristics, such as optic atrophy in ATX–SPG7 [10] and cone rod dystrophy in SCA7 [11].

Electroneuromyography findings are of paramount importance for categorizing ARCA [7], which can be divided into 3 groups (listed according to frequency of the genetic from among each group): (i) ARCA with sensory neuropathy, such as ATX–FXN and CANVAS/RFC1, POLG-related diseases and ataxia with vitamin E deficiency (ATX–TTPA); (ii) ARCA with both sensory and motor axonal neuropathy, such as ATX–ATM, ATX/HSP–SACS, ATX–SETX, ATX–APTX, ATX–CYP27A1, ATX–PHYH; (iii) ARCA with a supplemental demyelinating component, such as ATX/HSP–SACS, ATX–CYP27A1 and ATX–PHYH. Patients displaying peripheral neuropathy are usually more severely disabled and more frequently experience falls. In ADCA, peripheral neuropathy is also frequently found in SCA3/ATXN3 (with frequent disabling pain) or SCA2/ATXN2 for instance.

Brain MRI allows to identify the presence or the absence of a marked cerebellar atrophy. Obvious cerebellar atrophy is reminiscent of ATX–ATM, ATX/HSP–SACS, ATX–SETX, ATX–SYNE1, ATX–ADCK3, ATX–APTX (which are ARCA), or SCA14/PKRG, SCA5/STBN2, SCA13/KCNC3 (which are ADCA due to missense mutations). Conversely, the lack of cerebellar atrophy is suggestive of ATX–FXN or

ATX–TTPA. Facing a prominent pons atrophy combined with a more subtle cerebellar atrophy, CAs due to CAG triplet repeat expansions should be considered, such as (in order of relative frequency), SCA3/ATXN3, SCA2/ATXN2, SCA1/ATXN1, SCA7/ATXN7, SCA6/CACNA1A, SCA17/TBP and DRPLA/ATN1. Other imaging clues suggestive of a specific entity may also be found on brain MRI such as linear stripes of the pons in T2-weighted or FLAIR axial slides in ATX/HSP–SACS, white matter hyperintensities in corpus callosum, middle cerebellar peduncle and cerebral white matter in FXTAS/FMR1, bilateral dentate nuclei and olivary nuclei hyperintensities in POLG-related CA or ATX–PRDX3 as well as cortical hyperintensities during epileptic fits or stroke-like episodes in ATX–ADCK3.

## Genetic analysis strategy

### Expansion detection

ICA is the group of inherited diseases that includes the largest number of distinct short tandem repeat mutations, including dominant coding together with dominant and recessive noncoding expansions. Initial screening for the most frequent expansions, which are listed in Table 4, is an efficient initial approach for the diagnosis of ICA, even in the absence of a family history if the phenotype is thought



**Table 4** Genetics and presentation of hereditary ataxias due to repeat expansions to be tested before NGS analysis

Disease	Gene	Pathological expansion	Protein	Transmission	Age at onset	Clinical phenotype	MRI
FA ATX-FXN	<i>FXN</i>	> 38 GAA FA: > 700 GAA LOFA: < 500 GAA	Frataxin	Recessive Mostly isolated case, or $\geq 2$ sibs in same generation, unaffected parents	FA: 7–25 y LOFA: 25–40 y VLOFA: > 40 y	FA: sensory neuropathy, cerebellar ataxia, absent tendon reflexes, Babinski sign, scoliosis, pes cavus, impairment of position and vibratory senses, hearing loss, optic neuropathy, diabetes, cardiomyopathy LOFA: normal tendon reflexes, Babinski sign, spastic ataxia VLOFA: normal tendon reflexes, Babinski sign, spastic ataxia	Spine atrophy
CANVAS ATX-RFC1	<i>RFC1</i>	400–2000 AAGGG	Replication factor C	Recessive Mostly isolated case, or $\geq 2$ sibs in same generation, unaffected parents	54 y (35–73)	Cerebellar ataxia, sensory neuropathy, vestibular areflexia, chronic cough	Cerebellar vermis atrophy
SCA3 ATX-ATXN3	<i>ATXN3</i>	> 51 CAG	ATXN3	Dominant Founder mutation: Portugal (Azores Islands), Germany, Japan	0–20 y: 11% 21–40 y: 43% > 40 y: 46%	Small repeat: axonal neuropathy, dopa-responsive parkinsonism Medium repeat: cerebellar ataxia, pyramidal signs, diplopia Large repeat: dystonia, pyramidal signs Gaze-evoked nystagmus, hypometric saccades	Cerebellar, brainstem and spine atrophy
SCA2 ATX-ATXN2	<i>ATXN2</i>	> 32 CAG	ATXN2	Dominant with several cases in successive generations. Juvenile case can be apparently isolated Founder mutation: Cuba, West Indies	0–20 y: 17% 21–40 y: 45% > 40 y: 38%	Small repeat: postural tremor Medium repeat: cerebellar ataxia, decreased reflexes Large repeat: cerebellar ataxia, chorea, dementia, myoclonus, dystonia Very large repeat: cardiac failure, retinal degeneration Slow saccades	Cerebellar (vermis) and brainstem atrophy

**Table 4** (continued)

Disease	Gene	Pathological expansion	Protein	Transmission	Age at onset	Clinical phenotype	MRI
SCA6 ATX–CACNA1A	<i>CACNA1A</i>	> 19 CAG	$\alpha$ 1A-Subunit of voltage-dependent calcium channel of P/Q type	Dominant, but can be censured due to late onset	45y (19–73)	Small repeat: Episodic ataxia Downbeat nystagmus	Cerebellar atrophy
SCA1 ATX–ATXN1	<i>ATXN1</i>	> 38 CAG (without CAT interruption)	ATXN1	Dominant with several cases in successive generations	0–20 y: 15% 21–40 y: 42% > 40 y: 43%	Medium repeat: cerebellar ataxia, pyramidal syndrome Large repeat: amyotrophic lateral sclerosis-like disorder Very large repeat: developmental delay Hypermetric saccades	Cerebellar (vermis) and brainstem atrophy
SCA7 ATX–ATXN7	<i>ATXN7</i>	> 36 CAG	ATXN7	Dominant with several cases in successive generations. Juvenile case can be apparently isolated Founder mutation: Scandinavian countries, South Africa and Mexico	0–20 y: 25% 21–40 y: 48% > 40 y: 27%	Small repeat: cerebellar ataxia without visual loss Medium repeat: cerebellar ataxia, cone rod dystrophy Large repeat: visual loss (cone rod dystrophy) before cerebellar syndrome Very large repeat: cardiac and renal failure	Cerebellar and brainstem atrophy
SCA8 ATX–ATXN8	<i>ATXN8</i>	CTA/CTG repeat in 3' untranslated region	ATXN8	Dominant		Cerebellar ataxia, pyramidal syndrome, sensory neuropathy, cognitive impairment, depression,	Cerebellar atrophy
SCA36 ATX–NOP56	<i>NOP56</i>	> 650 GGCCTG (normal 3–14)	Nucleolar protein 56	Dominant	0–20 y: 21% 21–40 y: 10% > 40 y: 69%	Cerebellar ataxia, amyotrophy, hearing loss	Cerebellar atrophy
DRPLA ATX–ATN1	<i>ATN1</i>	> 47 CAG	DRPLA	Dominant	31y (1–67)	Small repeat: chorea, ataxia, psychiatric manifestations Large repeat: progressive myoclonus, epilepsy, developmental delay, mild ataxia Very large repeat: myoclonic epilepsy, chorea, cognitive impairment	Cerebellar and brainstem atrophy, white matter lesions in cerebrum, thalamus, globus pallidus

**Table 4** (continued)

Disease	Gene	Pathological expansion	Protein	Transmission	Age at onset	Clinical phenotype	MRI
SCA12 ATX–PPP2R2B	<i>PPP2R2B</i>	CAG repeat in 5' untranslated region	Protein phosphatase 2, regulatory subunit B	Dominant	10–55 y	Cerebellar ataxia, tremor, dystonia, dementia, polyneuropathy	Cerebellar atrophy
SCA31 ATX–TK2	<i>BEAN–TK2</i>	Intronic TGGAA repeat insertion	Brain-expressed protein associating with NEDD4 homologue	Dominant	56 y (45–72)	Pure cerebellar ataxia	Cerebellar atrophy
SCA17 ATX–TBP	<i>TBP</i>	>48 CAG	TATA-box-1-binding protein	Dominant, incomplete penetrance	34 y (3–75)	Small repeat: Huntington's disease-like phenotype, parkinsonism Medium repeat: ataxia, dementia, chorea and dystonia, pyramidal signs Large repeat: ataxia, dementia, spasticity, epilepsy Very large repeat: growth retardation	Diffuse cerebral atrophy
SCA10 ATX–ATXN10	<i>ATXN10</i>	Intronic ATTCT repeat insertion	ATXN10	Dominant	10–40 y	Cerebellar ataxia, epilepsy	Cerebellar atrophy
SCA37 ATX–DAB1	<i>DAB1</i>	ATTTC insertion in 5' untranslated region ranging from 31 to 75 repeats	Disabled homologue 1'	Dominant	48 y (18–64)	Cerebellar ataxia, saccadic pursuit (vertical > horizontal)	Cerebellar atrophy
FXTAS ATX–FMR1	<i>FMR1</i>	55–200 CGG	Fragile X mental retardation protein	X-linked	> 50 y	Intention tremor, cerebellar ataxia, parkinsonism, axonal neuropathy, cognitive impairment	White matter lesions in middle cerebellar peduncle, splenium of the corpus callosum and cerebrum Cerebral atrophy

The autosomal-dominant ataxias are listed according to available data regarding worldwide prevalence

*CANVAS* Cerebellar ataxia, neuropathy and vestibular are flexia syndrome, *DRPLA* Dentatorubral–pallidolysian atrophy, *FA* Friedreich ataxia, *FXTAS* Fragile X-associated tremor/ataxia syndrome, *SCA* Spinocerebellar ataxia, y years

compatible with these genes. Molecular diagnosis can be easily achieved by simple PCR fragment size analyses or by repeat-primed PCR amplifications, while this would be missed with classical short read exome sequencing. More sophisticated techniques including Southern blot analyses, long range PCR or repeat sequencing, might be required to detect some of these mutations, such as biallelic expansions in *RFC1* responsible for CANVAS. Future developments of long-read genome sequencing are awaited to hopefully detect both expansions and point mutations.

### Sanger sequencing

Dideoxynucleotide chain termination sequencing, also named Sanger sequencing, is a method of genetic sequencing that only allows detection of a few genetic variants per testing. Its use is now restricted to cases with prior knowledge of the defective gene (usually based on the biochemical screen, such as for ATX–TTPA or other metabolic diseases), confirmation of familial segregation for a mutation already identified in an affected relative, genetic counseling and confirmation of a mutation previously identified by Next-Generation Sequencing (NGS).

### Next-generation sequencing

Next-Generation Sequencing (NGS) is defined by the parallel sequencing of multiple genes in a single test. Given the large number of genes involved in ICA and the important clinical overlap between the different entities, NGS has become the method of choice for the genetic diagnosis of ICA. Panel sequencing, which consists in the testing of a predefined list of genes, is a suboptimal option because of low positive yield and the absence of the most recently identified genes [12]. Thus, exome (all protein-coding genes), “Mendelian”-exome (all known disease genes), and whole genome sequencing are increasingly being used as first tier diagnostic tools [13]. The major challenge for positive diagnosis is variant interpretation and sorting among the wealth of generated data. Thus, the most effective approach is usually trio analysis, which requires the parallel sequencing of the patient and both parents. Trio analyses solve the mode of inheritance issue: recessive mutations must be biallelic, i.e. each parent has to be heterozygous for the mutation while the patient has to be compound heterozygous or homozygous, dominant mutation must be inherited from the affected parent (or from the affected branch in case of reduced penetrance) or be de novo, meaning absent from both parents if they are both unaffected.

Another difficulty related to NGS is pathogenicity prediction for missense variants, which are defined by the replacement of a single amino acid by another one in a protein sequence, especially when facing atypical clinical

presentations. An average of 9000 missense variants are identified in each exome or genome sequencing, while only a single of them accounts for the phenotype in Mendelian disorders. Pathogenicity prediction based on conservation and structure (such as SIFT, PolyPhen2 and CADD algorithms) have a reasonable sensitivity but low specificity. In contrast, truncating variants (occurrence of a stop codon or short frameshift indel) and copy number variations (deletions and duplications) usually have a higher pathogenicity score but are less common. When a trio analysis is combined with pathogenicity assessment and matching with disease variants and common polymorphisms reported in public databases, the outcome usually yields a short list of variants that can be confronted with clinical data and subsequent targeted paraclinical investigations. Despite the recent advances in the genetics of ICA, the incapacity to identify the causative variant still occurs in many families, indicating that challenges lie ahead to unravel the missing genetic causes of this phenotype.

### The genetic nomenclature of ARCAs

A new transparent, adaptable nomenclature of ARCA has been proposed according to the International Parkinson and Movement Disorder Society [2]. Sixty-two entities were indicated with ATX prefix followed by gene name presenting ataxia as the main feature, and 30 have a double prefix when ataxia is combined with another prominent movement disorder (e.g. ATX/HSP, combination of ataxia and spastic paraparesis). Another interesting clinical and pathophysiological classification of ARCA was proposed excluding forms for which ataxia is minor or rare feature and identifying 59 main disorders [14].

### Clue clinical features for the diagnosis of inherited cerebellar ataxia

#### Friedreich–ataxia (ATX–FXN)

ATX–FXN is a multisystem disorder with an age at onset mostly before 25, and a progressive evolution with CA, sensory neuropathy, pyramidal signs, leading to wheelchair after 10 years of evolution. Cardiomyopathy, diabetes, scoliosis, deafness and optic neuropathy may occur. Brain MRI usually demonstrates no cerebellar atrophy, but cervical spinal cord atrophy is common. Despite a less severe phenotype, late (> 25 years) and very late (> 40 years) onset Friedreich ataxia should not be missed. These forms are characterized by a spastic ataxia with preserved or even brisk deep tendon reflexes. Dysarthria, muscle wasting, ganglionopathy, scoliosis and cardiomyopathy occur less

frequently than in typical early onset Friedreich ataxia [15]. ATX–FXN is due in the majority of cases to biallelic GAA repeat expansions in the first intron of the *FXN* gene, and in 2% of cases, to combination of one GAA expansion and one *FXN* point mutation or deletion in the other allele [16]. Frataxin, encoded by *FXN*, is involved in mitochondrial iron homeostasis and the assembly and transfer of iron–sulfur clusters to various mitochondrial enzymes and components. *FXN* mutations should be searched for firstly in case of suspected ARCA when the phenotype is compatible.

### Cerebellar ataxia, neuropathy and vestibular areflexia syndrome (CANVAS)

Cerebellar ataxia with neuropathy and vestibular areflexia syndrome (CANVAS) was first described by Migliaccio et al. [17]. The classic phenotype-associated sensory neuropathy, cerebellar and sensory ataxia, vestibular areflexia, dysautonomia and chronic cough. Additional clinical features, including parkinsonism or motor neuron disorders have recently been described [18]. Brain MRI showed frequent cerebellar atrophy and optional cervical posterior columns changes. Biallelic intronic AAGGG repeat expansions in the *RFC1* gene encoding a subunit of a DNA polymerase accessory protein have been recently identified as the cause of CANVAS [19]. In CANVAS, the number of the pentanucleotide repeat expansion of *RFC1* is increased from 11 up to more than 400 repeats (400–2000) and there is a modification of the AAAAG or AAAGG reference sequence. Although further works are warranted to determine the mechanism underlying *RFC1*-related disorders, the absence of *RFC1* expression alteration in mutation carriers argue against a loss of function mechanism [19]. Owing to the frequency of the heterozygous AAGGG repeat expansion in the normal population (0.7%), CANVAS/*RFC1* appear to be a common cause of late-onset ARCA [19].

### Ataxia telangiectasia (ATX/ATM)

ATX–ATM, the second most frequent ARCA after ATX–FXN, is characterized by CA, telangiectasias, oculomotor apraxia, dystonia, sensorimotor axonal neuropathy as well as elevated AFP serum level (markedly increased in 90% of patients, often above 100 µg/L (normal < 5 µg/L) [20]. ATX–ATM mostly starts around 2 years of age then progressively worsens, leading to the loss of independent walking by 10 years and to death before 18 years [21], although some patients experience later onset, milder phenotype or longer life span. ATX–ATM patients are prone to recurrent infections because of immunodeficiency and to increased cancer risk (especially hematologic malignancies) and sensitivity to ionizing radiations. *ATM* gene encodes a phosphatidylinositol-3-kinase involved in cell

cycle progression, cellular response to DNA alterations and maintenance of genome stability [22].

### ATX/HSP-SPG7

Disease onset is generally in the fourth decade [23] and the CA can be the main feature and precede spastic paraparesis. Optic neuropathy, progressive external ophthalmoplegia, parkinsonism and cognitive impairment can enrich the phenotype [10]. In the last few years, SPG7 appeared as a frequent cause of slowly progressive CA [13] beyond spastic paraplegia. Brain MRI revealed cerebellar atrophy [23, 24], and in some cases dentate nucleus hyperintensity on T2 sequences [24]. SPG7 is due to mutation in the gene encoding paraplegin, a mitochondrial protein [25]. Genotype–phenotype correlations have been described for this gene since p.Ala510Val variants was associated with a later onset cerebellar phenotype as compared to loss of function variants with spasticity-predominant phenotype [23].

### SCA3/ATXN3

SCA3, or Machado–Joseph disease, is the most frequent SCA worldwide especially in Portugal, Brazil, China, the Netherlands, Japan and Germany [26]. Founder mutations are responsible for the higher prevalence in these countries, in particular for families of Portuguese–Azorean ancestry and other founder haplotypes are reported in Japan and Germany [27]. Disease occurs in adulthood, and the phenotype also includes pyramidal signs, parkinsonism, dystonia, hypometric saccades, diplopia, painful axonal neuropathy and depression [28]. Facial myokymia are also highly prevalent in SCA3 but not particularly specific. Polyglutamine (polyQ) expansion in *ATXN3* gene is responsible for SCA3 and provokes protein aggregates that form intranuclear inclusions with subsequent neuronal loss. Recent publications have suggested specific retinal architecture alteration in SCA3 [29].

### SCA36/NOP56

CA is associated with tongue atrophy and fasciculations then skeletal muscle atrophy in limbs and trunk, lower motor neuron disease being confirmed by electroneuromyography. Other clinical signs are ptosis, postural tremor, mild cerebellar cognitive affective syndrome (CCAS) [30] and deafness. For the latter, its association with cerebellar ataxia may guide the clinician toward a specific diagnosis as SCA36 [31]. Large hexanucleotide GGCCTG repeat expansions in the first intron of the *NOP56* gene are responsible for SCA36 [32]. Nop56 protein is highly expressed in Purkinje cells, motor neurons of hypoglossal nucleus and the spinal cord anterior horn explaining the phenotype [32].

### SCA37/DAB1

SCA37 is a late-onset pure, slowly progressive cerebellar ataxia with a severe lower limbs dysmetria, dysphagia and oculomotor abnormalities [33]. Indeed, a remarkable clinical feature is the early vertical eye movement disorders as saccadic pursuit and dysmetria, which may anticipate CA. SCA37 is the last reported SCA associated with repeat expansion and due to insertion of ATTTC pentanucleotide in the noncoding region of *DAB1* [34]. This insertion modifies the normal allele (ATTTT)<sub>7–400</sub> in the pathogenic variant (ATTTT)<sub>60–79</sub>(ATTTC)<sub>31–75</sub>(ATTTT)<sub>58–90</sub>, with a negative correlation between age at disease onset and repeat size of ATTTC.

### SCA48/STUB1

SCA48 is due to *STUB1* (STIP1 Homology And U-Box Containing Protein 1) gene mutation [35] encoding the CHIP protein, a ubiquitin ligase/co-chaperone. *STUB1* biallelic mutations were first described as responsible for ARCA with hypogonadism and short stature [36] then in a Spanish family for dominantly inherited CA and cognitive impairment [35]. CCAS or Schmahmann's syndrome, based on the concept of "dysmetria of thought" created in '90 s [37], which includes executive deficits, attentional dysfunctions, language difficulties, visual-spatial memory impairment, impaired socio-emotional processes with social cognition deficits, apathy and disinhibited behavior is commonly found in SCA48 [35]. The median age at disease onset is 42 years and in several cases cognitive impairment can precede cerebellar ataxia [35]. Novel *STUB1* mutations were reported in six Italian families and in a larger French cohort with dominant ataxia, confirming this phenotype and its high frequency among dominant ataxias [38].

### Ataxia-pancytopenia syndrome/SCA49/SAMD9L

Ataxia-pancytopenia syndrome is characterized by CA, cytopenia (that must be searched for) and myeloid malignancies. Missense mutations in *SAMD9L* cause the autosomal-dominant Ataxia-Pancytopenia syndrome [39]. *SAMD9L* acts as a tumor suppressor with antiproliferative function. Given the hematopoietic mosaicism, the germline variant should be searched for in skin fibroblasts rather than in blood. It is important to test family members because of the risk for the carriers to develop hematological malignancies and the possibilities to be healthy hematopoietic stem cells donors [40].

### FXTAS/FMR1

Fragile X-associated tremor/ataxia syndrome (FXTAS) includes action tremor, CA, cognitive decline, peripheral neuropathy, parkinsonism, depression and anxiety [41]. Typical MRI findings are brain atrophy including cerebellar atrophy and typical but not specific middle cerebellar peduncles, periventricular area and corpus callosum splenium hyperintensities. FXTAS is due to fragile X premutation (55 up to 200 CGG triplet repeat) that is a 5' untranslated region of the *FMR1* gene (whose complete mutation is responsible for fragile X syndrome (FXS) mainly characterized by intellectual deficiency) [42]. FXTAS is due to sequestration of proteins by abnormal FMR1 mRNA, production of toxic FMRPolyG protein as well as consequences of DNA damage repair process activation [42]. FXTAS affects 40–75% of ageing male premutation carriers and 15–20% of women premutation carriers. The diagnosis of FXTAS is crucial to provide appropriate genetic counseling especially to patients' daughters who are at risk of developing FXTAS, primary ovarian insufficiency and of having sons affected with Fragile X syndrome.

### What is controversial or remains to be elucidated?

#### Conditions with both dominant and recessive presentations

Both dominant and recessive inheritance patterns are described for several genes involved in cerebellar ataxia. Few cases with dominant inheritance have been reported for *SPG7*. In the largest cohort of 241 *SPG7* patients, carrying two variants, 6% of patients presented with a dominant pattern of transmission [23]. Heterozygous relatives may present impaired balance and mild cerebellar atrophy, occurring later than homozygous carriers do [10]. Some variants seem to be associated with dominant cases, as p.Arg485\_Glu487del [43]. However, for these cases, the presence of pathogenic variant in another gene cannot be excluded.

Pathogenic *STUB1* variants were initially described in autosomal-recessive ATX-STUB1 [36] then in autosomal-dominant SCA48 [35].

*SPTBN2* can be inherited in both autosomal recessive and dominant fashion, responsible for ATX-SPTBN2 [44] and SCA5 [45], respectively. SCA5 is an adult-onset, slowly progressive pure CA whereas ATX-SPTBN2 is characterized by early-childhood onset and complicated phenotype.

*GRID2* may also be either recessively or dominantly inherited, the latter being reported with the variant p.Leu656Val [46]. Before that, only null mutations

in homozygous state were described as responsible for SCAR18 [47] with a more severe phenotype.

### Ataxia or spastic paraplegia?

It is frequent that clinicians encounter patients presenting with both spastic paraparesis and cerebellar features. Prominent spastic phenotype might lead to difficulties in assessing cerebellar ataxia. This is the case in polyQ SCAs, with clear genotype–phenotype correlation for large expansions in SCA1/ATXN1, SCA3/ATXN3 and SCA7/ATXN7 presenting as spastic paraplegia. In addition, ATX/HSP–SACS (ARSACS) in childhood and ATX/HSP–SPG7 in adulthood, present as spastic ataxia, both with autosomal-recessive transmission [48]. A slow progression and a clinical triad characterize the first: cerebellar ataxia, lower-limb spasticity and axonal and demyelinating sensorimotor neuropathy. Some investigations can help in diagnosis as fundoscopy allowing the identification of myelinated retinal nerve fibers and brain MRI showing linear pontine hypointensities and cerebellar atrophy. Adulthood onset, though rare, has been reported [49]. Other important spastic ataxias are cerebrotendinous xanthomatosis (ATX–CYP27A1), late-onset Friedreich ataxia and adult-onset Alexander disease. Among new genes, *CAPN1* was identified initially as a HSP-related gene (SPG76), but has been recently linked to spastic ataxia [50].

### Unique genotyping strategies

With the emergence of NGS, which is increasingly available, cheap and efficient, and permit the identification of many variants (including those with unknown significance) one may be tempted to perform NGS early on in the diagnosis work for a given patient, sometimes even before any laboratory investigation. The strategy to first genotype, that could be less expensive and more pragmatic, requires a close collaboration between geneticists and clinicians to interpret the genetic results based on phenotype. However, suitable clinical examination, exclusion of acquired causes, a precise delineation of the phenotype and follow-up of the patients are thoroughly recommended.

### Treatments and future therapeutic development perspectives

Only a limited number of ICA patients can benefit from a specific disease-modifying treatment (in Table 3). A Guideline Development Group composed by ataxia experts from United Kingdom provided recommendations with levels of evidence for medical interventions [51]. Supportive treatments proposed to the patients are physical therapy, speech therapy and occupational therapy. With regular practice of physiotherapy, which is recommended, improvement of CA

was demonstrated [52]. Speech therapy is suggested for management of dysarthria and swallowing difficulties as well as psychological support. For more information, there are dedicated websites: <http://ataxia-global-initiative.net/>, a platform for clinical research. <https://spatax.wordpress.com>, international research network; <https://ataxia.org> and <https://www.ataxia.org.uk/> for research support and education, as well as the website of the European Rare Disease network for webinars and fellowship applications <http://www.ern-rnd.eu>. Transcranial direct current stimulation (tDCS), aiming to modulate the excitability of the cerebellum, reported encouraging, but not replicated, results [53].

Curative therapies are in development for several CA. As for Huntington Disease, they derive from antisense oligonucleotides (ASOs) for SCA1/ATXN1 [54], SCA2/ATXN 2[55], SCA3/ATXN3 [56] and SCA7/ATXN7 [57] mice model. For SCA36/NOP56, ASOs showed RNA-foci reduction in patient iPSCs [58]. The perspective of ASOs clinical trials in humans in the next few years is realistic and the first clinical trial for SCA3 patients began in early 2022 (NCT05160558). Accumulated ataxin 1, 2, 3 and 7 proteins are promising target engagement biomarkers. Specific bioassays to quantify mutant ataxin-3 in blood, CSF, peripheral blood mononuclear cells and fibroblasts are used [59]. Allele-specific approaches are advisable since consequences due to wild type protein decrease could be harmful. Other therapies targeting RNA inhibiting gene expression are RNA interference (RNAi), micro RNA (miRNA), short hairpin RNA (shRNA) [60], gene editing strategies (CRISPR/Cas9) [61]. For now, in ATX-FXN, the only treatment that has shown positive results is omaveloxolone. In a phase 2 trial, omaveloxolone administration (150 mg/day) for 48 weeks showed significant neurological improvement as decreased of mFARS scores as compared to placebo [62, 63]. In ATX–FXN, delivery of frataxin-expressing AAV showed sensory neuropathy rescue in a conditional mouse model with complete frataxin deletion [64]. Another strategy to restore the frataxin expression was tested on mouse model YG8R by CRISPR/Cas9-mediated genome editing [65].

Although, gene therapies have been successful in mice models, major difficulties as technological challenges, lack of biomarkers and economic efforts arise in using these therapies in patients [61].

### Genetic counseling

Genetic counseling covers transmission pattern in the family, information about possibilities of presymptomatic testing especially in dominant diseases and prenatal diagnosis. For entities that present both, autosomal dominant and recessive inheritance patterns, genetic counseling is challenging. In diseases where no preventive measures exist, but the severity leads to the wish to find out about the genetic status,



presymptomatic testing is a choice that is not only medical in the absence of preventive treatment. The major reason for taking the test for SCAs is to plan a family, but a minority of expansion carriers choose to perform prenatal testing or preimplantation genetic diagnosis [66]. A specific care setting should be provided to support parents and families through these life choices.

## Conclusion

In this review, we provide to clinicians the key points for clinical, laboratory and genetic investigations when inherited cerebellar ataxia is suspected. The most frequent entities for each transmission pattern are discussed more in detail in order not to miss the diagnosis. New genes are constantly identified thanks to the increased availability of exome/genome and the development of new techniques as long-read sequencing. This lead to broaden phenotypic spectrum for some genes and to describe either recessive or dominant inheritance patterns, complicating the diagnostic process. As for therapy, curative treatments are not available, except for some subtypes, which is why gene therapies are eagerly awaited.

**Supplementary Information** The online version contains supplementary material available at <https://doi.org/10.1007/s00415-022-11383-6>.

**Author Contributions** GC: research project: A. conception, B. organization, C. execution; manuscript preparation: A. writing of the first draft, B. review and critique. TW: research project: A. conception, B. organization, C. execution; manuscript preparation: A. writing of the first draft, B. review and critique. CT: research project: A. conception, B. organization, C. execution; manuscript preparation: A. writing of the first draft, B. review and critique. MK: research project: A. conception, B. organization, C. execution; manuscript preparation: A. writing of the first draft, B. review and critique. AD: research project: A. conception, B. organization, C. execution; manuscript preparation: A. writing of the first draft, B. review and critique. MA: research project: A. conception, B. organization, C. execution; manuscript preparation: A. writing of the first draft, B. review and critique.

## Declarations

**Conflicts of interest** The authors report no competing interests.

## References

- Joyce MR, Nadkarni PA, Kronemer SI et al (2022) Quality of life changes following the onset of cerebellar ataxia: symptoms and concerns self-reported by ataxia patients and informants. *Cerebellum Lond Engl* 21:592–605. <https://doi.org/10.1007/s12311-022-01393-5>
- Rossi M, Anheim M, Durr A et al (2018) The genetic nomenclature of recessive cerebellar ataxias: genetic nomenclature of recessive ataxias. *Mov Disord* 33:1056–1076. <https://doi.org/10.1002/mds.27415>
- Marras C, Lang A, van de Warrenburg BP et al (2016) Nomenclature of genetic movement disorders: recommendations of the international Parkinson and movement disorder society task force. *Mov Disord* 31:436–457. <https://doi.org/10.1002/mds.26527>
- Salman MS (2018) Epidemiology of cerebellar diseases and therapeutic approaches. *Cerebellum Lond Engl* 17:4–11. <https://doi.org/10.1007/s12311-017-0885-2>
- Moscovich M, Okun MS, Favilla C et al (2015) Clinical evaluation of eye movements in spinocerebellar ataxias: a prospective multicenter study. *J Neuro-Ophthalmol Off J N Am Neuro-Ophthalmol Soc* 35:16–21. <https://doi.org/10.1097/WNO.0000000000000167>
- Stephen CD, Schmahmann JD (2019) Eye movement abnormalities are ubiquitous in the spinocerebellar ataxias. *Cerebellum Lond Engl* 18:1130–1136. <https://doi.org/10.1007/s12311-019-01044-2>
- Anheim M, Tranchant C, Koenig M (2012) The autosomal recessive cerebellar ataxias. *N Engl J Med* 366:636–646. <https://doi.org/10.1056/NEJMra1006610>
- Renaud M, Tranchant C, Martin JVT et al (2017) A recessive ataxia diagnosis algorithm for the next generation sequencing era. *Ann Neurol* 82:892–899. <https://doi.org/10.1002/ana.25084>
- Jacobi H, du Montcel ST, Romanzetti S et al (2020) Conversion of individuals at risk for spinocerebellar ataxia types 1, 2, 3, and 6 to manifest ataxia (RISCA): a longitudinal cohort study. *Lancet Neurol* 19:738–747. [https://doi.org/10.1016/S1474-4422\(20\)30235-0](https://doi.org/10.1016/S1474-4422(20)30235-0)
- Klebe S, Depienne C, Gerber S et al (2012) Spastic paraplegia gene 7 in patients with spasticity and/or optic neuropathy. *Brain* 135:2980–2993. <https://doi.org/10.1093/brain/aws240>
- Marianelli BF, Filho FMR, Salles MV et al (2021) A proposal for classification of retinal degeneration in spinocerebellar ataxia type 7. *Cerebellum Lond Engl* 20:384–391. <https://doi.org/10.1007/s12311-020-01215-6>
- Montaut S, Tranchant C, Drouot N et al (2018) Assessment of a targeted gene panel for identification of genes associated with movement disorders. *JAMA Neurol* 75:1234. <https://doi.org/10.1001/jamaneurol.2018.1478>
- Coutelier M, Hammer MB, Stevanin G et al (2018) Efficacy of exome-targeted capture sequencing to detect mutations in known cerebellar ataxia genes. *JAMA Neurol* 75:591. <https://doi.org/10.1001/jamaneurol.2017.5121>
- Beaudin M, Matilla-Dueñas A, Soong B-W et al (2019) The classification of autosomal recessive cerebellar ataxias: a consensus statement from the society for research on the cerebellum and ataxias task force. *Cerebellum Lond Engl* 18:1098–1125. <https://doi.org/10.1007/s12311-019-01052-2>
- Lecocq C, Charles P, Azulay J-P et al (2016) Delayed-onset Friedreich's ataxia revisited. *Mov Disord Off J Mov Disord Soc* 31:62–69. <https://doi.org/10.1002/mds.26382>
- Cossée M, Campuzano V, Koutnikova H et al (1997) Frataxin fragas. *Nat Genet* 15:337–338. <https://doi.org/10.1038/ng0497-337>
- Migliaccio AA, Halmagyi GM, McGarvie LA, Cremer PD (2004) Cerebellar ataxia with bilateral vestibulopathy: description of a syndrome and its characteristic clinical sign. *Brain J Neurol* 127:280–293. <https://doi.org/10.1093/brain/awh030>
- Huin V, Coarelli G, Guemy C et al (2021) Motor neuron pathology in CANVAS due to RFC1 expansions. *Brain*. <https://doi.org/10.1093/brain/awab449>
- Cortese A, Simone R, Sullivan R et al (2019) Biallelic expansion of an intronic repeat in RFC1 is a common cause of late-onset ataxia. *Nat Genet* 51:649–658. <https://doi.org/10.1038/s41588-019-0372-4>
- Rothblum-Oviatt C, Wright J, Lefton-Greif MA et al (2016) Ataxia telangiectasia: a review. *Orphanet J Rare Dis* 11:159. <https://doi.org/10.1186/s13023-016-0543-7>
- Micol R, Ben Slama L, Suarez F et al (2011) Morbidity and mortality from ataxia-telangiectasia are associated with ATM



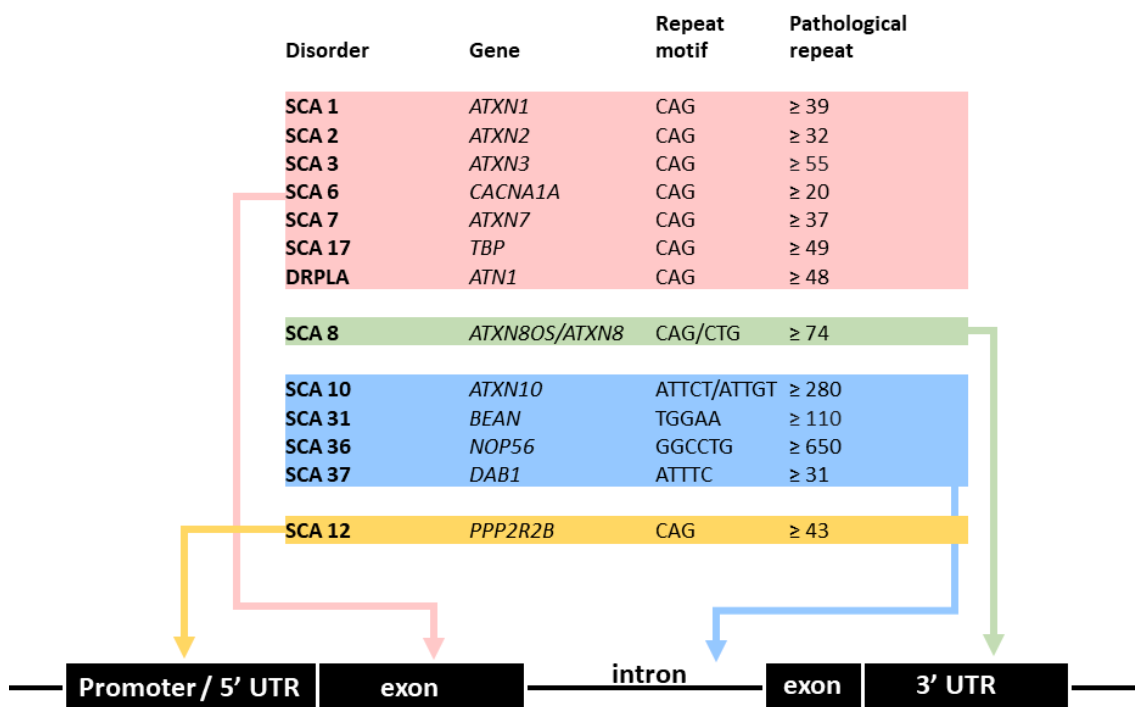
- genotype. *J Allergy Clin Immunol* 128:382–389.e1. <https://doi.org/10.1016/j.jaci.2011.03.052>
22. Savitsky K, Bar-Shira A, Gilad S et al (1995) A single ataxia telangiectasia gene with a product similar to PI-3 kinase. *Science* 268:1749–1753. <https://doi.org/10.1126/science.7792600>
  23. Coarelli G, Schule R, van de Warrenburg BPC et al (2019) Loss of paraplegin drives spasticity rather than ataxia in a cohort of 241 patients with *SPG7*. *Neurology* 92:e2679–e2690. <https://doi.org/10.1212/WNL.00000000000007606>
  24. Hewamadduma CA, Hoggard N, O'Malley R et al (2018) Novel genotype-phenotype and MRI correlations in a large cohort of patients with *SPG7* mutations. *Neurol Genet* 4:e279. <https://doi.org/10.1212/NXG.0000000000000279>
  25. Casari G, De Fusco M, Ciarmatori S et al (1998) Spastic paraplegia and OXPHOS impairment caused by mutations in paraplegin, a nuclear-encoded mitochondrial metalloprotease. *Cell* 93:973–983. [https://doi.org/10.1016/S0092-8674\(00\)81203-9](https://doi.org/10.1016/S0092-8674(00)81203-9)
  26. Klockgether T, Mariotti C, Paulson HL (2019) Spinocerebellar ataxia. *Nat Rev Dis Primer* 5:24. <https://doi.org/10.1038/s41572-019-0074-3>
  27. Martins S, Calafell F, Gaspar C et al (2007) Asian origin for the worldwide-spread mutational event in Machado-Joseph disease. *Arch Neurol* 64:1502–1508. <https://doi.org/10.1001/archneur.64.10.1502>
  28. Durr A (2010) Autosomal dominant cerebellar ataxias: polyglutamine expansions and beyond. *Lancet Neurol* 9:885–894. [https://doi.org/10.1016/S1474-4422\(10\)70183-6](https://doi.org/10.1016/S1474-4422(10)70183-6)
  29. Rezende Filho FM, Jurkute N, de Andrade JBC et al (2021) Characterization of retinal architecture in spinocerebellar ataxia type 3 and correlation with disease severity. *Mov Disord*. <https://doi.org/10.1002/mds.28893>
  30. Martínez-Regueiro R, Arias M, Cruz R et al (2020) Cerebellar cognitive affective syndrome in Costa da Morte ataxia (SCA36). *The Cerebellum* 19:501–509. <https://doi.org/10.1007/s12311-020-01110-0>
  31. Barsottini OG, Pedroso JL, Martins CR et al (2019) Deafness and vestibulopathy in cerebellar diseases: a practical approach. *Cerebellum Lond Engl* 18:1011–1016. <https://doi.org/10.1007/s12311-019-01042-4>
  32. Kobayashi H, Abe K, Matsuura T et al (2011) Expansion of intronic GGCCTG hexanucleotide repeat in NOP56 causes SCA36, a type of spinocerebellar ataxia accompanied by motor neuron involvement. *Am J Hum Genet* 89:121–130. <https://doi.org/10.1016/j.ajhg.2011.05.015>
  33. Matilla-Dueñas A, Volpini V (1993) Spinocerebellar Ataxia Type 37. In: Adam MP, Mirzaa GM, Pagon RA, et al (eds) GeneReviews®. University of Washington, Seattle, Seattle (WA)
  34. Seixas AI, Loureiro JR, Costa C et al (2017) A Pentanucleotide ATTTC repeat insertion in the non-coding region of DAB1, mapping to SCA37, causes spinocerebellar ataxia. *Am J Hum Genet* 101:87–103. <https://doi.org/10.1016/j.ajhg.2017.06.007>
  35. Genis D, Ortega-Cubero S, San Nicolás H et al (2018) Heterozygous *STUB1* mutation causes familial ataxia with cognitive affective syndrome (SCA48). *Neurology* 91:e1988–e1998. <https://doi.org/10.1212/WNL.0000000000006550>
  36. Shi Y, Wang J, Li J-D et al (2013) Identification of CHIP as a novel causative gene for autosomal recessive cerebellar ataxia. *PLoS ONE* 8:e81884. <https://doi.org/10.1371/journal.pone.0081884>
  37. Schmähmann J (1998) The cerebellar cognitive affective syndrome. *Brain* 121:561–579. <https://doi.org/10.1093/brain/121.4.561>
  38. SPATAX network, Roux T, Barbier M et al (2020) Clinical, neuropathological, and genetic characterization of *STUB1* variants in cerebellar ataxias: a frequent cause of predominant cognitive impairment. *Genet Med*. <https://doi.org/10.1038/s41436-020-0899-x>
  39. Chen D-H, Below JE, Shimamura A et al (2016) Ataxia-pancytopenia syndrome is caused by missense mutations in *SAMD9L*. *Am J Hum Genet* 98:1146–1158. <https://doi.org/10.1016/j.ajhg.2016.04.009>
  40. Ahmed IA, Farooqi MS, Vander Lugt MT et al (2019) Outcomes of hematopoietic cell transplantation in patients with germline *SAMD9/SAMD9L* mutations. *Biol Blood Marrow Transplant J Am Soc Blood Marrow Transplant* 25:2186–2196. <https://doi.org/10.1016/j.bbmt.2019.07.007>
  41. Salcedo-Arellano MJ, Dufour B, McLennan Y et al (2020) Fragile X syndrome and associated disorders: clinical aspects and pathology. *Neurobiol Dis* 136:104740. <https://doi.org/10.1016/j.nbd.2020.104740>
  42. Hagerman RJ, Hagerman P (2016) Fragile X-associated tremor/ataxia syndrome—features, mechanisms and management. *Nat Rev Neurol* 12:403–412. <https://doi.org/10.1038/nrneurol.2016.82>
  43. van Gassen KLI, van der Heijden CDCC, de Bot ST et al (2012) Genotype-phenotype correlations in spastic paraplegia type 7: a study in a large Dutch cohort. *Brain J Neurol* 135:2994–3004. <https://doi.org/10.1093/brain/aws224>
  44. Lise S, Clarkson Y, Perkins E et al (2012) Recessive mutations in *SPTBN2* implicate  $\beta$ -III spectrin in both cognitive and motor development. *PLoS Genet* 8:e1003074. <https://doi.org/10.1371/journal.pgen.1003074>
  45. Elsayed SM, Heller R, Thoenes M et al (2014) Autosomal dominant SCA5 and autosomal recessive infantile SCA are allelic conditions resulting from *SPTBN2* mutations. *Eur J Hum Genet EJHG* 22:286–288. <https://doi.org/10.1038/ejhg.2013.150>
  46. Coutelier M, Burglen L, Mundwiller E et al (2015) *GRID2* mutations span from congenital to mild adult-onset cerebellar ataxia. *Neurology* 84:1751–1759. <https://doi.org/10.1212/WNL.0000000000001524>
  47. Utine GE, Haliloğlu G, Salanci B et al (2013) A homozygous deletion in *GRID2* causes a human phenotype with cerebellar ataxia and atrophy. *J Child Neurol* 28:926–932. <https://doi.org/10.1177/0883073813484967>
  48. Pedroso JL, Vale TC, França Junior MC et al (2021) A diagnostic approach to spastic ataxia syndromes. *Cerebellum Lond Engl*. <https://doi.org/10.1007/s12311-021-01345-5>
  49. Briand M-M, Rodrigue X, Lessard I et al (2019) Expanding the clinical description of autosomal recessive spastic ataxia of Charlevoix-Saguenay. *J Neurol Sci* 400:39–41. <https://doi.org/10.1016/j.jns.2019.03.008>
  50. Shetty A, Gan-Or Z, Ashtiani S et al (2019) *CAPN1* mutations: Expanding the *CAPN1*-related phenotype: from hereditary spastic paraparesis to spastic ataxia. *Eur J Med Genet* 62:103605. <https://doi.org/10.1016/j.ejmg.2018.12.010>
  51. de Silva R, Greenfield J, Cook A et al (2019) Guidelines on the diagnosis and management of the progressive ataxias. *Orphanet J Rare Dis* 14:51. <https://doi.org/10.1186/s13023-019-1013-9>
  52. Milne SC, Corben LA, Georgiou-Karistianis N et al (2017) Rehabilitation for individuals with genetic degenerative ataxia: a systematic review. *Neurorehabil Neural Repair* 31:609–622. <https://doi.org/10.1177/1545968317712469>
  53. Benussi A, Dell'Era V, Cantoni V et al (2018) Cerebello-spinal tDCS in ataxia: a randomized, double-blind, sham-controlled, crossover trial. *Neurology* 91:e1090–e1101. <https://doi.org/10.1212/WNL.0000000000006210>
  54. Friedrich J, Kordasiewicz HB, O'Callaghan B et al (2018) Antisense oligonucleotide-mediated ataxin-1 reduction prolongs survival in SCA1 mice and reveals disease-associated transcriptome profiles. *JCI Insight*. <https://doi.org/10.1172/jci.insight.123193>

55. Scoles DR, Meera P, Schneider MD et al (2017) Antisense oligonucleotide therapy for spinocerebellar ataxia type 2. *Nature* 544:362–366. <https://doi.org/10.1038/nature22044>
56. McLoughlin HS, Moore LR, Chopra R et al (2018) Oligonucleotide therapy mitigates disease in spinocerebellar ataxia type 3 mice. *Ann Neurol* 84:64–77. <https://doi.org/10.1002/ana.25264>
57. Niu C, Prakash TP, Kim A et al (2018) Antisense oligonucleotides targeting mutant Ataxin-7 restore visual function in a mouse model of spinocerebellar ataxia type 7. *Sci Transl Med*. <https://doi.org/10.1126/scitranslmed.aap8677>
58. Matsuzono K, Imamura K, Murakami N et al (2017) Antisense oligonucleotides reduce RNA foci in spinocerebellar ataxia 36 patient iPSCs. *Mol Ther Nucleic Acids* 8:211–219. <https://doi.org/10.1016/j.omtn.2017.06.017>
59. Prudencio M, Garcia-Moreno H, Jansen-West KR et al (2020) Toward allele-specific targeting therapy and pharmacodynamic marker for spinocerebellar ataxia type 3. *Sci Transl Med*. <https://doi.org/10.1126/scitranslmed.abb7086>
60. Mitoma H, Manto M, Gandini J (2019) Recent advances in the treatment of cerebellar disorders. *Brain Sci*. <https://doi.org/10.3390/brainsci10010011>
61. Vázquez-Mojena Y, León-Arcia K, González-Zaldivar Y et al (2021) Gene therapy for polyglutamine spinocerebellar ataxias: advances, challenges, and perspectives. *Mov Disord Off J Mov Disord Soc* 36:2731–2744. <https://doi.org/10.1002/mds.28819>
62. Lynch DR, Johnson J (2021) Omaveloxolone: potential new agent for Friedreich ataxia. *Neurodegener Dis Manag* 11:91–98. <https://doi.org/10.2217/nmt-2020-0057>
63. Ghanekar SD, Kuo S-H, Staffetti JS, Zesiewicz TA (2022) Current and emerging treatment modalities for spinocerebellar ataxias. *Expert Rev Neurother* 22:101–114. <https://doi.org/10.1080/14737175.2022.2029703>
64. Piguet F, de Montigny C, Vaucamps N et al (2018) Rapid and complete reversal of sensory ataxia by gene therapy in a novel model of Friedreich ataxia. *Mol Ther* 26:1940–1952. <https://doi.org/10.1016/j.ymthe.2018.05.006>
65. Rocca CJ, Rainaldi JN, Sharma J et al (2020) CRISPR-Cas9 gene editing of hematopoietic stem cells from patients with Friedreich's ataxia. *Mol Ther Methods Clin Dev* 17:1026–1036. <https://doi.org/10.1016/j.omtm.2020.04.018>
66. Goizet C, Lesca G, Dürr A (2002) Presymptomatic testing in Huntington's disease and autosomal dominant cerebellar ataxias. *Neurology* 59:1330–1336. <https://doi.org/10.1212/01.wnl.0000032255.75650.c2>

Springer Nature or its licensor holds exclusive rights to this article under a publishing agreement with the author(s) or other rightsholder(s); author self-archiving of the accepted manuscript version of this article is solely governed by the terms of such publishing agreement and applicable law.

## Chapter 2 – Spinocerebellar ataxias

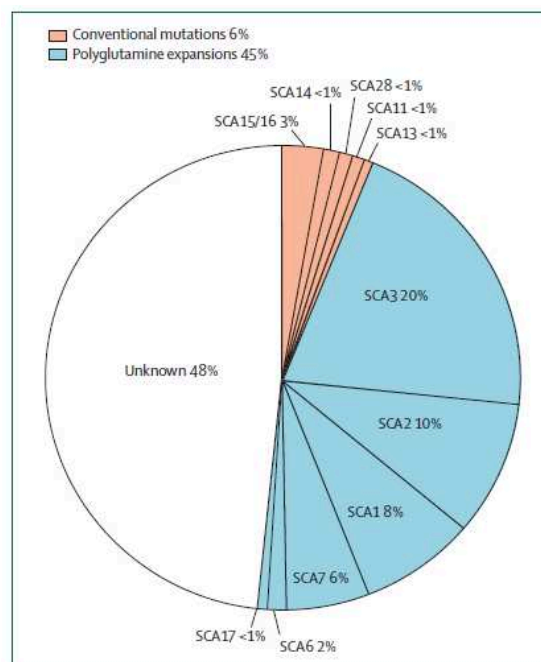
In this chapter, I will discuss in details the autosomal dominant cerebellar ataxias, the subject of my PhD thesis. Spinocerebellar ataxias (SCAs) are rare autosomal dominant neurodegenerative disorders, characterized by high heterogeneity regarding both their clinical manifestations and genetic background.<sup>9,13</sup> Onset usually occurs in mid-life, but childhood or older age onset have also been reported. SCAs are classified into three groups, based on the mutational mechanism: polyglutamine expansions (Figure 1), non-coding expansions (Figure 1), and conventional mutations including large rearrangements. To date, 49 SCA have received an official number. However, this classification is suboptimal for several reasons: for some loci, causative genes have not yet been identified (e.g., 16q22 for SCA4 or 7q31 for SCA18); some loci are duplicated (e.g., *ITPR1*, 3p26 for SCA15/16/29); some genes implicated in SCAs are not registered (e.g., *NPTX1*, *SLC1A3*); some loci or genes are not identified or confirmed (e.g., SCA9).



**Figure 1. Autosomal dominant cerebellar ataxias caused by repeat expansions.**

Repeat expansions can be located in coding or noncoding regions. In this figure, it is reported the disorder and the corresponding gene, repeat motif, and threshold size for pathological expansions. UTR: untranslated region.

SCAs lead to disability, significantly impacting the quality of life of patients and caregivers, especially for polyQ ones. Accounting for ~50% of SCAs worldwide, with varying prevalence depending on the country<sup>9,13,14</sup> (Figure 2), polyQ SCAs have been among the first SCAs subtypes to be investigated, and genes responsible for polyQ SCA were the earliest to be identified. Throughout the years, multiple studies have indeed greatly enhanced our knowledge of different aspects of polyQ SCAs, such as their pathophysiology, natural history, biomarkers identification, and potential treatments. This was possible thanks to the many international initiatives, such as SPATAX: Clinical and Genetic Analysis of Cerebellar Ataxias and Spastic Paraplegias (NCT00140829), EUROSCA: Study to determine and compare the rate of disease progression in SCA1, SCA2, SCA3 and SCA6 (NCT02440763), RISCA: Prospective Study of Individuals at Risk for SCA1, SCA2, SCA3, SCA6, SCA7 (NCT01037777), ESMI: European Spinocerebellar Ataxia type 3/Machado Joseph Disease Initiative, BIG-PRO: Biomarkers and Genetic Modifiers in a Study of Pre-ataxic and Ataxic SCA3/MJD Carriers (NCT04419974, NCT04229823), CRC-SCA (Clinical Research Consortium for Spinocerebellar Ataxias): Natural History Study and Genetic Modifiers in Spinocerebellar Ataxias (SCA) (NCT01060371), and READISCA: Clinical Trial Readiness for SCA1 and SCA3 (NCT03487367), with the involvement of more than 2000 patients with many thousand visits and follow-up.



**Figure 2. Relative prevalence of SCAs based on SPATAX cohort, after Durr A., Lancet Neurol. 2010.<sup>13</sup>**

Despite great advances in characterizing SCAs clinical manifestations and their genetic underpinnings, much still needs to be done to identify effective therapeutic strategies. Even though over the years a few randomized clinical trials have been conducted,<sup>15,16</sup> adequate curative therapies are currently still missing and clinicians dispose only of treatments aimed at alleviating symptoms combined with supportive treatments such as physical, speech, and occupational therapies. Encouraging results of RNA-targeting therapies for polyQ SCAs have been reported in several mouse models.<sup>17-20</sup> These approaches, among which the most advanced are the administration of antisense oligonucleotides (ASOs), aim to downregulate levels of the pathological polyQ protein. In this context, it is important to highlight that SCAs monogenic inheritance makes these diseases the perfect candidates for the development of gene therapies. Despite that, the heterozygous presence of the repeat expansion and the normal allele with a polymorphic repeat further complicates the strategy to decrease the mutant protein.

The clinical differences between polyQ and non-polyQ SCA subtypes, the recent advances in new genes identification, and the potential treatments have been widely discussed in the review “Autosomal dominant cerebellar ataxias: new genes and progress towards treatments” submitted to *Lancet Neurology* in September 2022.

*Review submitted in September 2022 to Lancet Neurology (following a request by the editorial board)*

**Autosomal dominant cerebellar ataxias: new genes and progress towards treatments**

Giulia Coarelli, MD,<sup>1</sup> Marie Coutelier, MD, PhD,<sup>1</sup> Alexandra Durr, MD, PhD<sup>1</sup>

<sup>1</sup>Sorbonne Université, Paris Brain Institute (ICM Institut du Cerveau), INSERM, CNRS, Assistance Publique-Hôpitaux de Paris, Pitié-Salpêtrière University Hospital, Paris, France

**Corresponding author:** Pr Alexandra Durr, Paris Brain Institute, Pitié-Salpêtrière Paris CS21414, 75646 PARIS Cedex 13, France, alexandra.durr@icm-institute.org, tel. +33 1 57 27 46 82, fax +33 1 57 27 47 26.

Character count for the title: 80

Total word count of the manuscript: 4648

Total word count of the abstract: 150

Total number of figures and tables: 4; Number of figures: 3; Number of tables: 1

Number of supplemental tables: 1

Panels: 2

## Abstract

The phenotype of dominantly inherited spinocerebellar ataxias (SCAs) varies from pure cerebellar to multisystemic involvement. To prepare precision medicine and intervention at preataxic stages in heterozygous carriers of pathogenic variants in SCA genes, genetic diagnosis is required but still unequally available. Bioinformatics advances regarding next generation exome and genome sequencing have allowed to identify new genes, such as *NPTX1*, *PNPT1/SCA25*, *DABI/SCA37*, *STUB1/SCA48*, *SAM9DL/SCA49*. Digenic inheritance for *STUB1/SCA48* and intermediate polyglutamine expansion in *TBP/SCA17* allowed to explain the more severe phenotypes in carriers of both heterozygous mutations. Given that extreme genetic heterogeneity, exome sequencing should become the diagnostic tool of choice. Treatments tested in Phase II-III studies such as riluzole and cerebellospinal transcranial direct current stimulation have given disputed results. Neurofilament light chain and brain MRI are reliable biomarkers to distinguish preataxic from manifest patients. The development of ataxin-specific bioassays might facilitate monitoring of the effects of treatment in upcoming trials.

**Search strategy and selection criteria:** We searched PubMed for English-language articles between 2017 and August, 2022, although well-known and seminal older articles were also considered. The search terms “spinocerebellar ataxia”, “SCA”, “polyglutamine diseases”, “SCA and biomarkers”, “SCA and gene therapy”, “SCA and treatment”, and all individual SCA genes were used. The final reference list was generated based on the relevance to the topics covered in this Review. Additionally, we searched the ClinicalTrials.gov registry using “spinocerebellar ataxia” and “SCA”.



## Introduction

Cerebellar ataxias transmitted as a dominant trait are a group of rare neurological diseases with a wide clinical and genetic heterogeneity, presenting with various neurological or non-neurological signs besides cerebellar ataxia. There are 39 genes for 43 spinocerebellar ataxias (SCAs) loci registered in the Online Mendelian Inheritance of Men (OMIM) database to date. At the same time, dominant causative SCA variants have been described in other genes but not yet registered as SCA.<sup>1</sup> The prevalence of each subtype is not well defined since the access to the detection of the different underlying causal repeat expansions and/or pathogenic variants is limited in many countries. A systematic review reported a global SCA prevalence average of 2.7/100,000 individuals but does not rely on a comprehensive screening method.<sup>2</sup> The most frequent SCA subtypes are caused by heterozygous translated CAG repeat expansions encoding polyglutamine (PolyQ) stretches in the corresponding protein: *ATXN1/SCA1* (MIM 164400), *ATXN2/SCA2* (MIM 183090), *ATXN3/SCA3* (MIM 109150), *CACNA1A/SCA6* (MIM 183086), *ATXN7/SCA7* (MIM 164500), *TBP/SCA17* (MIM 607136), and *ATN/DRPLA* (MIM 125370). Among them, SCA3 is the most prevalent worldwide; founder expansions were described in the Portuguese population, in families of Portuguese-Azorean ancestry; in Japan, and in Germany.<sup>3</sup> For SCA2, founder effects are reported in the Holguin province of Cuba with a common Spanish ancestry, the French West Indies, and India.<sup>3</sup> SCA6 is the third most prevalent subtype, particularly represented in Japan, Taiwan, Australia, Germany, the United Kingdom, and the USA.<sup>3</sup> SCA1 is the most prevalent form in Poland, Russia, and South Africa. For SCA7, founder events are reported in Scandinavian countries, South Africa, and Mexico.<sup>3</sup> DRPLA and SCA17 are very rare, even though the former accounts for a significant percentage of Japanese, Spanish and Portuguese SCA families. Non-coding repeat expansions or conventional mutations are responsible for less than 6% of SCAs.<sup>3,4</sup> However, some subtypes are highly represented in specific countries, such as SCA10 in Central and South America,

SCA12 in India, or SCA31 and SCA36 in Japan.<sup>3</sup> In this review, we will discuss the clinical differences between polyQ and non-polyQ SCA subtypes, the recent advances in new genes identification and resulting diagnostic tools, the potential treatments, and the existence of diagnostic and prognostic biomarkers.

### **Clinical features of SCAs**

- **Age at onset and genetic modifiers of polyglutamine SCAs**

The common clinical feature of SCAs is cerebellar ataxia expressed as lack of coordination, gait imbalance, clumsy voluntary limbs movements, dysarthria, dysphagia, and oculomotor abnormalities. Other neurological and extra-neurological signs can occur depending on the subtype. Disease onset is typically in the third or fourth decades in polyQ SCAs. Age at onset is determined by CAG repeat size and can be estimated based on CAG repeat length.<sup>5</sup> An interaction also exists between normal and expanded alleles in *trans* for *ATXN1*, *CACNA1A*, and *ATXN7*. A polygenic effect from allele sizes of the other SCA genes has furthermore been described in a large cohort of 1255 patients (SCA1, 2, 3, 6, and 7).<sup>6</sup> Other (CAG)<sub>n</sub>-containing genes influence the age at onset: *ATXN7* in SCA2; *ATXN2*, *ATN1* and *HTT* in SCA3; *ATXN1* and *ATXN3* in SCA6; and *ATXN3* and *TBP* in SCA7.<sup>6</sup> Anticipation is a hallmark phenomenon of polyQ subtypes: younger ages at onset and more severe phenotypes are found in successive generations. This is due to the instability of CAG repeat expansions in germline cell division, which also explains the stronger association of paternal inheritance with infantile forms.<sup>7</sup> Infantile and juvenile forms have been reported for very large CAG repeats in SCA2 and SCA7 (130 to more than 200 CAG repeats, versus usual pathogenic threshold sizes of 32 and 37, respectively).<sup>7,8</sup> In SCA7, congenital phenotypes are paternally transmitted and include cardiac and renal impairment, leading to death at age 0.4-2.3 years; while juvenile forms are from maternal descent in up to 40% of cases, do not show extraneurological involvement, and

initially present with isolated visual loss in 80 % of patients.<sup>7</sup> Finally, interruptions in CAG repeats also modify the age at onset. CAT codons in *ATXN1* delays the disease onset compared to uninterrupted CAG repeats.<sup>9</sup> CAA interruptions in *ATXN2* CAG tracks switch the classical phenotype of cerebellar ataxia to autosomal dominant parkinsonism.<sup>10</sup>

- **The severity of polyglutamine SCAs**

The severity of the polyQ SCAs phenotype also correlates with the CAG repeat size.<sup>4</sup> These subtypes have been better characterized than non-polyQ SCAs, as their natural history has been explored by different consortia. The EUROSCA study provided quantitative data on clinical progression for SCA1, 2, 3, and 6, based on the Scale for the Assessment and Rating of Ataxia (SARA) score.<sup>11</sup> It increased more rapidly for SCA1 (2.11 point per year), followed by SCA3, SCA2, and SCA6 (1.56, 1.49, and 0.8, respectively).<sup>11</sup> This study also established the 10-year survival rate at 57% for SCA1, 74% for SCA2, 73% for SCA3, and 87% for SCA6.<sup>12</sup> The predictors for shorter survival were dysphagia and higher SARA score for SCA1, CAG repeat length, higher SARA score, and older age at inclusion for SCA2 as well as for SCA3, together with dystonia.<sup>12</sup> Severe bulbar dysfunction due to motor neuron degeneration, in particular in hypoglossal nucleus, has been reported in SCA1 mice, which is in line with dysphagia as a predictor of poor SCA1 survival.<sup>13</sup> A French cohort<sup>14</sup> and the Clinical Research Consortium for Spinocerebellar Ataxias of North America<sup>15</sup> also confirmed SCA1 as the most severe SCA subtype.

The EUROSCA study also explored the patients' quality of life with the Unified Huntington's Disease Rating Scale (UHDRS-IV), assessing their functional capacity in daily life; the visual analogue scale of the EuroQol Five Dimensions Questionnaire (EQ-5D VAS) for health-related quality of life; and the Patient Health Questionnaire (PHQ-9) for depressive symptoms. The decline of functional outcome was linked to higher INAS count for SCA3, and higher SARA

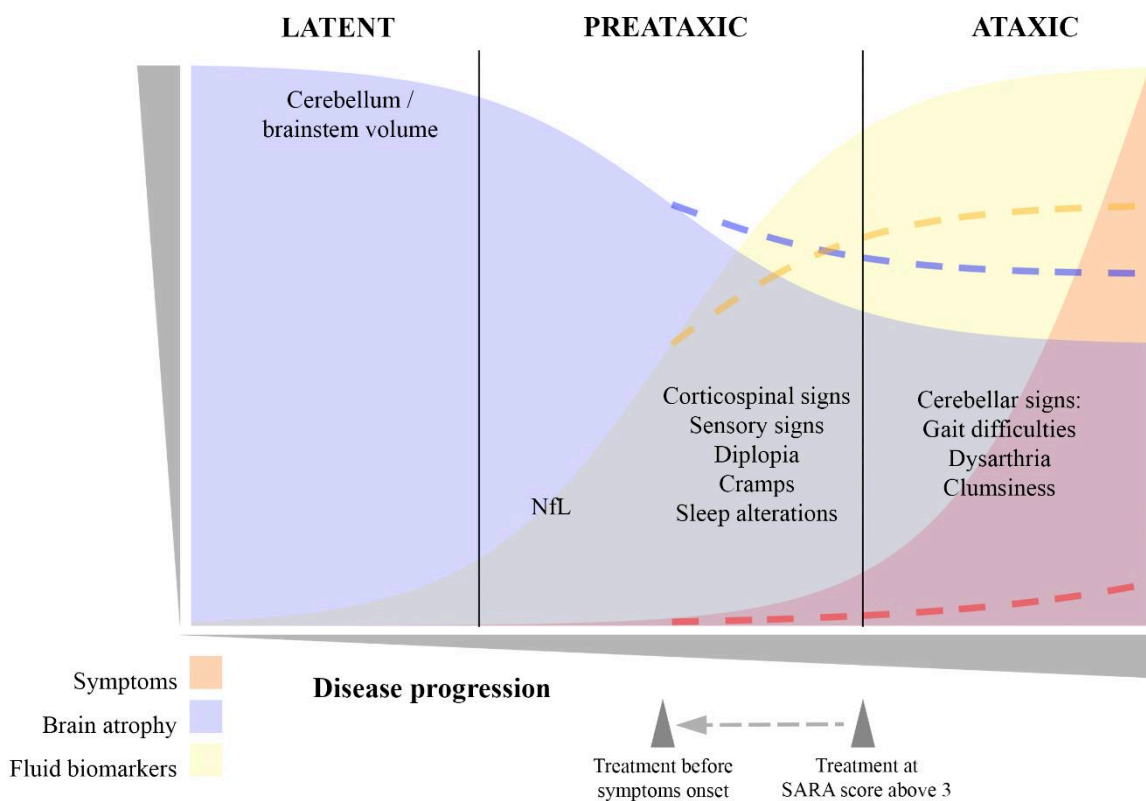
score, cognitive impairment, and longer CAG expansion for SCA1. Depression was also more frequent in SCA1 patients with cognitive impairment.<sup>11</sup> We can extrapolate that the quality of life is not primarily impacted by cerebellar ataxia but by other neurologic signs and mood disorders. In a cohort of mild SCA3 patients, the quality of life was determined by fatigue level rather than ataxia severity, and depression was correlated with disease duration and fatigue more than motor impairment,<sup>16</sup> outlining the discrepancy between clinicians' and patients' point of view. Depression and fatigue symptoms should hence be taken into consideration in clinical trial outcome measures. In the cohort from American continents and the Caribbean regions (PAHAN consortium), a questionnaire for health professionals showed that lower socio-economic status was associated with poorer management of the disease, from diagnosis to rehabilitation care.<sup>17</sup>

We can take advantage of preataxic carriers of pathogenic CAG repeats to investigate the changes in the latent and preataxic phase of the diseases (Figure 1). The RISCA study showed that the SARA score and the grey-matter loss of brainstem and cerebellum progressed faster in SCA1, 2, 3, and 6 preataxic carriers closer to ataxia phenotype conversion.<sup>18</sup> READISCA, an ongoing NIH-funded international clinical trial readiness study for SCA1 and SCA3, aims at exploring both preataxic and manifest or ataxic patients to identify reliable biomarkers as readouts in clinical trials.

- **Clinical differences between polyglutamine SCAs and non-polyQ SCAs**

SCAs due to conventional mutations or rearrangements (*SPTBN2/SCA5*, *TTBK2/SCA11*, *KCNC3/SCA13*, *PRKCG/SCA14*, *ITPR1/SCA15/16/29*, *KCND3/SCA19/22*, *TMEM240/SCA21*, *PDYN/SCA23*, *PNPT1/SCA25*, *EEF2/SCA26*, *FGF14/SCA27*, *AFG3L2/28*, *ELOVL4/SCA34*, *TGM6/SCA35*, *ELOVL5/SCA38*, *CCDC88C/SCA40*, *TRPC3/SCA41*, *CACNA1G/42*, *MME/SCA43*, *GRM1/SCA44*, *FAT2/SCA45*, *PLD3/SCA46*,

*PUM1/SCA47*, *STUB1/SCA48*, *SAM9DL/SCA49*) and noncoding repeat expansions (*ATXN8OS/SCA8*, *ATXN10/SCA10*, *PPP2R2B/SCA12*, *SCA31*, *NOP56/36*, and *DABI/SCA37*) are not as well described, as their rarity makes it difficult to gather data from large cohorts.



**Figure 1. Schematics representation of disease stages in polyglutamine SCAs.**

The natural history of polyglutamine SCAs can be divided into three main phases: the latent phase, where no signs or symptoms are present; the pre ataxic phase, where clinical signs and symptoms unrelated to ataxia can be detected; then the ataxic phase, with clear cerebellar manifestations (red shaded area). Two types of biomarkers are altered earlier on. The biological biomarkers, such as NfL, show early increase and can be detected before the onset of symptoms (yellow). Brain imaging can also show early alterations, with a decrease in cerebellum and brainstem volume (blue). These two elements could be taken into account to determine the best timepoint for a potential treatment (blue arrow). The administration before the onset of symptoms could allow to limit or avoid their occurrence and lessen the brain atrophy (projections in dashed lines).

For this reason, in 2020, we launched an international multicenter cross-sectional study to collect clinical and genetic data for non-expansion spinocerebellar ataxias. Results show that the clinical presentations are even more heterogeneous among one gene. Even though non-polyQ SCAs can occur early in childhood, they are less severe and have a slower progression

than polyQ SCAs (Cunha P, in preparation). Pediatric forms, which are exceptional in polyQs SCAs, have been described for the same pathogenic variant as late onset ones. For example, *SPTBN2/SCA5* and *TMEM240/SCA21* can manifest with congenital onset mimicking cerebral palsy<sup>19,20</sup> or with adult-onset ataxia.<sup>21</sup> Intellectual deficiency is often associated with cerebellar ataxia, suggesting that non-polyQ SCAs are rather developmental than neurodegenerative disorders. Other abnormal non-ataxic movements are frequently associated, such as tremor for *PPP2R2B/SCA12*,<sup>22</sup> dystonia and myoclonus for *PRKCG/SCA14*<sup>23</sup> and *KCND3/SCA19*.<sup>24</sup> *STUB1/SCA48* is specifically associated with predominant cognitive impairment.<sup>25</sup> Conventional mutations in *CACNA1A* are frequent and present with a large phenotype spectrum, associating familial hemiplegic migraine, episodic ataxia type 2, and progressive ataxia.<sup>26</sup> Developmental delay, autism, epilepsy, migraine, and paroxysmal tonic upward gaze are also often reported, while the ataxic signs can be episodic then progressive, or immediately progressive, with either congenital or adult-onset.<sup>27</sup>

### **Cerebellar Cognitive Affective/Schmahmann Syndrome – Panel 1**

The implication of cerebellum in cognition was proposed over the last few decades and conceptualized under the “dysmetria of thoughts” hypothesis.<sup>28</sup> Cerebellar lesions due to vascular, traumatic, infectious, neoplastic, or degenerative processes result in behavioral changes, obsessive ideas, lack of empathy, difficulties in emotional recognition, dysphoria, and depression.<sup>28</sup> Advances in neuropsychology led to describe the Cerebellar Cognitive Affective/Schmahmann Syndrome, then to define a validated scale to assess it,<sup>29</sup> later translated in several languages. This scale covers the fields impacted in CCAS: executive functions, visuospatial cognition, language, and emotion-affect. The first three are linked to the connectivity of the posterior lobe, including the medial and hemispheric regions of lobule VIIA Crus I/II, HVI and HVIIIB, with the prefrontal, parietal, and frontotemporal cortical areas respectively. Lesions in the “limbic cerebellum” (vermis and fastigial nucleus) cause the social

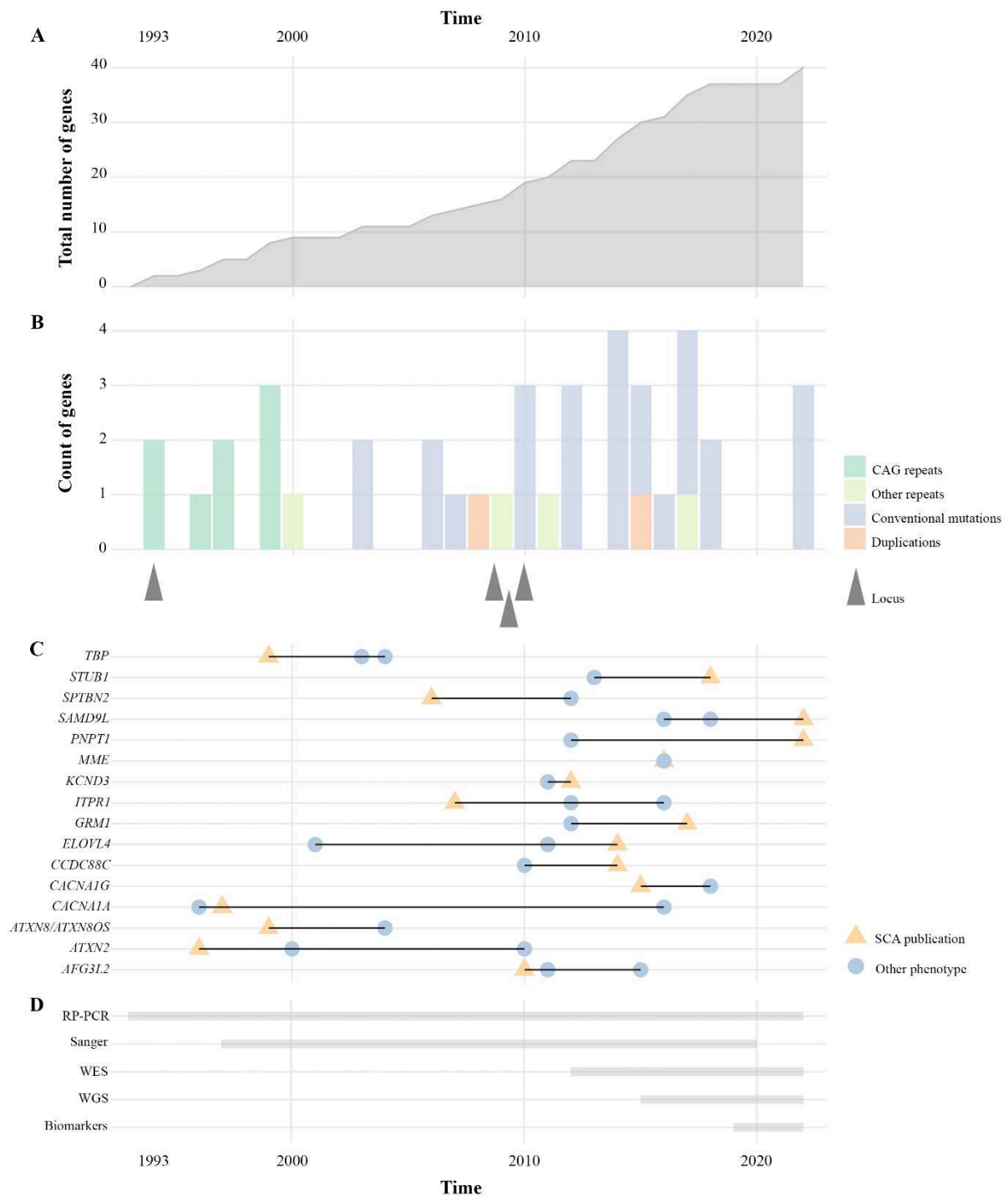
and emotional disturbances. In a cohort of 20 SCA3 patients, CCAS scale detected cognitive impairment at a mild or moderate disease stage.<sup>30</sup> CCAS score correlated with disease duration, SARA score, dominant hand 9 hole-peg test, and walking speed.<sup>30</sup> SCA3 carriers showed a significantly lower CCAS score compared to controls, which was not the case for SCA6, and Friedreich ataxia patients.<sup>31</sup> The word fluency test was the most appropriate to distinguish carriers from controls.<sup>31</sup> Language impairment has also been described in SCA36/*NOP56*, with decreased phonological verbal fluency in preataxic carriers, and impaired semantic fluency in symptomatic patients.<sup>32</sup> For 64 SCA2 patients, CCAS score was influenced by the level of education and ataxia severity.<sup>33</sup> The CCAS scale could detect mild cognitive impairments unnoticed by the Montreal Cognitive Assessment (MoCA) test, showing higher sensitivity.<sup>33</sup> Cognitive alterations are a hallmark for SCA48/*STUB1*, where cognition and emotion are altered early on, and focal atrophy of vermis, lobule V and VI are detected in the preataxic phase.<sup>34</sup>

These neurobehavioral alterations affect the quality of life of the patients and caregivers and should be considered in the patients' clinical management as well as in future clinical trials.

### **Diagnostic next-generation sequencing – Panel 2**

Given the profusion of genes implicated in SCAs and the lack of clear-cut genotype-phenotype correlations in most instances, the classical approach of testing candidate genes sequentially has proven limited efficiency (Figure 2). Molecular diagnosis is often limited to the most frequent polyQ SCAs and performed with targeted fragment analysis.<sup>4</sup> Panel-based approaches have been developed in several teams but are rapidly proving incomplete upon description of additional genes.<sup>26</sup> Whole exome sequencing (WES) is hence becoming a second-line diagnostic tool of choice, given that its lowering price makes it increasingly accessible and it allows post-hoc reexamination of data upon description of novel genes.<sup>35</sup> However, it is still hindered by its design, intrinsically limited to coding regions hence not detecting non-coding

mutations, while deep intronic variants have been shown to be causative, for example, in *SPG7*.<sup>36</sup>



**Figure 2. Evolution of SCAs mutational landscape, associated phenotypes, and diagnostic means.**

**A.** Cumulative number of genes and structural variants implicated in SCAs from 1993 to 2022. **B.** Repartition of the mutational types described in SCAs. CAG repeats were all reported before 2000, while the age of conventional mutations came later and flourished with the advent of exome sequencing. Non-CAG repeats are less frequent and described throughout the years. The locus mapped to dominant ataxia for which the causative genetic event could not be identified are represented separately by blue triangles. **C.** Phenotypic variability reported for SCA genes, based on the OMIM database. Yellow triangles represent the time of the gene implication in the dominant ataxia



phenotype, blue circles the description of divergent phenotypes, from extreme forms of the disease to completely unrelated affections. **D.** Schematic representation of the means of diagnosis available for SCAs. Repeat-primed PCR (RP-PCR) was and still is a major initial first step. Sequential Sanger sequencing for conventional mutations developed progressively, to be replaced by next-generation sequencing approaches. Nowadays, whole exome sequencing is the technique of choice in clinics, while the importance of whole genome sequencing is raising but is still limited for cost reasons. The development of algorithms to genotype repeats from next-generation sequencing data could see the end of RP-PCR.

Short-read sequencing is also not the technique of choice to identify repeat expansions, which can hardly be mapped to the reference sequence. In these regards, whole genome sequencing could be an effective alternative to WES, allowing altogether the identification of non-coding variants, of large structural changes,<sup>37</sup> and of expanded repeat tracks, thanks to a specifically designed tool, Expansion Hunter.<sup>38</sup> Recent results suggest that the latter can also be used on WES data to identify coding repeat expansions; WES could thus constitute a good compromise between time, cost, and expected results yield in clinical practice.

### **New SCA genes**

Over the past five years, several SCA genes have been identified (Figure 2). An intronic expansion in *DABI*, comprising a pathological AT TTC pentanucleotide repeat (range 31-75 repeats) flanked by AT TTT repeats ((AT TTT)<sub>60-79</sub>(AT TTC)<sub>31-75</sub>(AT TTT)<sub>58-90</sub>), is responsible for SCA37, clinically presenting as ataxia with predominantly vertical abnormal eye movements. A negative correlation seems to exist between the age at onset and the AT TTC repeat size.<sup>39</sup>

*PUM1/SCA47* is caused by lowered PUM1 protein levels, with a variable degree of disease severity depending on dosage deficiency. Patients present with a developmental syndrome, Pumilio1-Associated Developmental Disability, Ataxia and Seizure (PADDAS) upon a 50% reduction of protein levels, or a late onset ataxia with incomplete penetrance for a 25% decrease.<sup>40</sup>

The SCA25 locus, on chromosome 2p, was identified in 2004, by a linkage study based on 18 individuals from a large French family with cerebellar ataxia and sensory neuropathy. The causative variant, resulting in exon skipping in *PNPT1*, was only recently identified. Two other French or Australian families carried either another splice or nonsense variants.<sup>41</sup>

*STUB1* was already implicated in the autosomal recessive ataxia subtype SCAR16. In 2018, in six patients from a pedigree with a late-onset ataxia and CCAS, exome sequencing identified a heterozygous frameshift *STUB1* variant (p.Leu275Aspfs\*16).<sup>34</sup> The gene has subsequently been confirmed as responsible for dominant adult ataxia with cognitive impairment, sometimes in families with phenotypes reminiscent of Huntington's disease or frontotemporal dementia.<sup>25,42</sup> The sex ratio of *STUB1* patients is biased towards women, suggesting incomplete penetrance in men. This could possibly be due to lower *STUB1* expression in the central nervous system in women, making them more sensitive to haploinsufficiency.<sup>25</sup> Neuropathological studies found severe depletion of Purkinje cells, predominant in the vermis over the cerebellum hemispheres, without atrophy of the brainstem, hippocampus or cerebral cortex<sup>25</sup>. These data corroborate the implication of cerebellum in cognition (see Panel 1).

The last registered SCA subtype, SCA49, is caused by heterozygous variants in *SAMD9L*, previously involved in the dominant ataxia-pancytopenia and MIRAGE syndromes (Myelodysplasia, Infection, Restriction of growth, Adrenal hypoplasia, Genital problems, and Enteropathy). It was described in a Spanish family with nine affected subjects, cerebellar ataxia, dysarthria, gaze-evoked nystagmus, pyramidal syndrome, and axonal sensory polyneuropathy. Ataxia onset ranged from 30 to 60 years, but hyperreflexia, nystagmus or brain MRI white matter changes occurred earlier.<sup>43</sup> Mutations in this gene are also linked to myeloid malignancies and bone marrow failure that may be treated by hematopoietic cell transplantation,<sup>44</sup> hence the importance to identify them. Of note, given the acquired monosomy in hematopoietic cells, genetic tests should be performed on skin fibroblast.

Recently, *NPTX1* was identified to be causal of dominant cerebellar ataxia, through either dominant negative or haploinsufficiency phenotypes, leading to endoplasmic reticulum stress (Coutelier 2022).<sup>45</sup> The *NPTX1*-linked spectrum was later on extended to infantile cerebellar ataxia with secondary generalized epilepsy,<sup>35</sup> underlining the overlap between adult and childhood onset ataxic diseases.

### **Digenic inheritance and intermediate alleles as genetic modifiers**

It is not uncommon to detect two plausible variants in known SCA genes. In some cases, this may explain atypical presentations with either a more severe course or unusual signs. The concept of “two hits”, known in oncology, has also been proposed in neurology. For example, in a French *STUB1*/SCA48 cohort of 50 patients, exome sequencing and gene panels detected additional variants in *AFG3L2*/SCA28, *PRKCG*/SCA14, and *TBP*/SCA17.<sup>25</sup> The phenotype of a patient with *AFG3L2* p.Ala484Pro variant was not presenting the typical SCA28 ophthalmoplegia, but the gene implication cannot be excluded. The *PRKCG* variant was classified as Variant of Unknown Significance. Typical pathogenic *TBP* alleles of  $\geq 49$  CAG/CAA are fully penetrant, while intermediate alleles ranging from 41 to 48 CAG/CAA have incomplete penetrance, with about 50% of carriers still healthy at 50<sup>46</sup>. One patient carried both a *STUB1* variant and 46 CAG/CAA repeats in *TBP*, suggesting that this intermediate expansion could play a pathological role.<sup>25</sup> The relationship between *TBP* and *STUB1* was further studied in an Italian cohort: in 31 families with an intermediate *TBP*<sub>41-46</sub> allele and a SCA17/HD-like phenotype, 30 carried a pathogenic *STUB1* variant.<sup>47</sup> In a German family, the synergetic effect of two *TBP* intermediate alleles was suggested, based on a more severe phenotype.<sup>48</sup> Heterozygosity for an intermediate *TBP* allele of >39 CAG repeats was associated with higher cognitive impairment in half of 34 families with *STUB1*/SCA48 (Barbier 2022, in press). *TBP* intermediate alleles seem to have more general involvement in neurodegeneration, since alleles of 41 CAG/CAA repeats were found in four MSA index cases out of a cohort of

28.<sup>49</sup> In a Taiwanese cohort of 325 ALS patients and 1500 healthy controls, one ALS patient carried an intermediate *TBP* allele of 44 repeats and another one a *TBP* allele of 46 repeats together with a pathological expansion in *C9ORF72*. This could suggest that intermediate *TBP* allele  $\geq 44$  CAG/CAA repeats may represent a risk factor for ALS with an odds ratio of 23.2.<sup>50</sup>

Intermediate *ATXN2/SCA2* alleles (27-32 repeats) are known to be a risk factor or a modifier for ALS since *ATXN2* protein increases the toxicity of TDP-43 in *Drosophila* and human cells.<sup>51</sup> Almost 5% of sporadic and familial ALS patients carried an intermediate *ATXN2* polyQ allele ranging from 27 to 33 repeats. This was validated in other series and in an Italian cohort; survival was inversely correlated to repeat length with shorter survival in patients carrying more than 31 repeats.<sup>52</sup> In a recent study on more than 9000 DNA sample of patients suffering from ALS, ALS with frontotemporal dementia (FTD), FTD alone, Lewy body dementia, and healthy controls, the presence of *ATXN2* intermediate allele ( $\geq 31$  repeats) was confirmed to be a risk factor for ALS, ALS-FTD and FTD, with odds ratios of 6.3, 27.5 and 3.1, respectively.<sup>53</sup> However, the authors did not replicate the observation of earlier onset and shorter survival in ALS patients carrying the *ATXN2* intermediate allele.<sup>53</sup> For FTD, the role of *ATXN2* is not so well elucidated. An Italian cohort of FTD patients did not show higher frequency of intermediate *ATXN2* allele than controls.<sup>54</sup> However, if carried, the phenotype was more severe with earlier age at onset, parkinsonism, and psychotic symptoms at onset.<sup>54</sup> In a 70-year-old FTD patient, carrying 39 and 27 CAG *ATXN2* alleles, *post-mortem* analysis found TDP-43 positive cytoplasmic inclusions in the upper layers of the cortex while cerebellum examination was unremarkable without ubiquitin or p62 inclusion.<sup>55</sup> TDP43 inclusions have already been described in other polyQ diseases such as Huntington Disease, SCA3, and SCA7, suggesting that common pathological pathways are involved.<sup>55</sup> In TDP43 mice, administration of antisense oligonucleotides (ASOs) targeting *ATXN2* mRNA to the central nervous system increased the survival,<sup>56</sup> paving the way for therapeutic perspectives for ALS. A clinical trial (NCT04494256)

with an *ATXN2* ASO is ongoing for ALS patients with or without *ATXN2* expansion, based on results of Glass et al.<sup>53</sup>

Other PolyQ SCA genes might also be risk factors for ALS. In a study of 11700 subjects (ALS patients and controls), intermediate *ATXN1* allele (33-39 CAG/CAT repeats) were significantly associated with ALS.<sup>57</sup> As reported for *ATXN2*, *ATXN1* increases the mislocalization of TDP43 in *Drosophila* through a cytoplasmic gain of function. In addition, polyQ *ATXN1* aggravates the *Drosophila C9orf72* phenotype.<sup>57</sup> In another Italian cohort, intermediate *ATXN1* alleles were found in almost 20% of *C9orf72* patients, for both sporadic and familial cases.<sup>58</sup>

A recent study on more than 14000 DNA samples from five European population-based cohorts found a high prevalence of individuals carrying an intermediate (10.7%) or small pathological (1.3%) allele of one SCA gene, which must be considered for genetic counseling and for further research given their role as modifiers.<sup>46</sup> In fact, a modifying role has been described for intermediate alleles in *HTT/HD*, in breast cancer,<sup>59</sup> and in atypical Parkinson.<sup>60</sup>

## **Treatments**

- **Pharmacological treatments**

Because of the rarity and genetic complexity of SCAs, clinical trials are often conducted on cohorts mixing different genotypes. This may be appropriate for physical and/or speech training but is more questionable for mechanistically targeted approaches. There are so far no curative or neuroprotective treatments for SCAs approved by the Food and Drug Administrations (FDA) of the United States or by the European Medicines Agency (EMA). The widespread neurodegeneration documented by neuropathological studies in polyQ SCAs makes it difficult to target a specific brain region. In clinical practice, symptoms should be addressed using L-Dopa or dopamine agonists, baclofene and botulinum toxin injections for associated spasticity,

and treatments for urinary dysfunctions and neuropathic pain when needed. Antidepressants such as SSRIs are very useful to help decrease anxiety without increasing dizziness.

Some molecules have been tested but no benefits were seen (Table 1). For riluzole, used as disease-modifying therapy in ALS, results are controversial. A trial focused on hereditary ataxias, including 20 Friedreich ataxia patients and 40 patients with SCA1, 2, 6, 8, or 10, treated for 12 months, found an improvement of one SARA score point for the riluzole arm.<sup>61</sup> Because of the heterogeneity in genetic causes and disease stages in the cohort, we conducted a study in a clinically and genetically homogenous group of 45 SCA2 individuals.<sup>62</sup> This study did not show any clinical or radiological improvement after 12 months of treatment.<sup>62</sup> In addition, a prodrug of riluzole, the troriluzole, was administered in a phase III trial with 218 enrolled patients (SCA1, 2, 3, 6, 7, 8, and 10) (NCT03701399). After 48 weeks, no significant change between the two arms were found on the modified functional Scale for the Assessment and Rating of Ataxia (m-SARA) (<https://www.biohavenpharma.com/investors/news-events/press-releases/05-23-2022>).

The causal gene for SCA38, *ELOVL5*, codes for an elongase involved in very long-chain fatty acids synthesis, highly expressed in Purkinje cells. In a randomized, placebo-controlled study, the supplementation with 600 mg/day of docosahexaenoic acid (DHA), an omega-3 polyunsaturated fatty acid, for 16 weeks, followed by an open-label study until week 40, proved safe, improved gait and balance with a decrease of 2-points on the SARA score as well as cerebellar hypometabolism at week 40.<sup>63</sup> These positive results persisted after a 2-year follow-up.<sup>64</sup>

- **Non-pharmacological treatments**

Cerebellar transcranial direct current stimulation (tDCS) is a non-invasive treatment aiming at modulating the excitability of cerebellum connections. A two-weeks treatment improved SARA

score, ICARS score, 9-Hole Peg Test, and 8-m walking time compared to controls.<sup>65</sup> The treatment was extended for a group of 61 patients (five SCA1, 12 SCA2, one SCA14, one SCA28, five SCA38, 10 MSA type C, seven Friedreich's ataxia, 17 sporadic adult-onset ataxia and three individuals with CANVAS) randomized into two groups, with either cerebellar and spinal tDCS or placebo stimulation for two weeks. After 12-week follow-up, all patients underwent a second cycle of tDCS for two weeks, then were followed until week 52.<sup>66</sup> Significant improvement in clinical scores, CCAS scale, and quality of life were found.<sup>66</sup> Only one study focused on a defined genotype, SCA3, and found no evidence of SARA score improvement in twenty ataxic SCA3 individuals after two weeks of treatment and twelve months of follow-up.<sup>67</sup> The speech subscore, the PATA repetition task, and the INAS count however improved at six months, in particular for hyperreflexia, dystonia, and urinary symptoms.<sup>67</sup>

Speech therapy is strongly recommended for ataxia patients while only few studies systematically assessed it. Recently, intensive tailored biofeedback speech treatment for 20 days in 16 SCA1, 2, 3, and 6 patients reported intelligibility improvement.<sup>68</sup> Physical therapy has been investigated more, which demonstrated the improvement of ataxia symptoms. Intensive treatment, six hours per weekday for 24 weeks, led to significant decreases in SARA scores in SCA2.<sup>69</sup> Moderate (two hours three times per week) as well as intensive (two hours five times per week) training for 24 weeks improved SARA score in SCA7 patients.<sup>70</sup> To make treatment more financially and motivationally accessible, video games and home-based targeted training have been explored in children and adults with ataxia.<sup>71</sup>

- **Future therapeutic options**

Gene editing techniques such as zinc-finger nucleases, CRISPR/cas9, or transcription activator-like effector nucleases, seem to be far from being used in patients. One of the first feasibility

tests using CRISPR/Cas9 to correct the expanded CAG allele was reported in SCA3 induced pluripotent stem cells (iPSCs).<sup>72</sup> The expanded allele of 74 CAG was replaced by a normal allele of 17 CAG.<sup>72</sup> Several cellular abnormalities, such as polyQ aggregates, were improved, demonstrating the potential of this therapeutic strategy. Antisense oligonucleotides (ASOs) targeting the mRNA transcript are currently the most advanced therapeutic option. Promising results were obtained in SCA1, SCA2, SCA3, and SCA7 mice models<sup>73–76</sup> (Supplementary Table 1). ASOs therapies are already approved for other neurological diseases, such as spinal muscular atrophy, with remarkable results.<sup>77</sup> The first clinical trial with a non-allele-specific ASO for SCA3 patients started early 2022 (NCT05160558) (Table 1). However, the enthusiasm for ASOs in the ataxia community decreased somewhat after the discontinuation of the phase III study in Huntington Disease (NCT03761849), due to worsening of clinical rating scales and increase in neurofilament light chain (NfL) CSF level in patients who received higher doses, compared to low doses and placebo groups.<sup>78</sup> Tominersen, the ASOs used in this trial, was non-allele-selective and reduced both wild-type and mutant protein expression. This can be a challenge for huntingtin, a ubiquitous protein with several functions. The negative result might be linked to strong decrease of wild-type protein, weak delivery to target neurons, or inclusion of patients with advanced disease stage. Nevertheless, allele-specific ASO trials (NCT03225833, NCT03225846) were also stopped in Huntington disease, since the mHTT levels were not decreased as expected. Gene regulation and cellular functions of proteins involved in polyQ SCA are not fully elucidated, and we cannot predict the effects of a reduction of their expression, especially with a non-allele-selective ASO. For example, ataxin-1 protein reduction leads to a decrease of Capicua (CIC), a tumor suppressor protein, and an increased activity of protease  $\beta$ -secretase 1 (BACE1) implicated in the cleavage of amyloid precursor protein.<sup>79</sup> For these reasons, a safety assessment was conducted for a non-selective ASO in a SCA1 mouse model.<sup>80</sup> The authors concluded that ataxin-1 suppression did not impact *CIC* and

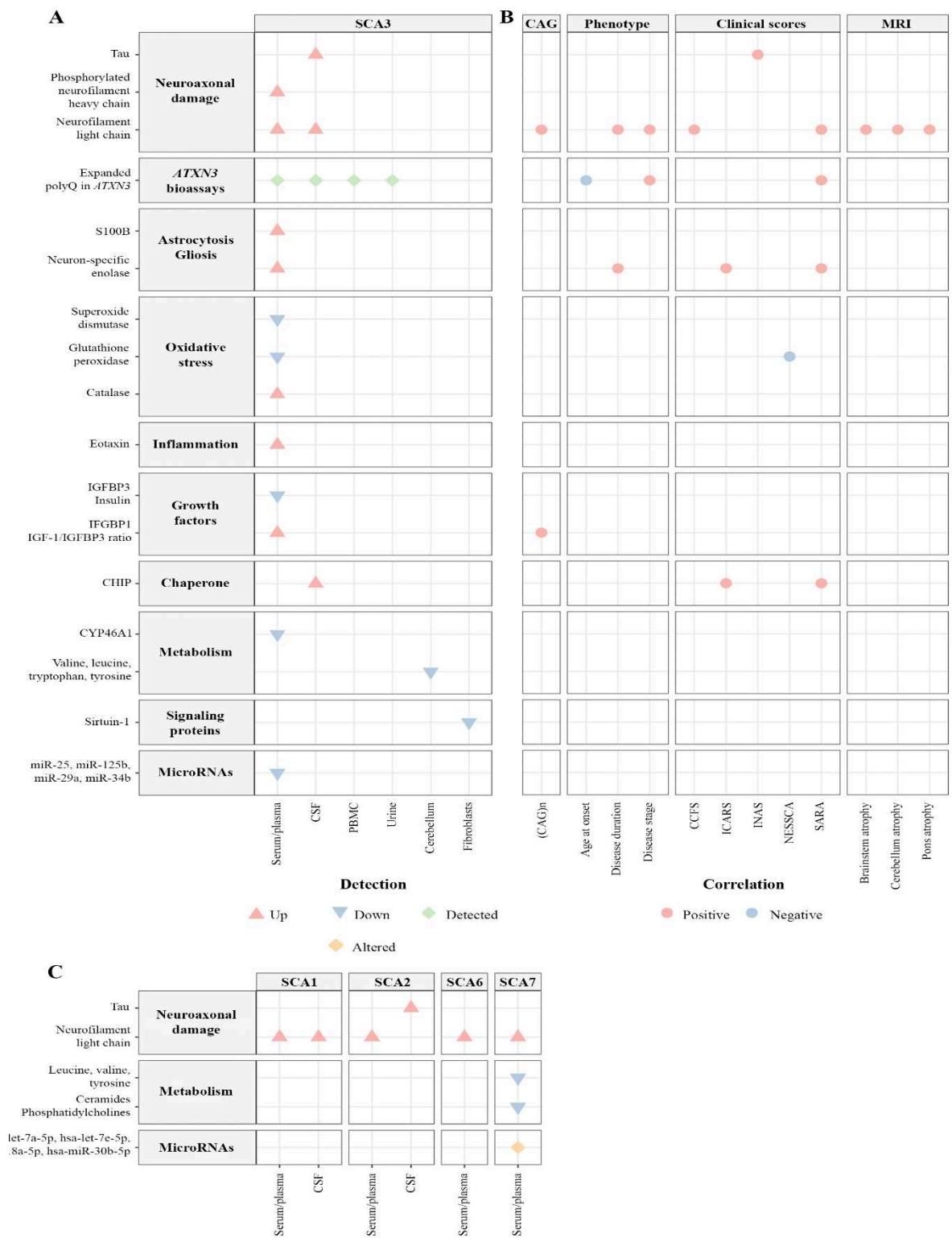


*BACE1* expression,<sup>80</sup> supporting the safety of this approach. PolyQ stretches are also present in several proteins, therefore ASO targeting polyQ repeats could trigger off-target mechanisms. Moreover, we still do not know the appropriate rate of pathogenic protein decrease we have to achieve. Reliable readouts to conduct clinical trials in a reasonable timeframe and not several years before having results.

## **Biomarkers**

Advancements in the therapeutic field render the need for reliable biomarkers even more compelling, to monitor treatment, detect patients with more rapid progression, distinguish healthy individuals from SCA carriers, and predict the conversion from pre-ataxic to manifest stages. Here, we detail some examples of biomarkers studied in SCAs (Figure 3). One of the most studied fluid biomarkers is the neurofilament light chain protein, NfL, a subunit of the neuronal cytoskeleton, whose levels increase in blood and CSF after axonal damage. NfL can be detected in blood with a strong correlation with its CSF levels. In polyQ SCAs, NfL levels have predictive, diagnostic, and prognostic values (Figure 3). As a predictive and diagnostic biomarker, it allows distinguishing carriers at presymptomatic and symptomatic stages, as well as from controls, with established cut-off levels.<sup>81,82</sup> Serum NfL already increases 7.5 and 5 years before the expected age at onset in SCA3 and SCA1 carriers, respectively.<sup>82,83</sup> Among polyQ SCAs, SCA3 carriers present the highest NfL levels, followed by SCA7, SCA1, and SCA2 carriers.<sup>81</sup> However, in a unique longitudinal study performed in polyQ SCAs, NfL levels did not change after two-year follow-up.<sup>81</sup> This may be due to the slow progression of the disease or because a plateau level was reached. As a prognostic biomarker, NfL levels correlate with disease severity in polyQ SCAs,<sup>81</sup> which has extensively been explored in SCA3,<sup>82,84,85</sup> and in SCA2.<sup>84</sup> Moreover, in polyQ SCAs, NfL predicts faster clinical and radiological progression: patients with higher NfL levels at baseline presented higher SARA scores and decreased cerebellum volume at 2-years follow-up.<sup>81</sup> For future clinical trials, these data could

help stratifying symptomatic carriers with faster progression and presymptomatic carriers approaching the phenoconversion.



**Figure 3. Schematic representation of fluid biomarkers and their correlation with clinical and radiological parameters.** At the top, fluid biomarkers explored in SCA3 and their correlations with CAG repeats, phenotype, clinical scores, and brain MRI. At the bottom, biomarkers for SCA1, SCA2, SCA6, and SCA7.

Ataxin-specific bioassays are of great interest and identifying these proteins in various biosamples could ease the follow-up of treatment responses (Figure 3). To date, ataxin-3 assays only are available in CSF, plasma, and urine.<sup>85-87</sup> PolyQ-expanded ataxin-3 level in plasma and CSF correlates with pathological CAG repeat expansion and SARA score.<sup>85,87</sup> In urine samples, expanded ataxin-3 was also detected in symptomatic and presymptomatic carriers and showed strong correlation with plasma levels and earlier age at onset.<sup>86</sup>

Tau, manifesting neuronal damage, is another potential fluid biomarker. In a pilot study conducted in SCA1, SCA2, and SCA6 patients, tau concentration in CSF was higher in SCA2 carriers than in controls.<sup>88</sup> In a recent study on SCA3 carriers, plasma t-tau levels were increased compared to controls.<sup>89</sup> Presymptomatic carriers however had higher CSF concentrations than patients, perhaps indicating the validity of the biomarker in early phases of the disease. Other fluid biomarkers are listed in Figure 3.

Radiological biomarkers are more powerful than clinical scores to track longitudinal progression in SCAs.<sup>90</sup> The hallmark of SCAs is the cerebellum atrophy, even if the brainstem is the most affected region in polyQ SCAs, with the exception of SCA6.<sup>4</sup> During the preataxic phase already, cerebellum and pons atrophy are evident in SCA2<sup>91</sup> and SCA3 carriers.<sup>92</sup> For the latter, medulla oblongata, pallidum, and C2-C3 spinal cord segment volumes are also reduced in preataxic carriers.<sup>92</sup> In a study including SCA1 carriers, preataxic individuals did not differ from controls.<sup>93</sup> After one-year of follow-up, however, a reduction in cerebellum volume was demonstrated, highlighting its potential use as biomarker in preataxic stages. In SCA2 patients with moderate disease followed for 12 months, only two regions, the pons and the lobule Crus I, showed atrophy progression.<sup>62</sup> Based on previous MRI scans, the authors speculated that the annual progression of atrophy could be used as a biomarker.<sup>62</sup> The cervical spinal cord is another region of interest. In SCA1,<sup>94</sup> SCA3,<sup>92</sup> and SCA7 carriers,<sup>95</sup> cervical atrophy correlates with pathological CAG repeat size and SARA score. In addition to volume analysis,

microstructural changes of the white matter are evidenced by diffusion tensor MRI in polyQ SCAs,<sup>95</sup> already at premanifest phase in SCA3.<sup>96</sup> Magnetic resonance spectroscopy also provided promising biomarkers<sup>97</sup> with evidence of higher sensitivity than MRI at preclinical stage.<sup>98</sup> The correlations and temporal dynamics of the different biomarkers issued from fluid analyses, clinical assessments (disease scales, oculomotor, cognitive, postural assessments, etc.), and radiological examinations may be used to define a disease trajectory, to optimize treatments options for each individual patient (Figure 1).

## **Conclusions**

In dominant diseases, the identification of the causal mutation gives the opportunity to identify preataxic carriers, who could benefit from treatments preventing the disease development. Finding the optimal treatment window, either at the occurrence of the first symptoms or during the preataxic stage, is hence a key issue. Fluid biomarkers such as NfL in blood, or radiological ones such as cerebellum or brainstem atrophy, will allow to identify the ideal time point to initiate treatment. Evidently, one difficulty of running a clinical trial in SCAs lies in their rarity. The Ataxia Global Initiative (AGI, <https://ataxia-global-initiative.net/>), initiated in 2021, is a worldwide platform for clinical research in ataxias, gathering academic and industrial researchers, clinicians, and patients' associations. To design the best therapeutic approaches, we cannot afford ignoring the functions of SCA proteins, the regulation of their expression over the life of an individual with SCA, and their cellular effects.

**Authors' contributions:** G.C.: literature search, conceptualisation, writing – original draft, figures; M.C.: literature search, writing – original draft, figures; A.D.: conceptualisation, supervision, validation, writing– review & editing.

**Declaration of interests:** The authors report no competing interests.

## References

- 1 Coutelier M, Jacoupy M, Janer A, *et al.* NPTX1 mutations trigger endoplasmic reticulum stress and cause autosomal dominant cerebellar ataxia. *Brain* 2021; : awab407.
- 2 Ruano L, Melo C, Silva MC, Coutinho P. The Global Epidemiology of Hereditary Ataxia and Spastic Paraplegia: A Systematic Review of Prevalence Studies. *Neuroepidemiology* 2014; **42**: 174–83.
- 3 Klockgether T, Mariotti C, Paulson HL. Spinocerebellar ataxia. *Nat Rev Dis Primers* 2019; **5**: 24.
- 4 Durr A. Autosomal dominant cerebellar ataxias: polyglutamine expansions and beyond. *The Lancet Neurology* 2010; **9**: 885–94.
- 5 Tezenas du Montcel S, Durr A, Rakowicz M, *et al.* Prediction of the age at onset in spinocerebellar ataxia type 1, 2, 3 and 6. *J Med Genet* 2014; **51**: 479–86.
- 6 Tezenas du Montcel S, Durr A, Bauer P, *et al.* Modulation of the age at onset in spinocerebellar ataxia by CAG tracts in various genes. *Brain* 2014; **137**: 2444–55.
- 7 Bah MG, Rodriguez D, Cazeneuve C, *et al.* Deciphering the natural history of SCA7 in children. *Eur J Neurol* 2020; **27**: 2267–76.
- 8 Mao R, Aylsworth AS, Potter N, *et al.* Childhood-onset ataxia: testing for large CAG-repeats in SCA2 and SCA7. *Am J Med Genet* 2002; **110**: 338–45.
- 9 Kraus-Perrotta C, Lagalwar S. Expansion, mosaicism and interruption: mechanisms of the CAG repeat mutation in spinocerebellar ataxia type 1. *Cerebellum & Ataxias* 2016; **3**: 20.
- 10 Charles P, Camuzat A, Benammar N, *et al.* Are interrupted SCA2 CAG repeat expansions responsible for parkinsonism? *Neurology* 2007; **69**: 1970–5.
- 11 Jacobi H, du Montcel ST, Bauer P, *et al.* Long-term disease progression in spinocerebellar ataxia types 1, 2, 3, and 6: a longitudinal cohort study. *The Lancet Neurology* 2015; **14**: 1101–8.
- 12 Diallo A, Jacobi H, Cook A, *et al.* Survival in patients with spinocerebellar ataxia types 1, 2, 3, and 6 (EUROSCA): a longitudinal cohort study. *The Lancet Neurology* 2018; **17**: 327–34.
- 13 Orengo JP, van der Heijden ME, Hao S, Tang J, Orr HT, Zoghbi HY. Motor neuron degeneration correlates with respiratory dysfunction in SCA1. *Disease Models & Mechanisms* 2018; : dmm.032623.
- 14 Monin M, Tezenas du Montcel S, Marelli C, *et al.* Survival and severity in dominant cerebellar ataxias. *Ann Clin Transl Neurol* 2015; **2**: 202–7.
- 15 Ashizawa T, Figueroa KP, Perlman SL, *et al.* Clinical characteristics of patients with spinocerebellar ataxias 1, 2, 3 and 6 in the US; a prospective observational study. *Orphanet J Rare Dis* 2013; **8**: 177.
- 16 Maas RPPWM, Schutter DJLG, van de Warrenburg BPC. Discordance Between Patient-Reported Outcomes and Physician-Rated Motor Symptom Severity in Early-to-Middle-Stage Spinocerebellar Ataxia Type 3. *Cerebellum* 2021; **20**: 887–95.
- 17 Jardim LB, Hasan A, Kuo S-H, *et al.* An Exploratory Survey on the Care for Ataxic Patients in the American Continents and the Caribbean. *Cerebellum* 2022; published online July 7. DOI:10.1007/s12311-022-01442-z.

- 18 Jacobi H, Reetz K, du Montcel ST, *et al.* Biological and clinical characteristics of individuals at risk for spinocerebellar ataxia types 1, 2, 3, and 6 in the longitudinal RISCA study: analysis of baseline data. *Lancet Neurol* 2013; **12**: 650–8.
- 19 van der Put J, Daugeliene D, Bergendal Å, Kvarnung M, Svenningsson P, Paucar M. On Spinocerebellar Ataxia 21 as a Mimicker of Cerebral Palsy. *Neurol Genet* 2022; **8**: e668.
- 20 Gouvêa LA, Raslan IR, Rosa ABR, *et al.* Spinocerebellar Ataxia Type 5 (SCA5) Mimicking Cerebral Palsy: a Very Early Onset Autosomal Dominant Hereditary Ataxia. *Cerebellum* 2022; published online March 3. DOI:10.1007/s12311-022-01380-w.
- 21 Riso V, Galatolo D, Barghigiani M, *et al.* A next generation sequencing-based analysis of a large cohort of ataxic patients refines the clinical spectrum associated with spinocerebellar ataxia 21. *Eur J Neurol* 2021; **28**: 2784–8.
- 22 Ganaraja VH, Holla VV, Stezin A, *et al.* Clinical, Radiological, and Genetic Profile of Spinocerebellar Ataxia 12: A Hospital-Based Cohort Analysis. *Tremor Other Hyperkinet Mov (N Y)* 2022; **12**: 13.
- 23 Schmitz-Hübsch T, Lux S, Bauer P, *et al.* Spinocerebellar ataxia type 14: refining clinicogenetic diagnosis in a rare adult-onset disorder. *Ann Clin Transl Neurol* 2021; **8**: 774–89.
- 24 Paucar M, Bergendal Å, Gustavsson P, *et al.* Novel Features and Abnormal Pattern of Cerebral Glucose Metabolism in Spinocerebellar Ataxia 19. *Cerebellum* 2018; **17**: 465–76.
- 25 Roux T, Barbier M, Papin M, *et al.* Clinical, neuropathological, and genetic characterization of STUB1 variants in cerebellar ataxias: a frequent cause of predominant cognitive impairment. *Genet Med* 2020; **22**: 1851–62.
- 26 Coutelier M, Coarelli G, Monin M-L, *et al.* A panel study on patients with dominant cerebellar ataxia highlights the frequency of channelopathies. *Brain* 2017; **140**: 1579–94.
- 27 Hommersom MP, van Prooijje TH, Pennings M, *et al.* The complexities of CACNA1A in clinical neurogenetics. *J Neurol* 2022; **269**: 3094–108.
- 28 Schmähmann JD, Weilburg JB, Sherman JC. The neuropsychiatry of the cerebellum - insights from the clinic. *Cerebellum* 2007; **6**: 254–67.
- 29 Hoche F, Guell X, Vangel MG, Sherman JC, Schmähmann JD. The cerebellar cognitive affective/Schmähmann syndrome scale. *Brain* 2018; **141**: 248–70.
- 30 Maas RPPWM, Killaars S, van de Warrenburg BPC, Schutter DJLG. The cerebellar cognitive affective syndrome scale reveals early neuropsychological deficits in SCA3 patients. *J Neurol* 2021; **268**: 3456–66.
- 31 Thieme A, Faber J, Sulzer P, *et al.* The CCAS-scale in hereditary ataxias: helpful on the group level, particularly in SCA3, but limited in individual patients. *J Neurol* 2022; **269**: 4363–74.
- 32 Martínez-Regueiro R, Arias M, Cruz R, *et al.* Cerebellar Cognitive Affective Syndrome in Costa da Morte Ataxia (SCA36). *Cerebellum* 2020; **19**: 501–9.
- 33 Rodríguez-Labrada R, Batista-Izquierdo A, González-Melix Z, *et al.* Cognitive Decline Is Closely Associated with Ataxia Severity in Spinocerebellar Ataxia Type 2: a Validation Study of the Schmähmann Syndrome Scale. *Cerebellum* 2022; **21**: 391–403.

- 34 Genis D, Ortega-Cubero S, San Nicolás H, *et al.* Heterozygous STUB1 mutation causes familial ataxia with cognitive affective syndrome (SCA48). *Neurology* 2018; **91**: e1988–98.
- 35 Schöggel J, Siegert S, Boltshauser E, Freilinger M, Schmidt WM. A De Novo Missense NPTX1 Variant in an Individual with Infantile-Onset Cerebellar Ataxia. *Mov Disord* 2022; published online May 12. DOI:10.1002/mds.29054.
- 36 Verdura E, Schlüter A, Fernández-Eulate G, *et al.* A deep intronic splice variant advises reexamination of presumably dominant SPG7 Cases. *Ann Clin Transl Neurol* 2020; **7**: 105–11.
- 37 Coutelier M, Holtgrewe M, Jäger M, *et al.* Combining callers improves the detection of copy number variants from whole-genome sequencing. *Eur J Hum Genet* 2022; **30**: 178–86.
- 38 Ibañez K, Polke J, Hagelstrom RT, *et al.* Whole genome sequencing for the diagnosis of neurological repeat expansion disorders in the UK: a retrospective diagnostic accuracy and prospective clinical validation study. *Lancet Neurol* 2022; **21**: 234–45.
- 39 Seixas AI, Loureiro JR, Costa C, *et al.* A Pentanucleotide ATTC Repeat Insertion in the Non-coding Region of DAB1, Mapping to SCA37, Causes Spinocerebellar Ataxia. *Am J Hum Genet* 2017; **101**: 87–103.
- 40 Gennarino VA, Palmer EE, McDonnell LM, *et al.* A Mild PUM1 Mutation Is Associated with Adult-Onset Ataxia, whereas Haploinsufficiency Causes Developmental Delay and Seizures. *Cell* 2018; **172**: 924-936.e11.
- 41 Barbier M, Bahlo M, Pennisi A, *et al.* Heterozygous PNPT1 Variants Cause Spinocerebellar Ataxia Type 25. *Ann Neurol* 2022; **92**: 122–37.
- 42 De Michele G, Lieto M, Galatolo D, *et al.* Spinocerebellar ataxia 48 presenting with ataxia associated with cognitive, psychiatric, and extrapyramidal features: A report of two Italian families. *Parkinsonism & Related Disorders* 2019; **65**: 91–6.
- 43 Corral-Juan M, Casquero P, Giraldo-Restrepo N, *et al.* New spinocerebellar ataxia subtype caused by SAMD9L mutation triggering mitochondrial dysregulation (SCA49). *Brain Commun* 2022; **4**: fcac030.
- 44 Ahmed IA, Farooqi MS, Vander Lugt MT, *et al.* Outcomes of Hematopoietic Cell Transplantation in Patients with Germline SAMD9/SAMD9L Mutations. *Biology of Blood and Marrow Transplantation: Journal of the American Society for Blood and Marrow Transplantation* 2019; **25**: 2186–96.
- 45 Coutelier M, Jacoupy M, Janer A, *et al.* NPTX1 mutations trigger endoplasmic reticulum stress and cause autosomal dominant cerebellar ataxia. *Brain* 2022; **145**: 1519–34.
- 46 Gardiner SL, Boogaard MW, Trompet S, *et al.* Prevalence of Carriers of Intermediate and Pathological Polyglutamine Disease-Associated Alleles Among Large Population-Based Cohorts. *JAMA Neurol* 2019; **76**: 650–6.
- 47 Magri S, Nanetti L, Gellera C, *et al.* Digenic inheritance of STUB1 variants and TBP polyglutamine expansions explains the incomplete penetrance of SCA17 and SCA48. *Genet Med* 2022; **24**: 29–40.
- 48 Reis MC, Patrun J, Ackl N, *et al.* A Severe Dementia Syndrome Caused by Intron Retention and Cryptic Splice Site Activation in STUB1 and Exacerbated by TBP Repeat Expansions. *Front Mol Neurosci* 2022; **15**: 878236.

- 49 Wernick AI, Walton RL, Soto-Beasley AI, *et al.* Frequency of spinocerebellar ataxia mutations in patients with multiple system atrophy. *Clin Auton Res* 2021; **31**: 117–25.
- 50 Jih K-Y, Lin K-P, Tsai P-C, Soong B-W, Liao Y-C, Lee Y-C. Investigating TBP CAG/CAA trinucleotide repeat expansions in a Taiwanese cohort with ALS. *Amyotroph Lateral Scler Frontotemporal Degener* 2021; **22**: 442–7.
- 51 Elden AC, Kim H-J, Hart MP, *et al.* Ataxin-2 intermediate-length polyglutamine expansions are associated with increased risk for ALS. *Nature* 2010; **466**: 1069–75.
- 52 Borghero G, Pugliatti M, Marrosu F, *et al.* ATXN2 is a modifier of phenotype in ALS patients of Sardinian ancestry. *Neurobiol Aging* 2015; **36**: 2906.e1-5.
- 53 Glass JD, Dewan R, Ding J, *et al.* ATXN2 intermediate expansions in amyotrophic lateral sclerosis. *Brain* 2022; : awac167.
- 54 Rubino E, Mancini C, Boschi S, *et al.* ATXN2 intermediate repeat expansions influence the clinical phenotype in frontotemporal dementia. *Neurobiol Aging* 2019; **73**: 231.e7-231.e9.
- 55 Fournier C, Anquetil V, Camuzat A, *et al.* Interrupted CAG expansions in ATXN2 gene expand the genetic spectrum of frontotemporal dementias. *Acta Neuropathol Commun* 2018; **6**: 41.
- 56 Scoles DR, Dansithong W, Pflieger LT, *et al.* ALS-associated genes in SCA2 mouse spinal cord transcriptomes. *Hum Mol Genet* 2020; **29**: 1658–72.
- 57 Tazelaar GHP, Boeynaems S, De Decker M, *et al.* ATXN1 repeat expansions confer risk for amyotrophic lateral sclerosis and contribute to TDP-43 mislocalization. *Brain Commun* 2020; **2**: fcaa064.
- 58 Ungaro C, Sprovieri T, Morello G, *et al.* Genetic investigation of amyotrophic lateral sclerosis patients in south Italy: a two-decade analysis. *Neurobiol Aging* 2021; **99**: 99.e7-99.e14.
- 59 Thion MS, Tézenas du Montcel S, Golmard J-L, *et al.* CAG repeat size in Huntingtin alleles is associated with cancer prognosis. *Eur J Hum Genet* 2016; **24**: 1310–5.
- 60 Pérez-Oliveira S, Álvarez I, Rosas I, *et al.* Intermediate and Expanded HTT Alleles and the Risk for  $\alpha$ -Synucleinopathies. *Mov Disord* 2022; published online July 19. DOI:10.1002/mds.29153.
- 61 Romano S, Coarelli G, Marcotulli C, *et al.* Riluzole in patients with hereditary cerebellar ataxia: a randomised, double-blind, placebo-controlled trial. *The Lancet Neurology* 2015; **14**: 985–91.
- 62 Coarelli G, Heinzmann A, Ewencyk C, *et al.* Safety and efficacy of riluzole in spinocerebellar ataxia type 2 in France (ATRIL): a multicentre, randomised, double-blind, placebo-controlled trial. *Lancet Neurol* 2022; **21**: 225–33.
- 63 Manes M, Alberici A, Di Gregorio E, *et al.* Docosahexaenoic acid is a beneficial replacement treatment for spinocerebellar ataxia 38. *Ann Neurol* 2017; **82**: 615–21.
- 64 Gazulla J, Benavente I, García-González E, Berciano J. Two-year follow-up of docosahexaenoic acid supplementation in spinocerebellar ataxia type 38 (SCA38). *J Neurol* 2022; published online April 19. DOI:10.1007/s00415-022-11138-3.
- 65 Benussi A, Dell’Era V, Cantoni V, *et al.* Cerebello-spinal tDCS in ataxia: A randomized, double-blind, sham-controlled, crossover trial. *Neurology* 2018; **91**: e1090–101.



- 66 Benussi A, Cantoni V, Manes M, *et al.* Motor and cognitive outcomes of cerebello-spinal stimulation in neurodegenerative ataxia. *Brain* 2021; **144**: 2310–21.
- 67 Maas RPPWM, Teerenstra S, Toni I, Klockgether T, Schutter DJLG, van de Warrenburg BPC. Cerebellar Transcranial Direct Current Stimulation in Spinocerebellar Ataxia Type 3: a Randomized, Double-Blind, Sham-Controlled Trial. *Neurotherapeutics* 2022; published online May 2. DOI:10.1007/s13311-022-01231-w.
- 68 Vogel AP, Graf LH, Magee M, Schöls L, Rommel N, Synofzik M. Home-based biofeedback speech treatment improves dysarthria in repeat-expansion SCAs. *Ann Clin Transl Neurol* 2022; published online June 21. DOI:10.1002/acn3.51613.
- 69 Rodríguez-Díaz JC, Velázquez-Pérez L, Rodríguez Labrada R, *et al.* Neurorehabilitation therapy in spinocerebellar ataxia type 2: A 24-week, rater-blinded, randomized, controlled trial. *Mov Disord* 2018; **33**: 1481–7.
- 70 Tercero-Pérez K, Cortés H, Torres-Ramos Y, *et al.* Effects of Physical Rehabilitation in Patients with Spinocerebellar Ataxia Type 7. *Cerebellum* 2019; **18**: 397–405.
- 71 Lacorte E, Bellomo G, Nuovo S, Corbo M, Vanacore N, Piscopo P. The Use of New Mobile and Gaming Technologies for the Assessment and Rehabilitation of People with Ataxia: a Systematic Review and Meta-analysis. *Cerebellum* 2021; **20**: 361–73.
- 72 He L, Wang S, Peng L, *et al.* CRISPR/Cas9 mediated gene correction ameliorates abnormal phenotypes in spinocerebellar ataxia type 3 patient-derived induced pluripotent stem cells. *Transl Psychiatry* 2021; **11**: 479.
- 73 Friedrich J, Kordasiewicz HB, O’Callaghan B, *et al.* Antisense oligonucleotide-mediated ataxin-1 reduction prolongs survival in SCA1 mice and reveals disease-associated transcriptome profiles. *JCI insight* 2018; **3**. DOI:10.1172/jci.insight.123193.
- 74 Scoles DR, Meera P, Schneider MD, *et al.* Antisense oligonucleotide therapy for spinocerebellar ataxia type 2. *Nature* 2017; **544**: 362–6.
- 75 McLoughlin HS, Moore LR, Chopra R, *et al.* Oligonucleotide therapy mitigates disease in spinocerebellar ataxia type 3 mice. *Annals of Neurology* 2018; **84**: 64–77.
- 76 Niu C, Prakash TP, Kim A, *et al.* Antisense oligonucleotides targeting mutant Ataxin-7 restore visual function in a mouse model of spinocerebellar ataxia type 7. *Science Translational Medicine* 2018; **10**. DOI:10.1126/scitranslmed.aap8677.
- 77 Hoy SM. Nusinersen: First Global Approval. *Drugs* 2017; **77**: 473–9.
- 78 Tabrizi SJ, Estevez-Fraga C, van Roon-Mom WMC, *et al.* Potential disease-modifying therapies for Huntington’s disease: lessons learned and future opportunities. *The Lancet Neurology* 2022; **21**: 645–58.
- 79 Suh J, Romano DM, Nitschke L, *et al.* Loss of Ataxin-1 Potentiates Alzheimer’s Pathogenesis by Elevating Cerebral BACE1 Transcription. *Cell* 2019; **178**: 1159-1175.e17.
- 80 O’Callaghan B, Hofstra B, Handler HP, *et al.* Antisense Oligonucleotide Therapeutic Approach for Suppression of Ataxin-1 Expression: A Safety Assessment. *Mol Ther Nucleic Acids* 2020; **21**: 1006–16.
- 81 Coarelli G, Darios F, Petit E, *et al.* Plasma neurofilament light chain predicts cerebellar atrophy and clinical progression in spinocerebellar ataxia. *Neurobiol Dis* 2021; **153**: 105311.

- 82 Wilke C, Haas E, Reetz K, *et al.* Neurofilaments in spinocerebellar ataxia type 3: blood biomarkers at the preataxic and ataxic stage in humans and mice. *EMBO Mol Med* 2020; **12**: e11803.
- 83 Wilke C, Mengel D, Schöls L, *et al.* Levels of Neurofilament Light at the Preataxic and Ataxic Stages of Spinocerebellar Ataxia Type 1. *Neurology* 2022; : 10.1212/WNL.0000000000200257.
- 84 Yang L, Shao Y-R, Li X-Y, Ma Y, Dong Y, Wu Z-Y. Association of the Level of Neurofilament Light With Disease Severity in Patients With Spinocerebellar Ataxia Type 2. *Neurology* 2021; **97**: e2404–13.
- 85 Prudencio M, Garcia-Moreno H, Jansen-West KR, *et al.* Toward allele-specific targeting therapy and pharmacodynamic marker for spinocerebellar ataxia type 3. *Sci Transl Med* 2020; **12**. DOI:10.1126/scitranslmed.abb7086.
- 86 Koike Y, Jansen-West KR, Hanna Al-Shaikh R, *et al.* Urine levels of the polyglutamine ataxin-3 protein are elevated in patients with spinocerebellar ataxia type 3. *Parkinsonism Relat Disord* 2021; **89**: 151–4.
- 87 Hübener-Schmid J, Kuhlbrodt K, Peladan J, *et al.* Polyglutamine-Expanded Ataxin-3: A Target Engagement Marker for Spinocerebellar Ataxia Type 3 in Peripheral Blood. *Mov Disord* 2021; published online Aug 16. DOI:10.1002/mds.28749.
- 88 Brouillette AM, Öz G, Gomez CM. Cerebrospinal Fluid Biomarkers in Spinocerebellar Ataxia: A Pilot Study. *Dis Markers* 2015; **2015**: 413098.
- 89 Garcia-Moreno H, Prudencio M, Thomas-Black G, *et al.* Tau and neurofilament light-chain as fluid biomarkers in spinocerebellar ataxia type 3. *Eur J Neurol* 2022; published online April 28. DOI:10.1111/ene.15373.
- 90 Adanyeguh IM, Perlberg V, Henry P-G, *et al.* Autosomal dominant cerebellar ataxias: Imaging biomarkers with high effect sizes. *Neuroimage Clin* 2018; **19**: 858–67.
- 91 Reetz K, Rodríguez-Labrada R, Dogan I, *et al.* Brain atrophy measures in preclinical and manifest spinocerebellar ataxia type 2. *Ann Clin Transl Neurol* 2018; **5**: 128–37.
- 92 Faber J, Schaprian T, Berkan K, *et al.* Regional Brain and Spinal Cord Volume Loss in Spinocerebellar Ataxia Type 3. *Mov Disord* 2021; **36**: 2273–81.
- 93 Nigri A, Sarro L, Mongelli A, *et al.* Spinocerebellar Ataxia Type 1: One-Year Longitudinal Study to Identify Clinical and MRI Measures of Disease Progression in Patients and Presymptomatic Carriers. *Cerebellum* 2022; **21**: 133–44.
- 94 Martins Junior CR, Martinez ARM, Vasconcelos IF, *et al.* Structural signature in SCA1: clinical correlates, determinants and natural history. *J Neurol* 2018; **265**: 2949–59.
- 95 Hernandez-Castillo CR, Diaz R, Rezende TJR, *et al.* Cervical Spinal Cord Degeneration in Spinocerebellar Ataxia Type 7. *AJNR Am J Neuroradiol* 2021; **42**: 1735–9.
- 96 Li M, Chen X, Xu H-L, *et al.* Brain structural abnormalities in the preclinical stage of Machado-Joseph disease/spinocerebellar ataxia type 3 (MJD/SCA3): evaluation by MRI morphometry, diffusion tensor imaging and neurite orientation dispersion and density imaging. *J Neurol* 2022; **269**: 2989–98.
- 97 Miranda CO, Nobre RJ, Paiva VH, *et al.* Cerebellar morphometric and spectroscopic biomarkers for Machado-Joseph Disease. *Acta Neuropathol Commun* 2022; **10**: 37.

- 98 Deelchand DK, Joers JM, Ravishankar A, *et al.* Sensitivity of Volumetric Magnetic Resonance Imaging and Magnetic Resonance Spectroscopy to Progression of Spinocerebellar Ataxia Type 1. *Mov Disord Clin Pract* 2019; **6**: 549–58.
- 99 Velázquez-Pérez L, Rodríguez-Chanfrau J, García-Rodríguez JC, *et al.* Oral Zinc Sulphate Supplementation for Six Months in SCA2 Patients: A Randomized, Double-Blind, Placebo-Controlled Trial. *Neurochem Res* 2011; **36**: 1793–800.
- 100 Saute JAM, de Castilhos RM, Monte TL, *et al.* A randomized, phase 2 clinical trial of lithium carbonate in Machado-Joseph disease. *Mov Disord* 2014; **29**: 568–73.
- 101 Lei L-F, Yang G-P, Wang J-L, *et al.* Safety and efficacy of valproic acid treatment in SCA3/MJD patients. *Parkinsonism Relat Disord* 2016; **26**: 55–61.
- 102 Zesiewicz TA, Greenstein PE, Sullivan KL, *et al.* A randomized trial of varenicline (Chantix) for the treatment of spinocerebellar ataxia type 3. *Neurology* 2012; **78**: 545–50.
- 103 Schulte T, Mattern R, Berger K, *et al.* Double-blind crossover trial of trimethoprim-sulfamethoxazole in spinocerebellar ataxia type 3/Machado-Joseph disease. *Arch Neurol* 2001; **58**: 1451–7.
- 104 Feil K, Adrion C, Boesch S, *et al.* Safety and Efficacy of Acetyl-DL-Leucine in Certain Types of Cerebellar Ataxia: The ALCAT Randomized Clinical Crossover Trial. *JAMA Netw Open* 2021; **4**: e2135841.
- 105 Nishizawa M, Onodera O, Hirakawa A, Shimizu Y, Yamada M, Rovatirelin Study Group. Effect of rovatirelin in patients with cerebellar ataxia: two randomised double-blind placebo-controlled phase 3 trials. *J Neurol Neurosurg Psychiatry* 2020; **91**: 254–62.

**Table 1. Treatments in mice and SCA patients.**

	<b>Technique, phase, NCT</b>	<b>Administration, dose, number of inclusions</b>	<b>Outcome measures and results</b>	<b>References</b>
<b>SCA1</b>				
Human trial completed				
	IIB/III, NCT01104649	Riluzole 100 mg/day n=21*	SARA change at month 12, clinical improvement (all genotypes mixed)*	Romano et al. 2015 <sup>61</sup>
	III, NCT03701399	Troriluzole 200 mg/day for 48 weeks, n=218**	m-SARA change at week 48, no improvement	Biohaven Pharmaceuticals
Ongoing				
	III, NCT03408080	BHV-4157 (prodrug of riluzole), n=24***	SARA change at week 12	University of California
<b>SCA2</b>				
Human trial completed				
	IIB/III, NCT01104649	Riluzole 100 mg/day, n=16*	SARA change at month 12, clinical improvement (all genotypes mixed)	Romano et al. 2015 <sup>61</sup>
	III, NCT03701399	Troriluzole, 200 mg/day for 48 weeks, n=218**	m-SARA change at week 48, no improvement	Biohaven Pharmaceuticals
	III, NCT03347344	Riluzole 100 mg/day, n=45	SARA change at month 12, no clinical and radiological improvement	Coarelli et al. 2022 <sup>62</sup>
	II	Zinc sulphate, 50 mg/day n=36	SARA change at month 6, safe, possible clinical improvement but study limitations	Velazquez-Perez et al. 2011 <sup>99</sup>
Ongoing				
	III, NCT03408080	BHV-4157 (prodrug of riluzole), n=24***	SARA change at week 12	University of California
<b>SCA3</b>				
Human trial completed				
	IIB/III, NCT01096082	Lithium 300 mg/day, n=62,	NESSCA change at week 48, safe but no clinical improvement	Saute et al. 2014 <sup>100</sup>
	II, ChiCTR-TRC10000754	Valproic acid 800 or 1200 mg/day, n=36	SARA change at week 12, safe, clinical improvement with high dose	Lei et al. 2016 <sup>101</sup>

	II, NCT00992771	Varenicline 2mg/day, n=18	SARA change at week 4, no improvement	Zesiewicz et al. 2012 <sup>102</sup>
	II	trimethoprim and sulfamethoxazole, 320/1600 mg/day for 2 weeks, followed by 160/800 mg/day for 5.5 months, n=22	Modified ataxia score, posturography, no improvement	Schulte et al. 2001 <sup>103</sup>
	III, NCT03701399	Troriluzole 200 mg/day for 48 weeks, n=218**	m-SARA change at week 48, no improvement	Biohaven Pharmaceuticals
	III, EudraCT 2015-000460- 34	Acetyl-DL-leucine 5g/day for 6 weeks, n=108****	SARA change at week 6	Feil et al. 2021 <sup>104</sup>
<b>Ongoing</b>				
	II, NCT04399265	Trehalose per os, n=40	SARA score at 3 and 6-month	National University of Malaysia
	IIB/III, NCT05490563	Trehalose injection, 0.75 g/kg or 0.50 g/kg by IV infusion once a week for 52 weeks, n=245	Change from baseline in m-SARA total score at week 52	Seelos Therapeutics
	III, NCT03408080	BHV-4157 (prodrug of riluzole), n=24***	SARA change at week 12	University of California
	I, NCT05160558	ASOBIIB132, intrathecal , 5 doses, Q4W up to day 85, n=48	Safety	Biogen
<b>SCA6</b>				
<b>Human trial completed</b>				
	III	Rovatiirelin 1.6 or 2.4 mg/day for 24 weeks, n=165 (cohort 1), n=83 (cohort 2)	SARA change at week 24, no improvment	Nishizawa et al. 2020 <sup>105</sup>
	III, NCT03701399	Troriluzole, 200 mg/day for 48 weeks, n=218**	m-SARA change at week 48, no improvement	Biohaven Pharmaceuticals
<b>Ongoing</b>				
	III, NCT03408080	BHV-4157 (prodrug of riluzole), n=24***	SARA change at week 12	University of California
<b>SCA7</b>				
<b>Human trial completed</b>				
	III, NCT03701399	Troriluzole, 200 mg/day for 48 weeks n=218**	m-SARA change at week 48, no improvement	Biohaven Pharmaceuticals

Ongoing				
	IIB/III, NCT03660917	Riluzole 100 mg/day for 12 months	Visual acuity expressed as log MAR units and SARA change at month 18	Sapienza University
<b>SCA31</b>				
Human trial completed				
	III	Rovatinirelin 1.6 or 2.4 mg/day for 24 weeks, n=72 (cohort 1), n=57 (cohort 2)	SARA change at week 24, no improvement	Nishizawa et al. 2020 <sup>105</sup>
<b>SCA38</b>				
Human trial completed				
	IIB, NCT03109626	DHA 600 mg/day, n=10	SARA change at week 16 and 40, SARA stabilization, limited sample size	Manes et al. 2017 <sup>63</sup>

For human trials: selection of completed double-blind, placebo-controlled, randomized clinical trials based on sample size >10 patients.

\*21 SCA1, 16 SCA2, 1 SCA6, 1 SCA8, 1 SCA10 patients

\*\*SCA1, 2, 3, 6, 7, 8, and 10

\*\*\*SCA1, 2, 3, 6

\*\*\*\*83 hereditary ataxia patients and 25 non- hereditary ataxia patients

Abbreviations: AAV: Adeno-associated virus; AE: adverse event; ASO: oligonucleotide antisense; DHA: docosahexaenoic acid; IV: intravenous; m-SARA: Modified Functional Scale for Assessment and Rating of Ataxia; NESSCA: Neurological Examination Score for the Assessment of Spinocerebellar Ataxia; SAE: Serious adverse events; SARA: Scale for Assessment and Rating of Ataxia; SNALP, stable nucleic acid lipid particles

## Supplementary materials

### Preclinical development of gene silencing and gene editing therapies in SCAs

Promising results of gene silencing therapies are reported in SCA mice models using viral vectors engineered microRNA (miRNA) or short hairpins RNA (shRNA). Here we describe some examples in SCA1 mice, the results for the other polyglutamine SCAs mice models are reported in Supplementary Table 1. In a SCA1 knock-in mouse model, reduction of mutant ataxin-1 expression by RNAi vectors targeting deep cerebellar nuclei preserved motor performance and cerebellum histology,<sup>1</sup> and improved phenotype after disease onset.<sup>2,3</sup> In another study, the combination of mutant *ATXN1* knockdown and overexpression of ataxin1-like (*ATXNIL*) improved motor performance and restored gene expression alterations.<sup>4</sup> Unexpected neurotoxicity occurred after AAV delivery of miS1, a miRNA targeting a conserved human/primate sequence in ataxin-1, in non-human primates.<sup>5</sup> The neurotoxicity was caused by the inverted terminal repeat (ITR) promoter activity of AAV and was also evidenced after injection of an AAV devoid of RNAi.<sup>5</sup> To design successful, safe, and efficient gene therapies, several technological issues have to be solved, such as delivery systems, in vivo stability, and the existence of off-target effects.

**Supplementary Table 1. Gene silencing and gene editing strategies in SCA mice models.**

SCA	Technique	Administration	Outcome measures and results	References
<b>SCA1</b>				
Mouse model				
	CRISPR/CAS9	Disruption of endogenous S776 phosphorylation site in ATXN1-154Q/2Q-knock-in mice	Phenotype improvement (coordination, respiratory capacity, survival extension)	Nitschke et al. 2021 <sup>6</sup>
	ASO	Intracerebroventricular in ATXN1-154Q/2Q-knockin mice	Clinical (ataxia and survival) and magnetic resonance spectroscopy rescue	Friedrich et al. 2018 <sup>7</sup>
	AAV-shRNA	Intracerebellar in transgenic SCA1 mice	Phenotype improvement, intranuclear inclusions reduction	Xia et al. 2004 <sup>2</sup>
	AAV-RNAi	Intracerebellar in ATXN1-154Q/2Q knock-in mice	Reduction of ATXN1, phenotype reversion, restoration of transcriptional abnormalities,	Keiser et al. 2014 <sup>1</sup>
	AAV-miRNA(miS1)	Intracerebellar in transgenic SCA1 B05 mice	Phenotype reversion	Keiser et al. 2016 <sup>3</sup>
	Dual component rAAV (hATN1L combined with miS1)	Intracerebellar in transgenic SCA1 B05 mice	Phenotype reversion, reduction of inflammatory markers and restoration of dysregulated gene expression	Carrell et al. 2022 <sup>4</sup>
<b>SCA2</b>				
Mouse model				
	ASO	Intracerebroventricular in ATXN2-Q127 mice	Reduced disease protein levels, clinical and electrophysiology improvement	Scoles et al. 2017 <sup>8</sup>
<b>SCA3</b>				
Mouse model				
	ASO	Intracerebroventricular in ATXN3-Q135 and Q4 mice	Reduced disease protein levels by >50%	Moore et al. 2017 <sup>9</sup>
	ASO	Intracerebroventricular ASO in ATXN3-Q75 mice	Reduced disease protein levels, prevention of ATXN3 oligomeric and nuclear accumulation, clinical and electrophysiology improvement	McLoughlin et al. 2018 <sup>10</sup>
	Lentivirus-shRNA	Intracerebellar in SCA3 transgenic C57BL/6J mice	Phenotype improvement, intranuclear inclusions reduction	Nobrega et al. 2013 <sup>11</sup>



	AAV-based RNAi (miR-Atx3-148)	Intracerebellar injection in SCA3/MJD84.2 mice	Intranuclear inclusions reduction, partial restoration of miRNA steady-state levels, mild phenotype	Rodríguez-Lébron et al. 2013 <sup>12</sup>
	Lentivirus-miRNA (mir-9, mir-181a, and mir-494)	Striatum injection in SCA3 mice	Reduction of intranuclear inclusions and mutant ATXN3	Carmona et al. 2017 <sup>13</sup>
	AAV5-miRNA (mir-451)	Striatum injection in SCA3 mice	Reduction of ATXN3 inclusions, rescue of striatal lesions of dopamine- and cAMP-regulated neuronal phosphoprotein	Nobre et al. 2022 <sup>14</sup>
	SNALPs-siRNAs	Intravenous in SCA3 mice	Phenotype improvement and reduction of intranuclear inclusions	Conceição et al. 2015 <sup>15</sup>
<b>SCA6</b>				
Mouse model				
	AAV9-mediated delivery of miR-3191-5p	Intracerebroventricular in SCA6 mice (C57/BL6J)	Disease phenotype rescue	Miyazaki et al. 2016 <sup>16</sup> Pastor et al. 2018 <sup>17</sup>
<b>SCA7</b>				
Mouse model				
	ASO	Intravitreal injection in ATXN7 266Q knock-in mice	Visual function and retinal histopathology improvement	Niu et al. 2018 <sup>18</sup>
	AAV1-miRNA(miS4)	Subretinal injection in BAC ATXN7-92Q transgenic mice	Preservation of normal retinal function, 50% reduction of wild-type and mutant ATXN7	Ramachandran et al. 2014 <sup>19</sup>

Abbreviations: AAV: Adeno-associated virus; ASO: oligonucleotide antisense; hATN1L: human ATXN1 like; miRNA: microRNA; rAAV: recombinant adeno-associated virus; RNAi: RNA interference; shRNA: short hairpin RNA; SNALP, stable nucleic acid lipid particle.

## References

- 1 Keiser MS, Boudreau RL, Davidson BL. Broad Therapeutic Benefit After RNAi Expression Vector Delivery to Deep Cerebellar Nuclei: Implications for Spinocerebellar Ataxia Type 1 Therapy. *Mol Ther* 2014; **22**: 588–95.
- 2 Xia H, Mao Q, Eliason SL, *et al.* RNAi suppresses polyglutamine-induced neurodegeneration in a model of spinocerebellar ataxia. *Nat Med* 2004; **10**: 816–20.
- 3 Keiser MS, Monteys AM, Corbau R, Gonzalez-Alegre P, Davidson BL. RNAi prevents and reverses phenotypes induced by mutant human ataxin-1. *Ann Neurol* 2016; **80**: 754–65.
- 4 Carrell EM, Keiser MS, Robbins AB, Davidson BL. Combined overexpression of ATXN1L and mutant ATXN1 knockdown by AAV rescue motor phenotypes and gene signatures in SCA1 mice. *Mol Ther Methods Clin Dev* 2022; **25**: 333–43.
- 5 Keiser MS, Ranum PT, Yrigollen CM, *et al.* Toxicity after AAV delivery of RNAi expression constructs into nonhuman primate brain. *Nat Med* 2021; **27**: 1982–9.
- 6 Nitschke L, Coffin SL, Xhako E, *et al.* Modulation of ATXN1 S776 phosphorylation reveals the importance of allele-specific targeting in SCA1. *JCI Insight* 2021; **6**: 144955.
- 7 Friedrich J, Kordasiewicz HB, O’Callaghan B, *et al.* Antisense oligonucleotide-mediated ataxin-1 reduction prolongs survival in SCA1 mice and reveals disease-associated transcriptome profiles. *JCI insight* 2018; **3**. DOI:10.1172/jci.insight.123193.
- 8 Scoles DR, Meera P, Schneider MD, *et al.* Antisense oligonucleotide therapy for spinocerebellar ataxia type 2. *Nature* 2017; **544**: 362–6.
- 9 Moore LR, Rajpal G, Dillingham IT, *et al.* Evaluation of Antisense Oligonucleotides Targeting ATXN3 in SCA3 Mouse Models. *Molecular Therapy Nucleic Acids* 2017; **7**: 200–10.
- 10 McLoughlin HS, Moore LR, Chopra R, *et al.* Oligonucleotide therapy mitigates disease in spinocerebellar ataxia type 3 mice. *Annals of Neurology* 2018; **84**: 64–77.
- 11 Nóbrega C, Nascimento-Ferreira I, Onofre I, *et al.* Silencing Mutant Ataxin-3 Rescues Motor Deficits and Neuropathology in Machado-Joseph Disease Transgenic Mice. *PLOS ONE* 2013; **8**: e52396.
- 12 Rodríguez-Lebrón E, Costa M doCarmo, Luna-Cancalon K, *et al.* Silencing Mutant ATXN3 Expression Resolves Molecular Phenotypes in SCA3 Transgenic Mice. *Molecular Therapy* 2013; **21**: 1909–18.
- 13 Carmona V, Cunha-Santos J, Onofre I, *et al.* Unravelling Endogenous MicroRNA System Dysfunction as a New Pathophysiological Mechanism in Machado-Joseph Disease. *Mol Ther* 2017; **25**: 1038–55.
- 14 Nobre RJ, Lobo DD, Henriques C, *et al.* miRNA-Mediated Knockdown of ATXN3 Alleviates Molecular Disease Hallmarks in a Mouse Model for Spinocerebellar Ataxia Type 3. *Nucleic Acid Ther* 2022; **32**: 194–205.

- 15 Conceição M, Mendonça L, Nóbrega C, *et al.* Intravenous administration of brain-targeted stable nucleic acid lipid particles alleviates Machado-Joseph disease neurological phenotype. *Biomaterials* 2016; **82**: 124–37.
- 16 Miyazaki Y, Du X, Muramatsu S-I, Gomez CM. An miRNA-mediated therapy for SCA6 blocks IRES-driven translation of the CACNA1A second cistron. *Sci Transl Med* 2016; **8**: 347ra94.
- 17 Pastor VB, Sahoo SS, Boklan J, *et al.* Constitutional SAMD9L mutations cause familial myelodysplastic syndrome and transient monosomy 7. *Haematologica* 2018; **103**: 427–37.
- 18 Niu C, Prakash TP, Kim A, *et al.* Antisense oligonucleotides targeting mutant Ataxin-7 restore visual function in a mouse model of spinocerebellar ataxia type 7. *Science Translational Medicine* 2018; **10**. DOI:10.1126/scitranslmed.aap8677.
- 19 Ramachandran PS, Bhattarai S, Singh P, *et al.* RNA Interference-Based Therapy for Spinocerebellar Ataxia Type 7 Retinal Degeneration. *PLOS ONE* 2014; **9**: e95362.

### Chapter 3: SCA biomarkers state of the art

The development of new therapeutic strategies goes hand in hand with the identification of clinical and imaging biomarkers. Biomarkers are defined as “objectively-measured characteristics that serve as indicators of normal biological processes, pathogenic processes or pharmacologic responses to therapeutic interventions”.<sup>21</sup> Ideally a biomarker should: i. Have a good reproducibility, ii. Be easily measurable (e.g., for biomarkers detected in urine or blood), and iii. Have a low cost. Despite being clinically silent, SCAs premanifest stage presents with both biological and radiological alterations. Blood tests performed in this phase can reveal the presence of high neurofilament light chain (NfL) concentrations in preataxic carriers if compared with healthy controls.<sup>22–25</sup> Similarly, cerebellum and pons atrophy can already be detected at this stage in some polyQ SCA subtypes.<sup>26–29</sup> The identification of reliable biomarkers, leading to early detection of SCA presymptomatic carriers could boost SCAs primary prevention, allowing to identify early on individuals that could benefit from preventive treatments.

Prognostic biomarkers are useful to predict the phenotype course and severity. Being able of stratifying carriers is crucial to understand the right timepoint to propose a treatment. Reliable biomarkers are also needed to monitor treatments’ efficacy. To date, in clinical trials for SCA patients, clinical scales are the primary outcome to be assessed. The Scale for the Assessment and Rating of Ataxia (SARA) (maximal value of 40) is the most frequently used. This scale, developed in 2006,<sup>30</sup> is fast, easy to administer, and sensitive to disease severity with global linear progression<sup>31</sup> (Moulaire 2022, in press). Since clinical scales are susceptible to variations related to the patient's physical conditions, in the context of multicenter clinical trials it would be preferable to use more objective measures resulting from fluids’ analysis, MRI measurements, or other digital assessments. Moreover, the SARA scale cannot be used to evaluate preataxic carriers and its small effect size would require the enrollment of a large number of patients, as calculated by the EUROSCA study. This study highlighted the need to recruit at least 142 patients for SCA1, 172 for SCA2, 202 for SCA3, and 602 for SCA6 to detect a 50% decrease in SARA score progression in a two-arm clinical trial of 12 months.<sup>32</sup> Given SCAs low prevalence, achieving these numbers of patients is extremely challenging. Hence, to allow to conducting trials on smaller sample sizes, the identification of biomarkers with effect sizes greater than clinical scores is highly needed. Biomarkers used for precision medicine are more complex to identify, but the research is expanding to include a combination of biomarkers issued from multi-omic sources.

In this context, at the beginning of my PhD, I wrote a review entitled “Recent advances in understanding dominant spinocerebellar ataxias from clinical and genetic points of view”, published in *F1000 Research* in November 2018.<sup>33</sup> This review is an overview of fluid, clinical, and radiological SCAs biomarkers currently available. In addition, I recently reported validated and emerging fluid biomarkers in a chapter “Blood and CSF biomarkers in autosomal dominant cerebellar ataxias” as contribution in a collected work entitled “Trials for Cerebellar Ataxias: From Cellular Models to Human Therapies” and edited by Dr. Bing-Wen Soong, Dr. Mario Manto, Dr. Alexis Brice, and Dr. Stefan M. Pulst.



## REVIEW

# Recent advances in understanding dominant spinocerebellar ataxias from clinical and genetic points of view [version 1; referees: 3 approved]

Giulia Coarelli<sup>1,2</sup>, Alexis Brice<sup>2,3</sup>, Alexandra Durr<sup>2,3</sup>

<sup>1</sup>Assistance Publique-Hopitaux de Paris (AP-HP), Department of Neurology, Avicenne Hospital, Paris 13 University, Bobigny, 93000, France

<sup>2</sup>Institut du Cerveau et de la Moelle épinière, ICM, Inserm U 1127, CNRS UMR 7225, Sorbonne University, Paris, 75013, France

<sup>3</sup>Assistance Publique-Hopitaux de Paris (AP-HP), Genetic department, Pitié-Salpêtrière University Hospital, Paris, 75013, France

**v1** First published: 12 Nov 2018, 7(F1000 Faculty Rev):1781 (<https://doi.org/10.12688/f1000research.15788.1>)

Latest published: 12 Nov 2018, 7(F1000 Faculty Rev):1781 (<https://doi.org/10.12688/f1000research.15788.1>)

## Abstract

### Abstract

Spinocerebellar ataxias (SCAs) are rare types of cerebellar ataxia with a dominant mode of inheritance. To date, 47 SCA subtypes have been identified, and the number of genes implicated in SCAs is continually increasing. Polyglutamine (polyQ) expansion diseases (*ATXN1/SCA1*, *ATXN2/SCA2*, *ATXN3/SCA3*, *CACNA1A/SCA6*, *ATXN7/SCA7*, *TBP/SCA17*, and *ATN1/DRPLA*) are the most common group of SCAs. No preventive or curative treatments are currently available, but various therapeutic approaches, including RNA-targeting treatments, such as antisense oligonucleotides (ASOs), are being developed. Clinical trials of ASOs in SCA patients are already planned. There is, therefore, a need to identify valid outcome measures for such studies. In this review, we describe recent advances towards identifying appropriate biomarkers, which are essential for monitoring disease progression and treatment efficacy. Neuroimaging biomarkers are the most powerful markers identified to date, making it possible to reduce sample sizes for clinical trials. Changes on brain MRI are already evident at the premanifest stage in SCA1 and SCA2 carriers and are correlated with CAG repeat size. Other potential biomarkers have also been developed, based on neurological examination, oculomotor study, cognitive assessment, and blood and cerebrospinal fluid analysis. Longitudinal studies based on multimodal approaches are required to establish the relationships between parameters and to validate the biomarkers identified.

### Keywords

spinocerebellar ataxias, biomarkers, antisense oligonucleotides, clinical trials, neuroimaging

## Open Peer Review

Referee Status:

	Invited Referees		
	1	2	3
version 1 published 12 Nov 2018			

F1000 Faculty Reviews are commissioned from members of the prestigious F1000 Faculty. In order to make these reviews as comprehensive and accessible as possible, peer review takes place before publication; the referees are listed below, but their reports are not formally published.

- 1 Harry Orr, University of Minnesota, USA
- 2 Bing-wen Soong, Taipei Medical University, Taiwan
- 3 Vikram G Shakkottai, University of Michigan, USA

## Discuss this article

Comments (0)

**Corresponding author:** Alexandra Durr ([alexandra.durr@icm-institute.org](mailto:alexandra.durr@icm-institute.org))

**Author roles:** **Coarelli G:** Conceptualization, Data Curation, Writing – Original Draft Preparation, Writing – Review & Editing; **Brice A:** Supervision, Validation, Writing – Review & Editing; **Durr A:** Conceptualization, Supervision, Validation, Writing – Original Draft Preparation, Writing – Review & Editing

**Competing interests:** No competing interests were disclosed.

**Grant information:** The author(s) declared that no grants were involved in supporting this work.

**Copyright:** © 2018 Coarelli G *et al.* This is an open access article distributed under the terms of the [Creative Commons Attribution Licence](#), which permits unrestricted use, distribution, and reproduction in any medium, provided the original work is properly cited.

**How to cite this article:** Coarelli G, Brice A and Durr A. **Recent advances in understanding dominant spinocerebellar ataxias from clinical and genetic points of view [version 1; referees: 3 approved]** *F1000Research* 2018, 7(F1000 Faculty Rev):1781 (<https://doi.org/10.12688/f1000research.15788.1>)

**First published:** 12 Nov 2018, 7(F1000 Faculty Rev):1781 (<https://doi.org/10.12688/f1000research.15788.1>)

## Introduction

Spinocerebellar ataxias (SCAs) are a group of neurodegenerative diseases displaying autosomal dominant inheritance. To date, 47 SCA subtypes have been described, and 35 causal genes have been identified<sup>1</sup>. SCAs are considered a rare group of cerebellar ataxias, with a mean prevalence of 2.7/100,000<sup>2</sup>. Their most frequent forms are polyglutamine (polyQ) expansion diseases (*ATXN1/SCA1*, *ATXN2/SCA2*, *ATXN3/SCA3*, *CACNA1A/SCA6*, *ATXN7/SCA7*, *TBP/SCA17*, and *ATN1/DRPLA*)<sup>3</sup>. These diseases manifest above a threshold number of CAG repeats, which is different for each gene. The same mutational mechanism is found in Huntington disease<sup>4</sup> and in spinal bulbar muscular atrophy<sup>5</sup>. Disease onset generally occurs between the ages of 20 and 40 years, and age at onset and CAG repeat expansion size are inversely correlated<sup>6,7</sup>. Age at onset also displays variability due to interactions between polyQ genes, i.e. between the expanded allele and the alleles of normal repeat size in the other genes<sup>8,9</sup>. The instability of expanded alleles results in genetic anticipation in successive generations<sup>3</sup>. Unsteady gait and clumsiness are usually the first clinical symptoms at onset, followed by a progressive loss of the ability to walk. Cerebellar syndrome is often associated with extracerebellar signs (pyramidal syndrome, extrapyramidal syndrome, retinal degeneration, dementia, seizures, etc.)<sup>3</sup>. There is currently no preventive or curative treatment, but different therapeutic approaches are being tested, including the use of disease-modifying compounds and therapeutic approaches, which are described below. However, in SCAs, the lack of sensitive biomarkers and the small number of patients to be included in clinical trials are a challenge for the statistical sample size estimation. Outcome measures providing information about treatment efficacy are vital, particularly for these genetic diseases that can be treated before the onset of symptoms. This review provides an overview of findings for biomarkers, recent results of clinical trials in SCA patients, and future perspectives for treatment.

## Natural history of spinocerebellar ataxias (SCA1, 2, 3, and 6)

The natural history of SCA1, 2, 3, and 6 was established by the longitudinal European cohort study EUROSCA, which included 462 patients with at least one year of follow-up and a median of 49 months of observation<sup>10</sup>. This study used the Scale for the Assessment and Rating of Ataxia (SARA), an accurate measurement of cerebellar dysfunction<sup>11,12</sup> in SCA1, 2, 3, and 6 patients and premanifest individuals<sup>13</sup>. The most severe disease turned out to be SCA1, with an annual progression of 2.11 on the 40-point SARA, followed by SCA3 (1.56 points), SCA2 (1.49 points), and SCA6 (0.8 points)<sup>10</sup>. SCA1 has also been reported to have the most severe prognosis for progression in other studies, such as one in Europe<sup>14</sup> and another conducted by the North American consortium (the Clinical Research Consortium for Spinocerebellar Ataxias)<sup>15</sup>. This may be because of motoneuron involvement, which, particularly in this form, leads to bulbar dysfunction and, thus, to respiratory and swallowing failure<sup>16</sup>. These results are consistent with 10-year survival, which is lowest for SCA1 patients, intermediate for SCA2 and SCA3, and highest for SCA6 patients<sup>17</sup>. A high SARA score has also been identified as one of the strongest risk factors for death in all

subtypes. Other associated risk factors include dysphagia for SCA1, longer CAG length in pathologic allele for SCA2, and dystonia and interaction between age and CAG length in SCA3<sup>17</sup>. The Composite Cerebellar Functional Severity (CCFS) score is another quantitative score for assessing cerebellar ataxia that has been validated in adults and children<sup>18,19</sup>. This score is calculated from scores for two tasks for the dominant hand—the nine-hole pegboard test and the click test—and is age dependent and available from an open source (<https://icm-institute.org/en/tutorial-for-making-ccfs-board/>). In a study on Friedreich ataxia and SCA1, 2, 3, and 7 patients, SARA and CCFS scores were higher in SCAs than in Friedreich ataxia after adjustment for disease duration, revealing a slower progression in Friedreich ataxia than in SCAs. Considering each SCA subtype separately, SCA2 and SCA1 patients had higher CCFS scores than did patients with other subtypes, despite an absence of difference in SARA scores<sup>20</sup>, probably because of the more accentuate cerebellar syndrome.

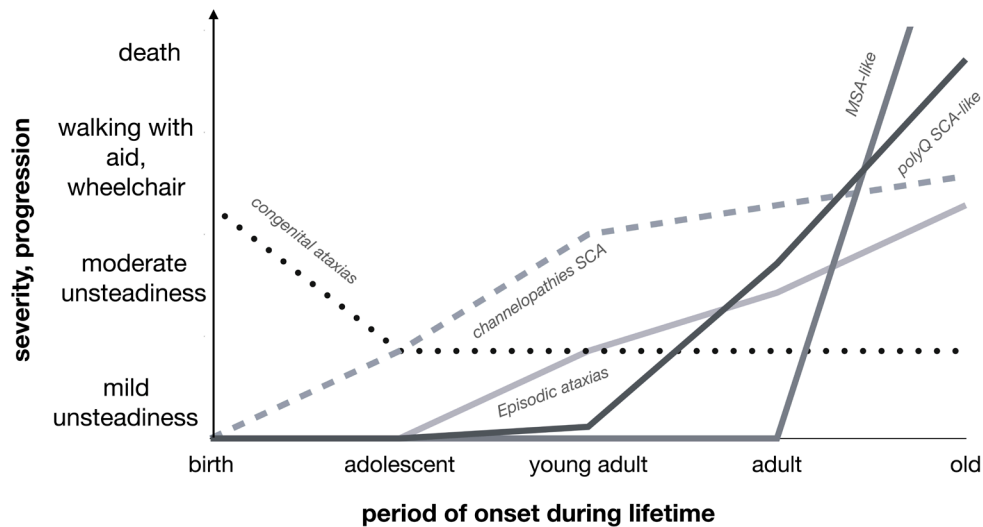
Based on SARA score progression, the EUROSCA study identified, for each genotype, the sample sizes required to detect a 50% decrease in SARA score progression in a two-arm clinical trial lasting one year: 142 patients for SCA1, 172 for SCA2, 202 for SCA3, and 602 for SCA6<sup>10</sup>. These are large numbers of patients for such rare diseases, making it necessary to carry out clinical trials at an international level. Additional biomarkers are required to overcome this problem. Furthermore, these dominantly inherited cerebellar ataxias have very different progression profiles, as shown in [Figure 1](#). Given the progressive nature of the disease and the sample sizes required, biomarkers are very important and essential.

## Biomarkers

### Neuroimaging biomarkers

The most powerful biomarkers identified to date are derived from neuroimaging examinations. Specific patterns of brain atrophy have been described *in vivo* in polyQ SCAs<sup>21,22</sup> and confirmed in post-mortem studies<sup>23,24</sup>. Changes in brain MRI findings are already evident at the premanifest stage in SCA1 and SCA2 carriers in the form of losses of gray matter from the cerebellum and brainstem. In SCA2 carriers only, an additional decrease in brainstem volume relative to non-carriers has also been reported<sup>13</sup>. A recent case-control study on a Cuban-German cohort of premanifest and manifest SCA2 carriers reported remarkable decreases in cerebellum and pontine volume and in the anteroposterior diameter of the pontine brainstem. A negative correlation was found between CAG repeat size and brainstem and cerebellum volume in premanifest individuals<sup>25</sup>. Cerebellar and pons atrophy was more pronounced in manifest patients<sup>25</sup>, representing a potential outcome measure. By contrast, midbrain and medulla volumes did not differ significantly between the preclinical and clinical stages<sup>25</sup>. In SCA2, white matter alterations in the parietal lobe and anterior corona radiata (detected by fractional anisotropy), and in the cerebellum and middle cerebellar peduncle (detected by mean diffusivity), were found to be correlated with SARA scores, leading the authors of the report concerned to suggest that connections between the motor and sensory integration areas might be impaired<sup>26</sup>. However, with





**Figure 1. Progression and severity profiles in cerebellar ataxias by underlying etiology.** Multisystem atrophy (MSA) is a rapidly progressing non-monogenic alpha-synucleinopathy. It is the most severe of these diseases, followed by polyglutamine (polyQ) spinocerebellar ataxias (SCAs), such as *ATXN1/SCA1*, *ATXN2/SCA2*, *ATXN3/SCA3*, *CACNA1A/SCA6*, *ATXN7/SCA7*, *TBP/SCA17*, and *ATN1/DRPLA*. Very different profiles are present in the forms because of missense mutations in channel genes (*CACNA1A*, *KCND3*, *KCNC3*, and *KCNA1*).

the exception of rare follow-up studies<sup>21,27</sup>, only cross-sectional brain MRI studies have been performed to date. Longitudinal studies will be required to establish the rate of progression of cerebellar and brainstem atrophy.

Cervical spinal cord atrophy has been proposed as a possible biomarker for SCA1, as it is correlated with SARA score, CAG repeat length, and disease duration<sup>28</sup>. Indeed, the clinical presentation of this subtype can include pyramidal signs and it may, at early stages, mimic spastic paraplegia<sup>29</sup>. Cervical spinal cord atrophy has also been identified as a potential biomarker for SCA3<sup>30</sup>.

Neurochemical abnormalities can be detected by MRI spectroscopy (MRS), as demonstrated by the group headed by Gulin Oz<sup>31</sup>. Decreases in N-acetylaspartate and glutamate levels reflect a loss of neurons, whereas increases in myoinositol serve as a marker of gliosis. N-acetylaspartate and N-acetylaspartylglutamate levels are significantly lower in the vermis and pons of SCA1, 2, 3, and 7 patients than in controls. Myoinositol levels are higher in SCA1, 2, and 3 patients than in controls. This neurochemical profile is particularly evident in SCA2 and SCA3 patients and is correlated with SARA score<sup>32</sup>. Interestingly, multicenter acquisition of this technique has been validated<sup>32</sup>.

Such alterations have been demonstrated by ultra-high-field MRS, even at the premanifest stage, with SCA2 patients showing the most compromised profile, followed by SCA1, SCA3, and SCA6 variant carriers<sup>31</sup>.

Another recent neuroimaging technique applied to SCAs is functional MRI (fMRI) at rest<sup>33</sup> or during a task<sup>34</sup>. This technique can be used to characterize circuitry reorganization, making it possible to identify specific patterns of cerebellar activation<sup>35,36</sup>.

Using this approach in the early phase of SCA3 disease, Duarte *et al.* discovered a reorganization of the motor network that could potentially serve as a biomarker<sup>37</sup>. However, more detailed analyses of fMRI outcomes are required for future application.

Neuroimaging biomarkers are more powerful than clinical scores for the detection of disease progression. In a cohort of SCA1, 2, 3, and 7 patients, greater longitudinal effect size was detected for brain volumetry (>1.2) than SARA and CCFS scores (<0.8)<sup>27</sup>. In conclusion, measures of pons and cerebellum atrophy seem to be the most promising biomarkers.

### Oculomotor biomarkers

Oculomotor involvement is present at an early phase of SCA and is detectable even at premanifest stages as a higher rate of gaze-evoked nystagmus or other alterations, such as a square-wave jerk during central fixation, impaired vertical smooth pursuit, slow saccade, and a higher antisaccade error rate in SCA3 carriers than controls<sup>13,38,39</sup>. These alterations have been studied in detail in SCA2 patients, all of whom present specific oculomotor abnormalities (slow horizontal saccades up to saccade paresis)<sup>40</sup>. Preclinical SCA2 carriers present a reduced saccade velocity and antisaccade task errors<sup>41</sup>.

Moreover, in manifest and premanifest SCA2 carriers, both the progression of oculomotor impairment and the slowing of horizontal saccade velocity are correlated, respectively, with CAG repeat size<sup>42</sup> and pontine atrophy<sup>25</sup>. The annual decrease in saccade velocity and saccade accuracy and an increase in saccade latency may soon be used as biomarkers. This correlation between saccade measurements and other parameters, such as brain MRI and/or cognitive assessment, may make it possible to reduce sample size in future trials<sup>42</sup>.

## Biological biomarkers

No biological biomarkers for SCAs have yet been identified, a situation contrasting with other neurodegenerative diseases, such as Alzheimer's disease and frontotemporal dementia. There is, therefore, a need to search for blood or cerebrospinal fluid (CSF) biomarkers of these diseases. In addition to guiding diagnostic process, biomarkers may be of use in clinical management if linked to disease progression.

In this respect, several recent studies in patients with SCA3, the most frequent SCA subtype, have yielded promising results. *SIRT1* encodes sirtuin-1, an NAD<sup>+</sup>-dependent deacetylase involved in several cellular functions, including chromatin modulation, the cell cycle, apoptosis, and autophagy regulation in response to DNA damage. *SIRT1* mRNA levels are lower in SCA3 mice than in wild-type mice and are also low in the fibroblasts of SCA3 patients<sup>43</sup>. In SCA3 mice, the rescue of *SIRT1* by caloric restriction or the administration of resveratrol induces motor improvement and neuropathological changes, such as a decrease in neuroinflammation and reactive gliosis with an activation of autophagy<sup>43</sup>. *SIRT1* overexpression has been shown to activate autophagy and thus to induce higher levels of mutant protein clearance. For these reasons, resveratrol may be a useful neuroprotective drug, as shown in some assays in *Drosophila* models of SCA3<sup>44</sup> and in the rat 3-acetylpyridine-induced cerebellar ataxia model<sup>45</sup>. Other studies have also demonstrated an imbalance between autophagy and apoptosis in SCA3. For example, an increase has been reported in the levels of *BECN1*, encoding the proautophagic Beclin 1 protein<sup>46</sup>, and *BCL2/BAX* ratio has been shown to be lower in pre-ataxic SCA3 carriers than in controls<sup>47</sup>, enhancing apoptotic processes.

Oxidative stress has been implicated in several neurodegenerative disorders, and SCA3 patients have been shown to produce abnormally large amounts of reactive oxygen species<sup>48</sup>. This phenomenon results from a decrease in antioxidant capacity: both superoxide dismutase and glutathione peroxidase (GPx) activities are lower in symptomatic than in pre-symptomatic carriers<sup>49</sup>. Moreover, the observed correlation of the decrease in GPx levels with disease severity suggests that GPx may be a reliable biomarker<sup>49</sup>.

Cytokines have also been investigated as possible markers of SCA3. Indeed, enhanced inflammation has been linked to stronger staining for IL1B and IL6 and higher levels of activated microglia and reactive astrocytes in the brains of SCA3 patients<sup>50</sup>. In a study on Brazilian SCA3 patients, no difference in cytokine levels was detected between 79 carriers and 43 controls. On the contrary, higher eotaxin levels were observed in asymptomatic carriers than in symptomatic carriers. It has been suggested that the levels of eotaxin released by astrocytes are inversely correlated with disease progression<sup>51</sup>. In another cohort of SCA3 patients recruited in the Azores, lower IL6 mRNA levels, due to the presence of the IL6\*C allele, were associated with an earlier age at onset than the presence of the IL6\*G allele<sup>52</sup>. In this study, the earlier age at onset (by about 10 years on average) resulted from the presence of the APOE\*e2 allele in IL6\*C

carriers, probably because of additional decreases in the levels of other cytokines, such as IL1B and TNF, due to the presence of the APOE\*e2 allele<sup>53</sup>.

In a recent study, serum neurofilament light chain (Nfl) was identified as a powerful potential serum biomarker in polyQ SCAs<sup>54</sup>. Neurofilaments are components of the neuron cytoskeleton, and their levels in the blood reflect damage to the axons of long fiber tracts<sup>55</sup>. In Huntington disease, which is also a polyQ disease, a correlation between serum Nfl levels and disease severity (UHDRS, cognitive decline, brain atrophy) has been reported, even after adjustment for age and CAG repeat size<sup>56</sup>. Nfl dosage is also useful for predicting disease onset in pre-symptomatic carriers and the progression of Huntington disease<sup>56</sup>. In a study by Wilke *et al.*, Nfl levels were higher in SCAs patients than in controls, particularly for SCA1 and SCA3<sup>54</sup>. The CSF has been only briefly explored in SCAs. CSF Nfl levels are a potential diagnostic and prognostic biomarker for SCAs, as in amyotrophic lateral sclerosis<sup>57</sup>. A study in SCA1, SCA2, and SCA6 patients evaluated  $\alpha$ -synuclein, DJ-1, and glial fibrillary acidic protein levels in CSF. The levels of all of these proteins were higher in CSF from patients than in control CSF, but this difference was significant only for tau, the levels of which were significantly higher in SCA2 patients. No correlations were found for CAG repeat size, disease severity, and disease duration<sup>58</sup>. It will be very interesting to determine polyQ protein levels in the CSF of SCA patients, as has been done already for Huntington disease.

## Cognition in spinocerebellar ataxias

Cognitive impairment, of various degrees of severity, can occur in polyQ SCAs. It involves mostly the executive functions and verbal memory, as shown in one of the first cognitive studies to compare the profiles of SCA1, 2, and 3 patients<sup>59</sup>. Cognitive decline was more prominent and rapid in SCA1 than in the other genotypes<sup>59-61</sup> and was associated with an increase in the incidence of depression<sup>61</sup>. In another study, SCA2 patients were found to have more visuospatial and visuo-perceptive deficits than SCA1 patients<sup>62</sup>. In a recent study focusing on cognitive dysfunction in SCA6 patients, mild impairments of executive functions, mental flexibility, and visuospatial skills were found to be correlated with decreased resting-state connectivity in the frontoparietal network<sup>63</sup>. These data support a role for the cerebellum in cognitive processes, given that the cerebellum is the principal cerebral structure affected and neuronal loss is less severe in SCA6 than in other polyQ diseases<sup>23</sup>. The scales most widely used to assess dementia, such as the Mini-Mental State Examination or Montreal Cognitive Assessment, are not appropriate for the detection of cognitive impairment in SCA patients, who present a cerebellar cognitive affective/Schmahmann's syndrome (CCAS)<sup>64</sup>. This syndrome includes executive dysfunctions, spatial cognition difficulties, language deficits, and personality changes. A CCAS scale has recently been validated in a large cohort of cerebellar patients with acquired, genetic, or idiopathic cause and shown to have a sensitivity of 95% and a selectivity of 78% for CCAS diagnosis<sup>64</sup>. This scale, which is easy and fast to administer, can be used for cognitive evaluation, which should be performed in longitudinal studies of patients.

### Genetic advances in spinocerebellar ataxias

The number of genes implicated in SCAs has steadily increased over time. The last causal gene to have been identified, in SCA47 patients, is *PUM1*, encoding Pumilio1, a member of the PUMILIO/FBF RNA-binding protein family. The loss of *Pum1* led to an SCA1-like phenotype in mice by causing a 30–40% increase in wild-type *Atxn1* protein levels in the cerebellum<sup>65</sup>. These two proteins are functionally related: in SCA1 mice, the disease is more severe if one copy of *Pum1* is removed, whereas the motor phenotype of *Pum1*-heterozygous mice is improved by the removal of one copy of *Atxn1*<sup>65</sup>. Mutations of *PUM1* were reported by Gennarino *et al.* in 15 patients, with different ages at disease onset (5 months to 50 years) and phenotypic presentations. A 50% loss of the protein resulted in a severe infantile disease and a developmental syndrome called Pumilio1-associated developmental disability, ataxia, and seizure (PADDAS), whereas the loss of 25% of the protein caused Pumilio1-related cerebellar ataxia (PRCA), with a later onset and incomplete penetrance<sup>66</sup>.

Using whole-exome sequencing (WES), Nibbeling *et al.* identified the genes associated with SCA46 and SCA45: *PLD3* and *FAT2*, respectively. These genes, which are strongly expressed in the cerebellum, cause pure adult-onset cerebellar ataxia. However, in some cases, SCA46 patients may present with a sensory neuropathy<sup>67</sup>.

Genes encoding ion channels are frequently involved in dominant cerebellar ataxia: mutations of *CACNA1A* are the most frequent genetic cause of autosomal dominant cerebellar ataxia in patients negative for polyQ SCAs, followed by other channel-coding genes, such as *KCND3*, *KCNC3*, and *KCNA1*<sup>68</sup>. These genes predispose the patient to an earlier disease onset, intellectual deficiency, and slower disease progression<sup>68</sup>. *CACNA1G* mutations, underlying SCA42<sup>69</sup>, lead to a slowly progressive pure<sup>70</sup> or complicated cerebellar ataxia associated with a spastic gait<sup>69</sup>. Patients with earlier onset may also present facial dysmorphism, microcephaly, digital abnormalities, and seizures<sup>71</sup>.

Another channel gene implicated in SCA44 is *GRM1*, encoding the metabotropic glutamate receptor 1 (mGluR1) responsible for two phenotypic manifestations: adult-onset cerebellar ataxia in the presence of gain-of-function mutations and early onset ataxia with intellectual deficiency when associated with loss-of-function mutations<sup>72</sup>.

The use of next-generation sequencing (NGS) techniques, such as WES, in everyday clinical practice has increased the diagnostic rate of complex neurological diseases<sup>73,74</sup>. The application of NGS in ataxia patients has revealed new SCA genes and improved our knowledge of the molecular pathways involved in cerebellar ataxia. It also affects the development of new therapeutic approaches: for example, elucidation of the role of mGluR1 in the excitability of Purkinje cells led to experiments modulating mGluR1 activity in SCA1 mice with drugs such as baclofen or the negative allosteric modulator JNJ16259685, both of which improved motor function<sup>75,76</sup>. As well, in a recent study by Bushart

*et al.*, the administration of potassium channel modulators induced improvement in SCA1 mice motor phenotype via electrophysiological changes<sup>77</sup>; the authors also showed that chlorzoxazone and baclofen co-administration was well tolerated by SCA1 patients and should be considered as a promising approach for treating symptoms<sup>77</sup>.

However, today, WES will not detect trinucleotide repeat disorders, mitochondrial DNA mutations, or large structural variants. Novel or *de novo* repeat expansions are still difficult to detect by short-read sequencing<sup>78</sup>. Tandem repeats are usually discarded by NGS pipelines, but bioinformatics efforts will be made to detect them. Recently, a novel intronic expansion, a pentanucleotide-repeat in *SAMD12*, has been identified in familial myoclonic epilepsy<sup>78</sup>. Long-read sequencing will probably allow one to identify more neurological repeat disorders.

### Therapeutic approaches in spinocerebellar ataxias

Over the last few years, several disease-modifying treatments have been tested with different outcomes. The most beneficial molecules to date are riluzole and valproic acid, whereas other drugs, such as lithium carbonate, trimethoprim-sulfamethoxazole, or zinc, have no significant effect<sup>79</sup>. A randomized placebo-controlled clinical trial in 40 SCA patients (SCA1, 2, 6, 8, and 10) and 20 Friedreich ataxia patients treated with riluzole (100 mg/day) for 12 months revealed a one-point improvement in SARA score in treated patients compared to the placebo group<sup>80</sup>. The use of valproic acid (1,200 mg/day) in SCA3 patients resulted in a SARA score at 12 weeks lower than that obtained for patients on placebo<sup>81</sup>. However, further trials are required to identify the genotype associated with a positive response to riluzole (ClinicalTrials.gov Identifier: NCT03347344).

Based on the hypothesis that one of the main omega-3 polyunsaturated fatty acids of the cerebellum, docosahexaenoic acid (DHA), is present at low levels in SCA38 patients owing to *ELOVL5* mutations, a clinical trial of DHA (600 mg/day) was performed<sup>82</sup>. This drug improved SARA score at 16 weeks in a small group of SCA38 patients and it also increased cerebellar metabolism, as shown by a brain 18-fluorodeoxyglucose positron emission tomography scan at 40 weeks<sup>82</sup>.

However, the most encouraging and innovative strategies developed to date are RNA-targeting therapies for polyQ SCAs, which have been validated in several mouse models<sup>83,84</sup>. These approaches mostly use antisense oligonucleotides (ASOs) to downregulate levels of the pathological polyQ protein. SCA2 mice treated with intrathecal ASOs display improvements in motor abilities, a recovery of Purkinje cell firing frequency, and lower levels of mutated ATXN2 protein<sup>85</sup>. ASOs have also been administered to SCA3 mice and were found to be well tolerated and to decrease the production of mutated protein<sup>86</sup>. A correlation was also found with electrophysiological changes in Purkinje cells<sup>87</sup>. These treatments may be used in patients with polyQ SCAs at early stages of the disease, even before the onset of symptoms. The long-term effects of decreasing levels of wild-type and mutated proteins and of decreasing the levels of other polyQ proteins remain unclear. The use of allele-

specific ASOs may be required<sup>88</sup>. A therapeutic approach based on ASOs is already at an advanced stage of development for Huntington disease<sup>89</sup>, and a phase 1A clinical trial in patients has yielded promising results<sup>90</sup>. ASO-based treatments are also being used for spinal muscular atrophy, in a different context, to retain exon 7 and produce a full-length SMN protein, with promising results<sup>91,92</sup>.

The advent of disease-modifying treatments for SCAs, including ASOs, will require the rapid identification and validation of robust biomarkers of disease progression or processes for the assessment of treatment response.

## Conclusion

This review summarizes recent clinical and genetic advances in dominant SCAs, including discoveries of novel SCAs, development of biomarkers, and therapeutic progress. The identification of biomarkers will be essential to demonstrate treatment efficacy. Future longitudinal studies based on multimodal approaches to elucidate the relationships between parameters will be required for the establishment of valid biomarkers. To date, gene suppression therapies are the most promising in polyQ SCAs, and clinical trials in the next few years are justified.

## Abbreviations

ASO, antisense oligonucleotide; CCAS, cerebellar cognitive affective/Schmahmann's syndrome; CCFS, Composite Cerebellar Functional Severity; CSF, cerebrospinal fluid; DHA, docosahexaenoic acid; fMRI, functional MRI; GPx, glutathione peroxidase; mGluR1, metabotropic glutamate receptor 1; MRS, MRI spectroscopy; Nfl, neurofilament light; NGS, next-generation sequencing; polyQ, polyglutamine; SARA, Scale for the Assessment and Rating of Ataxia; SCA, spinocerebellar ataxia; WES, whole-exome sequencing.

## Grant information

The author(s) declared that no grants were involved in supporting this work.

## Acknowledgments

We thank the patients' associations for their continuous support of our research: Association Connaitre les Syndromes Cérébelleux, Association Strumpell-Lorrain, Association Française de l'Ataxie de Friedreich, and the Tom Wahlig Foundation.

## References



1. **Online Mendelian inheritance in man.** OMIM Baltimore, MD: McKusick-Nathans Institute of Genetic Medicine, Johns Hopkins University. [Reference Source](#)
2. Ruano L, Melo C, Silva MC, *et al.*: **The global epidemiology of hereditary ataxia and spastic paraplegia: a systematic review of prevalence studies.** *Neuroepidemiology*. 2014; **42**(3): 174–83. [PubMed Abstract](#) | [Publisher Full Text](#)
3. Durr A: **Autosomal dominant cerebellar ataxias: polyglutamine expansions and beyond.** *Lancet Neurol*. 2010; **9**(9): 885–94. [PubMed Abstract](#) | [Publisher Full Text](#)
4. MacDonald ME, Ambrose CM, Duyao MP, *et al.*: **A novel gene containing a trinucleotide repeat that is expanded and unstable on Huntington's disease chromosomes. The Huntington's Disease Collaborative Research Group.** *Cell*. 1993; **72**(6): 971–83. [PubMed Abstract](#) | [Publisher Full Text](#)
5. La Spada AR, Wilson EM, Lubahn DB, *et al.*: **Androgen receptor gene mutations in X-linked spinal and bulbar muscular atrophy.** *Nature*. 1991; **352**(6330): 77–9. [PubMed Abstract](#) | [Publisher Full Text](#)
6. Stevanin G, Dürr A, Brice A: **Clinical and molecular advances in autosomal dominant cerebellar ataxias: From genotype to phenotype and pathophysiology.** *Eur J Hum Genet*. 2000; **8**(1): 4–18. [PubMed Abstract](#) | [Publisher Full Text](#)
7. Orr HT, Zoghbi HY: **Trinucleotide repeat disorders.** *Annu Rev Neurosci*. 2007; **30**: 575–621. [PubMed Abstract](#) | [Publisher Full Text](#)
8. Tezenas du Montcel S, Durr A, Bauer P, *et al.*: **Modulation of the age at onset in spinocerebellar ataxia by CAG tracts in various genes.** *Brain*. 2014; **137**(Pt 9): 2444–55. [PubMed Abstract](#) | [Publisher Full Text](#) | [Free Full Text](#)
9. Tezenas du Montcel S, Durr A, Rakowicz M, *et al.*: **Prediction of the age at onset in spinocerebellar ataxia type 1, 2, 3 and 6.** *J Med Genet*. 2014; **51**(7): 479–86. [PubMed Abstract](#) | [Publisher Full Text](#) | [Free Full Text](#)
10. Jacobi H, Du Montcel ST, Bauer P, *et al.*: **Long-term disease progression in spinocerebellar ataxia types 1, 2, 3, and 6: a longitudinal cohort study.** *Lancet Neurol*. 2015; **14**(11): 1101–8. [PubMed Abstract](#) | [Publisher Full Text](#)
11. Schmitz-Hübisch T, du Montcel ST, Baliko L, *et al.*: **Scale for the assessment and rating of ataxia: development of a new clinical scale.** *Neurology*. 2006; **66**(11): 1717–20. [PubMed Abstract](#) | [Publisher Full Text](#)
12. Schmitz-Hübisch T, Fimmers R, Rakowicz M, *et al.*: **Responsiveness of different rating instruments in spinocerebellar ataxia patients.** *Neurology*. 2010; **74**(8): 678–84. [PubMed Abstract](#) | [Publisher Full Text](#)
13. Jacobi H, Reetz K, du Montcel ST, *et al.*: **Biological and clinical characteristics of individuals at risk for spinocerebellar ataxia types 1, 2, 3, and 6 in the longitudinal RISCA study: analysis of baseline data.** *Lancet Neurol*. 2013; **12**(7): 650–8. [PubMed Abstract](#) | [Publisher Full Text](#) | [F1000 Recommendation](#)
14. Monin ML, Tezenas du Montcel S, Marelli C, *et al.*: **Survival and severity in dominant cerebellar ataxias.** *Ann Clin Transl Neurol*. 2015; **2**(2): 202–7. [PubMed Abstract](#) | [Publisher Full Text](#) | [Free Full Text](#)
15. Ashizawa T, Figueroa KP, Perlman SL, *et al.*: **Clinical characteristics of patients with spinocerebellar ataxias 1, 2, 3 and 6 in the US; a prospective observational study.** *Orphanet J Rare Dis*. 2013; **8**: 177. [PubMed Abstract](#) | [Publisher Full Text](#) | [Free Full Text](#)
16. Orengo JP, van der Heijden ME, Hao S, *et al.*: **Motor neuron degeneration correlates with respiratory dysfunction in SCA1.** *Dis Model Mech*. 2018; **11**(2): pii: dmm032623. [PubMed Abstract](#) | [Publisher Full Text](#) | [Free Full Text](#) | [F1000 Recommendation](#)
17. Diallo A, Jacobi H, Cook A, *et al.*: **Survival in patients with spinocerebellar ataxia types 1, 2, 3, and 6 (EUROSCA): a longitudinal cohort study.** *Lancet Neurol*. 2018; **17**(4): 327–34. [PubMed Abstract](#) | [Publisher Full Text](#)
18. du Montcel ST, Charles P, Ribai P, *et al.*: **Composite cerebellar functional severity score: validation of a quantitative score of cerebellar impairment.** *Brain*. 2008; **131**(Pt 5): 1352–61. [PubMed Abstract](#) | [Publisher Full Text](#)
19. Filipovic Pierucci A, Mariotti C, Panzeri M, *et al.*: **Quantifiable evaluation of cerebellar signs in children.** *Neurology*. 2015; **84**(12): 1225–32. [PubMed Abstract](#) | [Publisher Full Text](#)
20. Tanguy Melac A, Mariotti C, Filipovic Pierucci A, *et al.*: **Friedreich and dominant ataxias: quantitative differences in cerebellar dysfunction measurements.** *J Neurol Neurosurg Psychiatry*. 2018; **89**(6): 559–65. [PubMed Abstract](#) | [Publisher Full Text](#)
21. Reetz K, Costa AS, Mirzazade S, *et al.*: **Genotype-specific patterns of atrophy progression are more sensitive than clinical decline in SCA1, SCA3 and SCA6.** *Brain*. 2013; **136**(Pt 3): 905–17. [PubMed Abstract](#) | [Publisher Full Text](#)



22. Mascalchi M, Diciotti S, Giannelli M, *et al.*: **Progression of brain atrophy in spinocerebellar ataxia type 2: a longitudinal tensor-based morphometry study.** *PLoS One*. 2014; 9(2): e89410.  
[PubMed Abstract](#) | [Publisher Full Text](#) | [Free Full Text](#)
23. Seidel K, Siswanto S, Brunt ERP, *et al.*: **Brain pathology of spinocerebellar ataxias.** *Acta Neuropathol*. 2012; 124(1): 1–21.  
[PubMed Abstract](#) | [Publisher Full Text](#)
24. Scherzed W, Brunt ER, Heinsen H, *et al.*: **Pathoanatomy of cerebellar degeneration in spinocerebellar ataxia type 2 (SCA<sub>2</sub>) and type 3 (SCA<sub>3</sub>).** *Cerebellum*. 2012; 11(3): 749–60.  
[PubMed Abstract](#) | [Publisher Full Text](#)
25. F Reetz K, Rodríguez-Labrada R, Dogan I, *et al.*: **Brain atrophy measures in preclinical and manifest spinocerebellar ataxia type 2.** *Ann Clin Transl Neurol*. 2018; 5(2): 128–37.  
[PubMed Abstract](#) | [Publisher Full Text](#) | [Free Full Text](#) | [F1000 Recommendation](#)
26. Hernandez-Castillo CR, Galvez V, Mercadillo R, *et al.*: **Extensive White Matter Alterations and Its Correlations with Ataxia Severity in SCA 2 Patients.** *PLoS One*. 2015; 10(8): e0135449.  
[PubMed Abstract](#) | [Publisher Full Text](#) | [Free Full Text](#)
27. Adanyeguh IM, Perlberg V, Henry PG, *et al.*: **Autosomal dominant cerebellar ataxias: Imaging biomarkers with high effect sizes.** *Neuroimage Clin*. 2018; 19: 858–67.  
[PubMed Abstract](#) | [Publisher Full Text](#) | [Free Full Text](#)
28. F Martins CR Jr, Martinez ARM, de Rezende TJR, *et al.*: **Spinal Cord Damage in Spinocerebellar Ataxia Type 1.** *Cerebellum*. 2017; 16(4): 792–6.  
[PubMed Abstract](#) | [Publisher Full Text](#) | [F1000 Recommendation](#)
29. Pedrosa JL, de Souza PV, Pinto WB, *et al.*: **SCA1 patients may present as hereditary spastic paraplegia and must be included in spastic-ataxias group.** *Parkinsonism Relat Disord*. 2015; 21(10): 1243–6.  
[PubMed Abstract](#) | [Publisher Full Text](#)
30. Fahl CN, Branco LM, Bergo FP, *et al.*: **Spinal cord damage in Machado-Joseph disease.** *Cerebellum*. 2015; 14(2): 128–32.  
[PubMed Abstract](#) | [Publisher Full Text](#)
31. F Joers JM, Deelchand DK, Lyu T, *et al.*: **Neurochemical abnormalities in premanifest and early spinocerebellar ataxias.** *Ann Neurol*. 2018; 83(4): 816–29.  
[PubMed Abstract](#) | [Publisher Full Text](#) | [Free Full Text](#) | [F1000 Recommendation](#)
32. Adanyeguh IM, Henry PG, Nguyen TM, *et al.*: **In vivo neurometabolic profiling in patients with spinocerebellar ataxia types 1, 2, 3, and 7.** *Mov Disord*. 2015; 30(5): 662–70.  
[PubMed Abstract](#) | [Publisher Full Text](#) | [Free Full Text](#)
33. Coccozza S, Saccà F, Cervo A, *et al.*: **Modifications of resting state networks in spinocerebellar ataxia type 2.** *Mov Disord*. 2015; 30(10): 1382–90.  
[PubMed Abstract](#) | [Publisher Full Text](#)
34. F Guell X, Gabrieli JDE, Schmahmann JD: **Triple representation of language, working memory, social and emotion processing in the cerebellum: convergent evidence from task and seed-based resting-state fMRI analyses in a single large cohort.** *Neuroimage*. 2018; 172: 437–49.  
[PubMed Abstract](#) | [Publisher Full Text](#) | [Free Full Text](#) | [F1000 Recommendation](#)
35. Stefanescu MR, Dohnalek M, Maderwald S, *et al.*: **Structural and functional MRI abnormalities of cerebellar cortex and nuclei in SCA3, SCA6 and Friedreich's ataxia.** *Brain*. 2015; 138(Pt 5): 1182–97.  
[PubMed Abstract](#) | [Publisher Full Text](#) | [Free Full Text](#)
36. Deistung A, Stefanescu MR, Ernst TM, *et al.*: **Structural and Functional Magnetic Resonance Imaging of the Cerebellum: Considerations for Assessing Cerebellar Ataxias.** *Cerebellum*. 2016; 15(1): 21–5.  
[PubMed Abstract](#) | [Publisher Full Text](#)
37. Duarte JV, Faustino R, Lobo M, *et al.*: **Parametric fMRI of paced motor responses uncovers novel whole-brain imaging biomarkers in spinocerebellar ataxia type 3.** *Hum Brain Mapp*. 2016; 37(10): 3656–68.  
[PubMed Abstract](#) | [Publisher Full Text](#)
38. F Wu C, Chen DB, Feng L, *et al.*: **Oculomotor deficits in spinocerebellar ataxia type 3: Potential biomarkers of preclinical detection and disease progression.** *CNS Neurosci Ther*. 2017; 23(4): 321–8.  
[PubMed Abstract](#) | [Publisher Full Text](#) | [F1000 Recommendation](#)
39. Raposo M, Vasconcelos J, Bettencourt C, *et al.*: **Nystagmus as an early ocular alteration in Machado-Joseph disease (MJD/SCA3).** *BMC Neurol*. 2014; 14: 17.  
[PubMed Abstract](#) | [Publisher Full Text](#) | [Free Full Text](#)
40. Moscovich M, Okun MS, Favilla C, *et al.*: **Clinical evaluation of eye movements in spinocerebellar ataxias: a prospective multicenter study.** *J Neuroophthalmol*. 2015; 35(1): 16–21.  
[PubMed Abstract](#) | [Publisher Full Text](#) | [Free Full Text](#)
41. Velázquez-Pérez L, Rodríguez-Labrada R, Cruz-Rivas EM, *et al.*: **Comprehensive study of early features in spinocerebellar ataxia 2: Delineating the prodromal stage of the disease.** *Cerebellum*. 2014; 13(5): 568–79.  
[PubMed Abstract](#) | [Publisher Full Text](#)
42. Rodríguez-Labrada R, Velázquez-Pérez L, Auburger G, *et al.*: **Spinocerebellar ataxia type 2: Measures of saccade changes improve power for clinical trials.** *Mov Disord*. 2016; 31(4): 570–8.  
[PubMed Abstract](#) | [Publisher Full Text](#)
43. Cunha-Santos J, Duarte-Neves J, Carmona V, *et al.*: **Caloric restriction blocks neuropathology and motor deficits in Machado-Joseph disease mouse models through SIRT1 pathway.** *Nat Commun*. 2016; 7: 11445.  
[PubMed Abstract](#) | [Publisher Full Text](#) | [Free Full Text](#)
44. F Wu YL, Chang JC, Lin WY, *et al.*: **Caffeic acid and resveratrol ameliorate cellular damage in cell and Drosophila models of spinocerebellar ataxia type 3 through upregulation of Nrf2 pathway.** *Free Radic Biol Med*. 2018; 115: 309–17.  
[PubMed Abstract](#) | [Publisher Full Text](#) | [F1000 Recommendation](#)
45. F Ghorbani Z, Farahani RM, Aliaghaei A, *et al.*: **Resveratrol Protects Purkinje Neurons and Restores Muscle Activity in Rat Model of Cerebellar Ataxia.** *J Mol Neurosci*. 2018; 65(1): 35–42.  
[PubMed Abstract](#) | [Publisher Full Text](#) | [F1000 Recommendation](#)
46. F Kazachkova N, Raposo M, Ramos A, *et al.*: **Promoter Variant Alters Expression of the Autophagic BECN1 Gene: Implications for Clinical Manifestations of Machado-Joseph Disease.** *Cerebellum*. 2017; 16(5–6): 957–63.  
[PubMed Abstract](#) | [Publisher Full Text](#) | [F1000 Recommendation](#)
47. F Raposo M, Ramos A, Santos C, *et al.*: **Accumulation of Mitochondrial DNA Common Deletion Since The Preataxic Stage of Machado-Joseph Disease.** *Mol Neurobiol*. 2018; 1–6.  
[PubMed Abstract](#) | [Publisher Full Text](#) | [F1000 Recommendation](#)
48. Pacheco LS, da Silveira AF, Trott A, *et al.*: **Association between Machado-Joseph disease and oxidative stress biomarkers.** *Mutat Res*. 2013; 757(2): 99–103.  
[PubMed Abstract](#) | [Publisher Full Text](#)
49. F de Assis AM, Saute JAM, Longoni A, *et al.*: **Peripheral Oxidative Stress Biomarkers in Spinocerebellar Ataxia Type 3/Machado-Joseph Disease.** *Front Neurol*. 2017; 8: 485.  
[PubMed Abstract](#) | [Publisher Full Text](#) | [Free Full Text](#) | [F1000 Recommendation](#)
50. Evert BO, Schelhaas J, Fleischer H, *et al.*: **Neuronal intranuclear inclusions, dysregulation of cytokine expression and cell death in spinocerebellar ataxia type 3.** *Clin Neuropathol*. 2006; 25(6): 272–81.  
[PubMed Abstract](#)
51. da Silva Carvalho G, Saute JAM, Haas CB, *et al.*: **Cytokines in Machado Joseph Disease/Spinocerebellar Ataxia 3.** *Cerebellum*. 2016; 15(4): 518–25.  
[PubMed Abstract](#) | [Publisher Full Text](#)
52. F Raposo M, Bettencourt C, Ramos A, *et al.*: **Promoter Variation and Expression Levels of Inflammatory Genes IL1A, IL1B, IL6 and TNF in Blood of Spinocerebellar Ataxia Type 3 (SCA<sub>3</sub>) Patients.** *Neuromolecular Med*. 2017; 19(1): 41–5.  
[PubMed Abstract](#) | [Publisher Full Text](#) | [F1000 Recommendation](#)
53. Zhang H, Wu LM, Wu J: **Cross-talk between apolipoprotein E and cytokines.** *Mediators Inflamm*. 2011; 2011: 949072.  
[PubMed Abstract](#) | [Publisher Full Text](#) | [Free Full Text](#)
54. F Wilke C, Bender F, Hayer SN, *et al.*: **Serum neurofilament light is increased in multiple system atrophy of cerebellar type and in repeat-expansion spinocerebellar ataxias: a pilot study.** *J Neurol*. 2018; 265(7): 1818–24.  
[PubMed Abstract](#) | [Publisher Full Text](#) | [F1000 Recommendation](#)
55. Menke RA, Gray E, Lu CH, *et al.*: **CSF neurofilament light chain reflects corticospinal tract degeneration in ALS.** *Ann Clin Transl Neurol*. 2015; 2(7): 748–55.  
[PubMed Abstract](#) | [Publisher Full Text](#) | [Free Full Text](#)
56. Byrne LM, Rodrigues FB, Blennow K, *et al.*: **Neurofilament light protein in blood as a potential biomarker of neurodegeneration in Huntington's disease: a retrospective cohort analysis.** *Lancet Neurol*. 2017; 16(8): 601–9.  
[PubMed Abstract](#) | [Publisher Full Text](#) | [Free Full Text](#)
57. F Rossi D, Volanti P, Brambilla L, *et al.*: **CSF neurofilament proteins as diagnostic and prognostic biomarkers for amyotrophic lateral sclerosis.** *J Neurol*. 2018; 265(3): 510–21.  
[PubMed Abstract](#) | [Publisher Full Text](#) | [F1000 Recommendation](#)
58. Brouillette AM, Öz G, Gomez CM: **Cerebrospinal Fluid Biomarkers in Spinocerebellar Ataxia: A Pilot Study.** *Dis Markers*. 2015; 2015: 413098.  
[PubMed Abstract](#) | [Publisher Full Text](#) | [Free Full Text](#)
59. Bürk K, Globas C, Bösch S, *et al.*: **Cognitive deficits in spinocerebellar ataxia type 1, 2, and 3.** *J Neurol*. 2003; 250(2): 207–11.  
[PubMed Abstract](#) | [Publisher Full Text](#)
60. Moriarty A, Cook A, Hunt H, *et al.*: **A longitudinal investigation into cognition and disease progression in spinocerebellar ataxia types 1, 2, 3, 6, and 7.** *Orphanet J Rare Dis*. 2016; 11(1): 82.  
[PubMed Abstract](#) | [Publisher Full Text](#) | [Free Full Text](#)
61. Jacobi H, du Montcel ST, Bauer P, *et al.*: **Long-term evolution of patient-reported outcome measures in spinocerebellar ataxias.** *J Neurol*. 2018; 265(9): 2040–51.  
[PubMed Abstract](#) | [Publisher Full Text](#)
62. Fancellu R, Paridi D, Tomasello C, *et al.*: **Longitudinal study of cognitive and psychiatric functions in spinocerebellar ataxia types 1 and 2.** *J Neurol*. 2013; 260(12): 3134–43.  
[PubMed Abstract](#) | [Publisher Full Text](#)
63. F Pereira L, Airan RD, Fishman A, *et al.*: **Resting-state functional connectivity and cognitive dysfunction correlations in spinocerebellar ataxia type 6 (SCA6).** *Hum Brain Mapp*. 2017; 38(6): 3001–10.  
[PubMed Abstract](#) | [Publisher Full Text](#) | [F1000 Recommendation](#)
64. F Hoche F, Guell X, Vangel MG, *et al.*: **The cerebellar cognitive affective/ Schmahmann syndrome scale.** *Brain*. 2018; 141(1): 248–70.  
[PubMed Abstract](#) | [Publisher Full Text](#) | [Free Full Text](#) | [F1000 Recommendation](#)
65. Gennarino VA, Singh RK, White JJ, *et al.*: **Pumilio1 haploinsufficiency leads to SCA1-like neurodegeneration by increasing wild-type Ataxin1 levels.** *Cell*.

- 2015; **160**(6): 1087–98.  
[PubMed Abstract](#) | [Publisher Full Text](#) | [Free Full Text](#)
66. **F** Gennarino VA, Palmer EE, McDonell LM, *et al.*: **A Mild PUM1 Mutation Is Associated with Adult-Onset Ataxia, whereas Haploinsufficiency Causes Developmental Delay and Seizures.** *Cell*. 2018; **172**(5): 924–936.e11.  
[PubMed Abstract](#) | [Publisher Full Text](#) | [Free Full Text](#) | [F1000 Recommendation](#)
67. **F** Nibbeling EAR, Duarri A, Verschuuren-Bemelmans CC, *et al.*: **Exome sequencing and network analysis identifies shared mechanisms underlying spinocerebellar ataxia.** *Brain*. 2017; **140**(11): 2860–78.  
[PubMed Abstract](#) | [Publisher Full Text](#) | [F1000 Recommendation](#)
68. Coutelier M, Coarelli G, Monin ML, *et al.*: **A panel study on patients with dominant cerebellar ataxia highlights the frequency of channelopathies.** *Brain*. 2017; **140**(6): 1579–94.  
[PubMed Abstract](#) | [Publisher Full Text](#)
69. Coutelier M, Blesneac I, Monteil A, *et al.*: **A Recurrent Mutation in CACNA1G Alters Cav3.1 T-Type Calcium-Channel Conduction and Causes Autosomal-Dominant Cerebellar Ataxia.** *Am J Hum Genet*. 2015; **97**(5): 726–37.  
[PubMed Abstract](#) | [Publisher Full Text](#) | [Free Full Text](#)
70. Kimura M, Yabe I, Hama Y, *et al.*: **SCA42 mutation analysis in a case series of Japanese patients with spinocerebellar ataxia.** *J Hum Genet*. 2017; **62**(9): 857–9.  
[PubMed Abstract](#) | [Publisher Full Text](#)
71. Chemin J, Siquier-Pernet K, Nicouleau M, *et al.*: **De novo mutation screening in childhood-onset cerebellar atrophy identifies gain-of-function mutations in the CACNA1G calcium channel gene.** *Brain*. 2018; **141**(7): 1998–2013.  
[PubMed Abstract](#) | [Publisher Full Text](#)
72. **F** Watson LM, Bamber E, Schneckenberg RP, *et al.*: **Dominant Mutations in GRM1 Cause Spinocerebellar Ataxia Type 44.** *Am J Hum Genet*. 2017; **101**(3): 451–458.  
[PubMed Abstract](#) | [Publisher Full Text](#) | [Free Full Text](#) | [F1000 Recommendation](#)
73. Jiang T, Tan MS, Tan L, *et al.*: **Application of next-generation sequencing technologies in Neurology.** *Ann Transl Med*. 2014; **2**(12): 125.  
[PubMed Abstract](#) | [Publisher Full Text](#) | [Free Full Text](#)
74. **F** Lee H, Deignan JL, Dorrani N, *et al.*: **Clinical exome sequencing for genetic identification of rare Mendelian disorders.** *JAMA*. 2014; **312**(18): 1880–7.  
[PubMed Abstract](#) | [Publisher Full Text](#) | [Free Full Text](#) | [F1000 Recommendation](#)
75. **F** Shuvaev AN, Hosoi N, Sato Y, *et al.*: **Progressive impairment of cerebellar mGluR signalling and its therapeutic potential for cerebellar ataxia in spinocerebellar ataxia type 1 model mice.** *J Physiol*. 2017; **595**(1): 141–64.  
[PubMed Abstract](#) | [Publisher Full Text](#) | [Free Full Text](#) | [F1000 Recommendation](#)
76. **F** Power EM, Morales A, Empson RM: **Prolonged Type 1 Metabotropic Glutamate Receptor Dependent Synaptic Signaling Contributes to Spinocerebellar Ataxia Type 1.** *J Neurosci*. 2016; **36**(18): 4910–6.  
[PubMed Abstract](#) | [Publisher Full Text](#) | [F1000 Recommendation](#)
77. **F** Bushart DD, Chopra R, Singh V, *et al.*: **Targeting potassium channels to treat cerebellar ataxia.** *Ann Clin Transl Neurol*. 2018; **5**(3): 297–314.  
[PubMed Abstract](#) | [Publisher Full Text](#) | [Free Full Text](#) | [F1000 Recommendation](#)
78. **F** Ishiura H, Doi K, Mitsui J, *et al.*: **Expansions of intronic TTCA and TTTTA repeats in benign adult familial myoclonic epilepsy.** *Nat Genet*. 2018; **50**(4): 581–90.  
[PubMed Abstract](#) | [Publisher Full Text](#) | [F1000 Recommendation](#)
79. Zesiewicz TA, Wilmot G, Kuo SH, *et al.*: **Comprehensive systematic review summary: Treatment of cerebellar motor dysfunction and ataxia: Report of the Guideline Development, Dissemination, and Implementation Subcommittee of the American Academy of Neurology.** *Neurology*. 2018; **90**(10): 464–71.  
[PubMed Abstract](#) | [Publisher Full Text](#) | [Free Full Text](#)
80. Romano S, Coarelli G, Marcotulli C, *et al.*: **Riluzole in patients with hereditary cerebellar ataxia: a randomised, double-blind, placebo-controlled trial.** *Lancet Neurol*. 2015; **14**(10): 985–91.  
[PubMed Abstract](#) | [Publisher Full Text](#)
81. Lei LF, Yang GP, Wang JL, *et al.*: **Safety and efficacy of valproic acid treatment in SCA/MJD patients.** *Parkinsonism Relat Disord*. 2016; **26**: 55–61.  
[PubMed Abstract](#) | [Publisher Full Text](#)
82. **F** Manes M, Alberici A, Di Gregorio E, *et al.*: **Docosahexaenoic acid is a beneficial replacement treatment for spinocerebellar ataxia 38.** *Ann Neurol*. 2017; **82**(4): 615–21.  
[PubMed Abstract](#) | [Publisher Full Text](#) | [Free Full Text](#) | [F1000 Recommendation](#)
83. Keiser MS, Kordasiewicz HB, McBride JL: **Gene suppression strategies for dominantly inherited neurodegenerative diseases: lessons from Huntington's disease and spinocerebellar ataxia.** *Hum Mol Genet*. 2016; **25**(R1): R53–64.  
[PubMed Abstract](#) | [Publisher Full Text](#) | [Free Full Text](#)
84. Matos CA, de Almeida LP, Nóbrega C: **Machado-Joseph disease/spinocerebellar ataxia type 3: lessons from disease pathogenesis and clues into therapy.** *J Neurochem*. 2018.  
[PubMed Abstract](#) | [Publisher Full Text](#)
85. **F** Scoles DR, Meera P, Schneider MD, *et al.*: **Antisense oligonucleotide therapy for spinocerebellar ataxia type 2.** *Nature*. 2017; **544**(7650): 362–6.  
[PubMed Abstract](#) | [Publisher Full Text](#) | [F1000 Recommendation](#)
86. **F** Moore LR, Rajpal G, Dillingham IT, *et al.*: **Evaluation of Antisense Oligonucleotides Targeting ATXN3 in SCA3 Mouse Models.** *Mol Ther Nucleic Acids*. 2017; **7**: 200–10.  
[PubMed Abstract](#) | [Publisher Full Text](#) | [Free Full Text](#) | [F1000 Recommendation](#)
87. **F** McLoughlin HS, Moore LR, Chopra R, *et al.*: **Oligonucleotide therapy mitigates disease in spinocerebellar ataxia type 3 mice.** *Ann Neurol*. 2018; **84**(1): 64–77.  
[PubMed Abstract](#) | [Publisher Full Text](#) | [Free Full Text](#) | [F1000 Recommendation](#)
88. **F** Toonen LJA, Rigo F, van Attikum H, *et al.*: **Antisense Oligonucleotide-Mediated Removal of the Polyglutamine Repeat in Spinocerebellar Ataxia Type 3 Mice.** *Mol Ther Nucleic Acids*. 2017; **8**: 232–42.  
[PubMed Abstract](#) | [Publisher Full Text](#) | [Free Full Text](#) | [F1000 Recommendation](#)
89. Skotte NH, Southwell AL, Østergaard ME, *et al.*: **Allele-specific suppression of mutant huntingtin using antisense oligonucleotides: providing a therapeutic option for all Huntington disease patients.** *PLoS One*. 2014; **9**(9): e107434.  
[PubMed Abstract](#) | [Publisher Full Text](#) | [Free Full Text](#)
90. **F** Wild EJ, Tabrizi SJ: **Therapies targeting DNA and RNA in Huntington's disease.** *Lancet Neurol*. 2017; **16**(10): 837–47.  
[PubMed Abstract](#) | [Publisher Full Text](#) | [Free Full Text](#) | [F1000 Recommendation](#)
91. **F** Finkel RS, Mercuri E, Darras BT, *et al.*: **Nusinersen versus Sham Control in Infantile-Onset Spinal Muscular Atrophy.** *N Engl J Med*. 2017; **377**(18): 1723–32.  
[PubMed Abstract](#) | [Publisher Full Text](#) | [F1000 Recommendation](#)
92. **F** Mercuri E, Finkel R, Kirschner J, *et al.*: **Efficacy and safety of nusinersen in children with later-onset spinal muscular atrophy (SMA): End of study results from the phase 3 CHERISH study.** *Neuromuscular Disorders*. 2017; **27**(2): S210.  
[Publisher Full Text](#) | [F1000 Recommendation](#)

## Open Peer Review

Current Referee Status:



### Editorial Note on the Review Process

**F1000 Faculty Reviews** are commissioned from members of the prestigious **F1000 Faculty** and are edited as a service to readers. In order to make these reviews as comprehensive and accessible as possible, the referees provide input before publication and only the final, revised version is published. The referees who approved the final version are listed with their names and affiliations but without their reports on earlier versions (any comments will already have been addressed in the published version).

### The referees who approved this article are:

#### Version 1

- 1 **Vikram G Shakkottai** Department of Neurology, University of Michigan, Ann Arbor, MI, 48109-2200, USA  
**Competing Interests:** No competing interests were disclosed.
- 2 **Bing-wen Soong** Department of Neurology, Shuang Ho Hospital, Taipei Medical University, Taipei, Taiwan  
**Competing Interests:** No competing interests were disclosed.
- 3 **Harry Orr** Institute for Translational Neuroscience, University of Minnesota, Minneapolis, Minnesota, 55455, USA  
**Competing Interests:** No competing interests were disclosed.

The benefits of publishing with F1000Research:

- Your article is published within days, with no editorial bias
- You can publish traditional articles, null/negative results, case reports, data notes and more
- The peer review process is transparent and collaborative
- Your article is indexed in PubMed after passing peer review
- Dedicated customer support at every stage

For pre-submission enquiries, contact [research@f1000.com](mailto:research@f1000.com)

**F1000Research**

**Chapter 15 of the collected work entitled “Trials for Cerebellar Ataxias: From Cellular Models to Human Therapies”**

**Blood and CSF biomarkers in autosomal dominant cerebellar ataxias**

**Authors and Affiliations:**

Giulia Coarelli<sup>1</sup> and Alexandra Durr<sup>1</sup>

<sup>1</sup>Sorbonne Université, Institut du Cerveau - Paris Brain Institute - ICM, Inserm, CNRS, APHP, Hôpital de la Pitié Salpêtrière, Paris, France

**E-mails:**

Giulia Coarelli: [giulia.coarelli@icm-institute.org](mailto:giulia.coarelli@icm-institute.org)

Alexandra Durr: [alexandra.durr@icm-institute.org](mailto:alexandra.durr@icm-institute.org)

**Corresponding author:** Dr Giulia Coarelli, Paris Brain Institute, Pitié-Salpêtrière Paris CS21414, 75646 PARIS Cedex 13, France ; [giulia.coarelli@icm-institute.org](mailto:giulia.coarelli@icm-institute.org), tel. +33 1 57 27 46 82, fax. +33 1 57 27 47 26

**Keywords:** spinocerebellar ataxias, SCAs, biomarkers, gene therapy



## **Abstract**

A biomarker can be defined as a measurable indicator of the presence or severity of a disease state, often present before clinical signs are evident. For the most frequent forms of spinocerebellar ataxias (SCAs), due to expansions of coding CAG repeats, *SCA1/ATXN1*, *SCA2/ATXN2*, *SCA3/ATXN3*, *SCA6/CACNA1A*, *SCA7/ATXN7*, *SCA17/TBP* and *DRPLA/ATN1*, gene therapy for presymptomatic carriers are planned. Reliable biomarkers should indicate the pathological onset or discriminate disease stages that would allow to stratify patients and to monitor drug efficacy. This chapter reviews the available blood and cerebrospinal fluid (CSF) biomarkers. One of the most promising biomarker is Neurofilament light chain (NfL) for which blood and CSF levels accurately correlate. Moreover, NfL concentrations are associated with disease progression, and cerebellum and brainstem atrophy. Specific ataxin bioassays are in development for polyglutamine SCAs, but only ataxin-3 can be measured in blood and CSF. Other biomarkers are related to oxidative stress, inflammation, astrogliosis, and insulin pathway. Others are in development regarding the metabolism of cholesterol, lipids, and amino acids, as well as the micro-RNAs that would be potential biological markers of disease and therapeutic targets.

## 15.1 Introduction

Autosomal dominant cerebellar ataxias (ADCAs) are a rare cause of cerebellar ataxias. In genetic nomenclature, they referred to spinocerebellar ataxias (SCAs), a group of diseases clinically and genetically heterogeneous (1). Nowadays, forty-eight SCAs subtypes have been identified. The most frequent SCAs are due to pathological CAG repeat expansions coding for polyglutamine (polyQ): *SCA1/ATXN1*, *SCA2/ATXN2*, *SCA3/ATXN3*, *SCA6/CACNA1A*, *SCA7/ATXN7*, *SCA17/TBP* and *DRPLA/ATN1*. Age at onset and disease severity are negatively correlated with the pathological CAG repeat expansion (2), and phenotype is clearly associated with CAG repeat size (3). Pediatric and juvenile forms can also occur, especially for *SCA2* and *SCA7* (4,5). PolyQ subtypes clinically share the cerebellar ataxia with gait and balance impairment, limb dysmetria, dysarthria, swallowing difficulties and oculomotor abnormalities. However, other extra-cerebellar signs are also present: pyramidal syndrome for *SCA1*, *SCA3*, *SCA7*, *SCA17*, parkinsonism for *SCA2*, *SCA3*, *SCA7*, fasciculations and wasting for *SCA2*, peripheral neuropathy for *SCA2* and *SCA3*, dystonia for *SCA2*, *SCA3*, *SCA7*, *SCA17*, choreic movements for *SCA17*, ophthalmological deficit for *SCA7*, etc. The Scale for the Assessment and Rating of Ataxia (SARA) (6), that includes eight items to assess cerebellar syndrome, does not catch these extra-cerebellar signs. This scale is used as the primary outcome in several therapeutic and non-therapeutic trials for SCAs. However, presymptomatic carriers, defined by a SARA score < 3 out of 40, can present other non-cerebellar signs and symptoms that are already expression of disease.

Individual variability, even among genetically homogeneous forms due to a same mutation, impedes prediction of progression of the imaging and clinical signs in ataxias. Broadly, a higher number of CAG repeats within the *HTT* gene predicts earlier onset, but two people with the same repeat length may differ in clinical onset by decades (7). This variability has to be tackled using biomarkers that allow to define the state of disease for a single patient and the challenge

for the evaluation of potential treatments, particularly in early stages, will rely on longitudinal biomarkers.

Gene therapies have made remarkable progress over the last decade, such as antisense oligonucleotides (ASOs) approach. These are targeted treatment based on the genetic status. The rationale relies on the fact that lowering the burden of mutated protein may improve the disease prognosis. ASOs form a complex with targeted mRNA recruiting an endoribonuclease (Ribonuclease H) that degrades the RNA-DNA hybrid complex (8). Following the impressive results of nusinersen in spinal muscular atrophy (9,10), major hopes have been put in the development of ASO directed to *ATXN1*, *ATXN2*, *ATXN3* and *ATXN7* mutants even though one recent phase-III clinical trial failed to show that ASOs halted the progression of Huntington disease (HD) (11,12). Promising results have been reported by the ASOs administration in several SCAs mouse models (13–16). Therefore, objective and quantitative biomarkers rather than clinical measures are of critical importance as prognostic or pharmacodynamic markers to monitor drug effects. The aim of this chapter is to review the blood and cerebrospinal fluid (CSF) biomarkers for SCAs (Table 15.1).

## **15.2 Biological biomarkers**

### **15.2.1 Neurofilament light chain**

Neurofilament light chain (NfL) is a subunit of neuronal cytoskeleton and its level increases in CSF and blood as a result of axonal damage due to different causes (neurodegeneration, infection, traumatic, etc) (17). Using the highly sensitive single-molecule array method (Simoa) is possible to measure NfL in blood and CSF more accurately than conventional ELISA and electrochemiluminescence-based method (ECL assay) (18). Close correlation exists between CSF and blood concentrations, making NfL an easily measurable biomarker of neurodegeneration (17,19). In several neurological disorders, NfL correlates with disease stages, clinical scores, and neuroimaging data. It is the case for amyotrophic lateral sclerosis

(ALS) (20,21), Alzheimer's disease (22–24), multiple sclerosis (25,26), HD (27–29). This latter disease shares with SCAs the same mutational mechanism, a translated pathological CAG repeat expansion. NfL showed a prognostic value with a significant increase for HD presymptomatic carriers of the pathological expansion close to the age at expected disease onset (29). Moreover, for HD, atrophy of cerebral regions, as the putamen and caudate, are associated with higher NfL concentrations (29).

For SCAs, some studies showed the higher NfL levels in carriers than healthy controls. The first pilot study included only 20 SCAs carriers (SCA1, SCA2, SCA3, SCA6) founding elevated NfL concentrations compared to controls (30). Then, other studies on large cohorts of SCA3 carriers confirmed the correlation between clinical progression and NfL in CSF (31) and blood (31–33). In a longitudinal study with 2-year interval of plasma NfL measurements, NfL confirmed to be a disease biomarker with significant difference between healthy controls (~10 pg/ml) and polyglutamine (polyQ) SCAs carriers [SCA1 (~24 pg/ml), SCA2 (~20 pg/ml), SCA3 (~35 pg/ml), and SCA7 (~26 pg/ml)] (34). Interestingly, NfL concentrations remained stable at 2-year follow-up despite clinical progression assessed by SARA (34). Considering all SCAs subtypes, higher plasma NfL levels at baseline predicted a higher SARA score progression as well as a decrease in cerebellar volume at 2-year follow-up (34). NfL correlated with pons atrophy at baseline and follow-up (34), confirmed for SCA3 group taken separately. For SCA3, another study also reported significant association between serum NfL and cerebellum and brainstem volumes (31).

Serum NfL increase already 7.5 years before the expected age at onset for SCA3 carriers (32). NfL levels for SCA3 presymptomatic carriers fall down between controls and symptomatic carriers levels (31–34). SCA7 premanifest carriers with non-cerebellar signs at examination present NfL concentration close or above the cut-off level determined to differentiate controls from carriers (34). Based on presymptomatic carriers' data (31,32) and longitudinal data (34),

NfL seems to be a biomarkers that may be used in clinical trials to stratify carriers based on their NfL levels. However, some points remain to be clarified: i) SCA3 patients present the highest concentration than the other SCAs despite a less severe clinical progression based on SARA score (34,35). One possible explanation may be the prominent peripheral nervous system involvement than the other polyQ SCAs; ii) NfL levels do not change over time in SCAs, similar to ALS, frontotemporal dementia, and atypical parkinsonian syndromes (17). We may suppose that for these diseases NfL levels reach a plateau that masks the increase due to age. iii) NfL concentrations for polyQ SCAs fall between the highest levels of ALS or multiple system atrophy and the lowest levels in Friedreich's ataxia or Parkinson disease (17,36). It may be due to by either different disease progression rates or different levels of peripheral nervous system dysfunction.

### **15.2.2 Tau**

Another biomarker of neuroaxonal damage is Tau protein that promotes microtubule assembly and stability. This protein is an established marker in Creutzfeldt Jakob disease and Alzheimer disease (37). In a study including few SCA1, SCA2, and SCA6 patients, Tau levels in CSF were significantly higher in SCA2 carriers than controls (38). Other proteins were also tested in CSF ( $\alpha$ -synuclein, DJ-1, and GFAP) showing a tendency to be higher especially for SCA2 (38) and indicating the necessity to be reproduced in a larger cohort of patients.

### **15.2.3 Astrocytosis and gliosis**

Neuron-specific enolase (NSE) and protein S 100 B (S100B) are markers of neuron damage and gliosis. Serum concentrations of these two proteins are higher in SCA3 patients than controls (39), not tested in other SCA patients. NSE presents a correlations with disease

duration and clinical scales (ICARS and SARA), instead of S100B that does not correlate with any clinical parameters (39). In another SCA3 study, only NSE serum level was significantly higher than controls and presented a correlation with depression score (40).

#### **15.2.4 Ataxin specific bioassays**

In view of upcoming therapeutic trials that aim to decrease the mutant protein, it seems to be crucial the development of ataxin specific assays to monitor the efficacy of these treatments. To date, a time-resolved fluorescence resonance energy transfer (TR-FRET) immunoassay can detect the polyQ-expanded and non-expanded ataxin-3 protein level in blood-derived mononuclear cells from presymptomatic and symptomatic SCA3 carriers (41). Moreover, polyQ-expanded ataxin-3 protein levels correlated with disease stage and clinical severity assessed by SARA (41). However, this highly sensitive TR-FRET-based immunoassay cannot measure ataxin-3 level in other fluids such as CSF or plasma and should be validated in other cohorts.

In another study, an electrochemiluminescence immunoassay using the Meso Scale Discovery system detected polyQ-expanded ataxin-3 in CSF and plasma distinguishing controls from SCA3 carriers (42). In addition, this study showed the strong association between *ATXN3* pathological CAG repeat expansion and the rs7158733 SNP located ~132 nucleotides downstream of the CAG repeat (42) that could facilitate the allele specific ASO treatment.

Another novel single molecule counting (SMC) ataxin-3 immunoassay is able to measure polyQ-expanded ataxin-3 in plasma and CSF (43). Clinical correlations (age at onset and SARA score) are reported with plasma polyQ-expanded ataxin-3 levels. Longitudinal data show that plasma levels remain stable over a 1-year period (43).

For the other ataxin proteins, specific bioassays are not yet available.

### **15.2.5 Oxidative stress biomarkers**

Oxidative stress has been implicated in several neurodegenerative disorders. Production of abnormally large amounts of reactive oxygen species was reported for SCA3 (44). This seems to be caused by a dysregulation of major enzymes implicated in antioxidant capacity: superoxide dismutase and glutathione peroxidase (GPx) activities are lower in symptomatic than in pre-symptomatic carriers (45). On the other hand, catalase activity is increased in the serum of SCA3 patients (44). The correlation of GPx decrease activity with disease severity suggests that GPx may be a reliable biomarker (45).

In SCA2 presymptomatic and symptomatic carriers, glutathione S-transferases (GST) activity is increased by 21.8% and 5.5%, respectively (46). The role of this enzyme is to protect against oxidative stress and prevent apoptosis. GST increase activity supports the role of free radical damage in SCAs physiopathology.

### **15.2.6 Inflammation biomarkers**

Inflammatory genes encoding endopeptidase matrix metalloproteinase 2 (MMP-2) and cytokine stromal cell-derived factor 1 $\alpha$  (SDF1 $\alpha$ ) are upregulated in a cell culture model of SCA3 as well as in human SCA3 pons (47). Other proteins involved in inflammation process are significantly increased: amyloid  $\beta$ -protein (A $\beta$ ), interleukin-1 receptor antagonist (IL-1ra), interleukin-1 $\beta$  (IL-1 $\beta$ ), and interleukin-6 (IL-6) (47). Activation of microglia and presence of reactive astrocytes is reported in the brains of SCA3 patients (48). Based on these data, a large panel of cytokines has been investigated in a large cohort of presymptomatic and symptomatic SCA3 compared to controls (49). No difference in cytokine levels was detected among the groups except for eotaxin. Higher eotaxin concentrations were observed in asymptomatic carriers than

in symptomatic carriers (49). In symptomatic carriers the level dropped after one year (49). One possible explanation may be that the levels of eotaxin released by astrocytes are inversely correlated with disease progression (49).

### **15.2.7 Insulin/insulin-like growth factor 1 (IGF-1) system**

Abnormalities in the signaling pathway of the insulin/insulin-like growth factor 1 (IGF-1) system (IIS), including IGF-1, IGF binding proteins (IGFBPs), and insulin, are thought to play a role in the physiopathological processes of neurodegenerative diseases as Alzheimer's disease, HD and polyQ SCAs (50–52). SCA3 patients show higher serum levels of IGFBP1 and IGF-1/IGFBP-3 ratio than controls (53). Inversely, serum levels of IGFBP-3 (that binds more than 80% of peripheral IGF-1 and increases its half-life) and insulin levels are reduced (53).  $\beta$ -cell function is preserved in SCA3 patients and the reduction of insulin level is due to an increased peripheral sensitivity to insulin. Higher sensitivity to insulin and lower insulin levels are both related to earlier disease onset (53).

IGFBP-1 levels are correlated significantly with CAG repeat expansion (53). IGFBP1 may be a biomarker for SCA3 even though its link with expanded ataxin-3 protein remains unclear. One possible explanation could be the endoplasmic reticulum stress induced by mutant ataxin-3 protein that increases IGFBP-1 production in liver (53). Even though IGF1 is not significantly higher, it inversely correlates with the volume of medulla oblongata and pons (53).

### **15.2.8 Co-chaperone protein**

The carboxyl terminus of Hsp-70 interacting protein (CHIP), a co-chaperone protein, is an endogenous binding partner of the mutant ataxin-3. In SCA3 patients, CHIP level is elevated in



both serum and CSF, indirectly reflecting mutant ataxin-3 level (54). CHIP correlates with disease severity assessed by SARA and ICARS. The main role of CHIP is protein quality control. Ataxin-3 protein directly interacts with CHIP. The affinity between these two proteins increases with CAG expansion causing a cellular homeostasis dysregulation.

### **15.3 Biomarkers in development**

#### **15.3.1 Brain cholesterol metabolism**

Deregulation of brain cholesterol turnover and metabolism have been associated with several neurodegenerative diseases. 24-hydroxylase (CYP46A1) is the key enzyme of efflux of brain cholesterol, converting the excess cholesterol into 24S-hydroxycholesterol (24OHC) released in systemic circulation (55). Plasma 24OHC is significantly reduced in neurological disorders as Alzheimer's disease, Parkinson's disease, Niemann–Pick disease type C, multiple sclerosis, and HD (56–60). For HD, 24OHC levels decrease with disease progression and striatal volume loss (55). In SCA3 cerebellum samples, CYP46A1 is reduced (61). The overexpression by an adeno-associated virus (AAV)-mediated expression of CYP46A1 decreases the ATXN-3 aggregates by activation of autophagy and leads to motor improvement in SCA2 mouse model (61). Plasma 24OHC may be a potential biomarker for SCAs as reported for HD, therefore further investigations should be carry on.

#### **15.3.2 Metabolic profile**

The serum metabolomics profile shows a difference between symptomatic SCA3 patients and presymptomatic carriers or controls (62). In SCA3 patients, there is a downregulation of branched-chain amino acids including valine and leucine, and aromatic amino acids as

tryptophan and tyrosine (62). These metabolites are precursors of some neurotransmitters (serotonin, dopamine, GABA) and have a role in energy metabolism. Fatty acid metabolism is also dysregulated in SCA3 patients with decrease of saturated fatty acid and increase of monounsaturated and polyunsaturated fatty acid fatty (62).

Plasma lipidomic analysis in a cohort of polyQ SCAs showed that SCA7 patients differentiate from other polyQ SCAs patients for some ceramides and phosphatidylcholines (63). These lipids are strongly expressed in retina and their deficit may be linked to the retinal alterations characteristic for SCA7 rather than other polyQ SCAs.

For SCA7 patients, another study has reported the decreased of branched-chain amino acids, leucine and valine, as well as of tyrosine, with a good sensitivity to discriminate from controls (64). Moreover, when regarding only SCA7 carriers, methionine level differentiates early onset from late onset patients (64).

### **15.3.3 Micro-RNAs**

Several studies investigated micro-RNAs (miRNAs) levels in SCAs patients reporting different results. Lower levels of miR-25, miR-125b, miR-29a, and miR-34b are found in serum of SCA3 patients compared to controls (65,66). Reduced concentrations of miR-9 and miR-181a from CSF derived exosomes of SCA3 patients are reported (67). Three miRNAs-mir-9, mir-181a, and mir-494 are decreased in SCA3 human neurons (68). These three miRNAs interact with the ATXN3-3' UTR downregulating its expression (68). In SCA3 mouse model, the overexpression of these miRNAs reduces the mutant ataxin-3 expression by translation inhibition and mRNA degradation (68). For SCA7, the plasma expressions of four miRNAs (hsa-let-7a-5p, hsa-let7e-5p, hsa-miR-18a-5p, and hsa-miR-30b-5p) differentiate carriers from controls and seem to have a prognostic value discriminating between juvenile and adult onset (69).

These data could suggest miRNAs as potential biological markers of disease and therapeutic targets. However, their use does not seem to be possible in the short term.

#### **15.3.4 Sirtuin-1**

Sirtuin-1 is a NAD<sup>+</sup>-dependent deacetylase taking part in several cellular functions as chromatin modulation, cell cycle, apoptosis, and autophagy regulation in response to DNA damage. In SCA3 mice and in SCA3 patients' fibroblasts, sirtuin-1 mRNA levels are lower than controls (70). In SCA3 mice, the caloric restriction rescues sirtuin-1 with motor improvement (70). Sirtuin-1 overexpression activates autophagy and increases the mutant protein clearance. This overexpression results in neuropathological changes: activation of autophagy, decrease in neuroinflammation, and reduction of reactive gliosis (70).

#### **Conclusion**

This chapter reviews the available biomarkers in blood and CSF for polyQ SCAs. However, the majority of the evidence are reported for SCA3, the most frequent subtype worldwide, and only few longitudinal studies have been conducted with a lower inclusion of presymptomatic carriers. Still many efforts need to obtain an optimal biomarker with diagnostic and prognostic values, reliable to be used in upcoming gene therapy trials. Neurofilaments light chain seems to be currently the best biomarker, already confirmed in several neurological diseases, with a role to monitor drug administration in spinal muscular atrophy (71) and multiple sclerosis (26). A great interest there is towards the development of ataxin bioassays that are the specific target of ASOs therapy. Other pathways presented in this chapter require validation in larger cohorts.

## References:

1. Klockgether T, Mariotti C, Paulson HL. Spinocerebellar ataxia. *Nat Rev Dis Primers*. 2019 Dec;5(1):24.
2. Durr A. Autosomal dominant cerebellar ataxias: polyglutamine expansions and beyond. *The Lancet Neurology*. 2010 Sep;9(9):885–94.
3. Stevanin G, Dürr A, Brice A. Clinical and molecular advances in autosomal dominant cerebellar ataxias: from genotype to phenotype and physiopathology. *Eur J Hum Genet*. 2000 Jan;8(1):4–18.
4. Mao R, Aylsworth AS, Potter N, Wilson WG, Breningstall G, Wick MJ, et al. Childhood-onset ataxia: testing for large CAG-repeats in SCA2 and SCA7. *Am J Med Genet*. 2002 Jul 15;110(4):338–45.
5. Bah MG, Rodriguez D, Cazeneuve C, Mochel F, Devos D, Suppiej A, et al. Deciphering the natural history of SCA7 in children. *Eur J Neurol*. 2020 Nov;27(11):2267–76.
6. Schmitz-Hübsch T, du Montcel ST, Baliko L, Berciano J, Boesch S, Depondt C, et al. Scale for the assessment and rating of ataxia: development of a new clinical scale. *Neurology*. 2006 Jun 13;66(11):1717–20.
7. Lee J-M, Ramos EM, Lee J-H, Gillis T, Mysore JS, Hayden MR, et al. CAG repeat expansion in Huntington disease determines age at onset in a fully dominant fashion. *Neurology*. 2012 Mar 6;78(10):690–5.
8. Wild EJ, Tabrizi SJ. Therapies targeting DNA and RNA in Huntington’s disease. *The Lancet Neurology*. 2017 Oct;16(10):837–47.
9. Finkel RS, Mercuri E, Darras BT, Connolly AM, Kuntz NL, Kirschner J, et al. Nusinersen versus Sham Control in Infantile-Onset Spinal Muscular Atrophy. *N Engl J Med*. 2017 Nov 2;377(18):1723–32.
10. Acsadi G, Crawford TO, Müller-Felber W, Shieh PB, Richardson R, Natarajan N, et al. Safety and efficacy of nusinersen in spinal muscular atrophy: The EMBRACE study. *Muscle Nerve*. 2021 May;63(5):668–77.
11. Tabrizi SJ, Leavitt BR, Landwehrmeyer GB, Wild EJ, Saft C, Barker RA, et al. Targeting Huntingtin Expression in Patients with Huntington’s Disease. *N Engl J Med*. 2019 Jun 13;380(24):2307–16.
12. Kingwell K. Double setback for ASO trials in Huntington disease. *Nat Rev Drug Discov*. 2021 Jun;20(6):412–3.
13. Friedrich J, Kordasiewicz HB, O’Callaghan B, Handler HP, Wagener C, Duvick L, et al. Antisense oligonucleotide-mediated ataxin-1 reduction prolongs survival in SCA1 mice and reveals disease-associated transcriptome profiles. *JCI insight*. 2018 02;3(21).
14. Scoles DR, Meera P, Schneider MD, Paul S, Dansithong W, Figueroa KP, et al. Antisense oligonucleotide therapy for spinocerebellar ataxia type 2. *Nature*. 2017 20;544(7650):362–6.

15. McLoughlin HS, Moore LR, Chopra R, Komlo R, McKenzie M, Blumenstein KG, et al. Oligonucleotide therapy mitigates disease in spinocerebellar ataxia type 3 mice. *Annals of Neurology*. 2018;84(1):64–77.
16. Niu C, Prakash TP, Kim A, Quach JL, Hury LA, Yang Y, et al. Antisense oligonucleotides targeting mutant Ataxin-7 restore visual function in a mouse model of spinocerebellar ataxia type 7. *Science Translational Medicine*. 2018 31;10(465).
17. Gaetani L, Blennow K, Calabresi P, Di Filippo M, Parnetti L, Zetterberg H. Neurofilament light chain as a biomarker in neurological disorders. *J Neurol Neurosurg Psychiatry*. 2019;90(8):870–81.
18. Kuhle J, Barro C, Andreasson U, Derfuss T, Lindberg R, Sandelius Å, et al. Comparison of three analytical platforms for quantification of the neurofilament light chain in blood samples: ELISA, electrochemiluminescence immunoassay and Simoa. *Clin Chem Lab Med*. 2016 Oct 1;54(10):1655–61.
19. Khalil M. Neurofilaments as biomarkers in neurological disorders. *Nat Rev Neurol* [Internet]. 2018;14. Available from: <https://doi.org/10.1038/s41582-018-0058-z>
20. Lu C-H, Macdonald-Wallis C, Gray E, Pearce N, Petzold A, Norgren N, et al. Neurofilament light chain: A prognostic biomarker in amyotrophic lateral sclerosis. *Neurology*. 2015 Jun 2;84(22):2247–57.
21. Benatar M, Wu J, Andersen PM, Lombardi V, Malaspina A. Neurofilament light: A candidate biomarker of presymptomatic amyotrophic lateral sclerosis and phenoconversion. *Ann Neurol*. 2018 Jul;84(1):130–9.
22. Mattsson N, Cullen NC, Andreasson U, Zetterberg H, Blennow K. Association Between Longitudinal Plasma Neurofilament Light and Neurodegeneration in Patients With Alzheimer Disease. *JAMA Neurol*. 2019 Jul;76(7):791–9.
23. Benedet AL, Leuzy A, Pascoal TA, Ashton NJ, Mathotaarachchi S, Savard M, et al. Stage-specific links between plasma neurofilament light and imaging biomarkers of Alzheimer’s disease. *Brain*. 2020 Nov 19;
24. Preische O, Schultz SA, Apel A, Kuhle J, Kaeser SA, Barro C, et al. Serum neurofilament dynamics predicts neurodegeneration and clinical progression in presymptomatic Alzheimer’s disease. *Nat Med*. 2019 Feb;25(2):277–83.
25. Bjornevik K, Munger KL, Cortese M, Barro C, Healy BC, Niebuhr DW, et al. Serum Neurofilament Light Chain Levels in Patients With Presymptomatic Multiple Sclerosis. *JAMA Neurol*. 2020 Jan 1;77(1):58–64.
26. Kuhle J, Kropshofer H, Haering DA, Kundu U, Meinert R, Barro C, et al. Blood neurofilament light chain as a biomarker of MS disease activity and treatment response. *Neurology*. 2019 Mar 5;92(10):e1007–15.
27. Byrne LM, Rodrigues FB, Blennow K, Durr A, Leavitt BR, Roos RAC, et al. Neurofilament light protein in blood as a potential biomarker of neurodegeneration in Huntington’s disease: a retrospective cohort analysis. *Lancet Neurol*. 2017;16(8):601–9.

28. Johnson EB, Byrne LM, Gregory S, Rodrigues FB, Blennow K, Durr A, et al. Neurofilament light protein in blood predicts regional atrophy in Huntington disease. *Neurology*. 2018 20;90(8):e717–23.
29. Scahill RI, Zeun P, Osborne-Crowley K, Johnson EB, Gregory S, Parker C, et al. Biological and clinical characteristics of gene carriers far from predicted onset in the Huntington’s disease Young Adult Study (HD-YAS): a cross-sectional analysis. *Lancet Neurol*. 2020;19(6):502–12.
30. Wilke C, Bender F, Hayer SN, Brockmann K, Schöls L, Kuhle J, et al. Serum neurofilament light is increased in multiple system atrophy of cerebellar type and in repeat-expansion spinocerebellar ataxias: a pilot study. *J Neurol*. 2018 Jul;265(7):1618–24.
31. Li Q-F, Dong Y, Yang L, Xie J-J, Ma Y, Du Y-C, et al. Neurofilament light chain is a promising serum biomarker in spinocerebellar ataxia type 3. *Mol Neurodegener*. 2019 04;14(1):39.
32. Wilke C, Haas E, Reetz K, Faber J, Garcia-Moreno H, Santana MM, et al. Neurofilaments in spinocerebellar ataxia type 3: blood biomarkers at the preataxic and ataxic stage in humans and mice. *EMBO Mol Med*. 2020 Jul 7;12(7):e11803.
33. Peng Y, Zhang Y, Chen Z, Peng H, Wan N, Zhang J, et al. Association of serum neurofilament light (sNFL) and disease severity in patients with spinocerebellar ataxia type 3. *Neurology*. 2020 Aug 14;
34. Coarelli G, Darios F, Petit E, Dorgham K, Adanyeguh I, Petit E, et al. Plasma neurofilament light chain predicts cerebellar atrophy and clinical progression in spinocerebellar ataxia. *Neurobiol Dis*. 2021 Jun;153:105311.
35. Jacobi H, du Montcel ST, Bauer P, Giunti P, Cook A, Labrum R, et al. Long-term disease progression in spinocerebellar ataxia types 1, 2, 3, and 6: a longitudinal cohort study. *The Lancet Neurology*. 2015 Nov;14(11):1101–8.
36. Bridel C, van Wieringen WN, Zetterberg H, Tijms BM, Teunissen CE, and the NFL Group, et al. Diagnostic Value of Cerebrospinal Fluid Neurofilament Light Protein in Neurology: A Systematic Review and Meta-analysis. *JAMA Neurol*. 2019 Jun 17;
37. Tumani H, Teunissen C, Süßmuth S, Otto M, Ludolph AC, Brettschneider J. Cerebrospinal fluid biomarkers of neurodegeneration in chronic neurological diseases. *Expert Rev Mol Diagn*. 2008 Jul;8(4):479–94.
38. Brouillette AM, Öz G, Gomez CM. Cerebrospinal Fluid Biomarkers in Spinocerebellar Ataxia: A Pilot Study. *Dis Markers*. 2015;2015:413098.
39. Zhou J, Lei L, Shi Y, Wang J, Jiang H, Shen L, et al. Serum concentrations of NSE and S100B in spinocerebellar ataxia type 3/Machado-Joseph disease. *Zhong Nan Da Xue Xue Bao Yi Xue Ban*. 2011 Jun;36(6):504–10.
40. Tort ABL, Portela LVC, Rockenbach IC, Monte TL, Pereira ML, Souza DO, et al. S100B and NSE serum concentrations in Machado Joseph disease. *Clinica Chimica Acta*. 2005 Jan 1;351(1):143–8.
41. Gonsior K, Kaucher GA, Pelz P, Schumann D, Gansel M, Kuhs S, et al. PolyQ-expanded ataxin-3 protein levels in peripheral blood mononuclear cells correlate with clinical parameters in SCA3: a pilot study. *J Neurol*. 2020 Oct 26;

42. Prudencio M, Garcia-Moreno H, Jansen-West KR, Al-Shaikh RH, Gendron TF, Heckman MG, et al. Toward allele-specific targeting therapy and pharmacodynamic marker for spinocerebellar ataxia type 3. *Sci Transl Med*. 2020 Oct 21;12(566).
43. Hübener-Schmid J, Kuhlbrodt K, Peladan J, Faber J, Santana MM, Hengel H, et al. Polyglutamine-Expanded Ataxin-3: A Target Engagement Marker for Spinocerebellar Ataxia Type 3 in Peripheral Blood. *Mov Disord*. 2021 Aug 16;
44. Pacheco LS, da Silveira AF, Trott A, Houenou LJ, Algarve TD, Belló C, et al. Association between Machado-Joseph disease and oxidative stress biomarkers. *Mutat Res Genet Toxicol Environ Mutagen*. 2013 Oct 9;757(2):99–103.
45. de Assis AM, Saute JAM, Longoni A, Haas CB, Torrez VR, Brochier AW, et al. Peripheral Oxidative Stress Biomarkers in Spinocerebellar Ataxia Type 3/Machado-Joseph Disease. *Front Neurol*. 2017;8:485.
46. Almaguer-Gotay D, Almaguer-Mederos LE, Aguilera-Rodríguez R, Estupiñán-Rodríguez A, González-Zaldivar Y, Cuello-Almarales D, et al. Role of glutathione S-transferases in the spinocerebellar ataxia type 2 clinical phenotype. *J Neurol Sci*. 2014 Jun 15;341(1–2):41–5.
47. Evert BO, Vogt IR, Kindermann C, Ozimek L, de Vos RA, Brunt ER, et al. Inflammatory genes are upregulated in expanded ataxin-3-expressing cell lines and spinocerebellar ataxia type 3 brains. *J Neurosci*. 2001 Aug 1;21(15):5389–96.
48. Evert BO, Schelhaas J, Fleischer H, de Vos R a. I, Brunt ER, Stenzel W, et al. Neuronal intranuclear inclusions, dysregulation of cytokine expression and cell death in spinocerebellar ataxia type 3. *Clin Neuropathol*. 2006 Dec;25(6):272–81.
49. da Silva Carvalho G, Saute JAM, Haas CB, Torrez VR, Brochier AW, Souza GN, et al. Cytokines in Machado Joseph Disease/Spinocerebellar Ataxia 3. *Cerebellum*. 2016 Aug;15(4):518–25.
50. Craft S, Watson GS. Insulin and neurodegenerative disease: shared and specific mechanisms. *Lancet Neurol*. 2004 Mar;3(3):169–78.
51. Cohen E, Dillin A. The insulin paradox: aging, proteotoxicity and neurodegeneration. *Nat Rev Neurosci*. 2008 Oct;9(10):759–67.
52. Emamian ES, Kaytor MD, Duvick LA, Zu T, Tousey SK, Zoghbi HY, et al. Serine 776 of ataxin-1 is critical for polyglutamine-induced disease in SCA1 transgenic mice. *Neuron*. 2003 May 8;38(3):375–87.
53. Saute JAM, da Silva ACF, Muller AP, Hansel G, de Mello AS, Maeda F, et al. Serum insulin-like system alterations in patients with spinocerebellar ataxia type 3. *Mov Disord*. 2011 Mar;26(4):731–5.
54. Hu Z-W, Yang Z-H, Zhang S, Liu Y-T, Yang J, Wang Y-L, et al. Carboxyl Terminus of Hsp70-Interacting Protein Is Increased in Serum and Cerebrospinal Fluid of Patients With Spinocerebellar Ataxia Type 3. *Front Neurol*. 2019;10:1094.
55. Leoni V, Long JD, Mills JA, Di Donato S, Paulsen JS. Plasma 24S-hydroxycholesterol correlation with markers of Huntington disease progression. *Neurobiology of Disease*. 2013 Jul;55:37–43.

56. Papassotiropoulos A, Wollmer MA, Tsolaki M, Brunner F, Molyva D, Lütjohann D, et al. A cluster of cholesterol-related genes confers susceptibility for Alzheimer's disease. *J Clin Psychiatry*. 2005 Jul;66(7):940–7.
57. Kölsch H, Lütjohann D, Jessen F, Popp J, Hentschel F, Kelemen P, et al. CYP46A1 variants influence Alzheimer's disease risk and brain cholesterol metabolism. *Eur Psychiatry*. 2009 Apr;24(3):183–90.
58. Shobab LA, Hsiung G-YR, Feldman HH. Cholesterol in Alzheimer's disease. *Lancet Neurol*. 2005 Dec;4(12):841–52.
59. Solomon A, Leoni V, Kivipelto M, Besga A, Oksengård AR, Julin P, et al. Plasma levels of 24S-hydroxycholesterol reflect brain volumes in patients without objective cognitive impairment but not in those with Alzheimer's disease. *Neurosci Lett*. 2009 Oct 2;462(1):89–93.
60. Leoni V, Masterman T, Diczfalusy U, De Luca G, Hillert J, Björkhem I. Changes in human plasma levels of the brain specific oxysterol 24S-hydroxycholesterol during progression of multiple sclerosis. *Neurosci Lett*. 2002 Oct 18;331(3):163–6.
61. Nóbrega C, Mendonça L, Marcelo A, Lamazière A, Tomé S, Despres G, et al. Restoring brain cholesterol turnover improves autophagy and has therapeutic potential in mouse models of spinocerebellar ataxia. *Acta Neuropathol*. 2019 Nov;138(5):837–58.
62. Yang Z, Shi C, Zhou L, Li Y, Yang J, Liu Y, et al. Metabolic Profiling Reveals Biochemical Pathways and Potential Biomarkers of Spinocerebellar Ataxia 3. *Frontiers in Molecular Neuroscience*. 2019;12:159.
63. Garali I, Adanyeguh IM, Ichou F, Perlberg V, Seyer A, Colsch B, et al. A strategy for multimodal data integration: application to biomarkers identification in spinocerebellar ataxia. *Briefings in Bioinformatics*. 2018 Nov 27;19(6):1356–69.
64. Nambo-Venegas R, Valdez-Vargas C, Cisneros B, Palacios-González B, Vela-Amieva M, Ibarra-González I, et al. Altered Plasma Acylcarnitines and Amino Acids Profile in Spinocerebellar Ataxia Type 7. *Biomolecules*. 2020 Mar 3;10(3):E390.
65. Huang F, Zhang L, Long Z, Chen Z, Hou X, Wang C, et al. miR-25 alleviates polyQ-mediated cytotoxicity by silencing ATXN3. *FEBS Lett*. 2014 Dec 20;588(24):4791–8.
66. Shi Y, Huang F, Tang B, Li J, Wang J, Shen L, et al. MicroRNA profiling in the serums of SCA3/MJD patients. *Int J Neurosci*. 2014 Feb;124(2):97–101.
67. Hou X, Gong X, Zhang L, Li T, Yuan H, Xie Y, et al. Identification of a potential exosomal biomarker in spinocerebellar ataxia Type 3/Machado-Joseph disease. *Epigenomics*. 2019 Jul;11(9):1037–56.
68. Carmona V, Cunha-Santos J, Onofre I, Simões AT, Vijayakumar U, Davidson BL, et al. Unravelling Endogenous MicroRNA System Dysfunction as a New Pathophysiological Mechanism in Machado-Joseph Disease. *Mol Ther*. 2017 Apr 5;25(4):1038–55.
69. Borgonio-Cuadra VM, Valdez-Vargas C, Romero-Córdoba S, Hidalgo-Miranda A, Tapia-Guerrero Y, Cerecedo-Zapata CM, et al. Wide Profiling of Circulating MicroRNAs in Spinocerebellar Ataxia Type 7. *Mol Neurobiol*. 2019 Sep;56(9):6106–20.



70. Cunha-Santos J, Duarte-Neves J, Carmona V, Guarente L, Pereira de Almeida L, Cavadas C. Caloric restriction blocks neuropathology and motor deficits in Machado-Joseph disease mouse models through SIRT1 pathway. *Nat Commun.* 2016 May 11;7:11445.
71. Olsson B, Alberg L, Cullen NC, Michael E, Wahlgren L, Kroksmark A-K, et al. NFL is a marker of treatment response in children with SMA treated with nusinersen. *J Neurol.* 2019 Sep;266(9):2129–36.
72. Shin H-R, Moon J, Lee W-J, Lee HS, Kim EY, Shin S, et al. Serum neurofilament light chain as a severity marker for spinocerebellar ataxia. *Sci Rep.* 2021 Jun 29;11(1):13517.

**Table 15.1 Blood and cerebrospinal fluid biomarkers in spinocerebellar ataxias.**

<b>Mechanism</b>	<b>Biomarker</b>	<b>Results</b>	<b>Correlations</b>
<b>Neuroaxonal damage</b>	NfL	<p>↑ in serum SCA1, SCA2, SCA3, SCA6 (30)</p> <p>↑ in plasma SCA1, SCA2, SCA3, SCA7 (34)</p> <p>↑ in plasma and CSF of pre-symptomatic and symptomatic SCA3 (31)</p> <p>↑ in serum of symptomatic SCA3 (32)</p>	<p>For SCA3: disease stage (31,32), CAG (32), SARA (31,32,34), CCFS (34), pons atrophy (34), cerebellum and brainstem atrophy (31)</p> <p>For polyQ SCAs: SARA, CCFS, pons atrophy (34); disease stage, disease duration, SARA (72)</p>
	Phosphorylated neurofilament heavy chain	↑ in serum of SCA3 (32)	
	Tau	↑ in CSF of SCA2 (38)	No
<b>Astricitosis and gliosis</b>	Neuron-specific enolase	↑ in serum of SCA3 (39)	Disease duration, ICARS, and SARA (39)
	S100B	↑ in serum of SCA3 (39)	No
<b>ATXN-3 bioassays</b>	Expanded polyQ ATXN-3	Detection in PBMC by TR-FRET immunoassay in pre-symptomatic and symptomatic SCA3 (41)	Disease stage and SARA (41)
		Detection in plasma and CSF by electrochemiluminescence immunoassay in pre-symptomatic and symptomatic SCA3 (42)	No
		Detection in plasma and CSF by single molecule counting in pre-symptomatic and symptomatic SCA3 (43)	Age at onset (negative correlations) and SARA for plasma ATXN-3 levels (43)
<b>Oxidative stress</b>	Superoxide dismutase	↓ in serum of symptomatic than in pre-symptomatic SCA3 carriers (45)	No
	Glutathione peroxidase	↓ in serum of symptomatic than in pre-symptomatic SCA3 carriers (45)	Negative correlation with NESSCA (45)

	Catalase	↑ in serum of SCA3 (44)	No
<b>Inflammation</b>	Eotaxin	↑ in serum of asymptomatic SCA3 carriers (49)	No
<b>Growth factors</b>	IGFBP1 IGF-1/IGFBP-3 ratio	↑ in serum of SCA3 patients (53)	CAG repeat expansion (53)
	IGFBP-3 insulin	↓ in serum of SCA3 patients (53)	No
<b>Chaperon</b>	CHIP	↑ in serum and CSF of SCA3 patients (54)	SARA and ICARS (54)
<b>Metabolism</b>	CYP46A1	↓ in SCA3 cerebellum samples (61)	No
	Valine, leucine, tryptophan, and tyrosine	↓ in serum of SCA3 patients (62)	No
	Leucine, valine, and tyrosine	↓ in serum of SCA7 patients (64)	No
	Ceramides and phosphatidylcholines	↓ in plasma of SCA7 patients (63)	No
<b>Enzyme</b>	Sirtuin-1	↓ mRNA in SCA3 patients' fibroblasts (70)	No
<b>Micro-RNAs</b>	miR-25, miR-125b, miR-29a, and miR-34b	↓ in serum of SCA3 patients (65,66)	No
	hsa-let-7a-5p, hsa- let7e-5p, hsa-miR-18a- 5p, and hsa-miR-30b- 5p	Alterations in plasma of SCA7 patients (69)	Disease onset (69)

Abbreviations: CCFS: Composite Cerebellar Functional Score; CHIP: carboxyl terminus of the Hsp70-interacting protein; ICARS: International Cooperative Ataxia Rating Scale; IGFBP: insulin-like growth factor-binding protein; NfL: neurofilament light chain; polyQ: polyglutamine; S100B: protein S 100 B; SARA: Scale for the Assessment and Rating of Ataxia; SCA: spinocerebellar ataxia.

## Objectives

My PhD was aimed at the identification of biological, clinical, and imaging biomarkers in polyQ SCAs at preataxic and ataxic stages. As discussed in the Introduction, reliable biomarkers are needed for upcoming clinical trials. To pursue this aim, I investigated three SCA cohorts issued from three different clinical studies:

- 1) BIOSCA cohort: 62 polyQ SCA carriers (17 SCA1, 13 SCA2, 19 SCA3, and 13 SCA7) and 19 age-matched controls, from the French National Reference Center for Rare Diseases “Neurogenetics” in Paris, Pitié-Salpêtrière Hospital, enrolled in the BIOSCA study between 2011 and 2015 (NCT01470729). In this longitudinal study, we assessed plasma NfL levels in SCAs carriers and explored their correlations with clinical and radiological parameters.
- 2) ATRIL cohort: 45 SCA2 patients from eight National Reference Centers for Rare Diseases in France enrolled between 2018 and 2019 in the multicenter, double-blind, randomized, placebo-controlled study evaluating the safety and efficacy of riluzole (NCT03347344). Along with the investigation of riluzole efficacy, we also have explored the progression of cerebellar and brainstem atrophy over one year.
- 3) CERMOI cohort: 15 SCA2 carriers, 15 SCA7 carriers, and 10 age-matched controls, from the French National Reference Center for Rare Diseases “Neurogenetics” in Paris, Pitié-Salpêtrière Hospital, enrolled between 2020 and 2021 in the study “Integrated Functional Evaluation of the Cerebellum” (NCT04288128). We leveraged a multimodal assessment including clinical, postural, ophthalmological, neuropsychological evaluations, as well as brain MRI and biosamples, to identify reliable biomarkers which could discriminate carriers from controls and track the disease progression over one year.

Each of these cohorts will be discussed in a separate chapter. The results of BIOSCA and ATRIL studies have been published in 2021 and 2022, respectively; I will shortly introduce them and refer to the publication. The results from the CERMOI study have not been published yet.

# Results

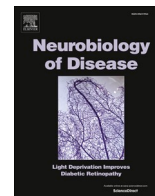
## Chapter 1 - BIOSCA study

In the past few years, Neurofilament light chain (NfL) has emerged as a reliable fluid biomarker in several neurological diseases, such as amyotrophic lateral sclerosis (ALS),<sup>34,35</sup> Alzheimer's disease,<sup>36-38</sup> Huntington's disease (HD),<sup>39-41</sup> Parkinson's disease (Pilotto 2021),<sup>42</sup> and multiple sclerosis.<sup>43,44</sup> This biomarker reflects neuronal damage resulting from different pathological triggers, such as vascular, inflammation, traumatic, or neurodegenerative injuries.<sup>45,46</sup> High correlation exists between CSF and blood NfL concentrations, making NfL an easily accessible biomarker.<sup>45</sup> As already shown in other neurological diseases, NfL levels correlate with disease severity, being useful for differential diagnostic in neurodegenerative diseases (e.g., to discriminate between different forms of parkinsonism).<sup>45,47,48</sup> In addition, it can be used to monitor a response to treatment, as shown in multiple sclerosis<sup>44</sup> and spinal muscular atrophy,<sup>49</sup> in which NfL levels decreased following the administration of disease modifying treatment.

Recently, NfL has been explored also in ataxias' research field, especially in SCA3, showing its extreme reliability in distinguishing carriers from controls. In addition, NfL levels proved useful to track the disease progression and were able to discriminate preataxic and ataxic carrier.<sup>22-25</sup> Furthermore, NfL levels can predict the disease onset,<sup>23</sup> as reported for HD,<sup>41</sup> since an increase of concentration occurs close to the phenoconversion phase. For these reasons, I aimed at expanding the investigation of NfL levels to other polyQ SCAs. I leveraged a preexisting cohort issued from the BIOSCA study<sup>50,51</sup> and measured NfL concentrations in plasma of SCA1, SCA2, SCA3, and SCA7 carriers (preataxic and ataxic carriers) at two time-points, with an interval of two years. We established the optimal NfL concentration cut-off to differentiate carriers from controls for each genotype. In addition, NfL levels were correlated with clinical and radiological parameters. In February 2021, the results of this first longitudinal study exploring NfL in polyQ SCAs have been published in *Neurobiology of Disease*.<sup>52</sup>

Contents lists available at [ScienceDirect](https://www.sciencedirect.com)

## Neurobiology of Disease

journal homepage: [www.elsevier.com/locate/ynbdi](http://www.elsevier.com/locate/ynbdi)

## Plasma neurofilament light chain predicts cerebellar atrophy and clinical progression in spinocerebellar ataxia

Giulia Coarelli<sup>a,b</sup>, Frederic Darios<sup>a</sup>, Emilien Petit<sup>a</sup>, Karim Dorgham<sup>c</sup>, Isaac Adanyeguh<sup>a</sup>,  
Elodie Petit<sup>a,b</sup>, Alexis Brice<sup>a</sup>, Fanny Mochel<sup>a,b</sup>, Alexandra Durr<sup>a,b,\*</sup>

<sup>a</sup> Sorbonne Université, ICM (Paris Brain Institute), AP-HP, INSERM, CNRS, University Hospital Pitié-Salpêtrière, Paris, France

<sup>b</sup> APHP Department of Genetics, Pitié-Salpêtrière University Hospital, Paris, France

<sup>c</sup> Sorbonne Université, INSERM, CNRS, Centre d'Immunologie et des Maladies Infectieuses-Paris (CIMI-Paris), F-75013 Paris, France

## ARTICLE INFO

## Keywords:

Spinocerebellar ataxias  
Neurofilament light chain  
Volumetric MRI  
Biomarker  
Cerebellum

## ABSTRACT

Neurofilament light chain (NfL) is a marker of brain atrophy and predictor of disease progression in rare diseases such as Huntington Disease, but also in more common neurological disorders such as Alzheimer's disease. The aim of this study was to measure NfL longitudinally in autosomal dominant spinocerebellar ataxias (SCAs) and establish correlation with clinical and imaging parameters. We enrolled 62 pathological expansions carriers (17 SCA1, 13 SCA2, 19 SCA3, and 13 SCA7) and 19 age-matched controls in a prospective biomarker study between 2011 and 2015 and followed for 24 months at the Paris Brain Institute. We performed neurological examination, brain 3 T MRI and plasma NfL measurements using an ultrasensitive single-molecule array at baseline and at the two-year follow-up visit. We evaluated NfL correlations with ages, CAG repeat sizes, clinical scores and volumetric brain MRIs. NfL levels were significantly higher in SCAs than controls at both time points ( $p < 0.001$ ). Age-adjusted NfL levels were significantly correlated at baseline with clinical scores ( $p < 0.01$ ). We identified optimal NfL cut-off concentrations to differentiate controls from carriers for each genotype (SCA1 16.87 pg/mL, SCA2, 19.1 pg/mL, SCA3 16.04 pg/mL, SCA7 16.67 pg/mL). For all SCAs, NfL concentration was stable over two years ( $p = 0.95$ ) despite a clinical progression ( $p < 0.0001$ ). Clinical progression between baseline and follow-up was associated with higher NfL concentrations at baseline ( $p = 0.04$ ). Of note, all premanifest carriers with NfL levels close to cut off concentrations had signs of the disease at follow-up. For all SCAs, the higher the observed NfL, the lower the pons volume at baseline ( $p < 0.01$ ) and follow-up ( $p = 0.02$ ). Higher NfL levels at baseline in all SCAs predicted a decrease in cerebellar volume ( $p = 0.03$ ). This result remained significant for SCA2 only among all genotypes ( $p = 0.02$ ). Overall, plasma NfL levels at baseline in SCA expansion carriers predict cerebellar volume change and clinical score progression. NfL levels might help refine inclusion criteria for clinical trials in carriers with very subtle signs.

### 1. Introduction

Interest in neurofilament light chain (NfL) has intensified in recent years due to mounting evidence that the level found in blood can serve as a biomarker for severity in neurological disorders (Gaetani et al., 2019; Bridel et al., 2019; Khalil, 2018). NfL is a subunit of the neuronal cytoskeleton and axonal damage provokes its release into cerebrospinal fluid (CSF) and blood (Gaetani et al., 2019). NfL concentrations in CSF

and blood are closely correlated, making it an easily measurable biomarker of neurodegeneration (Gaetani et al., 2019; Khalil, 2018). In several neurological diseases, NfL levels have been confirmed to be greater than in controls (Gaetani et al., 2019; Bridel et al., 2019; Khalil, 2018). NfL levels correlate with clinical scores, disease progression, and brain imaging in diseases such as amyotrophic lateral sclerosis (ALS) (Lu et al., 2015; Benatar et al., 2018), Alzheimer's disease (Mattsson et al., 2019; Benedet et al., 2020; Preische et al., 2019), and multiple sclerosis

**Abbreviations:** ALS, amyotrophic lateral sclerosis; ASOs, antisense oligonucleotides; AUC, area under the curve; CCFS, composite cerebellar functional severity score; CSF, cerebrospinal fluid; HD, Huntington disease; NfL, neurofilament light chain; PolyQ, polyglutamine; ROC, Receiver operating characteristics; SARA, scale for the assessment and rating of ataxia; SCA, spinocerebellar ataxia.

\* Corresponding author at: Paris Brain Institute, Pitié-Salpêtrière Paris CS21414, 75646 Paris, Cedex 13, France.

E-mail address: [alexandra.durr@icm-institute.org](mailto:alexandra.durr@icm-institute.org) (A. Durr).

<https://doi.org/10.1016/j.nbd.2021.105311>

Received 13 November 2020; Received in revised form 12 February 2021; Accepted 19 February 2021

Available online 23 February 2021

0969-9961/© 2021 The Author(s).

Published by Elsevier Inc.

This is an open access article under the CC BY-NC-ND license

(<http://creativecommons.org/licenses/by-nc-nd/4.0/>).

(Bjornevik et al., 2020; Kuhle et al., 2019). Moreover, Nfl dosage can help in the differential diagnosis of Parkinson's disease and atypical parkinsonian disorders (Hansson et al., 2017; Herbert et al., 2015; Hall et al., 2012). In inherited conditions, such as Huntington Disease, where pathological allele carriers can be identified before the onset of symptoms, NfL has been shown to increase significantly when carriers come close to the age at expected disease onset (Scahill et al., 2020). Loss of volume in cerebellar regions known to be affected in Huntington Disease, such as the caudate and putamen, were associated with higher NfL in plasma (Johnson et al., 2018). Higher NfL predicted subsequent occipital and white matter atrophy longitudinally (Johnson et al., 2018). Polyglutamine spinocerebellar ataxias (polyQ SCAs) share the same mutational mechanism with Huntington disease, a translated pathological CAG repeat expansion. For Huntington disease, there are targeted biomarkers, such as mutant huntingtin protein in CSF (Wild et al., 2015) for monitoring drug effects, or NfL as a prognostic blood biomarker of disease onset and progression (Byrne et al., 2017). Promising biomarkers for polyQ SCAs are being identified, as NfL (Wilke et al., 2018a), oxidative stress biomarkers (de Assis et al., 2017), ataxin-specific bioassays (Gonsior et al., 2020), and carboxy-terminus of Hsc70-interacting protein (CHIP) (Zhang et al., 2020). For both of these diseases, antisense oligonucleotides (ASOs) are in development. Research is more advanced for Huntington disease with phase 3 clinical trial (NCT03761849) as well as in an allele specific ASOs phase 1b/2a trial (NCT03225833). In SCAs, ASOs injections have shown encouraging results in SCA1 (Friedrich et al., 2018), SCA2 (Scoles et al., 2017), SCA3 (Moore et al., 2017; McLoughlin et al., 2018), and SCA7 (Niu et al., 2018) mouse models.

In the current study, we aimed to investigate whether blood NfL behaved similarly in various autosomal dominant ataxias. In a pilot study including 20 participants from families with dominant spinocerebellar ataxias (SCA1, SCA2, SCA3, SCA6) elevated NfL has been found (Wilke et al., 2018a). Three studies with large cohorts including SCA3 carriers showed NfL as a biomarker reflecting clinical state (Li et al., 2019; Wilke et al., 2020; Peng et al., 2020). We compared NfL levels from SCA1, SCA2, SCA3 and SCA7 carriers and healthy controls at baseline and a two-year follow-up visit. We also explored NfL correlations with clinical and brain imaging parameters.

## 2. Methods

We recruited 62 carriers of polyglutamine (polyQ) SCA (17 SCA1, 13 SCA2, 19 SCA3, and 13 SCA7) and 19 age-matched controls, from the French National Reference Center for Rare Diseases "Neurogenetics" in Paris, Pitié-Salpêtrière Hospital, between 2011 and 2015 as a part of the BIOSCA study (NCT01470729). The repeat length of the expanded and normal alleles was available for all SCA carriers. We assessed SCA carriers and controls by neurological examination, brain MRI, and NfL measurements at baseline and after two years. We used the scale for the assessment and rating of ataxia (SARA, max. value 40) (Schmitz-Hübisch et al., 2006) and the composite cerebellar functional severity score (CCFS) (du Montcel et al., 2008) to evaluate cerebellar syndrome. Pre-manifest carriers were considered to be those carriers of the pathological expansion without cerebellar signs, i.e. SARA score of <3 (Schmitz-Hübisch et al., 2006). Brain 3D T1-weighted magnetization-prepared rapid gradient-echo (MPRAGE) image ( $T_R = 2530$  ms,  $T_E = 3.65$  ms,  $T_I = 900$  ms, flip angle =  $9^\circ$ , 1 mm isotropic, field of view (FOV) =  $256 \times 256$  mm<sup>2</sup>) was acquired for 15 SCA1, 12 SCA2, 18 SCA3, 10 SCA7 carriers and 18 controls on a 3 T Siemens Trio scanner using a standard Siemens volume-transmit 32-channel receive coil array. Brain volumetric assessments of the cerebellum and pons were performed using Freesurfer, as previously described (Adanyeguh et al., 2018). To measure NfL, we collected fasted plasma samples using EDTA sample tube anticoagulant, frozen at  $-80^\circ\text{C}$  after collection, and stored in the local biobank. Plasma NfL levels were measured in duplicate using an ultra-sensitive single molecule array on the Simoa HD-1 Analyzer

(Quanterix), as previously established (Kuhle et al., 2016).

We compared clinical data, NfL levels, and volumes of the cerebellum and the pons between SCA populations and a control group at baseline and follow-up. We also compared NfL levels between each SCA genotype and the control group at baseline and follow-up. For each group, we analyzed the correlation between NfL levels and age at sampling, SARA score, CCFS, and volumetric brain MRI and, for SCA carriers only; correlations between pathological CAG repeat size and NfL and age at disease onset. We also investigated the difference between NfL level at follow-up and baseline ( $\Delta\text{NfL}$ ) for each group.

### 2.1. Standard protocol approvals, registrations, and patient consents

Local ethics committee (AOM10094, CPP Ile de France VI, Ref:105–10) approved the study. All participants agreed and signed a written informed consent form prior to participation in the study.

### 2.2. Statistical analysis

Statistical analyses were performed using SAS software. Data are expressed as the mean  $\pm$  standard deviation (SD) or frequency (n). Qualitative variables were compared between groups using Fischer's exact test and quantitative variables using non-parametric Kruskal-Wallis test, followed by a post-hoc Dunn pairwise test when necessary, with a Holm adjustment for multiple comparisons. Wilcoxon-Mann-Whitney test was used to assess the significance of the variation in clinical scores and NfL levels between baseline and follow-up. Pearson's correlation was performed between NfL levels and the volume of the cerebellum and pons using a step-down Bonferroni multiple correction. All correlations were adjusted for age and CAG repeat expansion. For each individual, the variation of clinical scores and volumetry between baseline and follow-up was computed. Using a linear model, we modeled these variations with the predictors: NfL, age, and the interaction between both. CAG repeat expansion was added as a covariable when considering the SCA subtype separately. The estimate of the NfL's effect ( $\beta$ ) is expressed in variation of the value of SARA score, CCFS and pons and cerebellum volume by pg/mL NfL concentration at baseline. Optimal cut-off values used to differentiate SCA symptomatic subjects from controls were determined using the Youden's procedure.

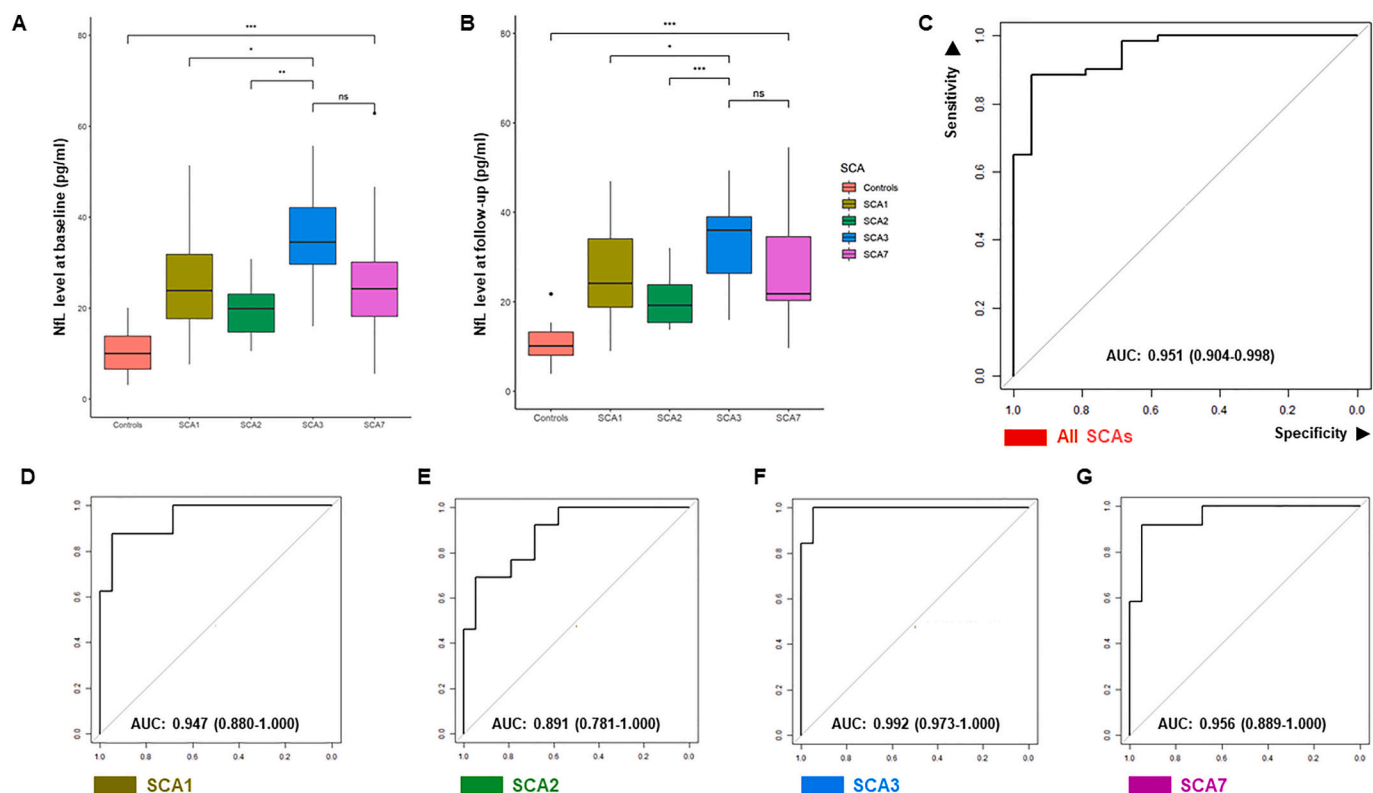
## 3. Results

### 3.1. Clinical characteristics and NfL correlations

NfL levels were significantly higher in SCA expansion carriers than in controls ( $27.25 \pm 12.16$  pg/mL vs  $10.24 \pm 4.48$  pg/mL,  $p < 0.001$ ), Fig. 1A, allowing for the differentiation of the two groups with high accuracy (AUC = 0.95 (0.9–0.99),  $p < 0.001$ , optimal cut-off at 16.04 pg/mL NfL, with 88% sensitivity and 95% specificity), Fig. 1C. NfL levels significantly correlated with age (baseline,  $r = 0.72$ ,  $p < 0.001$  and follow-up,  $r = 0.61$ ,  $p < 0.01$ ) in controls but not in SCA carriers (Table 1).

Across SCA groups, age at disease onset ( $p = 0.27$ ), age at examination ( $p = 0.52$ ), disease duration ( $p = 0.15$ ), SARA scores (baseline,  $p = 0.3$ ; follow-up  $p = 0.5$ ), and CCFS (baseline,  $p = 0.31$ ; follow-up  $p = 0.75$ ) were similar (Table 2). As expected, pathological CAG repeat sizes showed a negative correlation with age at disease onset for each SCA group (SCA1  $r = -0.929$ ,  $p < 0.001$ ; SCA2  $r = -0.696$ ,  $p < 0.01$ ; SCA3  $r = -0.701$ ,  $p < 0.01$ ; SCA7  $r = -0.89$ ,  $p < 0.001$ ). For all SCAs, the SARA score significantly increased by 2.24 in 2 years ( $12.16 \pm 6.93$  at baseline to  $14.4 \pm 7.75$  at follow-up,  $p < 0.0001$ ). For each genotype the SARA score was significantly higher at follow-up ( $10.67 \pm 6.23$  vs  $13.14 \pm 7.02$  for SCA1,  $p < 0.001$ ;  $13.26 \pm 6.16$  vs  $15.38 \pm 6.92$  for SCA2,  $p = 0.01$ ;  $14.1 \pm 7.26$  vs  $16.13 \pm 7.48$  for SCA3,  $p = 0.02$ ;  $10.15 \pm 7.79$  vs  $12.53 \pm 9.79$  for SCA7,  $p = 0.03$ ), with the largest increase for SCA1 (2.47/2 years) and the smallest for SCA3 (2.03/2 years), Table 2. In





**Fig. 1.** Plasma NfL concentrations and ROC curves differentiating SCAs carriers from controls.

A. NfL concentrations (pg/mL) at baseline were significantly different between controls and each SCA group. NfL levels in SCA3 were significantly higher than SCA1, SCA2 and SCA7. B. NfL concentrations (pg/mL) at two-year follow-up were significantly different between controls and each SCA group. SCA3 NfL levels were significantly higher than SCA1 and SCA2, but not SCA7. C. Receiver operating characteristics (ROC) curves at baseline showed the sensitivity and the specificity of plasma NfL to differentiate symptomatic SCA carriers and controls, AUC = 0.95 (0.9–0.99),  $p < 0.001$ , optimal cut-off: 16.04 pg/mL, 88% sensitivity, 95% specificity; D. ROC curve for symptomatic SCA1 carriers at baseline, AUC = 0.94 (0.88–1),  $p < 0.001$ , optimal cut-off: 16.87 pg/mL, 87% sensitivity, 95% specificity; E. ROC curve for SCA2 patients at baseline, AUC = 0.89 (0.78–1),  $p < 0.001$ , optimal cut-off: 19.1 pg/mL, 69% sensitivity, 95% specificity; F. ROC curve for symptomatic SCA3 carriers at baseline, AUC = 0.99 (0.97–1),  $p < 0.001$ , optimal cut-off: 16.04 pg/mL, 100% sensitivity, 95% specificity; G. ROC curve for symptomatic SCA7 carriers at baseline, AUC = 0.95 (0.88–1),  $p < 0.001$ , optimal cut-off: 16.67 pg/mL, 92 sensitivity, 95% specificity.

In the graph A and B, the boxes show upper and lower quartiles, horizontal lines in the boxes show median, and bar shows ranges. The point in the graph B for control group represents an outlier. \*  $p < 0.05$ ; \*\*  $p < 0.01$ ; \*\*\*  $p < 0.001$ ; ns: non significant.

**Table 1**

Correlation between plasma NfL concentrations and clinical and radiological characteristics in SCA carriers and controls.

	Controls (n = 19)		SCAs (n = 62)		SCA1 (n = 17)		SCA2 (n = 13)		SCA3 (n = 19)		SCA7 (n = 13)	
	r	p	r	p	r	p	r	p	r	p	r	p
Age V1	<b>0.72</b>	<b>&lt;0.001</b>	-0.14	0.25	-0.23	0.37	<b>-0.58</b>	<b>0.03</b>	-0.33	0.16	-0.15	0.62
Age V2	<b>0.61</b>	<b>&lt;0.01</b>	-0.06	0.59	-0.16	0.53	-0.53	0.06	-0.21	0.36	0.02	0.94
Disease duration V1	-	-	0.24	0.06	0.22	0.43	0.1	0.74	<b>0.57</b>	<b>0.02</b>	0.1	0.78
Disease duration V2	-	-	0.18	0.17	0.38	0.17	0.001	0.99	0.45	0.07	-0.12	0.75
SARA V1	0.18	0.46	<b>0.52</b>	<b>&lt;0.001</b>	0.25	0.35	0.32	0.32	<b>0.76</b>	<b>&lt;0.001</b>	0.33	0.30
SARA V2	-0.25	0.3	<b>0.48</b>	<b>&lt;0.001</b>	0.36	0.18	-0.01	0.96	<b>0.47</b>	<b>0.05</b>	0.40	0.21
CCFS V1	0.27	0.26	<b>0.36</b>	<b>&lt;0.01</b>	0.36	0.17	0.17	0.60	<b>0.59</b>	<b>0.01</b>	0.13	0.68
CCFS V2	0.15	0.53	<b>0.34</b>	<b>&lt;0.01</b>	0.38	0.15	-0.06	0.84	0.22	0.39	0.30	0.36
CAG V1	-	-	-	-	<b>0.52</b>	<b>0.03</b>	0.14	0.66	0.22	0.05	<b>0.93</b>	<b>&lt;0.001</b>
CAG V2	-	-	-	-	0.44	0.08	0.19	0.54	0.37	0.82	<b>0.85</b>	<b>&lt;0.001</b>
Cerebellar volume V1	0.10	0.69	-0.18	0.18	-0.45	0.12	-0.23	0.50	-0.43	0.09	-0.43	0.28
Cerebellar volume V2	0.01	0.95	-0.13	0.33	-0.49	0.08	-0.18	0.60	-0.08	0.74	-0.42	0.29
Cerebellum volume change	-0.22	0.39	<b>-0.29</b>	<b>0.03</b>	-0.4	0.17	<b>-0.68</b>	<b>0.02</b>	<b>-0.26</b>	0.34	-0.01	0.98
Pons volume V1	-0.02	0.93	<b>-0.35</b>	<b>&lt;0.01</b>	-0.26	0.37	-0.55	0.09	<b>-0.71</b>	<b>0.001</b>	-0.65	0.08
Pons volume V2	-0.07	0.78	<b>-0.30</b>	<b>0.02</b>	-0.30	0.31	-0.37	0.29	-0.47	0.06	-0.56	0.14

Abbreviations: CCFS: composite cerebellar functional severity scale, NfL: neurofilament light chain, SARA: scale for the assessment and rating of ataxia, SCA: spinocerebellar ataxia, V1: baseline, V2: two-year follow-up. Significant values are in bold.

addition, at follow-up, CCFS worsened in the SCA group ( $1.06 \pm 0.13$  vs  $1.09 \pm 0.16$ ,  $p < 0.001$ ), but when considering each genotype individually the progression was significant only for SCA3 ( $1.03 \pm 0.1$  vs  $1.08$

$\pm 0.12$ ,  $p < 0.01$ ) and SCA7 ( $1.05 \pm 0.18$  vs  $1.1 \pm 0.22$ ,  $p = 0.02$ ). In controls, no progression was found for SARA score ( $1.05 \pm 1.12$  vs  $0.76 \pm 0.69$ ,  $p = 0.3$ ) and CCFS ( $0.86 \pm 0.05$  vs  $0.84 \pm 0.04$ ,  $p = 0.26$ ),

**Table 2**

Comparison of clinical data and plasma NFL levels between the SCA population and control group.

	Age at onset (y)	Pathological CAG repeat	Disease duration at baseline	Baseline				2-year follow-up			
				Age at sampling (y)	SARA (max. Value 40)	CCFS	NfL (pg/mL)	Age at sampling (y)	SARA (max. Value 40)	CCFS	NfL (pg/mL)
Controls n = 19 (11 M-8 W)	–	–	–	49.53 ± 12.22	1.05 ± 1.12	0.86 ± 0.05	10.24 ± 4.48	51.53 ± 12.22	0.76 ± 0.69	0.84 ± 0.04	10.71 ± 4.2
SCAs n = 62 (32 M-30 W)	39.17 ± 11.71 (n = 59)	–	8.46 ± 5.4	46.85 ± 13.31	12.16 ± 6.93	1.06 ± 0.13	27.25 ± 12.16	49.83 ± 13.08	14.4 ± 7.75	1.09 ± 0.16	27.29 ± 10.92
p <sup>a</sup>	–	–	–	0.47	<b>&lt;0.001</b>	<b>&lt;0.001</b>	<b>&lt;0.001</b>	0.47	<b>&lt;0.001</b>	<b>&lt;0.001</b>	<b>&lt;0.001</b>
SCA1 n = 17 (9 M-8 W)	39.43 ± 12.53 (n = 16)	46.41 ± 6.16 (40–62)	6.5 ± 5.6	44.47 ± 15.17	10.67 ± 6.23	1.04 ± 0.09	24.79 ± 11.08	46.47 ± 15.17	13.14 ± 7.02	1.07 ± 0.15	26.20 ± 11.12
SCA2 n = 13 (8 M-4 W)	35.23 ± 10.74 (n = 13)	39.54 ± 2.81 (36–46)	10.2 ± 6.2	45.38 ± 12.2	13.26 ± 6.16	1.12 ± 0.15	20.28 ± 6.28	47.38 ± 12.2	15.38 ± 6.92	1.13 ± 0.18	20.12 ± 5.32
SCA3 n = 19 (8 M-11 W)	42.26 ± 10.88 (n = 19)	69.16 ± 5.55 (50–76)	8.6 ± 4.8	50.89 ± 12.02	14.1 ± 7.26	1.03 ± 0.1	34.92 ± 10.5	52.89 ± 12.02	16.13 ± 7.48	1.08 ± 0.12	33.14 ± 9.38
SCA7 n = 13 (7 M-6 W)	38.09 ± 12.99 (n = 11)	42.46 ± 5.1 (36–56)	9.0 ± 5.2	45.54 ± 13.78	10.15 ± 7.79	1.05 ± 0.18	26.25 ± 15.1	47.54 ± 13.78	12.53 ± 9.79	1.1 ± 0.22	27.33 ± 13
p <sup>**</sup>	0.27	–	0.15	0.52	0.28	0.31	<b>0.003</b>		0.47	0.75	<b>0.004</b>

Comparison of clinical data and plasma NfL levels between the SCA population and control group at baseline and follow-up and details for each SCA subtype. Data are presented as the mean ± standard deviation and significant values are in bold. Abbreviations: AO: age at disease onset, CCFS: composite cerebellar functional severity scale, M: men, NfL: neurofilament light chain, SARA: scale for the assessment and rating of ataxia, SCA: spinocerebellar ataxia, W: women, y: years.

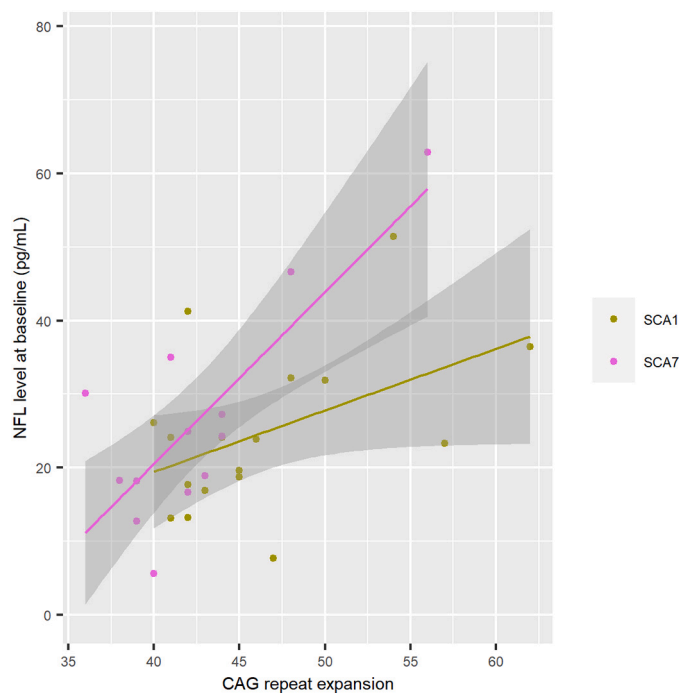
<sup>a</sup> p-value referred to comparison between control group and SCAs group.

<sup>\*\*</sup> p-value referred to comparison among SCAs groups.

**Table 2.**

Age-adjusted NfL levels for all SCAs were significantly correlated at baseline with SARA score ( $r = 0.52$ ,  $p < 0.001$ ) and CCFS ( $r = 0.36$ ,  $p < 0.01$ ), **Table 1**. In SCA population, the correlation between age-adjusted NfL levels with the SARA score and CCFS was confirmed at the two-year follow-up ( $r = 0.48$ ,  $p < 0.01$  and  $r = 0.34$ ,  $p < 0.01$ , respectively), **Table 1**. The increase of SARA scores between baseline and follow-up was associated with higher NfL concentrations at baseline ( $\beta = 0.07 \pm 0.03$ ,  $p = 0.04$ ). No correlation was found between NfL levels and disease duration (baseline,  $r = 0.24$ ,  $p = 0.06$ ; follow-up,  $r = 0.18$ ,  $p = 0.17$ ), **Table 1**.

At baseline, SCA3 had the highest NfL level among all subtypes,  $34.92 \pm 10.5$  pg/mL, significantly greater than SCA1 ( $24.79 \pm 11.08$  pg/mL,  $p = 0.03$ ), SCA2 ( $20.28 \pm 6.28$  pg/mL,  $p < 0.01$ ) and with the tendency to be higher than SCA7 ( $26.25 \pm 15.1$ ,  $p = 0.07$ ), **Fig. 1A**. These results were confirmed at follow-up (**Fig. 1B**). SCA3 was also found to have the most accurate pathological cut-off level, at 16.04 pg/mL, with 100% sensitivity and 95% specificity, AUC = 0.99 (0.97–1)  $p < 0.001$ , as shown in **Fig. 1F**, compared to SCA1 (**Fig. 1D**), SCA2 (**Fig. 1E**), and SCA7 (**Fig. 1G**). For SCA3, at baseline, NfL levels corrected for age and CAG repeat size, correlated with clinical scores (SARA,  $r = 0.76$ ,  $p < 0.001$ ; CCFS,  $r = 0.59$ ,  $p = 0.01$ ) and disease duration ( $r = 0.57$ ,  $p = 0.02$ ), **Table 1**. The tendency for correlation between NfL and SARA score persisted at the two-year follow-up ( $r = 0.47$ ,  $p = 0.05$ ) but not for CCFS ( $r = 0.22$ ,  $p = 0.39$ ) and disease duration ( $r = 0.45$ ,  $p = 0.07$ ), **Table 1**. Correlation between NfL levels at baseline and CAG repeat size was found for SCA1 and SCA7 ( $r = 0.52$ ,  $p = 0.03$  and  $r = 0.93$ ,  $p \leq 0.001$ ), **Table 1** and **Fig. 2**, but not for SCA2 and SCA3 ( $r = 0.14$ ,  $p = 0.66$  and  $r = 0.22$  and  $p = 0.05$ ), **Table 1**. For SCA7, the increase of CCFS between baseline and follow-up ( $1.05 \pm 0.18$  vs  $1.1 \pm 0.22$ ,  $p = 0.02$ , **Table 2**) was associated with greater NfL concentrations at baseline ( $\beta = 0.007 \pm 0.003$ ,  $p = 0.04$ ), and the correlation with CAG repeat

**Fig. 2.** Correlation between plasma NfL concentrations and CAG repeat size in SCA1 and SCA7.

The figure shows greater NfL concentrations (pg/mL) at baseline for greater CAG repeat length, significant for SCA1 ( $r = 0.52$ ,  $p = 0.03$ ) and SCA7 ( $r = 0.93$ ,  $p \leq 0.001$ ).

size was confirmed at follow-up,  $r = 0.85$ ;  $p < 0.001$  (Table 1).

### 3.2. NfL stability at 2-year follow-up

At the two-year follow-up visit, NfL concentrations were stable for controls ( $10.71 \pm 4.2$  pg/mL,  $p = 0.13$ ) and for all SCA carriers: both as a group ( $27.29 \pm 10.92$  pg/mL,  $p = 0.69$ ) and for each genotype taken separately ( $26.20 \pm 11.12$  pg/mL, SCA1  $p = 0.22$ ;  $20.12 \pm 5.32$  pg/mL, SCA2  $p = 0.83$ ;  $33.14 \pm 9.38$  pg/mL, SCA3  $p = 0.09$ ;  $27.33 \pm 13$  pg/mL, SCA7  $p = 0.12$ ), Table 2. SCA3 confirmed to have the higher NfL concentration compared to SCA1 and SCA2 (Fig. 1B, Table 2). Change over time in NfL levels for individuals ( $\Delta$ NfL) showed no significant differences between SCAs and controls ( $0.03 \pm 4.64$  vs  $0.46 \pm 1.57$ ,  $p = 0.69$ ), even across SCA subtypes ( $1.4 \pm 4.04$  for SCA1,  $-0.16 \pm 2.59$  for SCA2,  $-1.78 \pm 4.81$  for SCA3,  $1.08 \pm 6.1$  for SCA7,  $p = 0.16$ ).

### 3.3. Evolution of presymptomatic SCAs carriers

Two out of seven premanifest carriers had converted to the ataxic stage (SARA  $>3$ ) at follow-up: one SCA1 carrier with an NfL level of 13.3 pg/mL, close to the cut-off level of 16.87 pg/mL, and one SCA3 carrier with 15.9 pg/mL (cut-off at 16.04 pg/mL). The other premanifest carriers, despite a SARA score  $< 3$ , reported cramps and back pain (one SCA3 with NfL values of 19.2 pg/mL) or had pyramidal signs at examination (two SCA7 carriers with NfL levels of 13.9 pg/mL and 20.4 pg/mL respectively, for a cut-off value of 16.67 pg/mL). All premanifest carriers with NfL levels close to or above cut-off concentrations had moved into the disease stage at follow-up. This finding shows that NfL levels are sensitive to non-cerebellar manifestations of the disease in SCA3 and SCA7. Only the carriers with NfL levels below 10 pg/mL had no cerebellar and no extra-cerebellar signs (SCA1 carrier with 8.9 pg/mL and SCA7 carrier with 9.6 pg/mL).

### 3.4. MRI volumetry and NfL correlations

As previously reported, volumes of the cerebellum and pons decreased in all SCA groups between baseline and follow-up ( $p < 0.05$ ), while there was no change for controls (cerebellum volume,  $p = 0.12$ ; pons volume,  $p = 0.65$ ) (Adanyeguh et al., 2018).

For all SCAs, the higher the observed NfL, the lower the pons volume was found to be at baseline ( $r = -0.35$ ,  $p < 0.01$ ) (Fig. 3) and follow-up

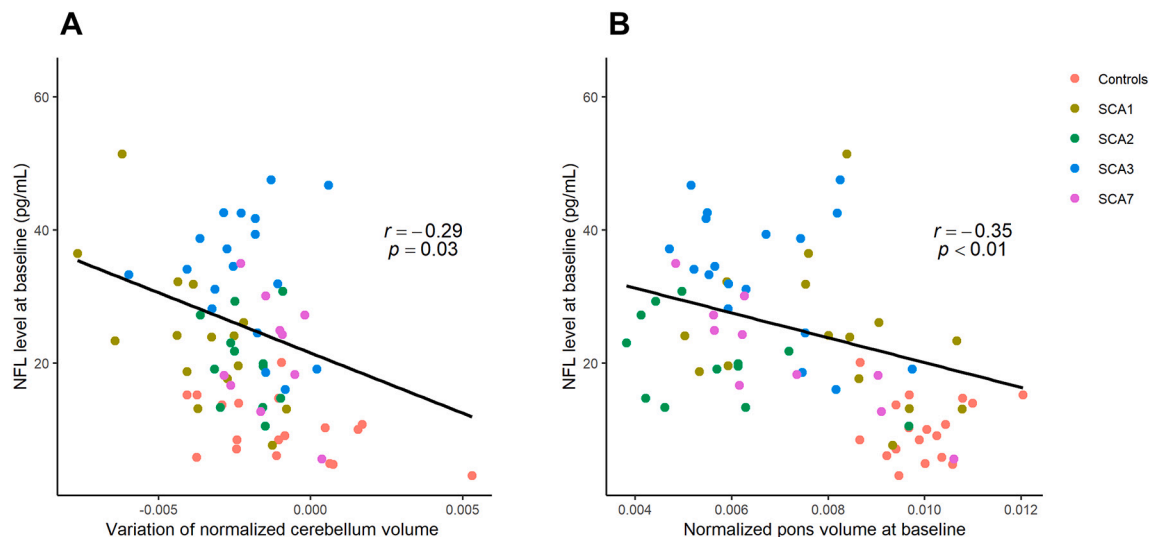
( $r = -0.30$ ,  $p = 0.02$ ), Table 1. This negative correlation was confirmed for SCA3 at baseline ( $r = -0.71$ ,  $p = 0.001$ ), with a tendency to persist at follow-up ( $r = -0.47$ ,  $p = 0.06$ ), Table 1. For all SCAs, there was a correlation between NfL levels at baseline and cerebellum volume change ( $r = -0.29$ ,  $p = 0.03$ ), Table 1.

Higher NfL levels at baseline predicted a decrease of cerebellar volume in all SCAs ( $\beta = -5.8 \times 10^{-5} \pm 2.7 \times 10^{-5}$ ,  $p = 0.03$ ), Fig. 3, Table 1. This result remained significant only for SCA2 when analyzing each individual genotype ( $\beta = -1.0 \times 10^{-4} \pm 3.7 \times 10^{-5}$ ,  $p = 0.02$ ), Table 1.

## 4. Discussion

We measured plasma NfL levels in SCA1, SCA2, SCA3, and SCA7 pathological expansion carriers in a longitudinal study and correlated those levels with clinical and imaging markers. The higher the NfL at baseline, the greater the SARA score and the greater the cerebellar volume loss at the two-year follow-up. Thus, NfL concentrations predicted cerebellar volume loss at two years in SCAs, as it has also been shown in Huntington Disease, where higher NfL levels predicted reduced volumes of the caudate and putamen bilaterally (Scabill et al., 2020). NfL levels do not change over time in SCAs in our study, this is also true in ALS (Lu et al., 2015), and they were not associated with age as for ALS, frontotemporal dementia, and atypical parkinsonian syndromes (Bridel et al., 2019) (Table 3). However, in other settings NfL levels increase, as for example in Alzheimer's disease (Mattsson et al., 2019), multiple sclerosis (Bjornevik et al., 2020), and also in SCA3 (Wilke et al., 2020) (Table 3). NfL concentrations in SCA patients fall between the highest levels observed in ALS (Lu et al., 2015) or multiple system atrophy (Wilke et al., 2018a) and the lowest levels in Friedreich's ataxia (Zeitlberger et al., 2018) or Parkinson's disease (Table 3) (Oosterveld et al., 2020). This could be explained by either different disease progression rates or different levels of peripheral nervous system dysfunction, as in ALS (Gaetani et al., 2019). Despite this, plasma NfL levels are not directly comparable in neurological disorders due to the different time points and different disease stages for which the plasma samples were collected (Table 3).

Because NfL concentrations reflect irreversible neuronal damage, we would expect levels to increase over time and parallel the visible clinical and radiological progression. The absence of NfL change over two years suggests this marker could be useful as a predictor to characterize



**Fig. 3.** Correlation between NfL concentrations and MRI volumetry in all SCA carriers and controls.

A. Correlation between NfL concentration at baseline and cerebellum volume change ( $r = -0.29$ ,  $p = 0.03$ ). For controls, no correlation was found ( $p = 0.38$ ). B. Correlation between NfL concentrations and pons volume was negative in all SCAs carriers at baseline ( $r = -0.35$ ,  $p < 0.01$ ). For controls, no correlation was found ( $p = 0.93$ ).

**Table 3**

Blood Neurofilament Light Chain concentrations in neurological diseases: from highest to lowest values.

Disease	Blood NfL (pg/mL, mean, range)	Type of study	Comments
Amyotrophic Lateral Sclerosis (Wilke et al., 2018b)	158.4 (93.2–246.3) n = 33	Cross-sectional	
Amyotrophic Lateral Sclerosis (Lu et al., 2015)	78 (40.2–146), <60 years 99.9 (57.6–167), 60–69 years 105 (61.7–154), 70–79 117.2 (54.9, 216.7), ≥80 years n = 67	Cross-sectional and longitudinal, age < 60 years	Cut-off value = 36.2 pg/mL NfL stable at 15 months follow-up
Multiple Systemic Atrophy type C <sup>18</sup>	60.7 (44.5–94) n = 25	Cross-sectional	
Dominant ataxias (SCA 1, 2, 3, 6) (Wilke et al., 2018a)	58.7 (45.3–74.0) n = 20	Cross-sectional	Moderate disease, SARA score 13.0 (7.8–17.1)
Huntington Disease (Byrne et al., 2017)	28.36 ± 22.24 (early premanifest, n = 58) 39.39 ± 14.19 (late premanifest, n = 46) 52.18 ± 20.52 (HD stage 1, n = 66) 57.48 ± 23.82 (HD stage 2, n = 31)	Cross-sectional	
Alzheimer Disease (Mattsson et al., 2019)	37.9 pg/mL (MCI, n = 855) 45.9 pg/mL (AD dementia, n = 327)	Longitudinal	Increase of 4.9 pg/mL per year
Multiple Sclerosis (Bjornevik et al., 2020)	Median 45.1 (IQR, 27.0–102.7) n = 30	Nested case-control	NfL increased 6 years before onset
SCA3 (Wilke et al., 2020)	34.8 (28.3–47.0) cohort 1 ESMI consortium, n = 75 85.5 (70.2–100.2) cohort 2 EuroSCA and RiSCA, n = 27	Cross-sectional	Moderate disease, SARA score 13.0 (10.0–21.5) cohort 1 Moderate disease, SARA score 11.5 (6.5– 15.0) cohort 2 Cut-off value cohort 2 = 20.3 pg/mL NfL higher than controls 7.5 years before onset
SCA3 (Li et al., 2019)	15.3 ± 7.5 (preclinical, n = 26) 37.5 ± 13.5 (manifest, n = 90)	Cross-sectional	Cut-off value = 20 pg/mL Moderate disease, SARA score 11.72 ± 6.02
SCA3 (Peng et al., 2020)	12.18 (10.2–13.9) (asymptomatic, n = 17) 21.84 (18.37–23.45) (premanifest, n = 20) 36.06 (30.04–45.9) (manifest, n = 198)	Cross-sectional	Moderate disease, SARA score 13 (10–17.5) for manifest group

**Table 3 (continued)**

Disease	Blood NfL (pg/mL, mean, range)	Type of study	Comments
Frontotemporal Dementia (Meeter et al., 2016)	31.5 (manifest, n = 35) 3.5 (premanifest, n = 44)	Cross-sectional	Cut-off value = 18.0 pg/mL (patients from presymptomatic carriers) Cut-off value = 8.3 pg/mL (presymptomatic carriers from controls)
<b>Dominant ataxias (Our study, 2020)</b>	<b>24.79 (7.6–51.4), n = 17</b> <b>SCA1 20.28 (10.5–30.8), n = 13</b> <b>SCA2 34.92 (16–55.7), n = 19</b> <b>SCA3 26.25 (5.5–62.8), n = 13</b>	<b>Longitudinal</b>	<b>NfL levels stable at 24-month follow-up</b> <b>Cut-off value = 16.87 pg/mL</b> <b>Cut-off value = 19.1 pg/mL</b> <b>Cut-off value = 16.04 pg/mL</b> <b>Cut-off value = 16.67 pg/mL (manifest from controls)</b>
Sporadic adult-onset ataxia (Wilke et al., 2018a)	28.0 (19.1–49.2) n = 25	Cross-sectional	
Inherited spastic paraparesis (Wilke et al., 2018b)	24.7 (18.1–40) n = 96	Cross-sectional	ROC analysis indicated the performance of NfL for differentiating HSP patients from ALS patients Cut-off value = 15.6 pg/mL
Parkinson Disease (Oosterveld et al., 2020)	18.7 (12.1–30.8) n = 139	Cross-sectional	Cut-off value = 15.6 pg/mL
Friedreich Ataxia (Zeitlberger et al., 2018)	17.10 (13.00–24.40) n = 33	Cross-sectional	No correlation with GAA repeat expansion size

Abbreviations: AD: Alzheimer's disease; ALS: amyotrophic lateral sclerosis; HSP: hereditary spastic paraplegia; MCI: mild cognitive impairment; NfL: neurofilament light chain; ROC: receiver operating characteristic; SCA: spinocerebellar ataxia.

premanifest cases, rather than as an outcome measure in patients with overt disease. The latter may have already reached a plateau NfL level that masks the age-dependent increase of NfL. Interestingly, premanifest SCA carriers in our study had normal, intermediate or elevated NfL levels. Pathological levels above or close to our cut-off were observed in non-ataxic carriers who had extra-cerebellar signs. One third of polyQ SCA carriers present with signs other than gait disturbances at onset (Globas et al., 2008). It is possible that NfL levels reflect the non-cerebellar signs of these diseases even before cerebellar ataxia clinically manifests.

Among genotypes, SCA3 carriers had higher NfL levels than SCA1 and SCA2, as has been previously reported (Wilke et al., 2018a). With our longitudinal data we can add that though NfL levels were the highest, SARA evolved the least in SCA3. This could be due to more prominent peripheral nervous system involvement, as painful axonal neuropathy is the hallmark of SCA3. Despite the finding that SCA3 had the smallest variation in SARA score, we confirmed the correlation between NfL and SARA score as previously reported for this subgroup as well (Li et al., 2019; Wilke et al., 2020; Peng et al., 2020). Only SCA3 subtype confirmed the correlation between NfL levels and pons atrophy that could be explained by the prominent involvement of pons nuclei compared to the other SCA groups (Seidel et al., 2012). For the SCA2



subtype, the smallest group among the SCAs in our cohort, NfL level at baseline still predicted cerebellar volume changes. This reflects a remarkable atrophy already present at a premanifest stage (Reetz et al., 2018; Jacobi et al., 2015).

In SCAs, age at onset is mainly predicted by expanded CAG sizes (Tezenas du Montcel et al., 2014), with larger CAG repeat sizes predicting more severe disease in younger patients. In our cohort, NfL levels correlated only with CAG repeat size for SCA1 and SCA7, a strong link which has already been reported for HD (Byrne et al., 2017). This may be because SCA1 and SCA7 in our sample showed the strongest correlation between CAG repeat size and age at onset. In one SCA3 study, including two cohorts with a total of 124 carriers, in addition to the correlation with disease progression and the prediction of the estimated age at onset, NfL levels also increased with CAG repeat size and age (Wilke et al., 2020). The limited sample size in our study compared to the Wilke et al., 2020<sup>28</sup> study could be a factor in the lack of correlation with CAG repeat length. While it is well established that blood and CSF NfL concentrations increase with age in healthy controls (Gaetani et al., 2019) (as we also observed in our study), we did not find an age-dependent increase in NfL levels in SCA carriers. Instead, a correlation between NfL levels and age at sampling is reported for SCA3 in two studies (Li et al., 2019; Wilke et al., 2020). In addition to the limited number of SCA3 patients included in our study, the lack of correlation with CAG repeat length could be explained in part by different age at sampling. In our study, SCA3 carriers had a mean age at baseline of almost 51 years old. In the study of Li et al. 2019<sup>27</sup> and Wilke et al., 2020 (Wilke et al., 2020), the ataxic SCA3 patients had similar age, but presymptomatic SCA3 carriers were included with a mean age between 31 and 36 years old representing 29 and 21% of the study samples respectively. The difference in ages between our study and the others, especially with presymptomatic carriers below the age of 50 in the two previous papers, could explain why we did not find a change in NfL level due to older age. In fact, previous studies have reported a non-linear association between age and NfL concentrations, which have been shown to reach a plateau (Li et al., 2019; Wilke et al., 2020). Compared to the studied of Li et al. 2019<sup>27</sup> and Wilke et al., 2020 (Wilke et al., 2020), we included patients with higher SARA score and less presymptomatic carriers. Careful inclusion criteria for cohorts using NfL concentrations as readouts of efficacy should be considered.

Our study presents certain limitations. The appropriate sample size for NfL has been estimated as 15 for SCA patients (Wilke et al., 2018a), in the present dataset SCA2 and SCA7 samples did not reach 15. In rare neurogenetic diseases, attaining large cohort of carriers remains a challenge. Our aim to have longitudinal data further reduced the sample size. While our study included data from baseline and a two-year follow-up visit, more assessment points over time and longer follow-up, may have allowed for a better understanding of NfL level evolution. In order to intervene prior to disease onset, studies of larger cohorts of presymptomatic carriers should be planned in the future. The use of NfL to determine disease onset in SCA3 has been explored (Wilke et al., 2020) and should be useful for other polyQ subtypes.

Clinical trials with antisense oligonucleotides (ASOs) are planned for polyQ SCAs over the next few years. This means there is an urgent need for a biomarker as an objective and reliable measure of biological processes to allow for the evaluation of a drug's effects. In contrast to HD, for which huntingtin in CSF can be measured, ataxin-specific bioassays are under development as recently reported in peripheral blood mononuclear cells for SCA3 (Gonsior et al., 2020). The main outcome measure of clinical trials is currently the SARA score. However, as we have shown in the current study, NfL detected the multisystem spread of pathology before ataxic onset in premanifest carriers with a SARA score < 3.

We also know that clinical measurements are rater-dependent and are not entirely accurate in detecting disease progression (Adanyeguh et al., 2018). To date, the most sensitive biomarkers for polyQ SCAs come from MRI studies (Adanyeguh et al., 2018), with brainstem and cerebellum atrophy already present at the presymptomatic stage for

SCA1 and SCA2 carriers (Reetz et al., 2018; Jacobi et al., 2013). Here, we show that brainstem and cerebellum atrophy is linked to NfL levels in SCAs. Even though, there is not a direct correlation with cerebellum volume, the cerebellum volume loss is greater for SCAs carriers with the highest level of NfL at baseline. The absence of an increase in NfL level at the two-year follow-up indicates that we cannot use NfL as a biomarker of disease progression during the short periods of time usually used in clinical trials, but as a biomarker of disease severity predicting the cerebellum atrophy. However, we can hypothesize on the role of NfL in clinical trials to monitor ASO effects; a decrease in blood NfL concentrations, subsequent to ASO injections, would be indirect evidence of a slowdown in neurodegeneration.

## 5. Conclusions

We defined disease cut off levels for SCA1, 2, 3 and 7 genotypes and showed that plasma NfL levels in SCAs predict cerebellar volume changes and clinical progression. This will be useful in refining clinical staging and may have use in future clinical trials.

## Funding

This study was supported by a grant from the French Ministry of Health "Programme Hospitalier de Recherche Clinique" (PHRC BIOSCA – ID RCB: 2010-A01324 35, AOM10094, NCT01470729).

## Declaration of Competing Interest

None.

## Acknowledgements

We would like to thank the SCA carriers and healthy volunteers for their participation in this study. We would like to thank Assistance-Publique des Hôpitaux de Paris, which sponsored the study.

## References

- Adanyeguh, I.M., Perlberg, V., Henry, P.-G., et al., 2018. Autosomal dominant cerebellar ataxias: imaging biomarkers with high effect sizes. *NeuroImage Clin.* 19, 858–867. <https://doi.org/10.1016/j.nicl.2018.06.011>.
- Benatar, M., Wu, J., Andersen, P.M., Lombardi, V., Malaspina, A., 2018. Neurofilament light: a candidate biomarker of presymptomatic amyotrophic lateral sclerosis and phenoconversion. *Ann. Neurol.* 84 (1), 130–139. <https://doi.org/10.1002/ana.25276>.
- Benedet, A.L., Leuz, A., Pascoal, T.A., et al., 2020. Stage-specific links between plasma neurofilament light and imaging biomarkers of Alzheimer's disease. *Brain J Neurol.* Published online November 19. <https://doi.org/10.1093/brain/awaa342>.
- Bjornevik, K., Munger, K.L., Cortese, M., et al., 2020. Serum Neurofilament light chain levels in patients with Presymptomatic multiple sclerosis. *JAMA Neurol.* 77 (1), 58–64. <https://doi.org/10.1001/jamaneurol.2019.3238>.
- Bridel, C., van Wieringen, W.N., Zetterberg, H., et al., 2019. Diagnostic value of cerebrospinal fluid Neurofilament light protein in neurology: a systematic review and meta-analysis. *JAMA Neurol.* <https://doi.org/10.1001/jamaneurol.2019.1534>. Published online June 17.
- Byrne, L.M., Rodrigues, F.B., Blennow, K., et al., 2017. Neurofilament light protein in blood as a potential biomarker of neurodegeneration in Huntington's disease: a retrospective cohort analysis. *Lancet Neurol.* 16 (8), 601–609. [https://doi.org/10.1016/S1474-4422\(17\)30124-2](https://doi.org/10.1016/S1474-4422(17)30124-2).
- de Assis, A.M., Saute, J.A.M., Longoni, A., et al., 2017. Peripheral oxidative stress biomarkers in Spinocerebellar Ataxia type 3/Machado-Joseph disease. *Front. Neurol.* 8, 485. <https://doi.org/10.3389/fneur.2017.00485>.
- du Montcel, S.T., Charles, P., Ribai, P., et al., 2008. Composite cerebellar functional severity score: validation of a quantitative score of cerebellar impairment. *Brain J. Neurol.* 131 (Pt 5), 1352–1361. <https://doi.org/10.1093/brain/awn059>.
- Friedrich, J., Kordasiewicz, H.B., O'Callaghan, B., et al., 2018. Antisense oligonucleotide-mediated ataxin-1 reduction prolongs survival in SCA1 mice and reveals disease-associated transcriptome profiles. *JCI Insight* 3 (21). <https://doi.org/10.1172/jci.insight.123193>.
- Gaetani, L., Blennow, K., Calabresi, P., Di Filippo, M., Parnetti, L., Zetterberg, H., 2019. Neurofilament light chain as a biomarker in neurological disorders. *J. Neurol. Neurosurg. Psychiatry* 90 (8), 870–881. <https://doi.org/10.1136/jnnp-2018-320106>.

- Globas, C., du Montcel, S.T., Baliko, L., et al., 2008. Early symptoms in spinocerebellar ataxia type 1, 2, 3, and 6. *Mov Disord Off J Mov Disord Soc.* 23 (15), 2232–2238. <https://doi.org/10.1002/mds.22288>.
- Gonsior, K., Kaucher, G.A., Pelz, P., et al., 2020. PolyQ-expanded ataxin-3 protein levels in peripheral blood mononuclear cells correlate with clinical parameters in SCA3: a pilot study. *J. Neurol.* 26 <https://doi.org/10.1007/s00415-020-10274-y>. Published online October.
- Hall, S., Öhrfelt, A., Constantinescu, R., et al., 2012. Accuracy of a panel of 5 cerebrospinal fluid biomarkers in the differential diagnosis of patients with dementia and/or parkinsonian disorders. *Arch. Neurol.* 69 (11), 1445–1452. <https://doi.org/10.1001/archneurol.2012.1654>.
- Hansson, O., Janelidze, S., Hall, S., et al., 2017. Blood-based NfL: a biomarker for differential diagnosis of parkinsonian disorder. *Neurology.* 88 (10), 930–937. <https://doi.org/10.1212/WNL.0000000000003680>.
- Herbert, M.K., Aerts, M.B., Beenes, M., et al., 2015. CSF Neurofilament light chain but not FLT3 ligand discriminates Parkinsonian disorders. *Front. Neurol.* 6, 91. <https://doi.org/10.3389/fneur.2015.00091>.
- Jacobi, H., Reetz, K., du Montcel, S.T., et al., 2013. Biological and clinical characteristics of individuals at risk for spinocerebellar ataxia types 1, 2, 3, and 6 in the longitudinal RISCA study: analysis of baseline data. *Lancet Neurol.* 12 (7), 650–658. [https://doi.org/10.1016/S1474-4422\(13\)70104-2](https://doi.org/10.1016/S1474-4422(13)70104-2).
- Jacobi, H., du Montcel, S.T., Bauer, P., et al., 2015. Long-term disease progression in spinocerebellar ataxia types 1, 2, 3, and 6: a longitudinal cohort study. *Lancet Neurol.* 14 (11), 1101–1108. [https://doi.org/10.1016/S1474-4422\(15\)00202-1](https://doi.org/10.1016/S1474-4422(15)00202-1).
- Johnson, E.B., Byrne, L.M., Gregory, S., et al., 2018. Neurofilament light protein in blood predicts regional atrophy in Huntington disease. *Neurology.* 90 (8), e717–e723. <https://doi.org/10.1212/WNL.0000000000005005>.
- Khalil, M., 2018. Neurofilaments as biomarkers in neurological disorders. *Nat. Rev. Neurol.* 14 <https://doi.org/10.1038/s41582-018-0058-z>.
- Kuhle, J., Barro, C., Andreasson, U., et al., 2016. Comparison of three analytical platforms for quantification of the neurofilament light chain in blood samples: ELISA, electrochemiluminescence immunoassay and Simoa. *Clin. Chem. Lab. Med.* 54 (10), 1655–1661. <https://doi.org/10.1515/cclm-2015-1195>.
- Kuhle, J., Kropshofer, H., Haering, D.A., et al., 2019. Blood neurofilament light chain as a biomarker of MS disease activity and treatment response. *Neurology.* 92 (10), e1007–e1015. <https://doi.org/10.1212/WNL.0000000000007032>.
- Li, Q.-F., Dong, Y., Yang, L., et al., 2019. Neurofilament light chain is a promising serum biomarker in spinocerebellar ataxia type 3. *Mol. Neurodegener.* 14 (1), 39. <https://doi.org/10.1186/s13024-019-0338-0>.
- Lu, C.-H., Macdonald-Wallis, C., Gray, E., et al., 2015. Neurofilament light chain: a prognostic biomarker in amyotrophic lateral sclerosis. *Neurology.* 84 (22), 2247–2257. <https://doi.org/10.1212/WNL.0000000000001642>.
- Mattsson, N., Cullen, N.C., Andreasson, U., Zetterberg, H., Blennow, K., 2019. Association between longitudinal plasma Neurofilament light and Neurodegeneration in patients with Alzheimer disease. *JAMA Neurol.* 76 (7), 791–799. <https://doi.org/10.1001/jamaneurol.2019.0765>.
- McLoughlin, H.S., Moore, L.R., Chopra, R., et al., 2018. Oligonucleotide therapy mitigates disease in spinocerebellar ataxia type 3 mice. *Ann. Neurol.* 84 (1), 64–77. <https://doi.org/10.1002/ana.25264>.
- Meeter, L.H., Dopfer, E.G., Jiskoot, L.C., et al., 2016. Neurofilament light chain: a biomarker for genetic frontotemporal dementia. *Ann Clin Transl Neurol.* 3 (8), 623–636. <https://doi.org/10.1002/acn3.325>.
- Moore, L.R., Rajpal, G., Dillingham, I.T., et al., 2017. Evaluation of antisense oligonucleotides targeting ATXN3 in SCA3 mouse models. *Mol Ther Nucleic Acids.* 7, 200–210. <https://doi.org/10.1016/j.omtn.2017.04.005>.
- Niu, C., Prakash, T.P., Kim, A., et al., 2018. Antisense oligonucleotides targeting mutant Ataxin-7 restore visual function in a mouse model of spinocerebellar ataxia type 7. *Sci. Transl. Med.* 10 (465) <https://doi.org/10.1126/scitranslmed.aap8677>.
- Oosterveld, L.P., Verberk, I.M.W., Majbour, N.K., et al., 2020. CSF or serum neurofilament light added to  $\alpha$ -Synuclein panel discriminates Parkinson's from controls. *Mov Disord Off J Mov Disord Soc.* 35 (2), 288–295. <https://doi.org/10.1002/mds.27897>.
- Peng, Y., Zhang, Y., Chen, Z., et al., 2020. Association of serum neurofilament light (sNfL) and disease severity in patients with spinocerebellar ataxia type 3. *Neurology.* 14. <https://doi.org/10.1212/WNL.0000000000010671>. Published online August.
- Preische, O., Schultz, S.A., Apel, A., et al., 2019. Serum neurofilament dynamics predicts neurodegeneration and clinical progression in presymptomatic Alzheimer's disease. *Nat. Med.* 25 (2), 277–283. <https://doi.org/10.1038/s41591-018-0304-3>.
- Reetz, K., Rodríguez-Labrada, R., Dogan, I., et al., 2018. Brain atrophy measures in preclinical and manifest spinocerebellar ataxia type 2. *Ann Clin Transl Neurol.* 5 (2), 128–137. <https://doi.org/10.1002/acn3.504>.
- Scahill, R.I., Zeun, P., Osborne-Crowley, K., et al., 2020. Biological and clinical characteristics of gene carriers far from predicted onset in the Huntington's disease young adult study (HD-YAS): a cross-sectional analysis. *Lancet Neurol.* 19 (6), 502–512. [https://doi.org/10.1016/S1474-4422\(20\)30143-5](https://doi.org/10.1016/S1474-4422(20)30143-5).
- Schmitz-Hübsch, T., du Montcel, S.T., Baliko, L., et al., 2006. Scale for the assessment and rating of ataxia: development of a new clinical scale. *Neurology.* 66 (11), 1717–1720. <https://doi.org/10.1212/01.wnl.0000219042.60538.92>.
- Scoles, D.R., Meera, P., Schneider, M.D., et al., 2017. Antisense oligonucleotide therapy for spinocerebellar ataxia type 2. *Nature.* 544 (7650), 362–366. <https://doi.org/10.1038/nature22044>.
- Seidel, K., Siswanto, S., Brunt, E.R.P., den Dunnen, W., Korf, H.-W., Rüb, U., 2012. Brain pathology of spinocerebellar ataxias. *Acta Neuropathol (Berl).* 124 (1), 1–21. <https://doi.org/10.1007/s00401-012-1000-x>.
- Tezenas du Montcel, S., Durr, A., Rakowicz, M., et al., 2014. Prediction of the age at onset in spinocerebellar ataxia type 1, 2, 3 and 6. *J. Med. Genet.* 51 (7), 479–486. <https://doi.org/10.1136/jmedgenet-2013-102200>.
- Wild, E.J., Boggio, R., Langbehn, D., et al., 2015. Quantification of mutant huntingtin protein in cerebrospinal fluid from Huntington's disease patients. *J. Clin. Invest.* 125 (5), 1979–1986. <https://doi.org/10.1172/JCI80743>.
- Wilke, C., Bender, F., Hayer, S.N., et al., 2018a. Serum neurofilament light is increased in multiple system atrophy of cerebellar type and in repeat-expansion spinocerebellar ataxias: a pilot study. *J. Neurol.* 265 (7), 1618–1624. <https://doi.org/10.1007/s00415-018-8893-9>.
- Wilke, C., Rattay, T.W., Hengel, H., et al., 2018b. Serum neurofilament light chain is increased in hereditary spastic paraplegias. *Ann Clin Transl Neurol.* 5 (7), 876–882. <https://doi.org/10.1002/acn3.583>.
- Wilke, C., Haas, E., Reetz, K., et al., 2020. Neurofilaments in spinocerebellar ataxia type 3: blood biomarkers at the preataxic and ataxic stage in humans and mice. *EMBO Mol Med.* 12 (7), e11803. <https://doi.org/10.15252/emmm.201911803>.
- Zeitlberger, A.M., Thomas-Black, G., Garcia-Moreno, H., et al., 2018. Plasma markers of Neurodegeneration are raised in Friedreich's Ataxia. *Front. Cell. Neurosci.* 12, 366. <https://doi.org/10.3389/fncel.2018.00366>.
- Zhang, S., Hu, Z., Mao, C., Shi, C., Xu, Y., 2020. CHIP as a therapeutic target for neurological diseases. *Cell Death Dis.* 11 (9), 1–12. <https://doi.org/10.1038/s41419-020-02953-5>.

## Chapter 2 - ATRIL study

In this multicenter, double-blind, randomized, placebo-controlled study we evaluated the safety and efficacy of riluzole in 45 SCA2 individuals. Based on the positive results obtained in two previous studies,<sup>53,54</sup> we decided to test riluzole in a clinically and genetically heterogeneous cohort.

Riluzole is used as disease-modifying therapy in ALS, but its mechanisms of action are not yet well elucidated.<sup>55</sup> In cerebellar ataxias, it was first tested in 2010 in Italy in a trial including 40 heterogeneous patients with hereditary and non-hereditary ataxia. After eight weeks of oral administration of 100 mg/day, treated patients improved by five points on the International Cooperative Ataxia Rating Scale (ICARS).<sup>53</sup> The Italian team pursued with the evaluation of this drug efficacy in hereditary forms of cerebellar ataxia only and I took part in this study as an associated investigator. This second trial enrolled 20 Friedreich ataxia patients and 40 SCA patients (SCA1, 2, 6, 8, and 10), treated for 12 months at 100 mg/day. The principal endpoint was the proportion of patients with improved SARA score of at least one point.<sup>54</sup> This proportion was higher in the riluzole arm, with no serious adverse events reported. However, this trial raised some questions, especially concerning the “best-practice” approaches while conducting a trial in rare diseases. Is it appropriate to mix different genotypes? The pathophysiology mechanisms for the entities included in the trial are different: abnormal signal transduction in SCA1, abnormal RNA metabolism in SCA2, channelopathy in SCA6,<sup>9</sup> and mitochondrial dysfunction in Friedreich’s ataxia.<sup>56</sup> The response to riluzole could therefore differ among the various genotypes. Moreover, we know based on disease natural history studies, that the disease progression is very different among polyQ SCAs. In fact, the SARA progression is faster for SCA1 (2.11 point per year), followed by SCA3, SCA2, and SCA6 (1.56, 1.49, and 0.8, respectively).<sup>32</sup> This could impact the response to riluzole administration. Another question regards the inclusion of carriers with SARA scores lower than 3/40. SARA scale presents only marginal and not linear progression in preataxic carriers, then increases linearly after ataxia onset<sup>31</sup> (Moulaire 2022 in press). Therefore, the SARA stabilization or 1-point decrease for preataxic individuals cannot be easily interpreted as an effective improvement due to riluzole intake. Other outcomes should be included in a clinical trial in addition to SARA score.

For all these reasons, we decided to restrict the trial only to SCA2 patients. The choice to target SCA2 was supported by the fact that intermediate *ATXN2* alleles (27-32 CAG) are

associated with an increased risk to develop ALS.<sup>57,58</sup> Moreover, SCA2 patients with large CAG expansion can present an ALS-like phenotype.<sup>13</sup> We used the same endpoint as Romano and colleagues,<sup>54</sup> and we added other outcomes, such as changes in Composite Cerebellar Functional Score (CCFS), Inventory of Non-Ataxia Signs (INAS) score, and decrease or stabilization of the rate of atrophy in the cerebellum and brainstem. Overall, this study allowed us to investigate longitudinal changes of clinical and radiological biomarkers in SCA2 patients. Post-hoc endpoints focused on performing baseline comparison of cerebellar and brainstem volumes between SCA2 patients and healthy controls, as well as analyzing the correlation between clinical scores and progression of atrophy, and measuring the annual volume loss leveraging preinclusion scans in patients for whom data were available.

In January 2022, the results of this clinical trial have been published in *Lancet Neurology*.<sup>59</sup>



# Safety and efficacy of riluzole in spinocerebellar ataxia type 2 in France (ATRIL): a multicentre, randomised, double-blind, placebo-controlled trial



Giulia Coarelli, Anna Heinzmann, Claire Ewencyk, Clara Fischer, Marie Chupin, Marie-Lorraine Monin, Hortense Hurmic, Fabienne Calvas, Patrick Calvas, Cyril Goizet, Stéphane Thobois, Mathieu Anheim, Karine Nguyen, David Devos, Christophe Verny, Vito A G Ricigliano, Jean-François Mangin, Alexis Brice, Sophie Tezenas du Montcel, Alexandra Durr

## Summary

**Background** Riluzole has been reported to be beneficial in patients with cerebellar ataxia; however, effectiveness in individual subtypes of disease is unclear due to heterogeneity in participants' causes and stages of disease. Our aim was to test riluzole in a single genetic disease, spinocerebellar ataxia type 2.

**Methods** We did a randomised, double-blind, placebo-controlled, multicentre trial (the ATRIL study) at eight national reference centres for rare diseases in France that were part of the Neurogene National Reference Centre for Rare Diseases. Participants were patients with spinocerebellar ataxia type 2 with an age at disease onset of up to 50 years and a scale for the assessment and rating of ataxia (SARA) score of at least 5 and up to 26. Patients were randomly assigned centrally (1:1) to receive either riluzole 50 mg orally or placebo twice per day for 12 months. Two visits, at baseline and at 12 months, included clinical measures and 3T brain MRI. The primary endpoint was the proportion of patients whose SARA score improved by at least 1 point. Analyses were done in the intention-to-treat population (all participants who were randomly assigned) and were done with only the observed data (complete case analysis). This trial is registered at ClinicalTrials.gov (NCT03347344) and has been completed.

**Findings** Between Jan 18, 2018, and June 14, 2019, we enrolled 45 patients. 22 patients were randomly assigned to receive riluzole and 23 to receive placebo. Median age was 42 years (IQR 36–57) in the riluzole group and 49 years (40–56) in the placebo group and 23 (51%) participants were women. All participants presented with moderate-stage disease, characterised by a median SARA score of 13·5 (IQR 9·5–16·5). The primary endpoint, SARA score improvement of at least 1 point after 12 months, was observed in seven patients (32%) in the treated group versus nine patients (39%) in the placebo group, with a mean difference of –10·3% (95% CI –37·4% to 19·2%;  $p=0\cdot75$ ). SARA score showed a median increase (ie, worsening) of 0·5 points (IQR –1·5 to 1·5) in the riluzole group versus 0·3 points (–1·0 to 2·5) in the placebo group ( $p=0\cdot70$ ). No serious adverse event was reported in the riluzole-treated group whereas four patients in placebo group had a serious adverse event (hepatic enzyme increase, fracture of external malleolus, rectorrhagia, and depression). The number of patients with adverse events was similar in both groups (riluzole 16 [73%] patients vs placebo 19 [83%] patients;  $p=0\cdot49$ ).

**Interpretation** We were able to recruit 45 patients moderately affected by spinocerebellar ataxia type 2 for this trial. Riluzole did not improve clinical or radiological outcomes in these patients. However, our findings provide data on progression of spinocerebellar ataxia type 2 that might prove to be valuable for the design of other clinical trials.

**Funding** French Ministry of Health.

**Copyright** © 2022 Elsevier Ltd. All rights reserved.

## Introduction

Spinocerebellar ataxias are a group of autosomal dominantly inherited progressive neurological diseases that are clinically and genetically heterogeneous,<sup>1</sup> with 48 subtypes. A subgroup of seven subtypes is caused by pathological expansions of a polymorphic CAG repeat and most commonly affects adults in midlife. These seven subtypes are spinocerebellar ataxia type 1 (associated with pathogenic variants in *ATXN1*), spinocerebellar ataxia type 2 (*ATXN2*), spinocerebellar ataxia type 3 (*ATXN3*), spinocerebellar ataxia type 6 (*CACNA1A*), spinocerebellar ataxia type 7 (*ATXN7*), spinocerebellar

ataxia type 17 (*TBP*), and dentatorubral pallidoluysian atrophy (*ATN1*). For these seven subtypes, mean age at onset and severity are closely and negatively correlated with the expanded CAG repeat size: the longer the pathological repeat, the earlier the age at onset. Paediatric and juvenile forms of the disease can also occur, especially for spinocerebellar ataxia type 2 and spinocerebellar ataxia type 7. The natural history of the disease for subtypes 1, 2, and 3 is well established, including the annual progression rate of the scale for the assessment and rating of ataxia (SARA) score.<sup>2</sup> No curative treatment exists for these diseases, although antisense

Lancet Neurol 2022

Published Online  
January 18, 2022  
[https://doi.org/10.1016/S1474-4422\(21\)00457-9](https://doi.org/10.1016/S1474-4422(21)00457-9)

See Online/Comment  
[https://doi.org/10.1016/S1474-4422\(22\)00028-X](https://doi.org/10.1016/S1474-4422(22)00028-X)

Department of Neurology, Sorbonne University, Paris Brain Institute (ICM Institut du Cerveau), INSERM, CNRS, Assistance Publique-Hôpitaux de Paris, Pitié-Salpêtrière University Hospital, Paris, France (G Coarelli MD, A Heinzmann MD, C Ewencyk MD, M-L Monin MD, H Hurmic MD, V A G Ricigliano MD, Prof A Brice MD, Prof A Durr MD); Department of Genetics, Neurogene National Reference Centre for Rare Diseases, Pitié-Salpêtrière University Hospital, Assistance Publique, Hôpitaux de Paris, Paris, France (G Coarelli, A Heinzmann, C Ewencyk, M-L Monin, H Hurmic, Prof A Durr); CATI, ICM, CNRS, Sorbonne University, Paris, France (C Fischer MS, M Chupin PhD, J-F Mangin PhD); University Paris-Saclay, CEA, CNRS, Baobab, Neurospin, Gif-sur-Yvette, France (C Fischer MS, M Chupin PhD, J-F Mangin PhD); Clinical Research Centre University Hospital, Toulouse, France (F Calvas MD); Department of Clinical Genetics, Purpan University Hospital, Toulouse, France (Prof P Calvas MD); Department of Medical Genetics, National Reference Centre for Neurogenetic Rare Diseases, Pellegrin Hospital, Bordeaux University Hospital, and INSERM U1211, Laboratory MRGM, Bordeaux University, Bordeaux, France (Prof C Goizet MD); Hospices Civils de Lyon, Department of Neurology C, Pierre Wertheimer

Neurological and Neurosurgical Hospital, Bron, France (Prof S Thobois MD); Faculty of Medicine Lyon Sud Charles Mérieux, Claude Bernard Lyon 1 University, Lyon, France (Prof S Thobois); CNRS, Institute of Cognitive Sciences Marc Jeannerod UMR, Bron, France (Prof S Thobois); Department of Neurology, Hôpital de Hautepierre, Univresity Hospital of Strasbourg, Strasbourg, France (Prof M Anheim MD); Fédération de Médecine Translacionnelle de Strasbourg, University of Strasbourg, Strasbourg, France (Prof M Anheim); Institute of Genetics and Molecular and Cellular Biology, Illkirch, France (Prof M Anheim); Department of Medical Genetics, Neurogene National Reference Centre for Rare Diseases, Marseille University Hospital, APHM/AMU, Marseille, France (Prof K Nguyen MD); University of Lille, INSERM, CHU Lille, LiNCog-Lille Neuroscience and Cognition, Lille, France (Prof D Devos MD); Neurology Department, Angers University Hospital, Angers, France (Prof C Verny MD); Sorbonne University, INSERM, Institute of Epidemiology and Public Health Pierre Louis, Assistance Publique-Hôpitaux de Paris, Pitié Salpêtrière University Hospital, Paris, France (S Tezenas du Montcel MD)

Correspondence to: Prof Alexandra Durr, Paris Brain Institute, Pitié-Salpêtrière Paris, 75646 Paris, France alexandra.durr@icm-institute.org

## Research in context

### Evidence before this study

We searched PubMed from inception to Nov 23, 2021, for the following terms without language restriction: “cerebellar ataxia”, “spinocerebellar ataxias (SCAs)”, “riluzole”, and “clinical trials”. We found two clinical trials with evidence of clinical improvement after riluzole treatment. The first, a pilot study, included 40 patients affected by genetic and other forms of ataxias with a treatment duration of 8 weeks (NCT00202397), and the second trial included 60 patients with different causes of inherited cerebellar ataxias and disease stages treated for 12 months (NCT01104649).

### Added value of this study

The ATRIL study assessed the safety and efficacy of riluzole in patients with spinocerebellar ataxia type 2. We enrolled a homogeneous cohort of patients with spinocerebellar ataxia type 2 recruited by the French network of rare neurogenetic diseases. This choice for replication was justified by three facts: patients with spinocerebellar ataxia type 2 are among those included in previous ataxia studies; spinocerebellar ataxia type 2

oligonucleotides have produced encouraging results in several mouse models.<sup>3,4</sup>

Several disease-modifying treatments have been tested in hereditary ataxias, such as valproic acid or lithium, without demonstrated efficacy to support their clinical use. However, the effect of riluzole has been reported as beneficial in two trials. The first trial, which was a pilot study with 40 patients affected by genetic and other forms of ataxia,<sup>5</sup> showed a decrease of 5 points on the international cooperative ataxia rating scale score after 4 weeks and 8 weeks of treatment with riluzole (100 mg/day) compared with placebo. The second trial, which was a placebo-controlled, randomised, double-blind study included 40 patients with spinocerebellar ataxias (spinocerebellar ataxia types 1, 2, 6, 8, or 10) and 20 patients with Friedreich ataxia, treated for 12 months.<sup>6</sup> That study confirmed the beneficial effect of riluzole with a 1 point decrease on the SARA score after 1 year. However, these two studies included patients with different forms of disease-causing variants and different disease stages, as well as presymptomatic carriers. This heterogeneity makes the generalisability of the positive effect unclear in individual disease subgroups. For this reason, we decided to do a trial in a population that was homogeneous in terms of genotype. Riluzole is widely used in amyotrophic lateral sclerosis with beneficial effects on survival,<sup>7</sup> patients with spinocerebellar ataxia type 2 frequently present with involvement of motor neurons,<sup>8</sup> and intermediate *ATXN2* alleles (27–32 CAG repeat expansion) are a risk factor for amyotrophic lateral sclerosis,<sup>9</sup> predisposing patients to more rapid progression.<sup>10</sup> We therefore did a placebo-controlled trial with riluzole for 12 months in patients with

can present an amyotrophic lateral sclerosis-like phenotype, and riluzole is widely used to treat amyotrophic lateral sclerosis; and intermediate *ATXN2* alleles (27–32 CAG repeats) are a risk factor for amyotrophic lateral sclerosis. In addition, we used pretrial cerebral MRI scans (cerebellum and brainstem volumes), added a quantitative measure of ataxia (the composite cerebellar functional severity score), and carefully analysed motor neuron involvement and quality-of-life measures. The ATRIL results showed no clinical or radiological improvement after riluzole treatment in patients with spinocerebellar ataxia type 2. However, we were able to measure significant volume loss over 12 months for specific brain regions in these patients.

### Implications of all the available evidence

We report the absence of improvement of clinical or radiological outcomes under riluzole treatment, despite satisfactory treatment compliance and absence of serious adverse events. However, our longitudinal imaging results might provide valuable biomarkers for upcoming clinical trials.

spinocerebellar ataxia type 2, the same primary clinical endpoint as the previously reported 1 year trial.<sup>6</sup>

## Methods

### Study design and participants

For this multicentre, double-blind, randomised, placebo-controlled study (the ATRIL study), patients were recruited from eight national reference centres for rare diseases in France. Eligible patients were aged at least 18 years, with a genetically confirmed diagnosis of spinocerebellar ataxia type 2 (CAG repeat lengths  $\geq 33$  in the *ATNX2* gene), a SARA score of at least 5 and up to 26, and an age at onset of up to 50 years. Patients received physiotherapy as standard care before and during the trial. Patients also all had to be able to give their informed consent and be covered by social security. Key exclusion criteria included ataxic syndromes other than spinocerebellar ataxia type 2, previous riluzole treatment, serious systemic illnesses or conditions known for enhancing the side-effects of riluzole (ie, severe cardiac or renal insufficiency, haematological and hepatic diseases with serum alanine amino transferase concentrations greater than or equal to twice the upper limit of normal, or abnormal values of several other hepatic markers), hypersensitivity to the active substance or to any of the excipients (dibasic calcium phosphate anhydrous, microcrystalline cellulose, croscarmellose sodium, colloidal silica anhydrous, magnesium stearate, hypromellose, or titanium dioxide [E171] macrogol 400), hypersensitivity to any of the placebo ingredients (lactose monohydrate, microcrystalline cellulose, colloidal silica, anhydrous, magnesium stearate, or Opadry II HP85F18422 White), contraindications for MRI examination, participation in another therapeutic trial (within the past

3 months), pregnancy or breastfeeding, non-abstinence or absence of effective contraception for women, inability to understand information about the protocol, and adults under legal protection or otherwise unable to consent.

Deviations from the protocol, which were minor, concerned the scheduling windows of the visits. Because of the COVID-19 pandemic, disease progression, or patient personal constraint, follow-up visits for two patients (one visit each) could not be scheduled as per protocol (12 months, 2 weeks before the scheduled date).

The trial was done according to Good Clinical Practice guidelines, the Declaration of Helsinki, and in line with French regulations. The study was approved by the French Ethics Committee and all participants provided written informed consent at the first visit before any study procedures or assessments. This trial is registered at ClinicalTrials.gov, number NCT03347344.

### Randomisation and masking

Randomisation was centralised and done by the Clinical Research Unit at Pitié-Salpêtrière University Hospital, under the supervision of the Agence Générale des Equipements et Produits de Santé (AGEPS) via the electronic reporting form. We used a block-randomisation scheme and a centralised procedure for randomisation, with stratification of participants included in Paris versus those recruited in other centres. After written consent and after checking inclusion and exclusion criteria, eligible patients were randomly assigned in a 1:1 ratio to receive either riluzole or placebo. AGEPS sent labelled pill boxes to the pharmacies of the eight different centres. Patients, investigators, and the trial team of the sponsor involved in the analysis remained masked to the randomised treatment assignments until the last study visit of each patient, with the exception of serious adverse events or medical emergency instances that required immediate unblinding.

### Procedures

Riluzole 100 mg was administered orally (50 mg every 12 h) for 12 months. Placebo 50 mg was presented as a round, biconvex, 8 mm in diameter, nearly-white film-coated tablet matching the appearance of the riluzole used in this study. The shipment was overseen by the clinical department of AGEPS, the central pharmacy of the Pitié-Salpêtrière Hospital. Treatments were stored at ambient temperature in a secured storage area and presented in numbered boxes, labelled for this study according to Good Manufacturing Practices by the AGEPS. Each numbered box contained 6 months of treatment: 20 blister packs of 20 active or placebo tablets. Patient compliance was checked by clinical research associates during monitoring throughout the study (amount of treatment returned used or unused and doses administered).

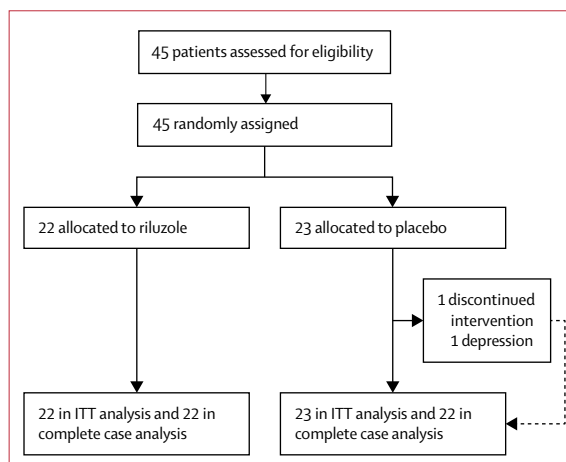
Eligible patients had blood analyses to check for normal liver function and blood cell count (bilirubin, aspartate transaminase [ASAT], alanine transaminase [ALAT],

$\gamma$  glutamyl transferase, alkaline phosphatases, albumin, and blood-cell count) less than 1 month before the baseline visit. The baseline visit (visit 1) included a clinical examination (weight, height, and blood pressure) and patient medical history (age, alcohol consumption, caffeine consumption, tobacco consumption, concomitant treatment, comorbidities, and frequency of physical therapy). Cerebellar function was assessed by SARA<sup>11</sup> and quantitatively measured by the composite cerebellar functional severity score (CCFS).<sup>12</sup> Neurological examination used the inventory of non-ataxia signs (INAS)<sup>13</sup> to report on motor neuron involvement and other signs. 3T cerebral MRI was done on site-specific MRI scanners. We assessed quality of life using the French version of the 36-item short-form health survey questionnaire (SF-36).<sup>14</sup>

At visit 2 (12 months, 2 weeks before or after the scheduled date), a clinical and neurological examination was done (SARA and CCFS scores and INAS count), as well as an evaluation of compliance, collection of adverse events, collection of concomitant medication, assessment of quality of life (SF-36 questionnaire), and cerebral MRI.

The severity of adverse events was evaluated using the Common Terminology Criteria for Adverse Events. The investigators also assessed the causal relationship between adverse events and the investigational medicinal product or the study procedures.

Hepatic measurements (bilirubin, ASAT, ALAT,  $\gamma$  glutamyl transferase, alkaline phosphatases, and albumin) and blood-cell counts were monitored in a local laboratory at month 1, month 2, month 3, a week before month 6, month 9, and a week before month 12. Women also underwent a urine pregnancy test at month 0 and a blood pregnancy test at month 1, month 2, month 3, month 6, month 9, and month 12 to exclude any possibility of pregnancy. Examinations were done locally, always in the same laboratory for each patient.



**Figure 1: Trial profile**

45 patients were included in the primary intention-to-treat and safety analyses, and 44 patients were included in the complete case analysis. ITT=intention to treat.

	Riluzole (n=22)	Placebo (n=23)
Sex		
Women	8 (36%)	15 (65%)
Men	14 (64%)	8 (35%)
Age	42 (36–57)	49 (40–56)
Age at onset	32 (25–43)	38 (29–44)
Disease duration	11 (5–12)	11 (6–18)
Repeat length of expanded alleles	39 (39–41)	39 (38–40)
Repeat length of short alleles	22 (22–22)	22 (22–22)
SARA score (maximum value 40)	15.3 (10.0–20.5)	12.5 (9.0–16.0)
CCFS	1.089 (1.004–1.226)	1.075 (1.008–1.185)
INAS count	4 (3–6)	4 (3–5)†
Sensory symptoms	18 (82%)	17 (74%)
Areflexia	14 (64%)	18 (78%)
Upper motor neuron signs*	11 (55%)	10 (43%)
Extensor plantar	7 (35%)	6 (26%)*
Spasticity	6 (27%)	6 (26%)‡
Hyperreflexia	4 (18%)	4 (17%)
Lower motor neuron signs*	8 (36%)	7 (32%)
Fasciculations	6 (27%)	4 (18%)‡
Paresis	2 (9%)	2 (9%)
Muscle atrophy	2 (9%)	2 (9%)
Cramps	16 (73%)	17 (74%)
Urinary dysfunction	8 (36%)	12 (52%)

(Table continues in next column)

## Outcomes

The primary outcome was a 1 point improvement of the SARA score after 12 months, as used by Romano and colleagues.<sup>6</sup> Prespecified secondary endpoints were: to evaluate the quantitative progression of cerebellar symptoms by showing a decrease in the SARA score; decrease in the SARA score compared with the natural evolution (this analysis is based on results of a previous study combined with results of the ATRIL trial); decrease in the CCFS score; change in the INAS score, including signs of involvement of lower motor neurons (presence of fasciculations, muscle atrophy, or paresis); decrease in or stabilisation of the rate of atrophy in the cerebellum and brainstem (midbrain, pons, and medulla oblongata), measured using volumetric 3T MRI; patient quality of life assessed using the SF-36 questionnaire; long-term tolerance of riluzole confirmed by clinical examination at study visits and by blood analysis (hepatic measurements, blood cell count) every month during the first 3 months of treatment, then every 3 months; and survival. Post-hoc endpoints concerned the baseline comparison with healthy controls of cerebellar and brainstem volumes, the correlation of baseline clinical scores with MRI data, and preinclusion progression of atrophy on MRI in patients for whom data were available.

	Riluzole (n=22)	Placebo (n=23)
(Continued from previous column)		
Extrapyramidal signs*	8 (36%)	5 (23%)
Dystonia	6 (27%)	4 (17%)
Resting tremor	5 (23%)	1 (5%)‡
Rigidity	1 (5%)	1 (4%)
Chorea/dyskinesia	3 (14%)	2 (9%)
Myoclonus	3 (14%)	2 (9%)
Brainstem oculomotor signs	9 (41%)	10 (45%)
Abnormal saccades*	20 (91%)	22 (96%)
Saccadic dysmetria*	18 (86%)†	18 (78%)
Double vision	3 (14%)	9 (39%)
Nystagmus*	3 (14%)	8 (9%)
Dysarthria	21 (95%)	21 (91%)
Dysphagia	13 (59%)	13 (57%)
Vertigo	7 (32%)	6 (26%)
Problems with handwriting	22 (100%)	22 (96%)
Cognitive dysfunction	0	2 (9%)
Alcohol consumption (at least once a week)	1 (4%)	4 (17%)
Physiotherapy	17 (77%)	15 (65%)
Number of hours per week	1 (1–3)	1 (1–2)

Data are n (%) or median (IQR). Ethnic background was not assessed. Upper motor neuron signs are defined as extensor plantar (unilateral or bilateral), spasticity, or hyperreflexia. Lower motor neuron signs are defined as fasciculations, paresis, or muscle atrophy. Brainstem oculomotor signs are defined as ophthalmoparesis on horizontal gaze, ophthalmoparesis on vertical gaze, or slowing of saccades. Extrapyramidal signs are defined as dystonia, resting tremor, or rigidity. Abnormal saccades are defined as broken up smooth pursuit or slowing saccades. Saccadic dysmetria is defined as hypometric saccades or hypermetric saccades. Nystagmus is defined as downbeat nystagmus on fixation, horizontal gaze-evoked nystagmus, or vertical gaze-evoked nystagmus. Other clinical characteristics have been defined in previous publications. SARA=scale for the assessment and rating of ataxia. CCFS=composite cerebellar functional severity score. INAS=inventory of non-ataxia signs. \*N=20. †N=21. ‡N=22.

**Table 1: Clinical and genetic characteristics at baseline**

## Statistical analysis

On the basis of Romano and colleagues' report,<sup>6</sup> we expected a positive effect in both groups. The primary criterion was a decrease in SARA score of at least 1 point after 12 months of treatment. We expected that 5% of patients in the placebo group would improve their SARA score and 45% of the patients in the treated group would improve their score. Using a two-sided Fisher's exact test (bilateral test), and an  $\alpha$  of 5%, the inclusion of 21 patients in each group allows for 80% power with a 40%  $\delta$  between the two groups.

Quantitative variables were described by their mean and SE or SD or their median (IQR) for each treatment group separately. Frequency, percentage, and a 95% CIs were used to describe qualitative variables for each treatment group separately. A Fisher's exact test was used to compare the proportion of patients with an improvement in SARA score of at least 1 point at 12 months between the

	Riluzole (n=22)	Placebo (n=22)	Mean difference (95% CI)	p value
Primary outcome: SARA score improvement of at least 1 point at month 12	7 (32%)	9 (39%)*	-10.3% (-37.4 to 19.2)	0.75
Secondary outcomes				
Change in the SARA score between inclusion and month 12	0.5 (-1.5 to 1.5)	0.3 (-1.0 to 2.5)	0.23 (-1.06 to 1.51)	0.70
Change in the CCFS between inclusion and month 12	0.055 (0.014 to 0.086)	0.004 (-0.040 to 0.020)	0.064 (0.015 to 0.110)	0.0050
Change in the INAS between inclusion and month 12	0 (-1 to 1)	-1 (-2 to 0)	-0.8 (-1.7 to 0.0)	0.070
Change in SF-36 PCS between inclusion and month 12	-1.9 (-6.2 to 11.1)	0.7 (-5.4 to 8.6)	-2.1 (-6.4 to 2.3)	0.89
Change in SF-36 MCS between inclusion and month 12	-0.8 (-4.7 to 3.5)	-4.7 (-6.8 to 3.2)	-1.5 (-8.4 to 5.5)	0.31
Percentage of MRI volume variation between inclusion and month 12				
Vermis	-4.86 (-7.32 to -0.03)	-3.35 (-6.36 to -0.25)	-0.79 (-4.52 to 2.94)	1.00
Left cerebellum	-1.73 (-3.95 to -1.25)	-1.27 (-3.29 to -0.33)	-0.83 (-2.45 to 0.79)	1.00
Right cerebellum	-1.25 (-3.03 to -0.47)	-1.58 (-2.23 to -0.35)	-0.83 (-2.57 to 0.9)	1.00
Midbrain	-1.63 (-3.44 to 0.96)	-3.34 (-5.82 to -0.69)	0.58 (-2.44 to 3.61)	1.00
Pons	-1.92 (-3.51 to -1.28)	-2.28 (-3.13 to -1.07)	0.45 (-1.1 to 2.01)	1.00
Medulla oblongata	1.59 (-5.20 to 6.77)	-1.41 (-6.72 to 2.75)	5.18 (-0.45 to 10.82)	1.00

Data are reported as n (%) or median (IQR) unless otherwise stated. The progression of brain atrophy for each region at month 12 is reported as median (IQR) of percentage change. Only one patient discontinued, and therefore secondary outcome results were presented by complete case analysis. SARA=scale for the assessment and rating of ataxia. CCFS=composite cerebellar functional severity score. INAS=inventory of non-ataxia signs. SF-36=36-item short-form health survey questionnaire. PCS=physical component score. MCS=mental component score. \*The primary endpoint analysis was done by intention to treat, with n=23 in the placebo group.

**Table 2: Primary and secondary outcomes**

two treatment groups. The primary analysis was done on an intention-to-treat (ITT) basis with missing data for one patient replaced by values for the worst evolution in the treatment group and by mean values for evolution in the placebo group. An additional analysis of the primary endpoint and analyses of secondary endpoints were done with only the observed data (complete case analysis). Changes in quantitative scores (CCFS, INAS, SF-36, and MRI data) between baseline and month 12 were first calculated and then compared using a Mann-Whitney test. In addition to the month 0 and month 12 data from the trial, for the quantitative evolution of the SARA score compared with its expected natural evolution, a mixed model including the 2 years of pretrial data when available was used to test differences in progression between groups. Frequency of adverse events was compared between groups using Fisher's exact test. P values of less than 0.05 were considered significant, except for in MRI analysis, in which the Holm step-down Bonferroni method was used to consider multiple comparisons.

The prespecified MRI analyses included analysis of volume loss at month 12 compared with baseline in the placebo group and comparison between the two groups. Post-hoc analyses were as follows: comparison of baseline volumes between the ATRIL population and a healthy control group of 18 individuals acquired from the Paris Center and involved in the study PHRC AOM03059 (they had no neurological disease history and a normal neurological examination; the atrophy rates for cerebellum and

pons as well as changes in white-matter density at month 12 were compared between both groups and between patients with spinocerebellar ataxia type 2 and healthy controls with Student *t* test); the correlations between baseline clinical scores, SARA, CCFS, and brain MRI data were determined using a linear-regression model adjusted for age at the baseline visit and the CAG repeat on the expanded allele, with p values being adjusted for multiple comparisons (Holm); and the atrophy progression for patients in the riluzole group, for whom two previous brain MRI scans had been acquired before the start of the trial. Statistical analyses were done with SAS software (version 9.4).

#### Role of the funding source

The funder of the study had no role in study design, data collection, data analysis, data interpretation, or writing of the report.

#### Results

Between Jan 18, 2018, and June 14, 2019, we enrolled 45 patients with spinocerebellar ataxia type 2 recruited in eight national reference centres for rare disease: the Pitié-Salpêtrière University Hospital in Paris (n=26), the Purpan University Hospital in Toulouse (n=5), the Pellegrin University Hospital in Bordeaux (n=3), the Pierre Wertheimer Neurological Hospital in Bron (n=3), the University Hospital of Angers (n=2), the University Hospital of Lille (n=2), the La Timone Hospital in



Marseille (n=2), and the Haute-pierre University Hospital in Strasbourg (n=2).

22 patients were randomly assigned to receive riluzole and 23 patients to receive placebo (figure 1). In the placebo group, one patient left the study because of depression.

Clinical characteristics at baseline are shown (table 1). Participants complained about handwriting difficulties (44 [98%] of 45 patients) and cramps (33 [73%] of 45 patients). Median SARA score was 13.5 of 40 (IQR 9.5–16.5) with a median disease duration of 11 years (IQR 6–16); the most prevalent signs were cerebellar ataxia (45 [100%]), dysarthria (43 [93%]), brainstem involvement (with abnormal saccades in 43 [93%]) and dysphagia in 26 [58%]), neuropathy (areflexia in 32 [71%]), and deep sensory decrease (35 [78%]). Upper motor neuron signs were found in 21 (49%) patients and lower motor neuron signs were found in 15 (34%).

For the primary endpoint (ie, the proportion of patients with a 1-point SARA-score improvement, meaning a decrease in SARA score), no significant variations in SARA score were found between treated and untreated patients on the basis of the ITT analysis (seven [32%] vs nine [39%];  $p=0.75$ ; table 2). Complete case analysis confirmed this result (seven [32%] vs nine [41%];  $p=0.75$ ).

No significant differences in SARA improvement were found in patients with or without motor neuron involvement (table 2). The SARA score after 12 months

was not significantly different between the riluzole and placebo groups and showed a median increase (meaning worsening) of 0.5 (IQR –1.5 to 1.5) in the riluzole group versus 0.3 (–1.0 to 2.5) in the placebo group ( $p=0.70$ ; table 2).

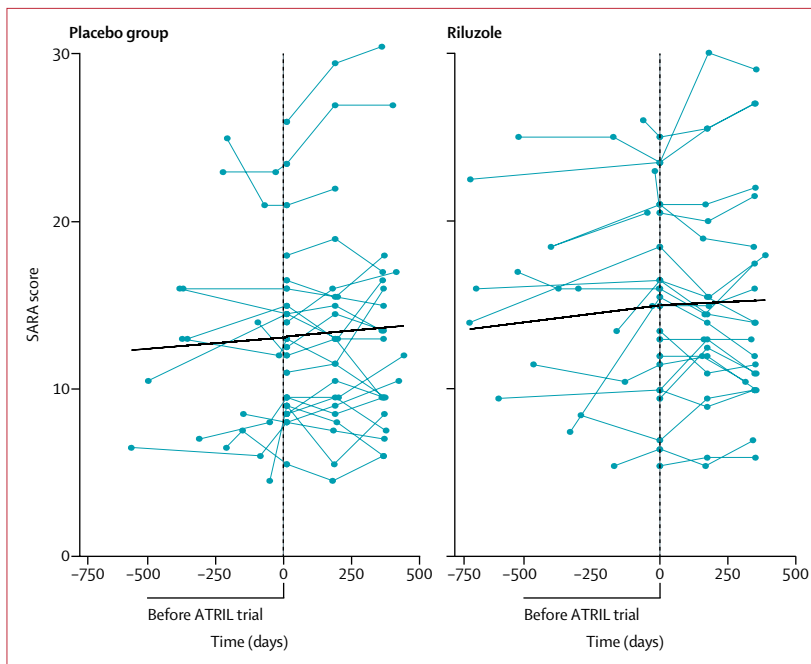
The quantitative change of SARA compared with the extended pretrial 2-year slope of SARA (analysed in all participants for whom at least one SARA score was available,  $n=43$ ) showed no significant change in SARA progression before and during the trial for both groups (figure 2).

CCFS worsened significantly in the riluzole group compared with the placebo group (0.055, IQR 0.014 to 0.086, vs 0.004, –0.040 to 0.020;  $p=0.0050$ ; table 2). INAS change was similar (0, IQR –1 to 1 vs –1 to –2 to 0;  $p=0.070$ ) in both groups (table 2). We did not detect a statistically significant upper or lower motor neuron improvement in the riluzole group compared with the placebo group (table 2).

Quality of life, as assessed by the SF-36 questionnaire, showed that for all dimensions except pain, patients had lower scores in physical and mental states than the French General Population (appendix p 3). At month 12, a tendency towards worsening of the composite SF-36 score was observed in both groups compared with baseline. This difference from baseline was not significant in either group (table 2; appendix p 3).

In the riluzole group, no patient had clinically significant blood-analysis abnormalities. Liver enzymes did not increase with treatment except in one patient (ALAT increase less than two times the normal value at month 2 of treatment followed by regression at month 3). In the placebo group, one patient had an ALAT increase (five times the normal value). No serious adverse event was reported in the riluzole group whereas four patients in the placebo group had a serious adverse event. The number of patients with adverse events was similar in both groups (riluzole 16 [73%] vs placebo 19 [83%];  $p=0.49$ ). No death occurred during the trial. All adverse events are listed (table 3). Treatment compliance was high in both groups, 94% (SD 9.75) in the riluzole group and 94% (5.77) in the placebo group.

All patients underwent brain MRI at baseline and at 12 months. One patient was excluded from brainstem analysis because of suboptimal segmentation. Baseline cerebellum and brainstem volumes are reported in the appendix (pp 4–5). Compared with healthy controls, baseline volumes were significantly lower in patients with spinocerebellar ataxia type 2, with the exception of the superior cerebellar peduncle (appendix pp 4–5). No significant difference was found between the two groups in percentage of volume change between baseline and the 12 month visit (table 2; appendix pp 6–7). A significant change of volume at month 12 compared with baseline was found in the placebo group for the left lobule crus I (Holm  $p=0.0013$ ) and pons (Holm  $p=0.0002$ ) appendix pp 6–7).



**Figure 2: Change in SARA score 2 years before and during ATRIL**

Change in SARA score in the placebo (A) and riluzole (B) groups. Each blue line represents a single patient. The black lines for each group represent the mean line of SARA progression estimated from the model (a mixed model including the 2 years of pre-trial data when available to test differences in progression between groups). Time in days is represented on the x-axis, with 0 indicating the beginning of the ATRIL study. The negative values represent time before the ATRIL study. For SARA score, 0 indicates least severe impairment and 40 most severe impairment. SARA=Scale for the Assessment and Rating of Ataxia.

In post-hoc analyses, we investigated the correlations between baseline SARA and CCFS scores and MRI data. Cerebellar and brainstem atrophy was greater in patients with higher SARA scores at baseline, but the change from baseline was not significant after adjustment for age and pathological CAG repeat length (appendix p 8). Higher CCFS scores were significantly correlated with higher vermiform grey-matter atrophy (appendix p 10), even after adjustment (Holm  $p=0.044$ ; appendix p 9).

For five patients in the riluzole group, two previous brain MRI scans at 2-year intervals were available. The progression of atrophy for each region on the basis of two previous MRI scans and the two clinical trial MRI scans is shown in the appendix (p 11). On the basis of these data, mean annual volume loss showed significant progression over the course of the 12 months for the pons ( $-277 \text{ mm}^3$  [SE 41] per year,  $p<0.0001$ ) and for the left lobule crus I ( $-171 \text{ mm}^3$  [SE 24] per year,  $p<0.0001$ ).

## Discussion

A regimen of 50 mg of riluzole twice per day for 12 months in adults with spinocerebellar ataxia type 2 did not result in a 1 point decrease of the SARA score at month 12 more often than did placebo. Therefore, we could not confirm a beneficial effect of riluzole, as has been previously reported.<sup>6</sup>

The mechanism of action of riluzole is not yet clear. This molecule has a pleiotropic effect on several ion channels and neurotransmitters. Riluzole seems to have a neuroprotective action enhancing the synaptic reuptake of glutamate and decreasing its release,<sup>15</sup> thereby preventing excitotoxicity; it also regulates the release of other excitatory neurotransmitters such as acetylcholine, dopamine, and serotonin by reducing cellular  $\text{Ca}^{2+}$  influx.<sup>15</sup> The most interesting potential mechanism for improving cerebellar ataxia is linked to its function as an opener of small-conductance  $\text{Ca}^{2+}$ -activated  $\text{K}^+$  channels, regulating the increased firing frequency of deep cerebellar nuclei neurons resulting from loss of Purkinje cells. When considering patients with Friedreich's ataxia separately from those with spinocerebellar ataxias in the trial by Romano and colleagues,<sup>6</sup> the improvement in SARA score was not different between patients from the treated and placebo groups. The absence of benefit from riluzole in Friedreich's ataxia could be explained by the prominent loss of deep cerebellar nuclei neurons with spared Purkinje cells. Furthermore, in a mouse model of spinocerebellar ataxia type 3, treatment with riluzole for 10 months showed decreased motor performance.<sup>16</sup> This study revealed a reduction of soluble normal ataxin 3 in riluzole-treated mice associated with an increased accumulation of mutated ataxin 3 protein.<sup>16</sup>

Even though patients with spinocerebellar ataxia type 2 represented the third largest group ( $n=16$  of 60) after those with spinocerebellar ataxia 1 and those with Friedreich's ataxia in the previous trial,<sup>6</sup> the heterogeneous nature of the cohort could have affected previous results.

	Riluzole (n=22)	Placebo (n=23)	p value
Patients with serious adverse events	0	4 (17%)*	0.10
Patients with adverse events	16 (73%)	19 (83%)	0.49
Number of adverse events	2 (1-3-5)	3 (1-5-4)	..
Severity of the adverse event			0.32
Slight	24 (69%)	43 (61%)	..
Moderate	11 (31%)	23 (32%)	..
Severe	0	5 (7%)	..
Treatment stopped because of adverse event	0	3 (13%)†	0.23
Types of adverse events			
Blood and lymphatic system disorders	0	4 (17%)	0.10
Hepatic disorders	1 (5%)	3 (13%)	0.60
Cardiac disorders	1 (5%)	2 (9%)	1.00
Skin disorders	3 (14%)	1 (4%)	0.34
Musculoskeletal disorders	1 (5%)	7 (30%)	0.040
Gastrointestinal disorders	2 (9%)	6 (26%)	0.24
Infections	4 (18%)	5 (22%)	1.00
Nervous system disorders	4 (18%)	6 (26%)	0.72
Ear and labyrinth disorders	0	2 (9%)	0.48
Other	9 (41%)	11 (48%)	0.76

Data are n (%) or median (IQR). \*Hepatic enzymes increase, fracture of external malleolus, rectorrhagia, and depression. †Depression, an alanine transaminase increase greater than five times the reference value, and one patient had hair loss and limb tremor.

**Table 3: Adverse and serious adverse events**

For this reason, we chose to enrol only patients with spinocerebellar ataxia type 2 with similar disease stages and did not include presymptomatic carriers (defined by a SARA score of less than 3 of 40). We included patients with a moderate stage of disease and a median SARA score of 13.5 of 40. We chose to enrol only patients with an age at onset up to 50 years, given that previous studies showed that patients with a later age at onset have a slower disease progression.<sup>2,17</sup> This choice would reduce the power for assessment of efficacy of the drug given the rare nature of this disease and the consequent small number of patients available.

In addition to the primary outcome, we evaluated the quantitative change of SARA score after 12 months that was not significantly different between the two groups. SARA is a validated assessment of cerebellar ataxia with a linear progression,<sup>2</sup> allowing us to do the analyses at only two timepoints. However, SARA is rater dependent and patient dependent (eg, it can be affected by physiotherapy, concomitant treatments or diseases, examination at different times of day)<sup>18</sup> and variations in scores could have potentially masked the beneficial effect of riluzole. For this reason, we used the CCFS, a validated, quantitative, and age-adjusted outcome measure that is rater independent, to assess upper-limb dysfunction.<sup>12</sup> Unexpectedly, CCFS measures significantly worsened in the riluzole-treated group. However, this measure did not

differ between baseline and 1 year follow-up in the placebo group, indicating that CCFS was not sensitive enough to pick up upper-limb disease progression within the time of the study. We also investigated motor neuron involvement but treatment was not accompanied by an improvement of the upper and lower motor neuron signs.

For brain MRI volumetry, which is reported to be more sensitive in detecting changes than clinical scores,<sup>19</sup> we used new automated tools (CEREBellum Segmentation [CERES] from the volBrain online platform) to obtain an accurate segmentation of the brainstem and a lobule-based parcellation of the cerebellum. Cerebellar and brainstem volumes decreased over 12 months in the placebo group, as expected and previously reported in other longitudinal studies.<sup>19,20</sup> Moreover, it has been previously reported that for carriers of the SCA2 mutation in *ATXN2* atrophy is already present at a presymptomatic stage in the brainstem,<sup>21</sup> especially the pons,<sup>20</sup> and in the cerebellum.<sup>21</sup> In this trial, volume loss was not prevented by riluzole, and volume changes did not differ between the two groups after 1 year. Two regions showed a significant decrease in volume compared with baseline, the pons and the left lobule crus I. The first region is one of the most important for oculomotor control. Saccade abnormalities, such as slow saccades, are common in spinocerebellar ataxia type 2.<sup>22</sup> In fact, more than one third of patients had oculomotor abnormalities at baseline and these did not improve after riluzole treatment. Lobule crus I has been implicated in cerebellar cognitive tasks, such as working memory and executive functions. Even though cerebellar motor alterations are usually the first signs observed in patients with spinocerebellar ataxia type 2, cerebellar cognitive affective syndrome (CCAS)<sup>23</sup> is common. However, we did not use a specific scale to assess CCAS. The presence of advanced atrophy at baseline could explain why we did not find a significant difference in volume change after 12 months for the other cerebellum or brainstem regions. We might explain this by a floor effect for change in the cerebellum, as has already been suggested, meaning that if the volume is already low at baseline, significant changes over time are not detected.<sup>24</sup>

CCFS score correlated significantly with vermis grey-matter atrophy, by contrast with SARA scores, which did not correlate with brain volume loss. However, the anatomical and physiological link between the vermis and upper-limb dysmetria is not established.

Future trials of gene therapy will likely be done in a multicentre setting because of the low prevalence of spinocerebellar ataxias. For this reason, objective and quantitative biomarkers rather than clinical measures are necessary to monitor drug effects and avoid inter-rater variability. We and others have shown that blood neurofilament light-chain concentrations correlate with clinical and radiological outcomes.<sup>25</sup> The absence of neurofilament measurement, which was not validated in spinocerebellar ataxias when this study began, represents a limitation of this study, as does the absence of other

objective biomarkers (eg, oculomotor recording or wearable sensors) that might have provided more accurate readouts. Cognitive assessment by the CCAS scale<sup>26</sup> could also have been useful for exploring correlations with specific cerebellum lobule volumes. Another limitation of our study is the low number of enrolled patients (45 patients) compared with the sample size calculations from the EUROSCA cohort (172 patients with spinocerebellar ataxia type 2 would be needed to detect a 50% reduction in SARA progression rate with a power of 80% in a 1 year trial).<sup>2</sup> The inclusion of 172 patients with same-stage spinocerebellar ataxia type 2 seems to not be feasible except for in a multicentre international setting. The ATRIL sample size estimation was based on the study by Romano and colleagues.<sup>6</sup> Considering their primary endpoint, the ATRIL sample size was sufficiently powered to show a difference between groups on the basis of the reported 50% of patients with SARA score improved by at least 1 point after 12 months.<sup>6</sup> However, with a 95% CI between  $-37.4\%$  and  $19.2\%$ , our data are consistent with a wide range of potential effects and do not exclude potential benefits (or harms) of riluzole.

In conclusion, using the same dose and duration of riluzole, and the same and additional readouts as Romano and colleagues,<sup>6</sup> in a large clinically and genetically homogeneous group of patients with spinocerebellar ataxia type 2, we found no improvement in clinical and radiological outcomes, despite satisfactory treatment compliance and an absence of serious adverse events. Although this result does not exclude a possible positive effect of riluzole on other forms of cerebellar ataxia, it illustrates the need to evaluate treatments in a homogeneous groups of patients, even in rare diseases.

#### Contributors

AD was the principal investigator. GC, STdM, and AD conceived and designed the study. GC, AH, CE, MLM, FC, PC, CG, ST, MA, KN, DD, CV, and AD followed up the patients and acquired the data. CF, MC, VR, and JFM analysed the radiological data. The statistical analyses were done by STdM. All authors reviewed, contributed to, and approved the final manuscript. All authors had full access to and verified the data and had final responsibility for the decision to submit the manuscript for publication.

#### Declaration of interests

We declare no competing interests.

#### Data sharing

Individual anonymised participant data and relevant clinical study documents (study protocol, statistical analysis plan, informed consent form, and clinical study report) will be available for qualified scientific and medical researchers as necessary for doing legitimate research. To request access to the data and submit a research proposal, please send a request to alexandra.durr@icm-institute.org.

#### Acknowledgments

We would like to thank the patients for their participation in this study. We would like to thank Assistance-Publique des Hôpitaux de Paris, which sponsored the study.

#### References

- 1 Durr A. Autosomal dominant cerebellar ataxias: polyglutamine expansions and beyond. *Lancet Neurol* 2010; **9**: 885–94.
- 2 Jacobi H, du Montcel ST, Bauer P, et al. Long-term disease progression in spinocerebellar ataxia types 1, 2, 3, and 6: a longitudinal cohort study. *Lancet Neurol* 2015; **14**: 1101–8.

For the volBrain: Automated MRI Brain volumetry system see <https://volbrain.upv.es>



- 3 Scoles DR, Meera P, Schneider MD, et al. Antisense oligonucleotide therapy for spinocerebellar ataxia type 2. *Nature* 2017; **544**: 362–66.
- 4 Moore LR, Rajpal G, Dillingham IT, et al. Evaluation of antisense oligonucleotides targeting ATXN3 in SCA3 mouse models. *Mol Ther Nucl Acid* 2017; **7**: 200–10.
- 5 Ristori G, Romano S, Visconti A, et al. Riluzole in cerebellar ataxia: a randomized, double-blind, placebo-controlled pilot trial. *Neurology* 2010; **74**: 839–45.
- 6 Romano S, Coarelli G, Marcotulli C, et al. Riluzole in patients with hereditary cerebellar ataxia: a randomised, double-blind, placebo-controlled trial. *Lancet Neurol* 2015; **14**: 985–91.
- 7 Fang T, Khleifat AA, Meurgey J-H, et al. Stage at which riluzole treatment prolongs survival in patients with amyotrophic lateral sclerosis: a retrospective analysis of data from a dose-ranging study. *Lancet Neurol* 2018; **17**: 416–22.
- 8 Pulst SM. Degenerative ataxias, from genes to therapies: the 2015 Cotzias Lecture. *Neurology* 2016; **86**: 2284–90.
- 9 Elden AC, Kim H-J, Hart MP, et al. Ataxin-2 intermediate-length polyglutamine expansions are associated with increased risk for ALS. *Nature* 2010; **466**: 1069–75.
- 10 Chiò A, Calvo A, Moglia C, et al. ATXN2 polyQ intermediate repeats are a modifier of ALS survival. *Neurology* 2015; **84**: 251–8.
- 11 Schmitz-Hübsch T, du Montcel ST, Baliko L, et al. Scale for the assessment and rating of ataxia: development of a new clinical scale. *Neurology* 2006; **66**: 1717–20.
- 12 du Montcel ST, Charles P, Ribai P, et al. Composite cerebellar functional severity score: validation of a quantitative score of cerebellar impairment. *Brain* 2008; **131**: 1352–61.
- 13 Jacobi H, Rakowicz M, Rola R, et al. Inventory of non-ataxia signs (INAS): validation of a new clinical assessment instrument. *Cerebellum* 2013; **12**: 418–28.
- 14 Ware JE, Sherbourne CD. The MOS 36-item short-form health survey (SF-36). I. Conceptual framework and item selection. *Med Care* 1992; **30**: 473–83.
- 15 Bellingham MC. A review of the neural mechanisms of action and clinical efficiency of riluzole in treating amyotrophic lateral sclerosis: what have we learned in the last decade? *CNS Neuro Ther* 2011; **17**: 4–31.
- 16 Schmidt J, Schmidt T, Golla M, et al. In vivo assessment of riluzole as a potential therapeutic drug for spinocerebellar ataxia type 3. *J Neurochem* 2016; **138**: 150–62.
- 17 Diallo A, Jacobi H, Cook A, et al. Survival in patients with spinocerebellar ataxia types 1, 2, 3, and 6 (EUROSCA): a longitudinal cohort study. *Lancet Neurol* 2018; **17**: 327–34.
- 18 Grobe-Einsler M, Taheri Amin A, Faber J, et al. Development of SARAtome, a new video-based tool for the assessment of ataxia at home. *Mov Disord* 2021; **36**: 1242–46.
- 19 Adanyeguh IM, Perlberg V, Henry P-G, et al. Autosomal dominant cerebellar ataxias: imaging biomarkers with high effect sizes. *Neuroimage Clin* 2018; **19**: 858–67.
- 20 Nigri A, Sarro L, Mongelli A, et al. Progression of cerebellar atrophy in spinocerebellar ataxia type 2 gene carriers: a longitudinal MRI study in preclinical and early disease stages. *Front Neurol* 2020; **11**: 616419.
- 21 Jacobi H, Reetz K, du Montcel ST, et al. Biological and clinical characteristics of individuals at risk for spinocerebellar ataxia types 1, 2, 3, and 6 in the longitudinal RISCA study: analysis of baseline data. *Lancet Neurol* 2013; **12**: 650–58.
- 22 Federighi P, Cevenini G, Dotti MT, et al. Differences in saccade dynamics between spinocerebellar ataxia type 2 and late-onset cerebellar ataxias. *Brain* 2011; **134**: 879–91.
- 23 Schmahmann JD. The cerebellum and cognition. *Neurosci Lett* 2019; **688**: 62–75.
- 24 Kosciuk TR, Sloat L, van der Plas E, et al. Brainstem and striatal volume changes are detectable in under 1 year and predict motor decline in spinocerebellar ataxia type 1. *Brain Commun* 2020; **2**: fcaa184.
- 25 Coarelli G, Darios F, Petit E, et al. Plasma neurofilament light chain predicts cerebellar atrophy and clinical progression in spinocerebellar ataxia. *Neurobiol Dis* 2021; **153**: 105311.
- 26 Hoche F, Guell X, Vangel MG, Sherman JC, Schmahmann JD. The cerebellar cognitive affective/Schmahmann syndrome scale. *Brain* 2018; **141**: 248–70.

### Supplementary appendix

This appendix formed part of the original submission and has been peer reviewed. We post it as supplied by the authors.

Supplement to: Coarelli G, Heinzmann A, Ewenczyk C, et al. Safety and efficacy of riluzole in spinocerebellar ataxia type 2 in France (ATRIL): a multicentre, randomised, double-blind, placebo-controlled trial. *Lancet Neurol* 2022; published online Jan 18. [https://doi.org/10.1016/S1474-4422\(21\)00457-9](https://doi.org/10.1016/S1474-4422(21)00457-9).

## Supplementary materials

### Brain MRI methods

3 Tesla cerebral MRI were acquired at baseline and after 12 months (Siemens Magnetom Verio n=28 patients, Siemens Prisma n=8 patients, Philips Achieva Dstream n=5 patients, Philips Achieva n=2 patients, Siemens Skyra n=2 patients). All MRIs were saved in a DICOM format and transferred to the platform for acquisition and processing of imaging: (CATI <https://cati-neuroimaging.com>) at the Paris Brain institute. The CATI was responsible for the harmonization, quality control, and analysis at M0 and M12. Acquired sequences included: i) a 3D T1-weighted magnetization prepared rapid gradient-echo (MPRAGE) volumetric image (for Siemens,  $T_R=2300$  ms,  $T_E=3$  ms,  $T_I=900$  ms, flip angle=  $9^\circ$ , voxel size= 1 mm isotropic, field of view =  $240 \times 256$  mm<sup>2</sup>; for Philips,  $T_R=7.2$  ms,  $T_E=3.3$  ms,  $T_I=904$  ms, flip angle=  $9^\circ$ , voxel size= 1 mm isotropic, field of view =  $240 \times 256$  mm<sup>2</sup>) was acquired at baseline and follow-up for volumetric analyses acquired for MRI volumetry to evaluate the atrophy of the cerebellum and brainstem; ii) a short T2-weighted image (for Siemens,  $T_R=5200$  ms,  $T_E=106$  ms, flip angle=  $90^\circ$ , voxel size= 1 mm isotropic, field of view =  $256 \times 256$  mm<sup>2</sup>; for Philips,  $T_R=8575$  ms,  $T_E=100$  ms, flip angle=  $90^\circ$ , voxel size= 1 mm isotropic, field of view =  $240 \times 240$  mm<sup>2</sup>) used by the neurologist when prominent artifacts were present on the T1 image. Brain images were inspected for major artifacts before they were processed. The MRI images were preprocessed using FreeSurfer 7.1.1<sup>1</sup> in order to use the sub-segmentation tool for the brainstem which extracts the volume of the midbrain, pons and medulla oblongata.<sup>2</sup> Since the cerebellum segmentation from FreeSurfer was not satisfactory for patients with an atrophic cerebellum, we processed the images using CERES<sup>3</sup> from the volBrain online platform.<sup>4</sup> We also added the volume of the vermis obtained by an atlas registration followed by manual corrections: the Brainnetome Atlas (<https://atlas.brainnetome.org>) was registered from the MNI space to the native image space using the deformation field previously obtained with CATI2

and only the vermis was kept for manual corrections. For more accurate and consistent segmentation, we corrected all the obtained regions of interest with the tissues classification of CAT12. The participant began treatment after the baseline MRI was performed.

To confirm the presence of cerebral atrophy, we compared baseline cerebellum and brainstem volumes of SCA2 patients with those extracted from the 3D T1-weighted images (Siemens Magnetom Verio) of a cohort of 18 healthy controls of a similar age. Pre-trial acquisitions in five patients allowed us to assess annual volume changes.

**Supplementary Table 1. Baseline and follow-up data of the 36-item short form health survey questionnaire (SF-36).**

Variable	Riluzole (n=22)	Placebo (n=23)	Total (n=45)	General population <sup>5</sup>
<b>Baseline</b>				
Physical functioning	50 [25;70] 50+/-28.7	50 [30;80] 52.8+/-30.1	50 [30;80] 51.4+/-29.1	86.5 +/- 19.7
Role limitations due to physical health	75 [0;100] 54.5+/-45.4	25 [0;75] 41.3+/-41.7	25 [0;100] 47.8+/-43.6	80.6+/-33.6
Role limitations due to emotional problems	50 [0;100] 53+/-44.4	33.3 [0;100] 53.6+/-44.7	33.3 [0;100] 53.3+/-44	67.8+/-19.7
Bodily pain	73 [42;100] 71.1+/-28.9	84 [41;100] 72.1+/-32.8	74 [41;100] 71.6+/-30.6	74.3+/-25.2
General health perceptions	53.5 [37;62] 51.1+/-21.2	42 [32;62] 45.5+/-21	47 [37;62] 48.2+/-21	69.0+/-20.9
Vitality	40 [25;60] 40.9+/-22.7	50 [30;60] 46.3+/-22.9	45 [25;60] 43.7+/-22.7	61.4+/-20.3
Social functioning	50 [37.5;75] 55.1+/-29	50 [37.5;62.5] 54.9+/-26.3	50 [37.5;75] 55+/-27.4	80.7+/-22.9
Mental Health	60 [48;76] 62+/-17.8	64 [52;76] 62.6+/-19.1	60 [52;76] 62.3+/-18.3	80.9+/-34.1
SF36: PCS, Physical component score	38 [34.6;54.5] 41.9+/-11.3	41.7 [35.6;50.3] 42.9+/-10.5	41.1 [35;50.5] 42.4+/-10.8	
SF36: MCS, Mental component score	42.1 [35.1;48.7] 41.5+/-10.8	39.4 [34.5;44.2] 40.1+/-10.6	41.3 [35.1;47.4] 40.8+/-10.6	
<b>Follow-up (month-12)</b>				
Variable	Riluzole (n=22)	Placebo (n=23)	p-value	
Physical functioning	0.0 [0.0;10.0]	-2.5 [-10.0;5.0]	0.26	
Role limitations due to physical health	0.0 [0.0;25.0]	0.0 [-25.0;0.0]	0.38	
Role limitations due to emotional problems	0.0 [0.0;66.7]	0.0 [-33.3;66.7]	0.62	
Bodily Pain	0.0 [-26.0;11.0]	-9.5 [-26.0;0.0]	0.36	
General Health perceptions	0.0 [-10.0;17.0]	2.5 [-7.0;10.0]	0.88	
Vitality	5.0 [-15.0;15.0]	2.5 [-15.0;10.0]	0.77	
Social Functioning	6.3 [-25.0;37.5]	0.0 [-25.0;25.0]	0.62	
Mental Health	6.0 [-4.0;12.0]	-4.0 [-12.0;8.0]	0.24	
Physical component score	-1.9 [-6.2;11.1]	0.7 [-5.4;8.6]	0.89	
Mental component score	-0.8 [-4.7;3.5]	-4.7 [-6.8;3.2]	0.31	

For the baseline data, we used the SF-36 Health Survey in French general population.<sup>5</sup> For all dimensions, except bodily pain, the mean value of the ATRIL patients are below those of the French General Population. The baseline data for riluzole and placebo group are reported as median scores [Q1;Q3].

At follow-up, we compared the variation between inclusion and M12 as median [Q1;Q3] of each of the SF-36 dimensions between the riluzole and placebo group.

**Supplementary Table 2. Brain MRI characteristics at baseline.**

Variable	Riluzole (n=22)	Placebo (n=23)	Total (n=45) Mean [95% CI]	Healthy controls (n=18) Mean [95% CI]	p-value*
Vermis	6400 [5952;7305]	6646 [5857;7292]	6576 [6258;6894]	10069 [9580;10559]	<0.001
Vermis grey matter	4628 [4209;4988]	5133 [4117;5233]	4751 [4466;5036]	7349 [7036;7663]	<0.001
Vermis white matter	1844 [1506;2169]	1781 [1357;2051]	1824 [1692;1957]	2719 [2447;2992]	<0.001
Left cerebellum	38666 [34601;46018]	37764 [33787;43574]	39645 [37548;41741]	58426 [55154;61698]	<0.001
Left cerebellum grey matter	27472 [24931;30987]	27598 [24031;30609]	28211 [26533;29889]	40771 [38691;42851]	<0.001
Left cerebellum white matter	11733 [9956;13686]	11309 [8524;12760]	11433 [10633;12233]	17655 [16242;19067]	<0.001
Left lobule III	219 [179;290]	254 [166;352]	236 [209;263]	313 [266;361]	0.004
Left lobule IV	1059 [906;1332]	1044 [856;1337]	1127 [1026;1229]	1583 [1448;1718]	<0.001
Left lobule V	2176 [2006;2862]	2139 [1680;2706]	2324 [2130;2517]	3463 [3192;3734]	<0.001
Left lobule VI	4803 [4376;5555]	4791 [4004;5463]	4906 [4603;5210]	7746 [7125;8367]	<0.001
Left lobule Crus I	9115 [7369;10237]	8388 [7358;9501]	8840 [8236;9444]	12065 [11412;12717]	<0.001
Left lobule Crus II	5999 [4979;6393]	5623 [4854;6543]	5828 [5446;6210]	7983 [7258;8707]	<0.001
Left lobule VIIIB	2869 [2339;3795]	2963 [2484;3310]	2975 [2747;3204]	4530 [4141;4919]	<0.001
Left lobule VIIIA	3695 [3292;4650]	3397 [2813;4410]	3829 [3520;4139]	685 [624;746]	<0.001
Left lobule VIIIB	2623 [2104;3018]	2324 [2016;2808]	2559 [2363;2755]	3821 [3530;4112]	<0.001
Left lobule IX	2360 [2007;2796]	2010 [1766;2250]	2250 [2066;2435]	3046 [2782;3309]	<0.001
Left lobule X	594 [493;678]	468 [409;590]	546 [506;585]	685 [624;746]	<0.001
Right cerebellum	39478 [36653;46105]	39255 [35958;44199]	40884 [38822;42946]	60429 [57071;63788]	<0.001
Right grey matter cerebellum	28226 [26111;32558]	28493 [25462;30374]	28882 [27229;30534]	41801 [39640;43961]	<0.001
Right white matter cerebellum	12158 [10080;13862]	11554 [9404;13061]	12002 [11270;12734]	18628 [17202;20053]	<0.001
Right lobule III	248 [206;304]	238 [187;345]	252 [222;283]	346 [310;382.93]	<0.001
Right lobule IV	1087 [964;1274]	957 [781;1280]	1082 [989;1175]	1557 [1387;1728]	<0.001
Right lobule V	2185 [1886;2482]	2148 [1604;2896]	2232 [2052;2411]	3288 [3558;3018]	<0.001
Right lobule VI	4761 [4192;6095]	4602 [3919;5323]	4892 [4572;5211]	8545 [7888;9202]	<0.001
Right lobule Crus I	9488 [8271;10110]	9868 [8004;10562]	9551 [8933;10170]	12427 [11577;13277]	<0.001
Right lobule Crus II	5817 [5220;6524]	5914 [4813;6836]	5883 [5486;6279]	8523 [7805;9242]	<0.001
Right lobule VIIIB	3064 [2534;3944]	2912 [2375;3483]	3118 [2878;3357]	4530 [4141;4919]	<0.001
Right lobule VIIIA	3933 [2998;4668]	3661 [2923;4332]	3892 [3597;4188]	5472 [5071;5872]	<0.001
Right lobule VIIIB	2687 [2003;3013]	2484 [2187;2774]	2571 [2408;2734]	3635 [3377;3893]	<0.001
Right lobule IX	2449 [2254;2862]	2072 [1826;2749]	2397 [2215;2580]	3293 [2990;3597]	<0.001
Right lobule X	668 [591;746]	565 [510;661]	608 [570;646]	721 [658;783]	0.002
SCP	200 [184;211]	191 [156;223]	198 [184;211]	187 [164;206]	0.39
Midbrain*	4673 [4287;5038]	4454 [4277;5272]	4742 [4553;4931]	6414 [6051;6776]	<0.001

Pons*	8277 [ 6748;8943]	7216 [6749;8127]	7943 [7422;8464]	16240 [15172;17308]	<0.001
Medulla oblongata*	3664 [3411;4194]	3871 [3611;4180]	3862 [3708;4017]	5358 [5056;5661]	<0.001

In this table, we reported the volume of cerebellum and brainstem regions for the riluzole group (as median scores [Q1;Q3]), the placebo group (as median scores [Q1;Q3]), the total ATRIL population (as median scores [Q1;Q3] in the first column, as mean [95% CI] in the second column), and healthy controls (as mean [95% CI]). The p-value refers to the comparison between the volumes (mean [95% CI]) of all ATRIL population (n=45) and healthy controls (n=18). For midbrain, pons and medulla oblongata, one patient in the placebo group was excluded from the analysis. All volumes are in mm<sup>3</sup>.

Abbreviations: SCP: superior cerebellar peduncle.

**Supplementary Table 3. Progression of MRI parameters after one year of treatment measured as percentage of variation.**

Variable	Riluzole (n=21)	Placebo (n=21)	Comparison between Riluzole and Placebo group Holm p-value*	Variation of the volume after one year for Placebo group Holm p-value**
Vermis	-4.86 [-7.32;-0.03]	-3.35 [-6.36;-0.25]	1	0.52
Vermis grey matter	-5.46 [-10.72;-0.66]	-4.82 [-7.94;0.93]	1	0.65
Vermis white matter	-4.35 [-5.72;5.78]	-2.02 [-6.55;8.15]	1	1
Left cerebellum	-1.73 [-3.95;-1.25]	-1.27 [-3.29;-0.33]	1	0.58
Left cerebellum grey matter	-2.55 [-3.95;-0.76]	-2.65 [-5.99;1.35]	1	0.56
Left cerebellum white matter	1.11 [-7.13;2.74]	-0.33 [-4.16;5.47]	1	1
Left lobule III	6.98 [-5.13;17.39]	3.61 [-6.30;22.29]	1	1
Left lobule IV	2.31 [-6.20;7.51]	-7.85 [-12.41;-1.26]	0.89	0.11
Left lobule V	-3.26 [-5.99;-0.99]	-1.48 [-5.47;0.59]	1	1
Left lobule VI	-3.60 [-6.44;-1.33]	-1.31 [-5.96;1.43]	1	1
Left lobule Crus I	-1.78 [-6.46;3.11]	-0.74 [-3.63;3.01]	1	<b>0.0013</b>
Left lobule Crus II	-3.52 [-4.51;-0.29]	-2.79 [-4.48;-0.96]	1	1
Left lobule VIIB	-2.59 [-4.50;1.15]	-3.06 [-7.31;3.48]	1	1
Left lobule VIIIA	-3.43 [-4.80;-1.71]	-1.84 [-4.71;1.99]	1	1
Left lobule VIIIB	-1.56 [-5.70;4.25]	-0.71 [-4.62;2.70]	1	1
Left lobule IX	-1.15 [-4.93;3.44]	0.58 [-1.47;2.78]	1	1
Left lobule X	3.25 [-3.98;8.01]	-0.34 [-4.40;8.54]	1	1
Right cerebellum	-1.25 [-3.03;-0.47]	-1.58 [-2.23;-0.35]	1	0.21
Right grey matter cerebellum	-1.88 [-4.04;0.77]	-2.38 [-6.08;0.30]	1	0.48
Right white matter cerebellum	-1.54 [-6.70;4.43]	-0.36 [-4.45;9.92]	1	1
Right lobule III	2.89 [-10.20;13.48]	1.17 [-7.52;25.82]	1	1
Right lobule IV	-0.66 [-8.19;5.86]	-4.43 [-10.23;0.31]	1	0.56
Right lobule V	0.61 [-7.34;3.15]	-0.39 [-4.34;4.25]	1	0.58
Right lobule VI	-1.66 [-6.25;3.35]	-2.07 [-7.28;-0.82]	1	0.05
Right lobule Crus I	-2.55 [-6.21;0.70]	-1.16 [-5.29;0.44]	1	0.17
Right lobule Crus II	-3.43 [-4.78;-1.02]	-2.28 [-3.90;-0.99]	1	1
Right lobule VIIB	-3.84 [-6.33;2.48]	-5.24 [-6.86;1.78]	0.89	1
Right lobule VIIIA	-2.19 [-5.80;0.78]	-3.31 [-4.43;-1.15]	1	1
Right lobule VIIIB	-3.28 [-7.49;1.40]	4.53 [-1.72;8.83]	1	1
Right lobule IX	1.25 [-3.77;5.67]	0.40 [-2.67;3.78]	1	1
Right lobule X	-0.80 [-3.97;2.53]	1.14 [-3.00;4.18]	1	1
SCP	3.09 [-5.37;6.60]	-2.11 [-7.74;2.52]	1	1
Midbrain	-1.63 [-3.44;0.96]	-3.34 [-5.82;-0.69]	1	0.12
Pons	-1.92 [-3.51;-1.28]	-2.28 [-3.13;-1.07]	1	<b>0.0002</b>
Medulla oblongata	1.59 [-5.20;6.77]	-1.41 [-6.72;2.75]	1	1

The progression of atrophy for each region at month-12 is reported as median [Q1;Q3] of percentage variation. No significant differences were found between the two groups.

\*Wilcoxon Two-Sample Test with t approximation.

\*\*Holm p-value is referred to placebo group analysis of percentage variation of volumes: left lobule Crus I and pons regions (Holm p-value in bold) presented a significant decrease after one year in untreated patients.



Abbreviations: SCP: superior cerebellar peduncle.

**Supplementary Table 4. Correlation between SARA score and MRI volumes.**

Variable	Unadjusted model			Adjusted model		
	Estimate	SE	Holm p-value	Estimate	SE	Holm p-value
Vermis	-0.00258	0.00069	0.01	-0.00191	0.00064	0.16
Vermis grey matter	-0.00272	0.00079	0.02	-0.00212	0.00070	0.14
Vermis white matter	-0.00232	0.00188	0.89	-0.00077	0.00166	1.00
Left cerebellum	-0.00044	0.00010	0.003	-0.00028	0.00011	0.43
Left cerebellum grey matter	-0.00056	0.00012	0.002	-0.00037	0.00014	0.28
Left cerebellum white matter	-0.00054	0.00031	0.83	-0.00017	0.00029	1.00
Left lobule III	-0.02368	0.00854	0.12	-0.01225	0.00834	1.00
Left lobule IV	-0.00625	0.00231	0.13	-0.00434	0.00210	0.72
Left lobule V	-0.00425	0.00114	0.01	-0.00314	0.00105	0.16
Left lobule VI	-0.00255	0.00074	0.02	-0.00133	0.00080	1.00
Left lobule Crus I	-0.00125	0.00037	0.03	-0.00080	0.00036	0.72
Left lobule Crus II	-0.00202	0.00059	0.02	-0.00127	0.00058	0.72
Left lobule VIIB	-0.00372	0.00095	0.01	-0.00272	0.00102	0.34
Left lobule VIIIA	-0.00296	0.00068	0.003	-0.00198	0.00075	0.34
Left lobule VIIIB	-0.00442	0.00110	0.007	-0.00314	0.00119	0.34
Left lobule IX	-0.00232	0.00133	0.83	-0.00080	0.00123	1.00
Left lobule X	-0.00960	0.00623	0.83	-0.00621	0.00541	1.00
Right cerebellum	-0.00041	0.00011	0.01	-0.00025	0.00011	0.72
Right cerebellum grey matter	-0.00053	0.00013	0.007	-0.00033	0.00014	0.57
Right cerebellum white matter	-0.00054	0.00034	0.83	-0.00024	0.00030	1.00
Right lobule III	-0.02000	0.00785	0.18	-0.00881	0.00780	1.00
Right lobule IV	-0.00636	0.00255	0.19	-0.00478	0.00226	0.72
Right lobule V	-0.00469	0.00121	0.01	-0.00312	0.00122	0.39
Right lobule VI	-0.00245	0.00070	0.02	-0.00129	0.00076	1.00
Right lobule Crus I	-0.00120	0.00037	0.03	-0.00077	0.00035	0.72
Right lobule Crus II	-0.00185	0.00057	0.03	-0.00119	0.00055	0.72
Right lobule VIIB	-0.00337	0.00092	0.01	-0.00245	0.00087	0.24
Right lobule VIIIA	-0.00284	0.00074	0.01	-0.00177	0.00078	0.66
Right lobule VIIIB	-0.00457	0.00139	0.03	-0.00340	0.00134	0.41
Right lobule IX	-0.00164	0.00137	0.89	0.00015	0.00126	1.00
Right lobule X	-0.00452	0.00663	0.89	-0.00158	0.00570	1.00
SCP	-0.02976	0.01866	0.83	0.00156	0.01825	1.00
Midbrain	-0.00386	0.00119	0.03	-0.00178	0.00133	1.00
Pons	-0.00165	0.00040	0.006	-0.00097	0.00049	0.79
Medulla oblongata	-0.00300	0.00152	0.60	-0.00143	0.00143	1.00

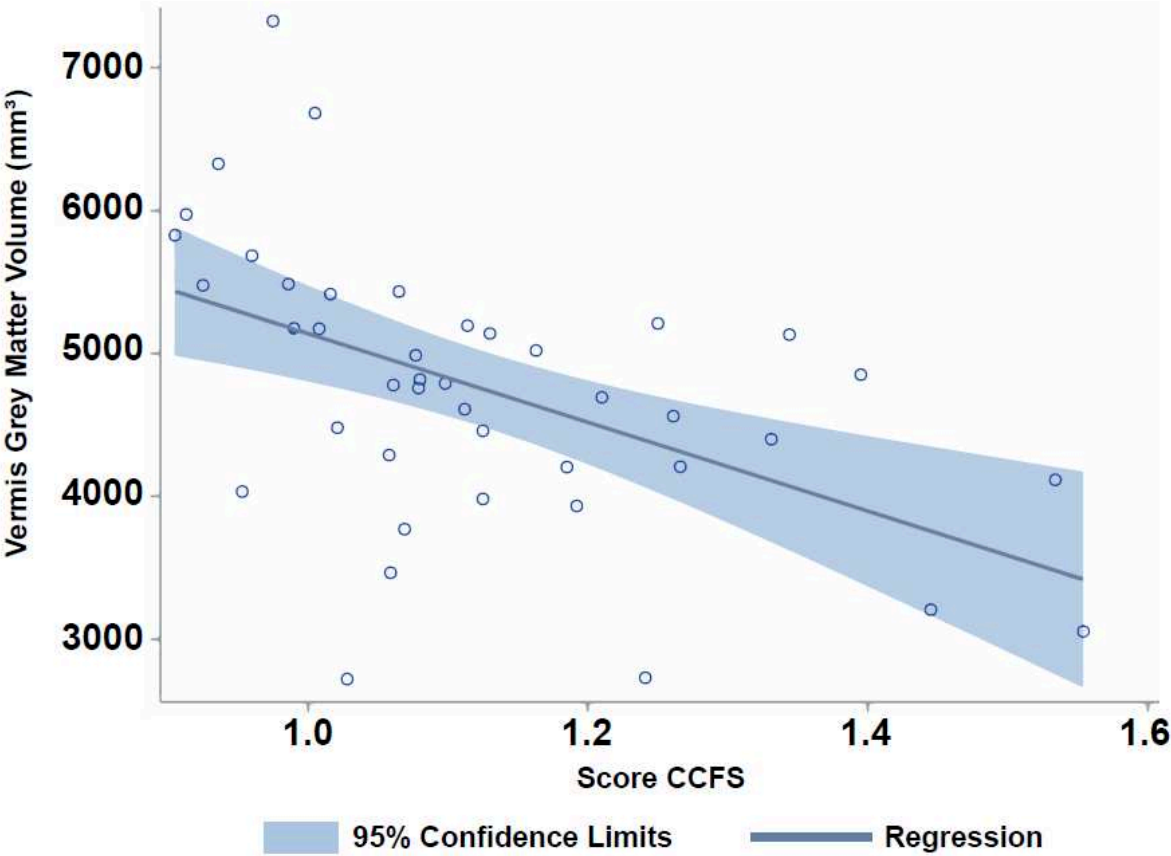
Cerebellar and brainstem atrophy was greater with higher SARA scores (in green), but not significant after adjustment for age and pathological CAG repeats (Holm p-value).

**Supplementary Table 5. Correlation between CCFS score and MRI volumes.**

Variable	Unadjusted model			Adjusted model		
	Estimate	SE	Holm p-value	Estimate	SE	Holm p-value
Vermis	-7.24E-05	2.14E-05	0.05	-6.43E-05	2.22E-05	0.22
Vermis grey matter	-8.57E-05	2.25E-05	0.0174	-7.89E-05	2.25E-05	0.0444
Vermis white matter	6.90E-06	6.24E-05	1.00	4.15E-05	6.17E-05	1.00
Left cerebellum	-1.02E-05	3.32E-06	0.09	-8.36E-06	4.03E-06	0.94
Left cerebellum grey matter	-1.26E-05	4.07E-06	0.09	-1.05E-05	4.73E-06	0.76
Left cerebellum white matter	-1.30E-05	9.66E-06	1.00	-4.96E-06	1.04E-05	1.00
Left lobule III	-3.97E-04	2.79E-04	1.00	-2.00E-04	3.00E-04	1.00
Left lobule IV	-1.13E-04	8.14E-05	1.00	-6.56E-05	8.31E-05	1.00
Left lobule V	-9.36E-05	4.10E-05	0.46	-7.12E-05	4.28E-05	1.00
Left lobule VI	-7.00E-05	2.21E-05	0.08	-6.18E-05	2.60E-05	0.63
Left lobule Crus I	-3.60E-05	1.15E-05	0.08	-3.09E-05	1.23E-05	0.53
Left lobule Crus II	-4.24E-05	1.87E-05	0.46	-3.09E-05	2.01E-05	1.00
Left lobule VIIIB	-9.51E-05	2.89E-05	0.06	-8.08E-05	3.43E-05	0.63
Left lobule VIIIA	-6.75E-05	2.41E-05	0.16	-5.13E-05	2.94E-05	1.00
Left lobule VIIIB	-1.32E-04	3.85E-05	0.0495	-1.19E-04	4.89E-05	0.60
Left lobule IX	-3.71E-05	4.38E-05	1.00	-2.12E-06	4.56E-05	1.00
Left lobule X	-4.73E-04	1.83E-04	0.26	-4.26E-04	1.80E-04	0.63
Right cerebellum	-1.03E-05	3.35E-06	0.09	-8.44E-06	3.88E-06	0.79
Right cerebellum grey matter	-1.34E-05	4.05E-06	0.06	-1.15E-05	4.70E-06	0.59
Right cerebellum white matter	-1.19E-05	1.06E-05	1.00	-5.49E-06	1.08E-05	1.00
Right lobule III	-2.20E-04	2.63E-04	1.00	-1.13E-05	2.84E-04	1.00
Right lobule IV	-1.47E-04	8.08E-05	0.97	-1.12E-04	8.12E-05	1.00
Right lobule V	-1.01E-04	4.12E-05	0.33	-7.39E-05	4.54E-05	1.00
Right lobule VI	-7.11E-05	2.11E-05	0.05	-6.38E-05	2.51E-05	0.51
Right lobule Crus I	-3.38E-05	1.11E-05	0.09	-2.87E-05	1.17E-05	0.59
Right lobule Crus II	-4.55E-05	1.80E-05	0.29	-3.53E-05	1.90E-05	1.00
Right lobule VIIIB	-9.03E-05	2.78E-05	0.07	-7.58E-05	2.94E-05	0.48
Right lobule VIIIA	-7.42E-05	2.48E-05	0.10	-5.95E-05	2.95E-05	0.96
Right lobule VIIIB	-1.32E-04	4.42E-05	0.10	-1.08E-04	4.89E-05	0.76
Right lobule IX	-1.61E-05	4.28E-05	1.00	1.77E-05	4.41E-05	1.00
Right lobule X	-3.93E-04	1.95E-04	0.75	-3.41E-04	1.91E-04	1.00
SCP	-6.16E-04	6.07E-04	1.00	2.93E-05	6.72E-04	1.00
Midbrain	-7.81E-05	3.99E-05	0.80	-3.73E-05	4.94E-05	1.00
Pons	-4.12E-05	1.30E-05	0.08	-3.51E-05	1.71E-05	0.94
Medulla oblongata	-3.88E-05	4.82E-05	1.00	-3.64E-07	5.03E-05	1.00

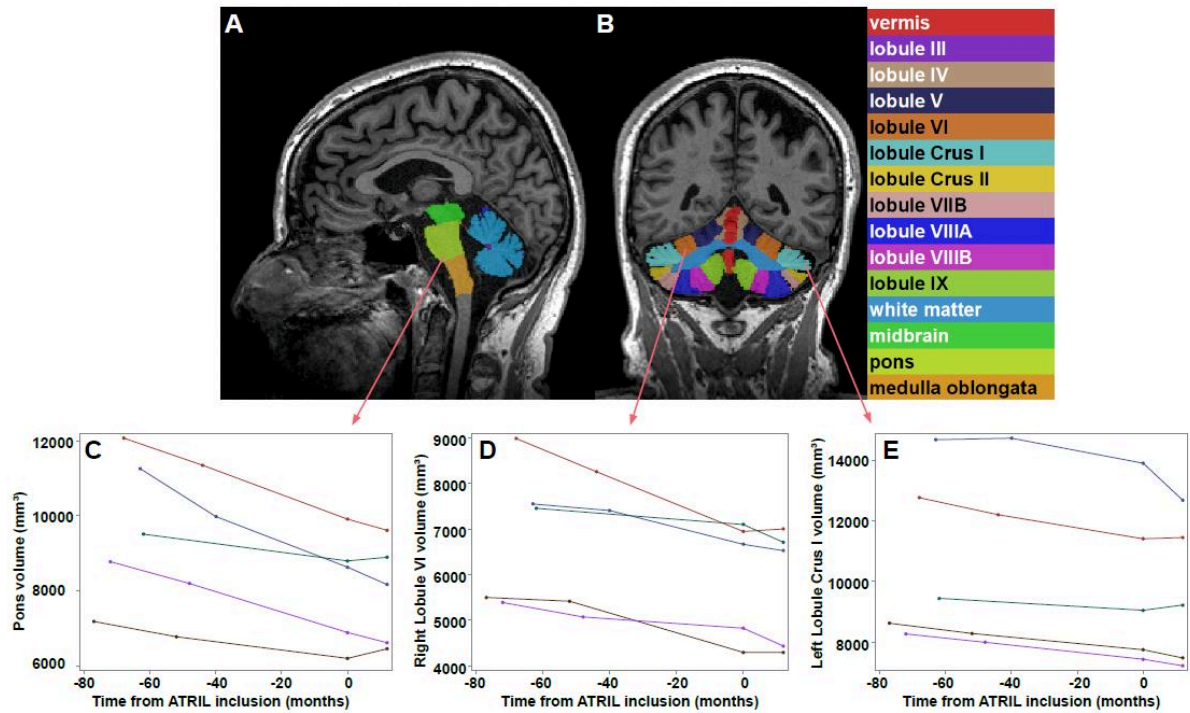
Only the negative correlation between CCFS and vermis grey matter was significant after adjustment for age and pathological CAG repeats (Holm p=0.04).

Supplementary Figure 1. Correlation between CCFS score and vermis grey matter volume at baseline.



The figure shows that lower vermis grey matter volumes correlate with higher Composite Cerebellar Functional Score (CCFS). Vermis grey matter volume is in mm<sup>3</sup>.

Supplementary Figure 2. Cerebellar and brainstem segmentation.



The figure shows the segmentation of cerebellum (A) and brainstem (B) using CERES software from the volBrain online platform. For five patients two brain MRIs (V1 and V2) at a two-year interval before the ATRIL study (M0 and M12) were available. The progression of volume loss is reported for the regions for which we found a significant change of volume after the 12 month ATRIL trial: pons (C), right cerebellum lobule VI (D) (almost significant volume change), and left cerebellum lobule Crus I (E).

## References:

- 1 Fischl B, Salat DH, Busa E, *et al.* Whole brain segmentation: automated labeling of neuroanatomical structures in the human brain. *Neuron* 2002; **33**: 341–55.
- 2 Iglesias JE, Van Leemput K, Bhatt P, *et al.* Bayesian segmentation of brainstem structures in MRI. *Neuroimage* 2015; **113**: 184–95.
- 3 Romero JE, Coupé P, Giraud R, *et al.* CERES: A new cerebellum lobule segmentation method. *NeuroImage* 2017; **147**: 916–24.
- 4 Manjón JV, Coupé P. volBrain: An Online MRI Brain Volumetry System. *Front Neuroinform* 2016; **10**: 30.
- 5 Leplège A, Ecosse E, Verdier A, Perneger TV. The French SF-36 Health Survey: translation, cultural adaptation and preliminary psychometric evaluation. *J Clin Epidemiol* 1998; **51**: 1013–23.

## Chapter 3 - CERMOI study

### Biomarkers in preataxic and early stage of SCA2 and SCA7

Giulia Coarelli,<sup>1</sup> Charlotte Dubec,<sup>1</sup> Sabrina Sayah,<sup>1</sup> Clara Fischer,<sup>2</sup> Marco Nassisi,<sup>3</sup> Emilie Dusclaux,<sup>4</sup> Karim Dorgham,<sup>5</sup> Lina Daghsen,<sup>1</sup> Bertrand Gaymard,<sup>6</sup> Pierre Daye,<sup>7</sup> Paulina Cunha,<sup>1</sup> Rania Hilab,<sup>1</sup> Hortense Hurmic,<sup>1</sup> Jean Charles Lamy,<sup>1</sup> Marie Laure Welter,<sup>1</sup> Marie Chupin,<sup>2</sup> Peggy Gatignol,<sup>4</sup> Isabelle Audo,<sup>3</sup> Jean François Mangin,<sup>2</sup> Roger Lane,<sup>8</sup> Moore Arnold,<sup>9</sup> Pierre Pouget,<sup>1</sup> Sophie Tezenas du Montcel,<sup>1</sup> Alexandra Durr<sup>1</sup>

<sup>1</sup>Sorbonne Université, Paris Brain Institute, Inserm, INRIA, CNRS, APHP, 75013 Paris, France

<sup>2</sup>CATI, ICM, CNRS, Sorbonne Université, Paris, France; Université Paris-Saclay, CEA, CNRS, Baobab, Neurospin, Gif-sur-Yvette, France

<sup>3</sup>Sorbonne Université, INSERM, CNRS, Institut de la Vision, 75012, Paris, France ; Centre Hospitalier National d'Ophthalmologie des Quinze-Vingts, National Rare Disease Center REFERET and INSERM-DGOS CIC 1423, F-75012 Paris, France

<sup>4</sup>Sorbonne Université, INSERM, UMRS1158 Neurophysiologie Respiratoire Expérimentale et Clinique, Paris, France

<sup>5</sup>Sorbonne Université, INSERM, CNRS, Centre d'Immunologie et des Maladies Infectieuses-Paris (CIMI-Paris), F-75013 Paris, France

<sup>6</sup>Service de Neurophysiologie, University Hospital Pitié-Salpêtrière, Paris, France

<sup>7</sup>P3lab, 1348 Louvain-la-Neuve, Belgique

<sup>8</sup>Ionis Pharmaceuticals, Carlsbad, CA, United States

<sup>9</sup>Biogen, Cambridge, MA, United States.

## Introduction

In the perspective of preventive treatments in preataxic stages of spinocerebellar ataxias (SCAs), the identification of reliable biomarkers providing objective measures to monitor disease and response to treatment is crucial. Antisense oligonucleotides (ASOs) are the most advanced option. Their administration at an early stage of the disease or even at the preataxic stage may be suitable to prevent clinical manifestations.<sup>60,61</sup> To date, in SCAs, imaging biomarkers present the strongest effect size than clinical scores.<sup>51</sup> Previous studies reported cerebellar and brainstem atrophy at the preataxic stages,<sup>26–29,62</sup> as well as microstructural damage of the white matter<sup>63–65</sup> and magnetic resonance spectroscopy (MRS) abnormalities<sup>66,67</sup>

in early disease phase. This suggests that biomarkers other than clinical scores could be better readouts in clinical trials. In this perspective, we aimed at identifying biological, clinical and/or imaging biomarkers in SCAs through a multimodal assessment. Our center is already involved in READISCA, an ongoing NIH-funded international clinical trial readiness study for SCA1 and SCA3. We therefore chose to focus on SCA2 and SCA7 mutation carriers only, either preataxic or affected at a very early stage (SARA score <15 out of 40). We enrolled 15 SCA2 and 15 SCA7 participants, together with ten control participants, for a 12-months study. The multimodal assessment consisted of neurological, neuropsychological, postural, oral mobility, ophthalmological, oculomotor, radiological, and biological evaluations.

## Methods

- **Study design and participants**

The “Integrated functional evaluation of the cerebellum” (CERMOI) study is a monocentric natural history study for SCA2 and SCA7 carriers, conducted between April 2020 and May 2022 at the Paris Brain Institute (ICM). Eligible criteria were: i. Be at least 18 years old, ii. With a genetically confirmed diagnosis of spinocerebellar ataxia type 2 (CAG repeat lengths  $\geq 32$  in the *ATNX2* gene) and spinocerebellar ataxia type 7 (CAG repeat lengths  $\geq 37$  in the *ATNX7* gene), iii. Have a SARA score between 0 and 15/40, iv. Be able to walk independently for a 30 feet distance without an assistive device, v. Be able to stand unassisted for 30 seconds, and vi. Be able to undergo cerebral MRI scanning. Eligible healthy controls had to test negative for SCA2 and SCA7, have a SARA score < 3, as well as no diagnosis of any other neurological disease. All participants had to be able to give their informed consent and be covered by social security. For all participants, key exclusion criteria included i. Contra-indications to MRI examination, ii. Currently receiving or having received any investigational drug in the prior two months, iii. Pregnancy or breastfeeding, iv. Inability to understand information about the protocol, which included individuals under legal protection or unable to consent, v. Genotype consistent with other inherited ataxias, vi. Changes in coordinative physical and occupational therapy for ataxia two months prior to study participation, vii. Concomitant disorder(s) or condition(s) potentially compromising the assessment of ataxia or its severity during this study.

The trial was carried out according to Good Clinical Practice guidelines, the Declaration of Helsinki, and in line with French regulations. The study was approved by the French Ethics



Committee and all participants provided written informed consent at the first visit before any study procedures or assessments. This trial is registered at ClinicalTrials.gov, under the number NCT04288128. This study was co-funded by the Biogen pharmaceutical lab and Ionis.

- **Procedures**

The study included three visits over a year: at baseline (V1, M0), at month 6 (V2, M6), and at month 12 (V3, M12), (Table 1). To avoid excessive fatigue, exams included in visit V1 and V3 were performed on two consecutive days. To accommodate participants' needs, V2 and V3 exams were performed in a range of  $\pm$  three weeks before or after the scheduled visit.

**Table 1. Evaluations performed at each visit of the CERMOI study.**

	<b>Visit 1 (M0)</b>	<b>Visit 2 (M6)</b>	<b>Visit 3 (M12)</b>
<b>Physical examination</b>	X	X	X
<b>Neurological examination</b>	X	X	X
<b>Quality of life questionnaires</b>	X	X	X
<b>Gait and postural analysis</b>	X	X	X
<b>Oro-facial motor assessment</b>	X	X	X
<b>Neuropsychological assessment</b>	X		X
<b>Ophthalmologic assessment*</b>	X	X**	X
<b>Oculomotor recording</b>	X	X	X
<b>Brain MRI</b>	X	X	X
<b>Blood sampling</b>	X	X	X
<b>CSF sampling***</b>	X		X
<b>Urine analysis</b>	X	X	X

\*Only for SCA2 and SCA7 carriers; \*\*Only visual acuity and optical coherence tomography; \*\*\*Optional.

This study was based on the following assessments (Table 1):

- Clinical and neurological examination including the Scale for the Assessment and Rating of Ataxia (SARA)<sup>30</sup> and Composite Cerebellar Functional Severity (CCFS)<sup>68</sup> scores, the Inventory of Non-Ataxia Signs (INAS),<sup>69</sup> the Most Bothersome Symptom (MBS) questionnaire in order to determine patients' most bothersome symptoms, and a collection of concomitant medication.

- Quality of life questionnaires: EQ-5D questionnaire (standardized instrument which measures health-related quality of life by five dimensions: mobility, self-care, usual activities, pain/discomfort and anxiety/depression),<sup>70</sup> Patient Health Questionnaire (PHQ-9, a self-administered depression module),<sup>71</sup> Fatigue Severity Scale (FSS),<sup>72</sup> and Friedreich's Ataxia Activities of Daily Living (FA-ADL).<sup>73</sup>

- Postural and gait assessment: The instrumented assessments of gait and posture were performed using an array of six body-worn inertial measurement units (Opal TM, Mobility Lab, APDM Inc., Portland,OR, USA) placed at both wrists, both feet, the sternum, and the lumbar region. The postural sway assessment included three tests: natural stance, feet-together stance, and tandem stance with eyes open and eyes closed condition for each test. The participants were asked to stand for 30 seconds with their feet apart, their hands on their sides. A foot template was placed on the ground and adjusted to ensure the same position for all participants. The gait assessment included four tests: natural gait (8 meters), forward tandem gait (3.6 meters), fast gait (10 meters), and 2-minutes natural gait in a hallway. Participants had to walk on a rectilinear trajectory and then turn and walk back the same distance for all tests, except for the fast gait.

- Oro-facial motor assessment: We used the Oral-Lingual-Facial Motility (MBLF) evaluation.<sup>74</sup> It is a computerized and calibrated evaluation of oral motor facial function. It accounts for the muscular coordination and degree of impairment of the lingual and facial muscles necessary for articulation, mimicry, and oral mobilization during the first stage of swallowing. Different items across five domains (face, eye, cheeks, lips, and tongue) were tested. The total MBLF score is derived by summing each category and ranges between 0 and 111 (worst-best). The nerves involved in the tasks [facial (VII), mandibular (V3 branch of the trigeminal nerve), lingual (from V3 branch of the trigeminal nerve), glossopharyngeal (IX), and hypoglossal (XII)] were also scored based on the movements in which they are involved (Table 2).

**Table 2. Facial and Lingual Motor Assessment (MBLF).**

Facial areas	Oral Motor Tasks	Muscles	Nerves	Score
<b>Face</b> /6	Symmetry at rest			/3
	Change of face when smiling			/3
<b>Eyes</b> /9	Close your eyes	Orbicularis oculi	VII	/3
	Raise your eyebrows	Occipito-frontalis	VII	/3
	Be frown	Corrugator supercilii	VII	/3
<b>Lips</b> /27	Pinch the lips	Compressor/buccinator	VII + V3	/3
	Stretch the lips	Zygomaticus/risorius	VII	/3
	Keep lips closed strongly	Orbicularis/masseter	VII+ V3	/3
	Smile as you open your mouth	Zygomaticus/risorius	VII	/3
	Discover the upper teeth	Levator labii superioris	VII	/3
	Discover the lower teeth	Mentalis	VII	/3
	Make « u »	Orbicularis oris	VII	/3
	Whistle	Orbicularis oris	VII	/3
	Blow	Orbicularis oris	VII	/3
<b>Cheeks and jaws</b> /30	Open your mouth	Buccinator/orbicularis oris	VII + V3	/3
	Close your mouth	Masseter/orbicularis oris	VII + V3	/3
	Puff off the cheeks	Buccinator/orbicularis oris	VII + V3	/3
	Puff left cheek	Buccinator/orbicularis oris	VII + V3	/3
	Puff right cheek	Buccinator/orbicular	VII + V3	/3
	Pass the air from one cheek to another	Buccinator/orbicularis oris	VII + V3	/3
	Tuck in the cheeks	Buccinator/orbicularis oris	VII + V3	/3
	Left jaw open mouth	Pterygoid	V3	/3
	Right jaw open mouth	Pterygoid	V3	/3
	Chew mouth closed			/3
<b>Tongue</b> /39	Stick the tongue out	Genioglossus/transverse muscle	XII + lingual nerve	/3
	Bring in the tongue	Hyoglossus/superior longitudinal muscle	XII	/3
	Put the tongue to the right	Pharyngoglossus	XII	/3
	Put the tongue to the left	Pharyngoglossus	XII	/3
	Put it on top	Superior longitudinal muscle	XII	/3
	Put it down	Superior longitudinal muscle	XII	/3
	Put your tongue on your teeth	Styloglossus/hypoglossus	VII + IX +XII	/3
	Move the tongue inside the right cheek			/3
	Move the tongue inside the left cheek			/3
	Raise the tip in the mouth	Pharyngoglossus	XII	/3
	Raise the tip out of the mouth	Styloglossus	VII + IX +XII	/3
	Click of the disapproval/disagreement	Styloglossus	VII + IX +XII	/3
	Rhythm of galloping horse	Styloglossus	VII + IX +XII	/3
<b>TOTAL</b>			<b>/111</b>	

Rating: 0 = no contraction; 1 = initiated movement; 2 = almost complete movement; 3 = normal contraction. Face symmetry: 0 = severe/complete asymmetry; 1 = significant asymmetry; 2 = slight asymmetry; 3 = no asymmetry.

- Neuropsychological evaluation: Neuropsychological assessment evaluated: i) global cognitive efficiency by the CCAS-Scale<sup>75</sup> and visual reasoning with Raven's progressive matrices 1938 (PM38)<sup>76</sup> (visual reasoning was assessed only on V1 since no change in intelligence was expected over one year); ii) attention and working memory by Digit Span (forward, backward and sequencing), Spatial Span (forward and backward) and the Paced Auditory Serial Addition Test (PASAT);<sup>77</sup> iii) executive functions by Trail Making test (TMT), Stroop, Modified Card Sorting test (MCST), verbal fluencies (semantic and literal);<sup>78</sup> iv) Emotions-Social cognition by faux-pas test and Ekman's emotional recognition<sup>79</sup> and a dynamic emotional recognition (FACES Battery),<sup>80</sup> on last visit; v) apathy by Starkstein scale score;<sup>81</sup> vi) visuoconstructive and visuospatial functions using Rey's figure on last visit (copy and memory) and subtests from the Visual Object and Space Perception (VOSP);<sup>82</sup> vii) language with a French naming test from the GRECO Neuropsychological Semantic Battery.<sup>83</sup>

- Ocular-motor recording: Horizontal and vertical movements of both eyes were recorded with a video-based eye tracker (Eyelink 2000) at a sampling rate of 1000 Hz that will allow an accurate analysis of saccades. Visual stimulation was displayed on a Iiyama monitor located 60 cm in front of them (visual angle: 56 ° x 35°). Each oculomotor session began with a calibration procedure (13 successive locations covering the entire screen). The data were stored and analyzed later with the EventID software. Each saccade paradigm was performed twice. Paradigms consisted in a visually guided saccade task (reflexive saccades triggered toward a suddenly presented visual target), a double saccade task (two saccades successively triggered toward that same target), a delayed saccade task (saccade triggered after a delay towards a visual target), a mirror saccade task (saccades triggered after a delay towards the mirror location of a stable visual target), a ramp saccade task (saccade triggered toward a visual target previously reached by a smooth ramp movement), and an antisaccade task (saccade performed toward the opposite direction a visual target).

- Ophthalmological assessment: At each visit, a detailed examination of the ocular structures with a slit lamp and eye fundus was performed. Since SCA7 patients present retinal dystrophy, two different protocols were followed for SCA2 and SCA7 carriers. For SCA2 carriers, the protocol included: best-corrected visual acuity (BCVA) using the Early Treatment Diabetic Retinopathy Study (ETDRS) charts, color vision tested by the Cambridge color test, static perimetry (Humphrey 24-2), visual evoked potential (VEP), electroretinogram (ERG) pattern, spectral-domain optical coherence tomography (SD-OCT), and retinal fundus

photograph. For SCA7 carriers: BCVA, Cambridge color test, mesopic microperimetry (Macular Integrity Assessment device, MAIA), full-field electroretinography (Ff-ERG), SD-OCT, retinal fundus photograph, near-infrared fundus autofluorescence (NIR-FAF), and short-wavelength fundus autofluorescence (SW-FAF) imaging. Healthy controls did not perform the ophthalmological assessment since we disposed of results from other control cohorts.

- Brain MRI: Three MRI sessions were acquired on a 3 Tesla cerebral MRI system (Siemens Magnetom PrismaFit). The MRI protocol was devised in the Center for Magnetic Resonance Research in Minneapolis and included sequences for volumetry and voxel-based morphometry (VBM), diffusion tensor imaging (DTI), and MR spectroscopy (MRS). All MRI scans were exported in DICOM format and transferred to the platform for acquisition and image processing (CATI <https://cati-neuroimaging.com>) at the Paris Brain institute. The CATI was responsible for the quality control, and analysis at M0, M6 and M12. Sequences acquired included: i) a 3D T1-weighted magnetization prepared rapid gradient-echo (MPRAGE) volumetric image (TR= 2400 ms, TE= 2.22 ms, TI= 1000 ms, flip angle= 8°, voxel size= 0.8 mm isotropic, field of view = 240 x 256 mm<sup>2</sup>) was acquired for volumetric analyses to evaluate the atrophy of the brain, cerebellum and brainstem; ii) a 3D T2-weighted image (SPACE sequence, TR=3200 ms, TE= 563 ms, voxel size= 0.8 mm isotropic, field of view = 256 x 240 mm<sup>2</sup>) used by the neurologist when prominent artifacts were present on the 3DT1 image. Brain images were inspected for major artifacts before they were processed. The MRI images were preprocessed using FreeSurfer 7.2.0 in order to get the cortical thicknesses of the brain and to use the sub-segmentation tool for the brainstem that extracts the volume of the midbrain, pons and medulla oblongata. We processed the images using CERES<sup>84</sup> and vol2Brain pipelines from the volBrain online platform for cerebellum segmentation (<https://www.volbrain.upv.es>). CERES is a tool dedicated to the cerebellum, it provides volumes of the main tissues (white and grey matter) and the cerebellum lobules. We also added the volume of the vermis, obtained by vol2Brain and automatically corrected especially for the first lobules (vermis I-III). For more accurate and consistent segmentation, we corrected all the obtained regions of interest with the tissues classification of CAT12.8.

- Biosample collections: We collected fasten blood, urine, and CSF (optional). All biosamples were frozen at - 80 °C after collection, and stored in the local biobank. We measured plasma NfL, and  $\alpha$ -synuclein, total tau, amyloid beta 40 (A $\beta$ 40), and amyloid beta 42 (A $\beta$ 42) in plasma and CSF. pTau181 was measured only in CSF. All biomarkers were measured in

duplicate using an ultrasensitive single molecule array on the Simoa HD-1 Analyzer (Quanterix), as previously established.<sup>85</sup>

Eligible participants underwent blood tests to check for normal blood cell count and hemostasis 72 hours prior to the lumbar puncture.

The severity of adverse events was evaluated using the Common Terminology Criteria for Adverse Events. The investigators also assessed the causal relationship between adverse events and the study procedures.

- **Objectives**

The objectives of the CERMOI study were: i. to determine, in SCA2 and SCA7 carriers compared with healthy controls, the cross-sectional and longitudinal variability for the different parameters/assessments over one year: neurological examination, quality of life, postural assessment, oro-facial motor assessment, neuropsychological assessment, ophthalmological assessment, oculomotor recording, brain MRI, CSF and blood biomarkers; ii. to correlate the different assessments in order to evaluate the progression in SCA2 and SCA7 carriers over one year.

- **Statistical analysis**

Frequency, percentage, and 95% confidence intervals (CI) were used to describe qualitative variables. Quantitative variables were described by their mean and standard error (SE) or standard deviation (SD) or their median and interquartile range (IQR). Qualitative variables were compared among groups using Fisher's exact test. Quantitative variables were compared among the three visits using non-parametric Kruskal-Wallis test, followed by Wilcoxon-Mann-Whitney pairwise test with Hochberg adjustment, when Kruskal-Wallis p-value was significant. In addition, for each assessment we calculated the quantitative progression of the scores using a mixed model with random effects for the patients and time as a fixed effect. The relations between baseline clinical scores and brain MRI data as well as other assessments' results were determined using a Spearman correlation model.

To account for multiple comparisons, P-values were considered significant based on a Holm-adjusted threshold within each set of assessments. Statistical analyses were done with R software (version 4.1.2).

## Results

Between May 28, 2020, and April 24, 2021, we enrolled 15 SCA2 carriers, 15 SCA7 carriers, and 10 controls recruited at the national reference center for rare disease of the Pitié-Salpêtrière University Hospital in Paris. All completed the assessments required by the study, except for one individual belonging to the control group, who did not complete the last visit (V3).

- **Clinical assessment and quality of life**

Clinical characteristics at baseline are shown in Table 3. Among SCAs carriers, five SCA2 and nine SCA7 were at pre-ataxia stage (SARA score < 3 out of 40). The first symptoms at onset presented by SCA2 patients were walking difficulties (n=8) and dysarthria (n=2), resulting in a median age at onset of 37 years (IQR 29.5, 44.7). For SCA7 carriers, they were walking difficulties (n=4), visual impairment (n=3), walking difficulties with visual impairment (n=1), walking and writing difficulties (n=1), for a median age at onset of 36 years (IQR 17, 48). Three pre-ataxic carriers of SCA7 expansions reported age at onset for walking difficulties. At baseline, median SARA score was 4 (IQR 1.25, 6.5) and 2 (IQR 0, 11.5) for SCA2 and SCA7, respectively, significantly different compared with controls (0, IQR 0, 0), but comparable between SCA groups (p=0.93, Table 3). A similar trend was also observed at V2 and V3 (p<0.001 between SCA2 and controls for the two visits; p=0.01 at V2 and p<0.01 at V3 between SCA7 and controls), reflecting an early disease stage. After 12 months, SARA score remained <3 in all five preataxic SCA2 carriers, while two preataxic SCA7 carriers converted to ataxia stage (SARA ≥3). Two SCA2 carriers with SARA score > 3 at baseline showed a decrease in the SARA score to pre-ataxic stage at V3 (from 4 to 2.5 and from 3.5 to 2).

CCFS score were significantly higher in SCA groups than control (p <0.01) and comparable between SCA2 and SCA7 carriers (p=0.45, Table 3).

INAS count was significant different between SCA subtypes and controls (p <0.001) and similar between SCA groups (p=0.36, Table 3). In Table 4, details of baseline INAS are reported. Upper motoneuron signs were significantly more frequent in SCAs (p <0.001), in particular for the SCA7 group presenting with hyperreflexia (<0.001). Dysmetric saccades were the other signs more detected in SCAs carriers than controls (p <0.0001). Urinary dysfunction was more reported by SCA7 carriers (p=0.02), probably driven by corticospinal involvement, even if it was not significant after Holm adjustment.

**Table 3. Clinical and genetic characteristics at baseline.**

	SCA2 (n=15)	SCA7 (n=15)	Control (n=10)	p-value*	p-value** SCA2-controls	p-value** SCA7-controls	p-value** SCA2-SCA7
<b>Sex</b>							
Women, n (%)	5 (33%)	8 (53%)	4 (40%)	0.61			
Men, n (%)	10 (67%)	7 (47%)	6 (60%)				
<b>CAG repeat length of short alleles</b>							
Median (Q1, Q3)	22 (22, 22)	10 (10, 10)		na			
Min – Max	22-24	10-14					
<b>CAG repeat length of expanded alleles<sup>§</sup></b>							
Median (Q1, Q3)	38 (36.5, 39)	41 (39, 46.5)		na			
Min – Max	35-40	38-62					
<b>Years of education</b>							
Median (Q1, Q3)	15 (14, 17)	16 (14.5, 17)	17 (15.5, 17)	0.43			
Min – Max	10-20	11-17	12-20				
<b>Age at baseline (years)</b>							
Median (Q1, Q3)	41 (37, 46)	38 (28.5, 39.8)	39.5 (31, 54.5)	0.78			
Min - Max	21-66	18-60	26-64				
<b>Age at first symptom (years)</b>							
n	n=8	n=9					
Median (Q1, Q3)	37 (29.5, 44.7)	36 (17, 48)		0.7			
Min – Max	26 – 60	6 – 60					
<b>Disease duration (years)</b>							
n	n=8	n=9					
Median (Q1, Q3)	8.5 (4.2, 11.7)	8 (5, 11)		0.8			
Min – Max	1 – 17	0 – 12					
<b>SARA score (max value 40)</b>							
Median (Q1, Q3)	4 (1.25, 6.5)	2 (0, 11.5)	0 (0, 0)	0.001	<0.001	<0.01	0.93
<b>CCFS (normal 0.85 ± 0.05)</b>							
Median (Q1, Q3)	0.89 (0.87, 0.95)	0.85 (0.84, 1.03)	0.82 (0.8, 0.84)	0.002	0.001	0.02	0.45
<b>INAS count (max value 16)</b>							
Median (Q1, Q3)	4 (2.5, 4.5)	5 (2.5, 5)	1 (1, 2)	<0.001	<0.001	<0.001	0.36
<b>EQ-5D (max value 100)</b>							
Median (Q1, Q3)	80 (62.5, 90)	80 (52.5, 90)	90 (85.5, 98.7)	0.12			
<b>PHQ-9 (max value 27)</b>							
Median (Q1, Q3)	1.5 (0, 2.75)	3 (2, 5)	4.5 (1.5, 6.7)	0.11			
<b>FSS (max value 7)</b>							
Median (Q1, Q3)	1.67 (1.2, 3.4)	2.22 (1.7, 3)	2.56 (2.3, 4.3)	0.22			
<b>FA-ADL (max value 36)</b>							
Median (Q1, Q3)	3 (0.5, 5)	4 (1, 10)	0 (0, 0)	0.001	<0.01	<0.01	0.28

Data are n (%) or median (Q1, Q3). In red, significant p value. \*p-value calculated by Kruskals-Wallis test; \*\* Hochberg adjusted p-value calculated by Wilcoxon test. Abbreviations: CCFS: composite cerebellar functional severity score; FA-ADL: Friedreich's Ataxia Activities of Daily Living; FSS: Fatigue Severity Scale; INAS:



inventory of non-ataxia signs, Patient Health Questionnaire (PHQ-9); SARA: scale for the assessment and rating of ataxia. <sup>s</sup>Normal *ATXN2*/SCA2 allele < 32 CAG, normal *ATXN7*/SCA7 allele < 36 CAG.

**Table 4. Comparison of baseline INAS items among the three groups.**

Item INAS	SCA2 (n=15) n (%)	SCA7 (n=15) n (%)	Control (n=10) n (%)	p-value	p-value SCA2- SCA7*	p-value SCA2- control*	p-value control- SCA7*	Holm p-value
<b>Areflexia</b>	3 (20%)	0 (0%)	0 (0%)	0.10	0.22	0.25	1	
<b>Upper motoneuron signs</b>	8 (53%)	11 (73%)	0 (0%)	<0.001	0.44	<0.001	<0.001	0.0024
Hyperreflexia	6 (40%)	11 (73%)	0 (0%)	<0.001	0.13	0.05	<0.001	0.0025
Extensor plantar	2 (13%)	2 (13%)	0 (0%)	0.65				
Spasticity	2 (13%)	7 (47%)	0 (0%)	0.02	0.10	0.5	0.02	0.0026
<b>Lower motoneuron signs</b>	3 (20%)	2 (13%)	0 (0%)	0.4				
Fasciculations	3 (20%)	0 (0%)	0 (0%)	0.1				
Muscle atrophy	0 (0%)	1 (7%)	0 (0%)	1				
Paresis	0 (0%)	2 (13%)	0 (0%)	0.3				
<b>Extrapyramidal signs</b>	6 (40%)	2 (13%)	0 (0%)	0.05				
Resting tremor	1 (6.7%)	0 (0%)	0 (0%)	1				
Rigidity	5 (33%)	2 (13%)	0 (0%)	0.09				
Dystonia	1 (7%)	0 (0%)	0 (0%)	1				
<b>Chorea/Dyskinesia</b>	0 (0%)	0 (0%)	0 (0%)	1				
<b>Impaired vibration sense at ankles</b>	11 (73%)	11 (73%)	4 (40%)	0.19				
<b>Nystagmus</b>	4 (27%)	2 (13%)	0 (0%)	0.20				
<b>Ophthalmoparesis</b>	2 (13%)	4 (27%)	0 (0%)	0.20				
<b>Dysmetric saccades</b>	11 (73%)	13 (87%)	0 (0%)	<0.0001	0.65	<0.001	<0.001	0.0023
<b>Diplopia</b>	2 (13%)	3 (20%)	0 (0%)	0.33				
<b>Urinary dysfunction</b>	2 (13%)	7 (47%)	0 (0%)	0.02	0.10	0.5	0.02	0.0026
<b>Dysphagia</b>	4 (27%)	5 (33%)	0 (0%)	0.07				
<b>Cramps</b>	3 (20%)	2 (13%)	1 (10%)	0.85				

Data are n (%). In red, significant p-value after Holm adjustment; in blue, significant p-value before Holm adjustment. \*p-value between groups calculated only for significant global p-value by Fisher's exact test.

Upper motor neuron signs are defined as hyperreflexia, extensor plantar (unilateral or bilateral), or spasticity. Lower motor neuron signs are defined as fasciculations, muscle atrophy, or paresis. Extrapyramidal signs are defined as resting tremor, rigidity, or dystonia. Nystagmus is defined as downbeat nystagmus on fixation, horizontal gaze-evoked nystagmus, or vertical gaze-evoked nystagmus. Ophthalmoparesis is defined as vertical or/and horizontal. Dysmetric saccades are defined as hypometric saccades or hypermetric saccades.

We analyzed the progression of clinical scores at V2 and V3, pooling SCA2 and SCA7 carriers (n=30, Table 5). Only SARA score showed a significant global progression, with a mean of  $5.05 \pm 5$  at baseline and of  $5.77 \pm 6.1$  at V3 ( $p < 0.01$  between baseline and V2,  $p < 0.01$  between baseline and V3, no progression between V2 and V3, Table 5). We analyzed SARA score progression for each SCA subgroup, observing that the score significantly progressed only in SCA7 individuals (global  $p < 0.01$ , baseline-V2  $p = 0.01$ , baseline-V3  $p < 0.001$ , Table 5).

At baseline, the quality of life questionnaires EQ-5D, PHQ-9, and FSS showed no significant difference between SCA groups and controls, while the activities of daily living assessed by FA-ADL were impaired in SCA groups compared with controls ( $p < 0.01$  for both comparisons between SCA2 and controls and between SCA7 and controls, Table 3). Quality of life did not worsen at V2 and V3 (Table 5).

**Table 5. Progression of clinical scores at month 6 (V2) and month 12 (V3) for SCA2 and SCA7 individuals pooled together.**

	Global p-value	Mean (SD) at baseline	Mean (SD) at V2	p-value baseline-V2	Mean (SD) at V3	p-value baseline-V3
<b>SARA*</b>	<b>0.03</b>	5.05 (5)	5.73 (6.1)	<b>0.006</b>	5.77 (6.1)	<b>0.004</b>
SCA2	0.25	4.57 (3.7)	4.93 (4.1)	0.12	4.63 (4.2)	0.77
SCA7	<b>0.002</b>	5.53 (6.1)	6.53 (7.7)	<b>0.01</b>	6.9 (7.5)	<b>&lt;0.001</b>
<b>CCFS</b>	0.11	0.9208 (0.1)	0.92 (0.1)	0.88	0.9101 (0.1)	0.16
<b>INAS count</b>	0.21	3.8 (1.5)	3.9 (2.07)	0.62	3.57 (1.9)	0.25
<b>EQ5D</b>	0.47	71.63 (25.1)	68.55 (25.2)	0.31	68.13 (27)	0.49
<b>PHQ-9</b>	0.27	3.38 (3.9)	3.73 (4)	0.49	4.37 (5)	0.09
<b>FSS</b>	0.15	2.49 (1.5)	2.78 (1.5)	0.09	2.8 (1.4)	0.07
<b>FA-ADL</b>	0.43	4.57 (4.7)	4.54 (4.2)	0.21	4.23 (5.2)	0.36

Analysis done by a mixed model with random effects for the patients and time as a fixed effect. In red, significant p-value. \*For SARA score only, the progression was calculated for all SCA individuals pooled together and for each SCA group separately.

Abbreviations: CCFS: composite cerebellar functional severity score; FA-ADL: Friedreich's Ataxia Activities of Daily Living; FSS: Fatigue Severity Scale; INAS: inventory of non-ataxia signs, Patient Health Questionnaire (PHQ-9); SARA: scale for the assessment and rating of ataxia; SD: standard variation.

We collected the Most Bothersome Symptom (MBS) with a dedicated questionnaire. In SCA2 carriers the most reported MBS at baseline was “walking difficulties” (n=9), followed by dysarthria (n=2), “vision problems” (n=1), “sleep disturbance” (n=1), “fatigue” (n=1), “lack of hand dexterity” (n=1), “pain” (n=1), and “cognitive impairment” (n=1). At month 12, “walking difficulties” (n=6) was confirmed as the main MBS followed by “fatigue” (n=3), “lack of hand dexterity” (n=2), “dysarthria” (n=1), “pain” (n=1), and “cognitive impairment” (n=1). In the SCA7 group, “vision problems” (n=4) was the most reported MBS at baseline, followed by “walking difficulties” (n=3), “dysarthria” (n=1), “lack of hand dexterity” (n=1), “legs rigidity” (n=1), “sleep disturbance” (n=1), and “cognitive impairment” (n=1). At month 12, “sleep disturbance” (n=3) became more frequent than “vision problems” (n=2), “walking difficulties” (n=2), “fatigue” (n=2), “cognitive impairment” (n=2), “dysarthria” (n=1), and “urinary dysfunction” (n=1). For controls, “fatigue” (n=3) and “sleep disturbance” (n=2) were the most reported MBS.

- **Gait and postural assessment**

Gait parameters tested for natural, fast, tandem, and 2-minutes gait are reported in Table 6 and illustrated in Figure 1. At baseline, the comparison among the three groups showed significant differences in fast gait speed of the SCA2 and SCA7 carriers compared with healthy controls ( $p=0.02$  and  $p=0.04$ , respectively), with a reduced cadence in SCA7 carriers ( $p=0.3$ ). In the SCA7 group, the stance phase of the gait cycle was longer than the healthy controls ( $p=0.4$ ), and was associated with a reduced swing phase ( $p=0.4$ ), both marked on the right side.

The 2-minutes natural gait test showed one significant result on the foot strike angle of the right leg, significantly increased in SCA2 carriers compared with controls ( $p=0.01$ ). For tandem gait, no differences were found, possibly because only SCA7 presymptomatic carriers (n=9) and presymptomatic and early ataxic SCA2 carriers (n=12) performed this task. In the standing in the natural position task, the sway area metric was significantly larger for the SCA population than for controls, for both open and closed eyes conditions ( $p<0.01$ ). This parameter was especially affected for SCA2 carriers ( $p<0.001$ , Table 6). However, none of these differences were significant after Holm adjustment.



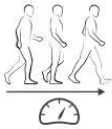





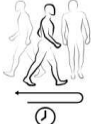


We analyzed the progression of all parameters over one year by multiple comparisons test. None reported a significant progression after Holm adjustment.

**Table 6. Comparison of baseline postural parameters among the three groups.**

Variable	SCA2 (n=15)	SCA7 (n=15)	Control (n=10)	p-value KW*	p-value SCA2- SCA7**	p-value SCA2- Control**	p-value SCA7- Control**
<b>Fast gait</b>							
<b>Cadence RLL (steps/min)</b>	122.5 (113.5-120)	123 (116.2-128)	133 (130-142)	0.02	0.90	0.05	0.02
<b>Cadence LLL (steps/min)</b>	123 (113.5-130)	124 (116.2-128)	133 (130-141)	0.03	0.94	0.07	0.03
<b>Gait speed RLL (m/s)</b>	1.55 (1.41-1.6)	1.6 (1.1475-1.7)	1.82 (1.7-1.9)	0.02	0.83	0.02	0.04
<b>Gait speed LLL (m/s)</b>	1.54 (1.3-1.7)	1.58 (1.1-1.7)	1.85 (1.7-1.9)	0.01	0.74	0.02	0.04
<b>Stance RLL (%)</b>	57.85 (56.5-58.9)	57.95 (56.7-60.6)	55.9 (54.3-57.2)	0.02	0.49	0.06	0.04
<b>Swing RLL (%)</b>	42.15 (41-43.4)	42.05 (39.3-43.2)	44.1 (42.8-45.7)	0.02	0.49	0.06	0.04
<b>2-minutes gait</b>							
<b>Foot strike angle RLL (°)</b>	28.6 (27.5-30.6)	25.15 (23.4-29.6)	23.35 (20.9-26.9)	0.03	0.26	0.01	0.44
<b>Static position</b>							
<b>Sway area open eyes (°2)</b>	1.04 (0.8-1.7)	0.94 (0.5-3.97)	0.26 (0.2-0.5)	0.003	0.77	0.001	0.02
<b>Sway area closed eyes (°2)</b>	1.58 (0.8-3.3)	1.18 (0.5-8)	0.39 (0.2-0.6)	0.004	0.53	<0.001	0.03

Data are expressed as median (Q1, Q3). In blue, significant p-value before Holm adjustment. \*p-value calculated by Kruskals-Wallis test; \*\* Hochberg adjusted p-value calculated by Wilcoxon test.

Abbreviations: LLL: left lower limb; RLL: right lower limb.

GAIT PARAMETERS		Definition
<b>DURATION (s)</b>		The duration of the trial
<b>CADENCE (steps/min)</b>		Number of steps per minutes counting steps of both feet
<b>GAIT SPEED (m/s)</b>		The forward speed of the subject measured at the forward distance traveled during the gait cycle divided by the gait cycle duration
<b>FOOT STRIKE ANGLE (°)</b>		The angle of the foot at the point of initial contact. The pitch of the foot when flat is zero and positive when the heel contacts first
<b>STANCE (% CGT)</b>		The percentage of the gait cycle in which the foot is on the ground
<b>STRIDE LENGTH (m)</b>		The forward distance tracked by the foot during a gait cycle
<b>SWING (% CGT)</b>		The percentage of the gait cycle in which the foot is not on the ground
<b>TOE OUT ANGLE (°)</b>		The lateral angle of the foot during the stance phase relative to the forward motion of the foot during the swing phase. Positive angles indicate an outward
<b>TURNS DURATION (s)</b>		The duration of the turn
<b>APA DURATION (s)</b>		The duration of the period standing form the first measurable change of the lateral lumbar acceleration from baseline to when the lateral acceleration goes back to baseline value
<b>Double support (% CGT)</b>		The percentage of gait cycle in which both feet are on the ground

**Figure 1. Gait parameters tested using APDM wearable sensors in CERMOI study.**

- **Oro-facial motor assessment**

We evaluated oro-facial motor performance by MBLF evaluation (Table 2). In SCA2 carriers, clinical observations found predominant tremor in the tongue and lips. Co-contractions were notable in the neck, cheeks, eyes, and mouth. Hypomimia was often observed in this group with weakness during the execution of movements, lack of mobility, and movements that were not wide and not maintained. The smile was very discreet in some patients. We found an overall slowness. The praxis "show the lower teeth" was laborious. The "Eye" examination caused labial and jugal synkinesia in some patients. Jugal praxias such as "puff off the cheeks" or "pass the air from one cheek to another" were slowed down and sometimes gave the impression of no air in the cheeks. The SCA7 carriers also showed tremors and co-contractions during the "Tongue" and "Lips" parts. These tremors were found on the tongue, neck and eyelids. The "Eye" examination part caused palpebral and oral tremors and often revealed a hypomimia with very restricted eyebrow movements. We also observed a slowness to perform lingual movements, more or less severe speech disorders and articulatory imprecision. Qualitatively, some controls presented a weakness in the cheeks, tremors of the tongue, neck and cheeks, and hypomimia.

At baseline, the median of total oral motor mobility score, the MBLF score, was similar among the three groups: 101 (98.5, 103.5) in SCA2, 103 (98.5, 107.5) in SCA7, and 105.5 (101.25, 108) in controls,  $p=0.33$  (Table 7). At month-12 (V3), MBLF score significantly worsened in SCA2 and SCA7 patients group compared with controls ( $p<0.001$ ), decreasing to 90 (86.5, 93) in SCA2 and to 96 (87, 99.5) in SCA7 carriers. All domains were significantly different between SCA2 carriers and controls, while for SCA7 the difference was found in the face, cheeks, and tongue domains (Table 7). These worsening trends were already detectable at the six-month follow-up (Table 7). In controls, MBLF score remained stable (median of 107, IQR 106, 108, Table 7).

For the movements tested by MBLF, we also evaluated the nerves involvement: facial (VII), mandibular (V3 branch of trigeminal nerve), lingual (from V3 branch of trigeminal nerve), glossopharyngeal (IX), and hypoglossal (XII) nerves (Table 7). Some movements required the involvement of more than one nerve (Table 2). At baseline, there was no difference of nerves scores among the three groups (Table 7). However, for SCA2 carriers, VII, XII, and VII-IX-XII nerves scores were significantly lower than controls at V2 ( $p<0.01$ ,  $p=0.01$ , and  $p<0.01$ , respectively), and all nerves scores were significantly decreased at V3 (Table 7). For SCA7

carriers, no differences were detected at baseline and at V2 (except for VII nerve score,  $p=0.01$ ) while at V3 the VII, XII, and the association of VII-IX-XII nerves scores were lower than controls ( $p<0.001$ ,  $p<0.01$ , and  $p<0.01$ , respectively) (Table 7).

For all SCAs, MBLF score significantly worsened at each time-point (between V1 and V2  $p<0.001$ , between V1 and V2  $p<0.001$ , between V2 and V3  $p<0.01$ , Table 8). All MBLF sub-scores and nerve scores (except for mandibular branch of trigeminal nerve) significantly progressed at V3 ( $p<0.001$ ). Given that these results were so remarkable, we analyzed the progression for each SCA group (Table 8). Significant decrease of MBLF score ( $p<0.001$ ), was early detected at 6-month follow-up for SCA7 carriers together with face and tongue sub-scores ( $p<0.01$ ), while for SCA2 only face score worsened ( $p=0.01$ , Table 8). For nerves scores, progression was detected at V2 in both SCA groups for hypoglossal nerve score ( $p=0.01$  for SCA2 and  $p<0.0001$  for SCA7, Table 8). In addition, for SCA2, VII nerve and VII-IX-XII nerves scores were worsened at V2 ( $p<0.0001$  and  $p=0.01$ , respectively), and for SCA7 VII-V3 score ( $p=0.04$ , Table 8). At month-12, all MBLF sub-scores and nerves scores were significantly decreased in both SCA groups (Table 8).

**Table 7. Comparison of MBLF scores among the three groups at baseline, month-6, and month-12.**

	SCA2 (n=15)	SCA7 (n=15)	Control (n=10)	p-value KW*	p-value SCA2- SCA7**	p-value SCA2- Control**	p-value SCA7- Control**	Holm p- value
<b>Baseline V1</b>								
Face	5 (5, 6)	5 (5, 6)	6 (6, 6)	0.03	0.55	0.04	0.06	0.008
Eyes	9 (8, 9)	9 (8.5, 9)	9 (8.2, 9)	0.75				
Lips	25 (23, 26)	25 (23, 25.5)	25 (24, 26)	0.54				
Cheeks	27 (25.5, 29.5)	29 (26.5, 29.5)	29 (28, 29)	0.54				
Tongue	36 (35, 37.5)	38 (34.5, 38.5)	36 (35.2, 38.7)	0.39				
<b>MBLF score/111</b>	101 (98.5, 103.5)	103 (98, 107.5)	105.5 (101, 108)	0.33				
VII score	27 (25, 28.5)	28 (26, 29)	28 (28, 29)	0.42				
VII + V3 score	26 (24.5, 27)	27 (24.5, 27)	26 (25, 26.7)	0.88				
V3 score	5 (4, 6)	5 (4.5, 6)	6 (5.25, 6)	0.19				
XII + lingual nerve score	3 (3, 3)	3 (3, 3)	3 (3, 3)	0.61				
XII score	17 (15, 18)	18 (16.5, 18)	16.5 (16, 17.7)	0.41				
VII + IX + XII score	11 (9.5, 11)	11 (9.5, 12)	12 (10.2, 12)	0.18				
<b>6 months-V2</b>								
Eyes	8 (7, 8.5)	8 (8, 9)	9 (9, 9)	0.01	0.09	0.01	0.09	0.05
Lips	23 (20, 25)	24 (22, 25)	26 (25, 26)	<0.01	0.55	<0.01	<0.01	0.017
Cheeks	26 (25, 27)	27 (26.5, 29)	30 (29.2, 30)	<0.001	0.09	<0.01	<0.01	0.0125
Tongue	33 (32, 34)	34 (32.5, 37)	37.5 (36.2, 38.7)	<0.001	0.10	<0.001	0.03	0.025
<b>MBLF score/111</b>	95 (92, 96.5)	99 (93.5, 103.5)	107 (107, 108.7)	<0.001	0.07	<0.001	<0.001	0.01
VII score	24 (22, 27)	26 (24.5, 28)	28.5 (28 – 29)	<0.01	0.25	<0.01	0.01	0.017
XII + lingual nerve score	2 (2 – 3)	3 (2.5, 3)	3 (3, 3)	0.02	0.06	0.06	0.73	0.05
XII score	15 (14, 16)	16 (14, 17)	17 (17, 18)	0.01	0.15	0.01	0.13	0.025
VII + IX + XII score	10 (10, 10)	11 (9, 11)	12 (11, 12)	<0.01	0.11	0.001	0.05	0.0125
<b>12 months-V3</b>								
Face	4 (4, 5)	5 (4, 5)	6 (6, 6)	<0.001	0.36	<0.001	<0.001	0.008
Eyes	8 (7, 9)	8 (7.5, 9)	9 (9, 9)	0.02	0.27	0.02	0.07	0.05
Lips	8 (7, 9)	8 (7.5, 9)	9 (9, 9)	0.02	0.27	0.02	0.07	0.025
Cheeks	26 (23, 27.5)	27 (24.5, 28)	29 (29, 30)	<0.001	0.30	<0.001	<0.01	0.017
Tongue	31 (28.5, 32)	31 (30.5, 34)	38 (37, 38)	<0.001	0.26	<0.001	<0.01	0.0125
<b>MBLF score/111</b>	90 (86.5, 93)	96 (87, 99.5)	107 (106, 108)	<0.001	0.27	<0.01	<0.001	0.01
VII score	25 (21, 26.5)	26 (23, 27)	29 (28, 29)	<0.001	0.46	<0.01	<0.001	0.017
VII + V3 score	23 (23, 25)	24 (23, 26)	26 (26, 27)	0.02	0.42	0.03	0.05	0.05
XII + lingual nerve score	2 (2, 2)	2 (2, 3)	3 (3, 3)	0.0053	0.13	<0.01	0.09	0.0125



XII score	13 (12, 15.5)	14 (13.5, 16)	17 (17, 17)	<0.001	0.20	<0.01	<0.01	0.025
VII + IX + XII score	10 (8, 10)	9 (9, 10.5)	12 (12, 12)	<0.001	0.62	<0.001	0.001	0.01

Data are expressed as median (Q1, Q3). In red, significant p-value <0.05 after Holm adjustment; in blue, significant p-value <0.05 before Holm adjustment. \*p-value calculated by Kruskals-Wallis test; \*\* Hochberg adjusted p-value calculated by Wilcoxon test.

Abbreviations: MBLF: Oral-Lingual-Facial Motility.

**Table 8. Progression of MBLF scores at month 6 (V2) and month 12 (V3) for SCA2 and SCA7 separately.**

	<b>Global p-value</b>	<b>Mean (SD) at baseline</b>	<b>Mean (SD) at V2</b>	<b>p-value V1-V2</b>	<b>Mean (SD) at V3</b>	<b>p-value V1-V3</b>	<b>Holm p-value</b>
<b>SCA2</b>							
Face	<0.001	5.2 (0.77)	4.8 (0.94)	0.01	4.33 (0.9)	<0.01	0.01
Eyes	<0.001	8.4 (0.91)	7.73 (1.03)	0.73	7.67 (1.18)	<0.001	0.025
Lips	<0.001	24.2 (2.81)	22.07 (3.59)	0.67	21.8 (3.57)	<0.001	0.017
Cheeks	0.01	26.93 (2.99)	25.13 (3.8)	0.55	24.67 (3.79)	<0.01	0.05
Tongue	<0.001	35.27 (3.49)	31.87 (5.07)	0.12	30.2 (3.71)	<0.01	0.0125
<b>MBLF score/111</b>	<0.01	100 (7.96)	91.6 (12.32)	0.2	88.67 (9.82)	<0.01	0.08
VII score	<0.001	26.73 (3.24)	24.07 (3.83)	<0.001	23.93 (4.11)	<0.001	0.0125
VII + V3 score	<0.01	25.33 (2.44)	24 (3.64)	0.06	23.13 (3.44)	<0.01	0.05
XII + lingual nerve score	<0.01	2.87 (0.35)	2.33 (0.49)	<0.01	2.2 (0.41)	<0.01	0.01
XII score	<0.01	16.07 (2.87)	14.4 (3.04)	0.01	13.67 (2.16)	<0.001	0.025
VII + IX + XII score	<0.001	10.33 (1.18)	9.53 (1.68)	0.01	9.13 (1.41)	<0.001	0.017
<b>SCA7</b>							
Face	<0.01	5.33 (0.82)	5.2 (0.68)	<0.01	4.6 (0.83)	0.001	0.0125
Eyes	0.12	8.6 (0.74)	8.4 (0.63)	0.24	8.13 (0.99)	0.04	0.05
Lips	0.01	24 (2.2)	23 (2.62)	0.33	22.47 (2.56)	<0.01	0.25
Cheeks	<0.01	27.33 (3.94)	26.53 (3.72)	0.13	25.87 (3.16)	<0.001	0.17
Tongue	<0.01	36.4 (2.77)	34.2 (3.45)	<0.01	31.67 (3.15)	<0.01	0.01
<b>MBLF score/111</b>	<0.01	101.67 (7.75)	97.33 (8.41)	<0.001	92.73 (8)	<0.01	0.008
VII score	0.01	26.93 (2.4)	25.73 (2.49)	0.06	25.07 (2.74)	<0.01	0.05
VII + V3 score	<0.01	25.2 (3.14)	24.4 (3.89)	0.04	23.93 (3.08)	0.001	0.025
XII + lingual nerve score	<0.001	2.93 (0.26)	2.73 (0.46)	0.08	2.47 (0.52)	<0.001	0.0125
XII score	<0.01	17.13 (1.13)	15.87 (1.55)	<0.001	14.53 (1.64)	<0.01	0.01
VII + IX + XII score	<0.01	10.53 (1.36)	10.13 (1.6)	0.19	9.53 (1.36)	0.001	0.01

Analysis done by a mixed model with random effects for the patients and time as a fixed effect. In red, significant p-value. \*p-value between baseline and V2; \*\*p-value between baseline and V3.

Abbreviations: MBLF: Oral-Lingual-Facial Motility SD: standard deviation.

- **Neuropsychological evaluation**

We analyzed data resulting from global cognitive efficiency tests, executive functions and attentional skills at baseline and V3. The CCAS score was similar among the three groups ( $p=0.06$ , Table 9). At baseline, the variables that were significantly different among the three groups were: Stroop color (global  $p=0.03$ ,  $p=0.04$  between SCA2 and SCA7 carriers), emotional recognition (global  $p=0.01$ ,  $p=0.02$  between SCA2 and controls, and  $p=0.02$  between SCA7 and controls), and semantic fluency (global  $p=0.01$ ,  $p=0.02$  between SCA2 and controls, and  $p=0.01$  between SCA7 and controls, Table 9). However, after Holm adjustment, these differences were not significant (Table 9). Of note, only SCA7 carriers with preserved color vision performed Stroop tasks. Hence, SCA7 carriers performed similar to controls and even better than SCA2 carriers on this test. At month-12 (V3), in SCA2 and SCA7 carriers pooled together, we only detected an improvement of phonemic fluency ( $22.27 \pm 6.69$  at baseline vs  $26.9 \pm 6.44$ ,  $p < 0.001$ , Table 10), as a result of previous training. The increase of the apathy scored by Starkstein scale did not reach significance after Holm adjustment (Table 10).

At V3, we added an assessment of emotional recognition with dynamic stimuli evaluated by the FACES battery. We found a significant worse performance for SCA7 in this test compared with SCA2 carriers [31 (29, 32.5) vs 34 (31.5, 34) respectively,  $p=0.04$ ] and controls [31 (29, 32.5) vs 34 (34, 34) respectively,  $p=0.02$ ]. For SCA7 carriers, the test was not impacted by vision problems since neutral and joyful faces were always recognized. The least recognized expression was sadness ( $3.8 \pm 1.45$ ), followed by anger ( $4.9 \pm 0.88$ ) and disgust ( $5.2 \pm 0.86$ ). No difference was found between SCA2 and controls ( $p=0.28$ ).

**Table 9. Baseline neuropsychological characteristics.**

	SCA2 (n=15)	SCA7 (n=15)	Controls (n=10)	p- value*	p-value SCA2- SCA7**	p-value SCA2- Controls**	p-value SCA7- Controls**	Holm p-value
<b>CCAS (max best 120)</b>	93 (86, 101.5)	101 (96, 106.5)	105 (102, 108.2)	0.06				
<b>CCAS fail (max worse 10)</b>	2 (1, 3)	0 (0, 1.5)	0.5 (0, 1)	0.08				
<b>PM38 (max best 60)</b>	50 (46.5, 52.5)	48.5 (43.2, 50)	49 (46.2, 49.7)	0.64				
<b>Digit span forward scaled score (max best 19)</b>	11 (9, 11.5)	11 (8.5, 12.5)	9.5 (8.2, 12.5)	0.98				
<b>Digit span backward scaled score (max best 19)</b>	9 (8, 11.5)	10 (8, 12)	13 (10.2, 14.7)	0.05				
<b>Digit span sequencing scaled score (max best 19)</b>	13 (10.5, 14.5)	12 (10, 12.5)	12 (10.5, 13.7)	0.81				
<b>Spatial span forward scaled score (max best 19)</b>	12 (9.5, 13)	11 (10.5, 12.5)	10.5 (9.25, 13.7)	0.94				
<b>Spatial span backward scaled score (max best 19)</b>	12 (10.5, 14)	11 (10.5, 12)	11 (10, 11)	0.37				
<b>Trail Making test (seconds)</b>	46.5 (40, 76.5)	36 (24.5, 49.2)	35 (27.5, 40.7)	0.12				
<b>Stroop color</b>	69.5 (65.5, 77)	88 (78, 91) n=9	78 (69, 88)	0.03	0.04	0.21	0.425	0.003
<b>Stroop word</b>	98.5 (89, 104.5)	117 (100, 118) n=9	103 (102, 116)	0.07				
<b>Stroop colorword</b>	44 (39.7, 51)	53 (51, 60) n=9	51 (50, 55)	0.10				
<b>Semantic fluency</b>	29 (26.5, 36)	30 (26, 33.5)	37.5 (34, 40.7)	0.01	0.91	0.02	0.01	0.0028
<b>Phonemic fluency</b>	22 (17, 25)	24 (20, 27.5)	23.5 (21, 30.2)	0.43				
<b>Emotional recognition (max best 35)</b>	28 (26, 29)	28 (27, 29)	30.5 (29.25, 31.7)	0.01	0.73	0.02	0.02	0.0029
<b>Faux pas test (max best 30)</b>	26 (23.5, 28.5)	29 (25.5, 29.5)	28.5 (24.7, 29.7)	0.31				
<b>Control stories (max best 10)</b>	10 (10, 10)	10 (10, 10)	10 (10, 10)	0.46				
<b>Starkstein scale (max worse 42)</b>	9 (5.5, 10)	10 (5.5, 11.5)	10 (7.25, 12.7)	0.60				

Data are expressed as median (Q1, Q3). In blue, significant p-value <0.05 before Holm adjustment. \*p-value calculated by Kruskals-Wallis test; \*\* Hochberg adjusted p-value calculated by Wilcoxon test. Abbreviations: CCAS: Cerebellar Cognitive Affective/Schmahmann syndrome; PM38: Raven's Progressive Matrices.

**Table 10. Progression of neuropsychological tests over one year for all SCAs carriers.**

	<b>Baseline V1 Mean (SD)</b>	<b>V3 (M12) Mean (SD)</b>	<b>p-value*</b>	<b>Holm p- value</b>
<b>CCAS</b>	96.1 (11.7)	99.1 (10.4)	0.06	
<b>CCAS fail</b>	1.5 (1.6)	1.3 (1.5)	0.30	
<b>PM38</b>	47.7 (6.6)	Not done	-	
<b>Digit span forward scaled score</b>	10.2 (3.1)	9.9 (2.6)	0.44	
<b>Digit span backward scaled score</b>	9.8 (2.7)	10.1 (3.2)	0.55	
<b>Digit span sequencing scaled score</b>	12.1 (3.2)	12.3 (3.3)	0.58	
<b>Spatial span forward scaled score</b>	11.4 (2.6)	11.6 (3.2)	0.65	
<b>Spatial span backward scaled score</b>	11.6 (2.6)	11.5 (3.1)	0.80	
<b>Trail Making test</b>	47.2 (26.6)	42.9 (25.3)	0.26	
<b>Stroop color</b>	75.3 (13.2)	74.9 (13.7)	0.75	
<b>Stroop word</b>	103.5 (12.8)	100.7 (16.2)	0.46	
<b>Stroop colorword</b>	48.7 (11.2)	49.1 (11.5)	0.11	
<b>Semantic fluency</b>	30.3 (6.1)	31.2 (6.4)	0.44	
<b>Phonemic fluency</b>	22.2 (6.7)	26.9 (6.4)	< 0.001	0.0028
<b>Emotional recognition</b>	27.5 (2.5)	28 (3.4)	0.38	
<b>Faux pas test</b>	25.9 (4.4)	24.9 (6.18)	0.26	
<b>Control stories</b>	9.8 (0.6)	9.7 (0.62)	0.96	
<b>Starkstein scale</b>	8.9 (4.1)	10.3 (5.17)	0.04	0.0029

Analysis done by a mixed model with random effects for the patients and time as a fixed effect. In red, significant p-value <0.05 after Holm adjustment; in blue, significant p-value <0.05 before Holm adjustment.

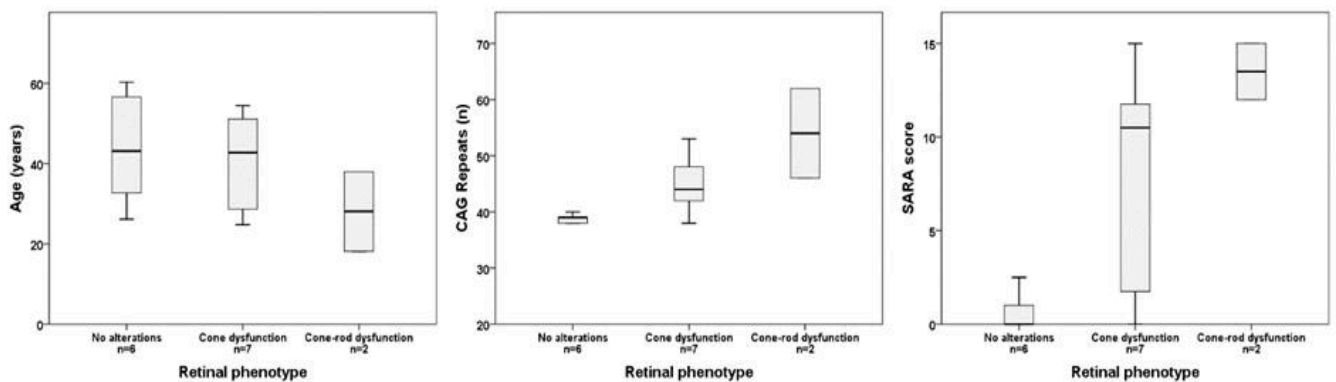
Abbreviations: CCAS: Cerebellar Cognitive Affective/Schmahmann syndrome; PM38: Raven's Progressive Matrices; SD: standard deviation.

- **Ophthalmological assessment**

At baseline, visual symptoms were reported by one SCA2 patient (photophobia) and nine SCA7 carriers (photophobia n=7, decreased visual acuity n=5, color vision disorders n=5, night vision disorders n=2, central scotoma n=2, phosphenes n=1). No major alterations were found for SCA2 carriers (sd-OCT analyses are ongoing), while for SCA7 retinal involvement was detected, as expected, in both functional and imaging exams detailed below:

Functional exams

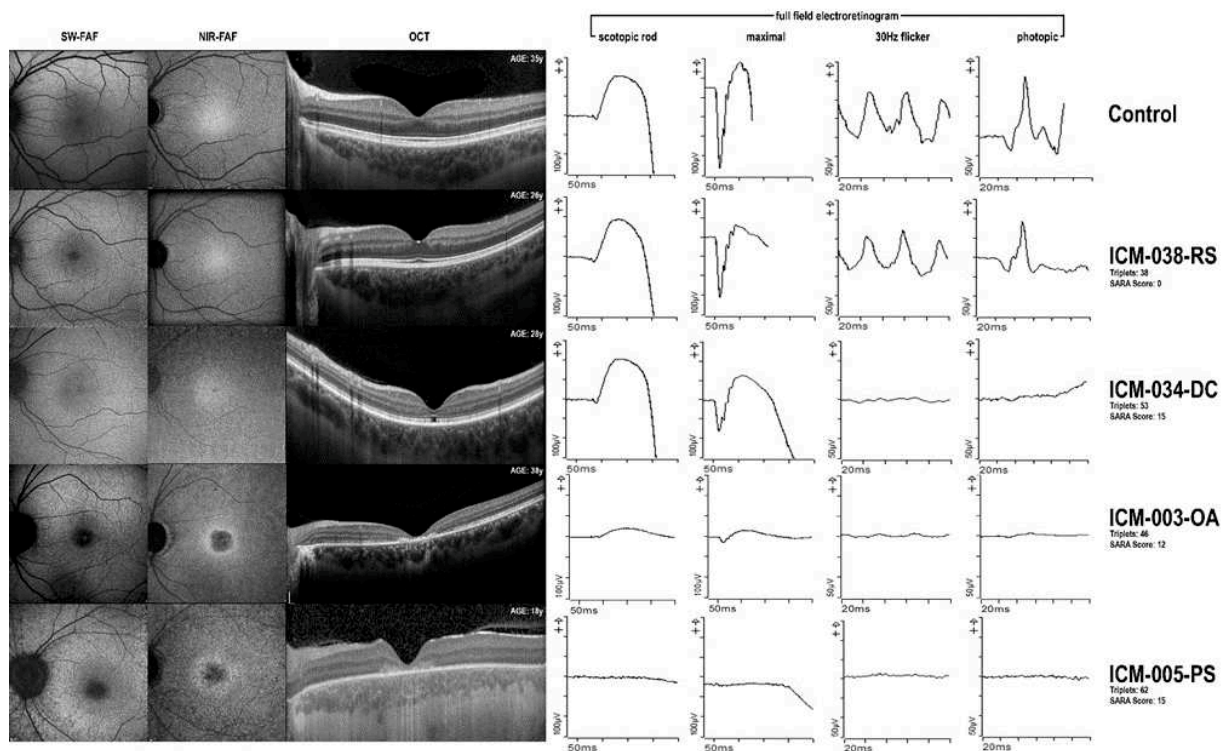
The mean best-corrected visual acuity (BCVA) was  $74.53 \pm 28.23$  ETDRS letters (about 20/32 Snellen equivalent, normal eyesight= 20/20) indicating a mild visual loss, and did not change over time. Color vision was impaired in five patients (33%), with no preferential axis. Thirteen carriers could complete the microperimetry, while two were excluded for the long exam duration due to low vision (20/200 and 20/800) and unstable fixation. The mean retinal sensitivity was  $23.9 \pm 3.9$  dB (reference database range: 24-36 dB). Ff-ERGs showed a significant impairment of the cone system in nine carriers (60%); two of them (13%), at the ataxic stage, had both photopic and scotopic functions altered, with undetectable traces in one patient (7%). In carriers with no photoreceptor impairment (n=6, median age: 43 years), CAG repeats were  $\leq 40$  and the SARA score was  $< 3$  out of 40 (Figure 2). The two patients with rod and cone dysfunction (18 and 38-year-old) had 62 and 46 CAG repeats with a SARA score of 15 and 12, respectively (Figure 2). Finally, the number of CAG repeats in carriers with only cone dysfunction (n=7, cone dystrophy [CD], median age: 42 years) ranged between 38 and 49, with a SARA score ranging between 0 and 15 (Figure 2). The Ff-ERG did not significantly worsen at month-12.



**Figure 2. Box plots showing the distribution of age, number of CAG repeats (pathogenic threshold sizes of 37 CAG repeats), and the SARA score based on the full field electroretinography alterations as cone dystrophy or cone-rod dystrophy.**

## Imaging analysis

Three patients (20%) had no retinal abnormalities on any imaging modality. They all had a SARA score  $\leq 1$  and a CCFS score  $<0.85$ . All other patients presented with a cone or cone-rod dystrophy at variable stages (Figure 3). Alterations included a central area of hypoautofluorescence on SW-FAF and NIR-FAF, a foveal disruption of the photoreceptors' ellipsoid zone and/or a central outer retinal atrophy on SD-OCT. Specifically, hypoautofluorescence was detectable and measurable in the SW-FAF of seven patients (47%, mean surface:  $0.54 \pm 0.72 \text{ mm}^2$ ) and in the NIR-FAF of 12 carriers (80%), half of them at preataxic stage, (mean surface:  $0.42 \pm 0.78 \text{ mm}^2$ ). The photoreceptors' ellipsoid zone was disrupted and measurable only in 10 carriers (67%, mean horizontal diameter:  $937.42 \pm 877.01 \mu\text{m}$ ; mean vertical diameter:  $1329.89 \pm 2600.8 \mu\text{m}$ ). The overall cohort had a mean central outer nuclear layer (ONL) thickness of  $69.97 \pm 31.25 \mu\text{m}$ . Longitudinal analyses are ongoing.



**Figure 3. Ophthalmological alterations in SCA7 carriers.**

Short-wavelength fundus autofluorescence (SW-FAF), near-infrared fundus autofluorescence (NIR-FAF), optical coherence tomography (OCT) and full field electroretinogram (ffERG) responses of four SCA7 carriers and one healthy control. Carrier ICM-038-RS (age at examination 25, 38 CAG, SARA score 0/40) had no ophthalmological and neurological alteration. Patient ICM-034-DC (age at examination 27, 53 CAG, SARA score 15/40) showed ocular abnormalities characterized by a focal interruption of the photoreceptor line on OCT (yellow arrow) and undetectable photopic responses on ffERG. Patients ICM-005-PS (age at examination 18, 64 CAG, SARA score

of 15/40) and ICM-003-OA (age at examination 38, 46 CAG, SARA score of 12/40) presented the most severe phenotype with cerebellar and pyramidal syndrome associated with diminished visual acuity, specifically outer retinal layers on OCT were diffusely thinner (with atrophy at the fovea) and both cones and rods responses were severely impaired.

- **Oculomotor biomarkers**

At baseline, the saccade main sequence, resulting from the relationship between amplitude, duration, and velocity of saccades, was altered in manifest SCA2 (n=10) and SCA7 (n=5) expansion carriers versus controls ( $p < 0.05$ ). This was also significant in preataxic SCA2 carriers (n=5) versus controls ( $p < 0.05$ ). There was no significant correlation with the expanded CAG repeat size or clinical scores (SARA and CCFS scores). This preliminary analysis indicates that abnormal saccades are very early signs, detectable in the absence of cerebellar features upon a neurological examination. The study of the other parameters, such as the presence of square waves, nystagmus, antisaccades, as well as the longitudinal analyses are still ongoing.

- **Brain MRI**

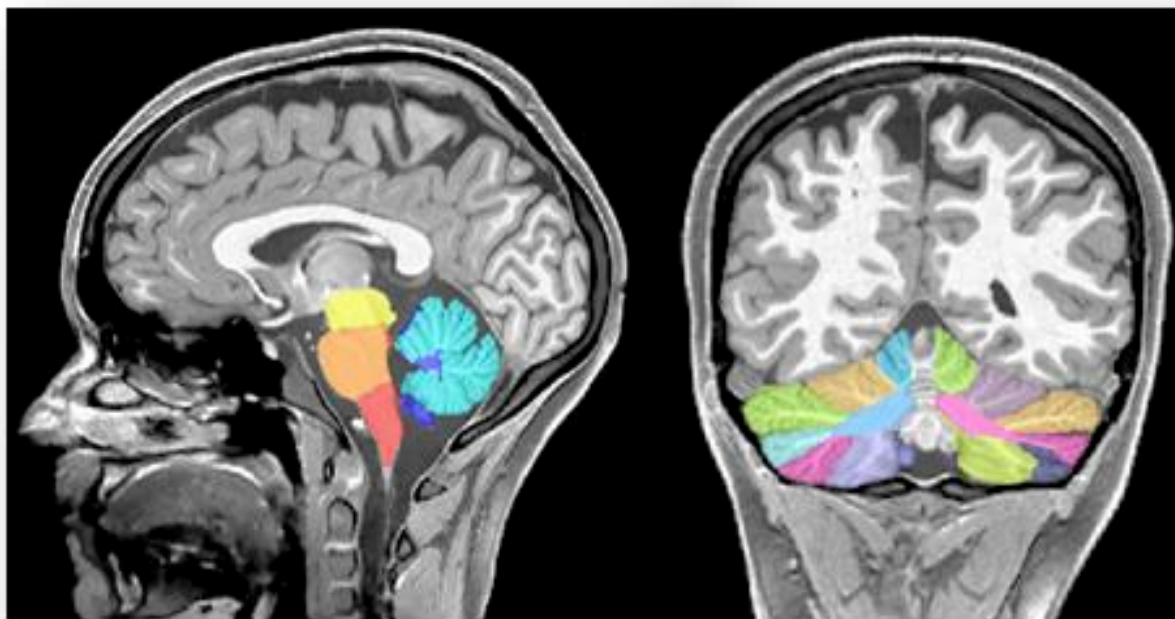
For brain MRI volumetry, we used new automated tools (CERES from the volBrain online platform) and we obtained an accurate segmentation of the brainstem and a lobule-based parcellation of the cerebellum (Figure 4). At baseline, we found significant differences for right and left cerebellum volumes between SCA2 carriers and both controls ( $p=0.001$ ) and SCA7 carriers ( $p=0.01$ ). Bilateral cerebellum grey matter was significantly reduced in SCA2 compared with control and SCA7 groups ( $p < 0.01$ ). The left cerebellum white matter was significantly reduced in both SCA2 and SCA7 carriers compared with controls ( $p=0.001$  and  $p=0.02$ , respectively), and between SCA subtype was significantly decreased in SCA2 ( $p=0.02$ , Table 11). For the right cerebellum hemisphere, white matter volume differences were not significant after Holm adjustment. Differences between SCA carriers and control individuals for midbrain, pons, medulla oblongata, and superior cerebellar peduncle volumes were not significant after Holm adjustment (Table 11).

For cerebellar lobules, after Holm adjustment, only the left VIIB lobule volume was significant smaller in SCA2 carriers compared with controls ( $p < 0.01$ ) and SCA7 carriers ( $p=0.03$ , Table 11).



For the subcortical regions of interest (accumbens, amygdala, hippocampus, basal forebrain, caudate, pallidum, and thalamus) as well as for the cortical thickness we did not find any difference between SCA carriers and controls (Table 12).

For SCA2 and SCA7 pooled together, progression of volume loss over one year was detected only for pons ( $p=0.004$ ), and already at month-6 ( $p<0.001$ ). When taking the two groups separately, this observation only remained significant for SCA2, at month-6 ( $p<0.01$ ) and month-12 ( $p=0.01$ ). For the other regions, only the putamen volume and the thickness of the right insula and left medial orbitofrontal cortex showed a trend to progress over one year, not reaching the Holm  $p$ -value threshold. MRS and DTI analyses are ongoing.



**Figure 4. Segmentation of brainstem (on the left) and cerebellum (on the right) using CERES software from the volBrain online platform.**

**Table 11. Comparison of baseline cerebellum and brainstem volumes between SCA carriers and controls.**

Variable	SCA2 (n=15)	SCA7 (n=15)	Control (n=10)	p-value*	p-value* SCA2- SCA7	p-value* SCA2- Control	p-value* SCA7- Control	Holm p- value
<b>Right cerebellum</b>	50618 (43927.9, 53153.4)	58130.9 (53452.9, 64982)	62966.85 (56498.8, 70177)	<b>0.001</b>	<b>0.01</b>	<b>0.001</b>	0.23	0.001
<b>-Grey matter</b>	37424.2 (33167.7, 38210.5)	42119.6 (40143.1, 45815)	45030.45 (42189, 47752.4)	<b>&lt;0.001</b>	<b>0.002</b>	<b>0.002</b>	0.39	0.001
<b>-White matter</b>	5116.79 (4605.5, 6179.1)	6242.65 (5280.3, 7394)	7646.96 (7028.5, 8694.5)	<b>0.002</b>	<b>0.04</b>	<b>0.002</b>	<b>0.04</b>	0.001
<b>Left cerebellum</b>	49890.5 (45066.1, 53373.5)	57837.1 (53176.7, 64163)	62735.1 (57039, 70049.4)	<b>0.001</b>	<b>0.01</b>	<b>&lt;0.001</b>	0.14	0.001
<b>-Grey matter</b>	37169.7 (33749.6, 39291.1)	43350.4 (40374.7, 45775)	45555.55 (4223., 49106.9)	<b>0.001</b>	<b>&lt;0.01</b>	<b>&lt;0.01</b>	0.28	0.001
<b>-White matter</b>	4938.11 (4587.6, 6209.8)	6184.28 (5234.5, 7343)	7565.8 (7086.6, 8539.6)	<b>0.001</b>	<b>0.02</b>	<b>0.001</b>	<b>0.02</b>	0.001
<b>Vermis</b>	6875.98 (6462.5, 7788.5)	7435.07 (7021.8, 8454)	8415.19 (7760.9, 8857.6)	0.05	-	-	-	0.007
<b>-Grey matter</b>	5360.5 (5029.2, 6084.3)	5895.01 (5594.7, 6430)	6284.12 (5964.9, 6563.3)	0.11	-	-	-	0.0125
<b>-White matter</b>	1648.6 (1469.1, 1813.7)	1673.68 (1404.1, 2000)	2049.74 (1739.8, 2379.7)	0.08	-	-	-	0.006
<b>Midbrain</b>	5626.21 (5266.5, 6235.4)	5561.71 (5111.1, 6041)	6509.39 (5995.7, 7108.4)	<b>0.03</b>	0.53	<b>0.06</b>	<b>0.04</b>	0.004
<b>Pons</b>	9671.93 (9220.1, 13401.6)	12921.01 (10780.3, 13778)	15992.15 (14566, 18496.8)	<b>0.002</b>	0.24	<b>0.002</b>	<b>0.01</b>	0.001
<b>Medulla oblongata</b>	4348.81 (4052.6, 4810.1)	4528.01 (4286.1, 4834)	5426.03 (5057.8, 5979.7)	<b>0.004</b>	0.51	<b>0.005</b>	<b>0.008</b>	0.001
<b>SCP</b>	225.27 (196.1, 257.5)	200.19 (190.4, 208)	280.82 (243.9, 308.3)	<b>0.003</b>	0.09	<b>0.03</b>	<b>0.004</b>	0.001
<b>Right cerebellum hemisphere</b>								
<b>Lobule III</b>	258.04 (237.56, 414.97)	389.62 (328.18, 410)	370.42 (330.1, 403.3)	0.39	-	-	-	0.05
<b>Lobule IV</b>	1350.62 (1155.04, 1482.45)	1376.73 (1268.7, 1565)	1558.22 (1358.1, 1668.1)	0.21	-	-	-	0.025
<b>Lobule V</b>	2844.08 (2705.34, 3333.28)	3325.35 (2849.2, 3840)	3368.87 (2947.8, 3437.3)	0.1	-	-	-	0.007
<b>Lobule VI</b>	7049.54 (6168.61, 7440.44)	8240.78 (7105.6, 9046)	8460.58 (7822.4, 9236.3)	<b>0.01</b>	<b>0.04</b>	<b>0.01</b>	0.72	0.002
<b>Lobule Crus I</b>	10741.5 (9859.06, 11995.3)	12314.8 (11297.2, 14452)	13554.55 (11541, 15407.2)	<b>0.01</b>	<b>0.03</b>	<b>0.03</b>	0.68	0.003
<b>Lobule Crus II</b>	6688.08 (6254.68, 8666.65)	8571.67 (7768.37, 9580)	8660.25 (7869.5, 9450.2)	<b>0.01</b>	<b>0.01</b>	<b>0.03</b>	0.93	0.002
<b>Lobule VIIIB</b>	4208.02 (3283.11, 4377.44)	4233.1 (4054.42, 4596)	4998.73 (4694.7, 5332.8)	<b>0.03</b>	0.2	<b>0.03</b>	0.18	0.004
<b>Lobule VIIIA</b>	4896.64 (4429.96, 5692.26)	5479.28 (5243.51, 6377)	5992.49 (5120.5, 7135.1)	0.10	-	-	-	0.01
<b>Lobule VIIIB</b>	3052.92 (2847.93, 3387.04)	3696.54 (2996.63, 3970)	3809 (3512, 4228)	<b>0.007</b>	0.12	<b>0.003</b>	0.19	0.002
<b>Lobule IX</b>	2675.64 (2208.71, 3080.62)	3237.8 (2805, 3418)	3519 (3137, 3855)	<b>0.01</b>	0.09	<b>0.02</b>	0.17	0.003
<b>Lobule X</b>	538.61 (499.95, 605.42)	645.1 (566.26, 732)	720.36 (670.5, 771.3)	<b>0.005</b>	0.06	<b>0.004</b>	<b>0.21</b>	0.002

Left cerebellum hemisphere								
<b>Lobule III</b>	250.36 (217.5, 354.2)	337.91 (264.95, 406)	406.26 (363.51, 497.27)	0.01	0.12	0.04	0.12	0.003
<b>Lobule IV</b>	1533.4 (1265.1, 1606)	1572.31 (1326.56, 1861)	1717.46 (1663.8, 1792.8)	0.1	-	-	-	0.008
<b>Lobule V</b>	3192.23 (2522, 3522.9)	3596.19 (3102.39, 4400)	3794.84 (3483, 4147)	0.01	0.1	0.01	0.73	0.003
<b>Lobule VI</b>	6959.94 (6316.3, 7405.3)	8042.79 (7148.86, 8597)	8253.22 (7615, 9823.9)	0.009	0.03	0.01	0.60	0.002
<b>Lobule Crus I</b>	10742.5 (9816.7, 11576)	12133.6 (10860.8, 13947)	13056.95 (11356.5, 15188)	0.03	0.06	0.06	0.68	0.005
<b>Lobule Crus II</b>	6429.52 (5800.2, 7644.1)	8233.76 (7361.8, 8805)	8794.04 (7725.3, 9290.3)	0.01	0.04	0.01	0.39	0.002
<b>Lobule VIIB</b>	3918.74 (3167.6, 4257.16)	4395.4 (4073.8, 4753)	4995.66 (4531.4, 5456)	0.001	0.03	0.002	0.05	0.001
<b>Lobule VIIIA</b>	5521.26 (4238.9, 6124.9)	5621.61 (5428.5, 6319)	6455.12 (5714.9, 6778.3)	0.1	-	-	-	0.01
<b>Lobule VIIIB</b>	3266.47 (3157.9, 3703.2)	3760.54 (3585.7, 4112)	3935.38 (3649.4, 4124)	0.009	0.02	0.01	0.64	0.002
<b>Lobule IX</b>	2695.1 (2164.6, 3046.5)	3116.46 (2629.5, 3490)	3549.35 (3046.8, 3949.7)	0.01	0.11	0.01	0.11	0.002
<b>Lobule X</b>	534.51 (498.4, 578.2)	581.62 (537.8, 722)	702.7 (623.4, 760.9)	0.004	0.12	0.001	0.11	0.002

In this table, we reported volume in mm<sup>3</sup> as median scores (Q1, Q3) of cerebellum and brainstem regions. In red, significant p-value <0.05 after Holm adjustment; in blue, significant p-value <0.05 before Holm adjustment. \*p-value calculated by Kruskals-Wallis test; \*\* Hochberg adjusted p-value calculated by Wilcoxon test.

Abbreviations: SCP: superior cerebellar peduncle.

**Table 12. Comparison of baseline cortical thickness and subcortical volumes of regions of interest between SCA carriers and controls.**

Variable	SCA2 (n=15)	SCA7 (n=15)	Control (n=10)	p-value*	Holm p-value
<b>Subcortical Grey Matter</b>	2.99 (2.87, 3.15)	2.94 (2.86, 3)	3.03 (2.97, 3.05)	0.98	
<b>Accumbens</b>	0.05 (0.04, 0.05)	0.05 (0.05, 0)	0.05 (0.05, 0.05)	0.34	
<b>Amygdala</b>	0.15 (0.14, 0.15)	0.14 (0.13, 0)	0.14 (0.14, 0.15)	0.81	
<b>Basal Forebrain</b>	0.06 (0.05, 0.06)	0.06 (0.05, 0)	0.06 (0.05, 0.06)	0.70	
<b>Caudate</b>	0.48 (0.47, 0.52)	0.52 (0.49, 1)	0.52 (0.5, 0.54)	0.06	
<b>Hippocampus</b>	0.58 (0.56, 0.61)	0.57 (0.56, 1)	0.58 (0.52, 0.6)	0.64	
<b>Pallidum</b>	0.2 (0.2, 0.22)	0.2 (0.19, 0)	0.2 (0.2, 0.21)	0.74	
<b>Putamen</b>	0.6 (0.55, 0.63)	0.6 (0.56, 1)	0.59 (0.58, 0.63)	0.90	
<b>Thalamus</b>	0.86 (0.81, 0.97)	0.84 (0.78, 1)	0.87 (0.8, 0.9)	0.32	
<b>Cortical thickness (left hemisphere)</b>					
<b>Left caudal anterior cingulate</b>	2.42 (2.31, 2.52)	2.47 (2.39, 3)	2.52 (2.38, 2.63)	0.47	
<b>Left caudal middle frontal</b>	2.62 (2.57, 2.65)	2.62 (2.54, 3)	2.73 (2.67, 2.75)	0.08	
<b>Left fusiform</b>	2.71 (2.64, 2.79)	2.67 (2.59, 3)	2.66 (2.6, 2.7)	0.42	
<b>Left inferior temporal</b>	2.73 (2.65, 2.78)	2.73 (2.69, 3)	2.77 (2.67, 2.81)	0.60	
<b>Left lateral orbitofrontal</b>	2.65 (2.58, 2.76)	2.62 (2.55, 3)	2.67 (2.61, 2.72)	0.27	
<b>Left medial orbitofrontal</b>	2.45 (2.33, 2.51)	2.45 (2.38, 2)	2.42 (2.34, 2.46)	0.82	
<b>Left middle temporal</b>	2.73 (2.7, 2.83)	2.78 (2.75, 3)	2.83 (2.72, 2.89)	0.65	
<b>Left paracentral</b>	2.47 (2.41, 2.53)	2.49 (2.41, 3)	2.45 (2.43, 2.52)	0.97	
<b>Left precentral</b>	2.7 (2.6, 2.73)	2.73 (2.61, 3)	2.7 (2.62, 2.8)	0.90	
<b>Left rostral anterior cingulate</b>	2.59 (2.53, 2.75)	2.7 (2.57, 3)	2.69 (2.65, 2.8)	0.33	
<b>Left rostral middle frontal</b>	2.41 (2.34, 2.47)	2.4 (2.34, 2)	2.44 (2.41, 2.5)	0.39	
<b>Left superior temporal</b>	2.75 (2.71, 2.9)	2.74 (2.68, 3)	2.83 (2.76, 2.84)	0.43	
<b>Left insula</b>	2.97 (2.9, 3.03)	2.94 (2.87, 3)	2.96 (2.92, 3.02)	0.34	
<b>Cortical thickness (right hemisphere)</b>					
<b>Right caudal anterior cingulate</b>	2.25 (2.22, 2.35)	2.34 (2.32, 2)	2.26 (2.14, 2.33)	0.02	0.001
<b>Right caudal middle frontal</b>	2.55 (2.5, 2.62)	2.54 (2.5, 3)	2.64 (2.54, 2.69)	0.28	
<b>Right fusiform</b>	2.72 (2.62, 2.82)	2.68 (2.64, 3)	2.72 (2.67, 2.76)	0.91	
<b>Right inferior temporal</b>	2.79 (2.71, 2.83)	2.79 (2.69, 3)	2.78 (2.69, 2.81)	0.56	
<b>Right lateral orbitofrontal</b>	2.66 (2.61, 2.7)	2.64 (2.61, 3)	2.67 (2.66, 2.72)	0.32	
<b>Right medial orbitofrontal</b>	2.43 (2.35, 2.52)	2.42 (2.39, 2)	2.48 (2.44, 2.51)	0.56	
<b>Right middle temporal</b>	2.84 (2.76, 2.88)	2.83 (2.76, 3)	2.87 (2.82, 2.92)	0.53	
<b>Right paracentral</b>	2.5 (2.42, 2.54)	2.49 (2.47, 3)	2.53 (2.46, 2.61)	0.36	
<b>Right precentral</b>	2.62 (2.45, 2.64)	2.67 (2.51, 3)	2.64 (2.58, 2.73)	0.21	

<b>Right rostral anterior cingulate</b>	2.62 (2.55, 2.65)	2.66 (2.59, 3)	2.59 (2.57, 2.71)	0.49	
<b>Right rostral middle frontal</b>	2.34 (2.3, 2.42)	2.33 (2.3, 2)	2.35 (2.3, 2.44)	0.79	
<b>Right superior temporal</b>	2.81 (2.76, 2.89)	2.8 (2.75, 3)	2.88 (2.78, 3.02)	0.32	
<b>Right insula</b>	2.95 (2.88, 3.02)	2.9 (2.88, 3)	3.05 (2.98, 3.16)	0.06	

In this table, we reported volume in mm<sup>3</sup> as median scores (Q1, Q3) and cortical thickness in mm.

\*p-value calculated by Kruskals-Wallis test

- **Fluid biomarkers**

At baseline, we found significant difference between SCA carriers and controls only for NfL plasma levels. The median NfL levels were 14.2 (11.52, 15.89) pg/ml, 15.53 (13.27, 23.23) pg/ml, and 4.88 (3.56, 6.17) pg/ml for SCA2, SCA7, and controls, respectively (Table 13). These concentrations were higher in SCA carriers compared with controls ( $p < 0.001$  for both groups). NfL levels remained stable after 12 months of follow-up (V3) for SCA2 and SCA7 groups ( $15.01 \pm 5.14$  pg/ml,  $p = 0.23$  and  $17.81 \pm 11.16$  pg/ml,  $p = 0.14$ , respectively). For controls, NfL significantly increased over one year ( $5.16 \pm 2.38$  pg/ml at baseline vs  $7.93 \pm 3.68$  pg/ml at V3,  $p < 0.001$ ). Among the other biomarkers, the progression was only significant detected only for  $\alpha$ -synuclein between baseline and month-6 (V2) for SCA carriers pooled together ( $p < 0.001$ ) and for SCA7 taken separately ( $p < 0.01$ ). All other biomarkers were stable over one year.

For CSF, we did not measure NfL since plasma levels highly correlate with CSF.<sup>45</sup> For the other biomarkers, there was no difference among the groups at baseline (Table 13). Moreover, anyone increased in SCA carriers and control individuals at V3.

**Table 13. Comparison of baseline fluid biomarkers among the three groups.**

Variable	SCA2 (n=15)	SCA7 (n=15)	Control (n=10)	p-value*	p-value SCA2- SCA7**	p-value SCA2- Control**	p-value SCA7- Control**	Holm p-value
<b>Plasma</b>								
<b>NfL pg/ml</b>	14.2 (11.5, 15.8)	15.53 (13.2, 3.2)	4.88 (3.5, 6.1)	<0.001	0.17	<0.001	<0.001	0.008
<b>Aβ40 pg/ml</b>	226.6 (197.7, 252.9)	249.9 (209.39, 264)	262.9 (230.2, 269)	0.29				
<b>Aβ42 pg/ml</b>	10.65 (9.2, 11.6)	10.24 (9.2, 12)	12.65 (11.52, 13.6)	0.13				
<b>Tau pg/ml</b>	5.9 (5.1, 7.2)	6.84 (5.73, 8)	6.48 (5.54, 7.6)	0.61				
<b>pTau181 pg/ml</b>	1.74 (1.5, 1.9)	1.39 (1.24, 3)	1.53 (1.36, 1.9)	0.52				
<b>αSyn pg/ml</b>	22700.5 (18059, 54444)	28937 (16249, 53844)	35142.5 (23809, 68628)	0.43				
<b>CSF</b>	n=15	n=14	n=8					
<b>Aβ40 pg/ml</b>	7764.7 (3478.1, 9672.7)	8195.7 (6514, 9756)	11229.6 (7547, 11567)	0.07				
<b>Aβ42 pg/ml</b>	533.8 (263.5, 806.6)	641.27 (545.8, 703)	898.9 (572, 989.1)	0.16				
<b>Tau pg/ml</b>	127.9 (65, 162.4)	136.5 (119.1, 191)	115.6 (74.3, 125.4)	0.12				
<b>pTau181 pg/ml</b>	26.67 (19.3, 34.1)	30.84 (26.65, 38)	27.3 (23.4, 29.6)	0.27				
<b>αSyn pg/ml</b>	866.7 (289.9, 1719)	1180.1 (750.8 1769)	1141.9 (471, 1598)	0.37				

Data are expressed as median (Q1, Q3). In red, significant p-value <0.05 after Holm adjustment; \*p-value calculated by Kruskals-Wallis test; \*\* Hochberg adjusted p-value calculated by Wilcoxon test. Abbreviations: Aβ40: amyloid beta 40; Aβ42: amyloid beta 42.

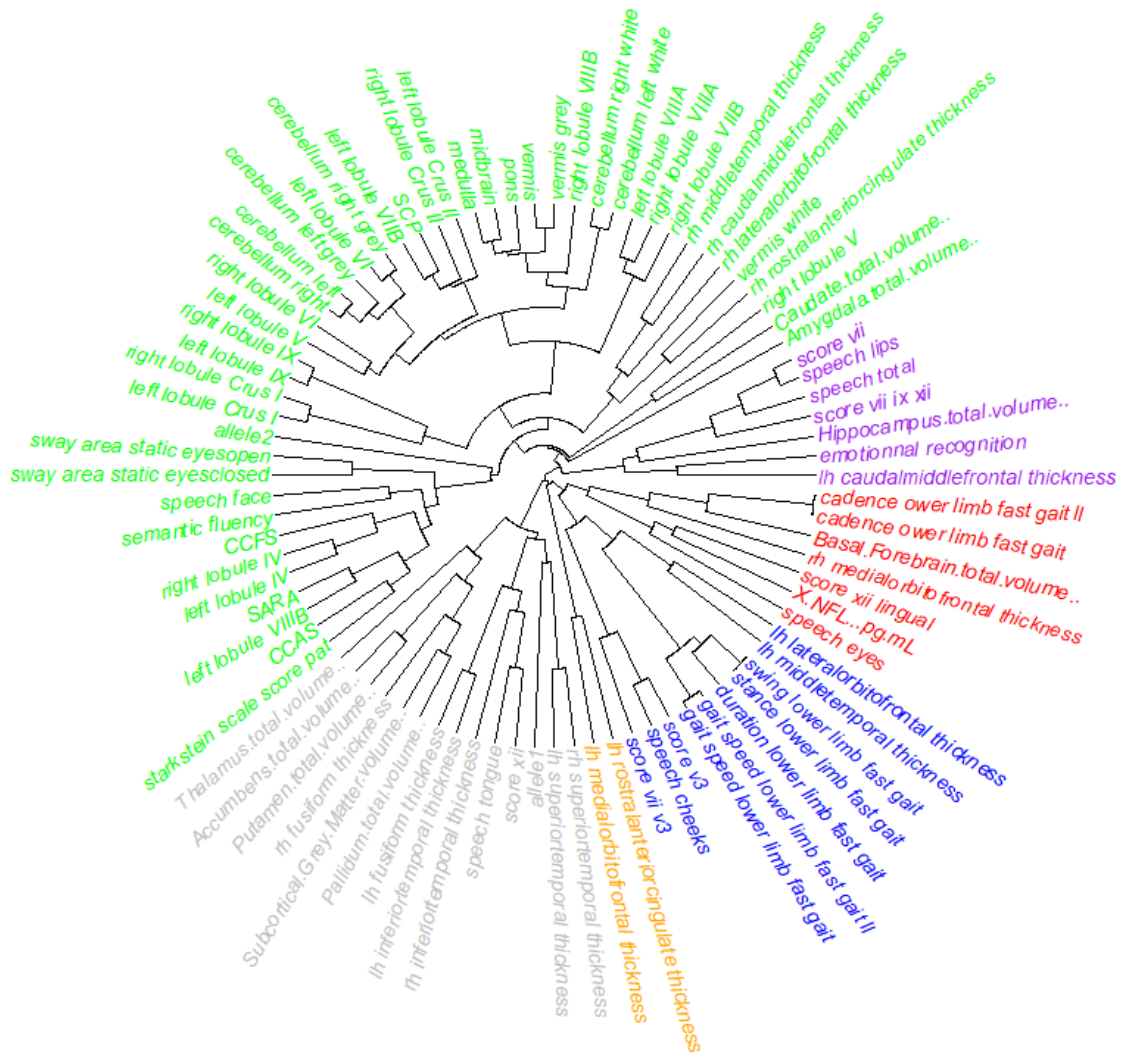
## Correlations among all parameters

Taking into account the huge number of variables belonging to the different assessments, we calculate a correlation matrix of parameters of interest in an exploratory manner without correction. The clustering of variables for SCA2 and SCA7 are shown in Figure 5 and Figure 6, respectively. The most relevant correlations for baseline SARA score, CCAS total score, MBLF total score, and plasma NfL concentrations with the other parameters of the study are reported in Table 14. For SCA2, SARA score showed to correlate with the other clinical scores (CCFS and CCAS) and brainstem volumes. For SCA7, SARA score correlated with the other clinical scores (CCFS, CCAS, MBLF), pathological CAG repeat size, ophthalmological findings, subcortical volumes, and brainstem volumes. Plasma NFL levels correlated with subcortical volumes of putamen, pallidum, thalamus, superior cerebellar peduncle, and pons.

**Table 14. Correlations between baseline clinical scores and plasma NfL concentrations with the other parameters of CERMOI multimodal assessment.**

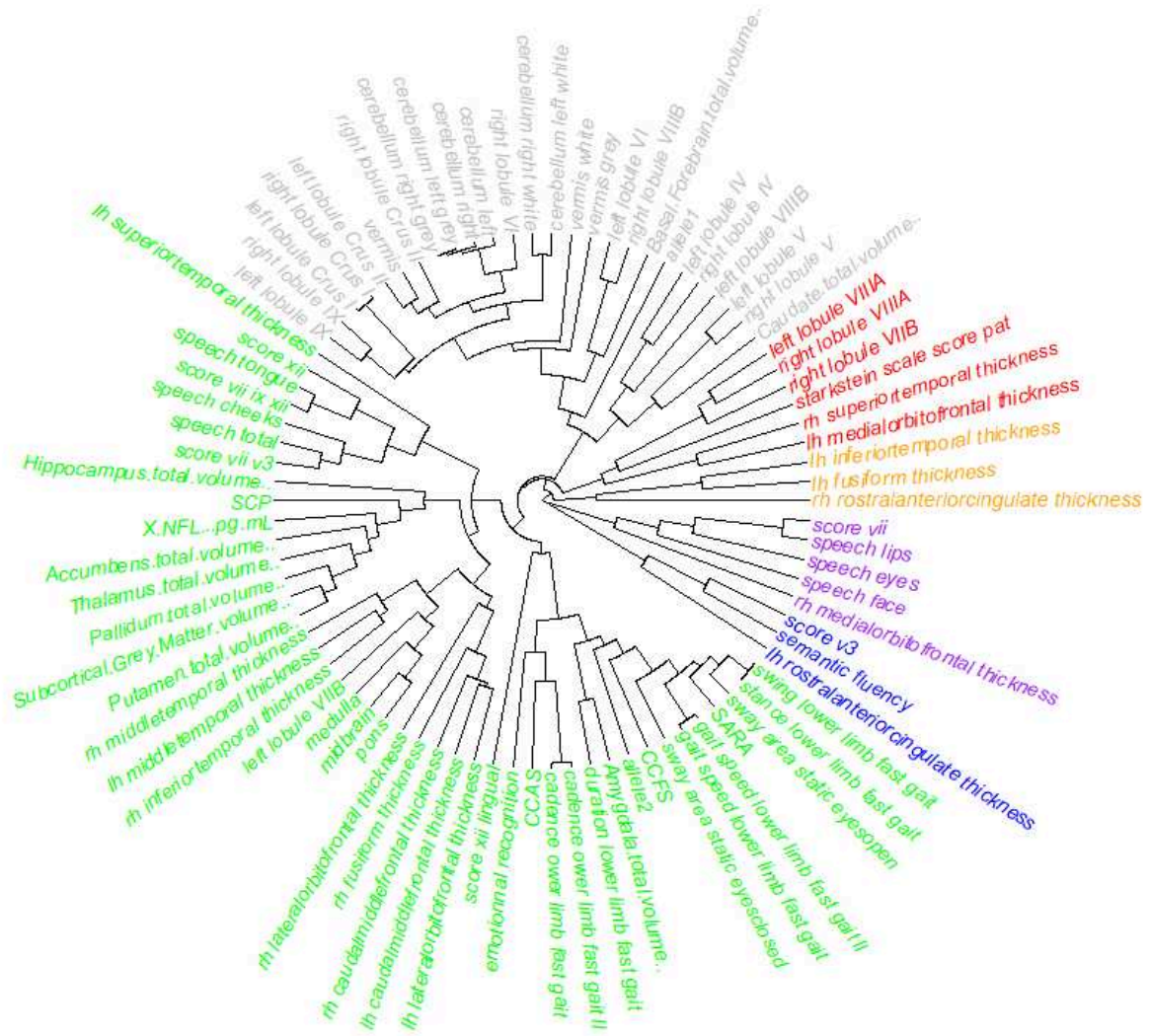
	SCA2		SCA7	
<b>SARA score</b>	CCFS	$\rho:0.68$ $p<0.01$	CCFS	$\rho:0.78$ $p<0.001$
	CCAS	$\rho:-0.75$ $p=0.001$	CCAS	$\rho:-0.74$ $p<0.01$
	Sway area open eyes	$\rho:-0.55$ $p=0.03$	Pathological CAG repeat	$\rho:0.69$ $p=0.001$
	Pallidum volume	$\rho:-0.55$ $p=0.03$	MBLF	$\rho:-0.57$ $p=0.02$
	Left lobule VIIIB	$\rho:-0.83$ $p<0.001$	BCVA	$\rho:0.89$ $p<0.001$
	SCP volume	$\rho:-0.9$ $p<0.001$	ONL	$\rho:-0.86$ $p<0.001$
	Pons volume	$\rho:-0.55$ $p=0.04$	NfL	$\rho:0.77$ $p<0.001$
	Medulla oblongata	$\rho:-0.6$ $p=0.02$	Sway area open eyes	$\rho:0.9$ $p<0.001$
<b>CCAS score</b>	CCFS	$\rho:-0.67$ $p<0.01$	Putamen volume	$\rho:0.76$ $p=0.001$
	Left lobule VIIIB	$\rho:0.62$ $p=0.01$	Pallidum volume	$\rho:0.73$ $p<0.001$
	Right lobule VIIIB	$\rho:0.53$ $p=0.04$	Thalamus volume	$\rho:-0.69$ $p<0.001$
			SCP volume	$\rho:-0.73$ $p=0.001$
			Pons volume	$\rho:-0.57$ $p=0.02$
<b>MBLF score</b>	Left lobule IX	$\rho:0.57$ $p=0.03$	Pathological CAG repeat	$\rho:-0.63$ $p=0.01$
	Right lobule IX	$\rho:0.61$ $p=0.01$		
<b>Plasma NfL</b>	XII nerve score	$\rho:-0.6$ $p=0.02$	Pons volume	$\rho:0.54$ $p=0.03$
			Thalamus volume	$\rho:0.55$ $p=0.03$
			Outer nuclear layer	$\rho:-0.82$ $p<0.001$
			Sway area open eyes	$\rho:0.6$ $p=0.01$
			Subcortical grey matter volume	$\rho:-0.72$ $p<0.01$
			Accumbens volume	$\rho:-0.71$ $p<0.01$
			Amygdala volume	$\rho:-0.56$ $p=0.02$
			Putamen volume	$\rho:-0.72$ $p<0.01$
		Pallidum volume	$\rho:-0.67$ $p<0.01$	
		Thalamus volume	$\rho:-0.63$ $p=0.01$	

Analysis done by Spearman correlation model. Abbreviations: BCVA: best-corrected visual acuity; CCAS: Cerebellar cognitive affective syndrome; CCFS: Composite Cerebellar Functional Score; MBLF: Oral-Lingual-Facial Motility; NfL: Neurofilament light chain; ONL: outer nuclear layer; SARA: Scale for the Assessment and Rating of Ataxia; SCP: superior cerebellar peduncle. The correlations were determined using Spearman correlation model (uncorrected for multiple comparisons).



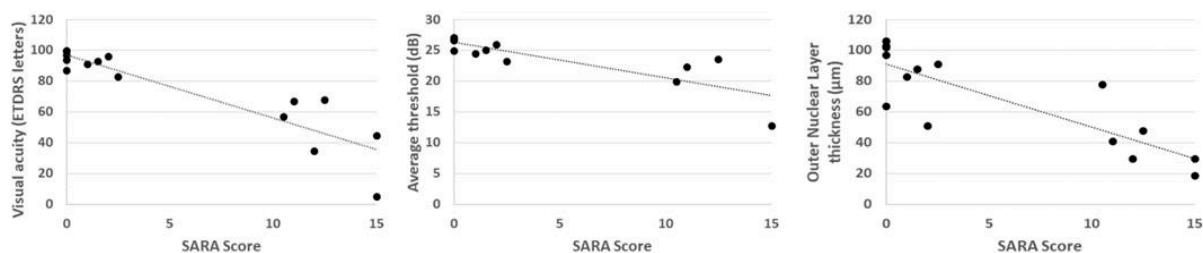
**Figure 5. Clustering of baseline variables of interest for SCA2 carriers.**





**Figure 6. Clustering of baseline variables of interest for SCA7 carriers.**

Concerning ophthalmological results for SCA7 carriers, SARA score showed a significant correlation with BCVA ( $\rho: 0.89$   $p < 0.001$ ) and the average retinal sensitivity from microperimetry test ( $\rho: -0.87$   $p < 0.001$ , Figure 7). Among all imaging parameters, central ONL thickness significantly correlated with both SARA score and NFL levels ( $\rho: -0.86$   $p < 0.001$  and  $\rho: -0.82$   $p < 0.001$ , respectively). No significant correlations were found between ophthalmic parameters and the pathological CAG repeat.

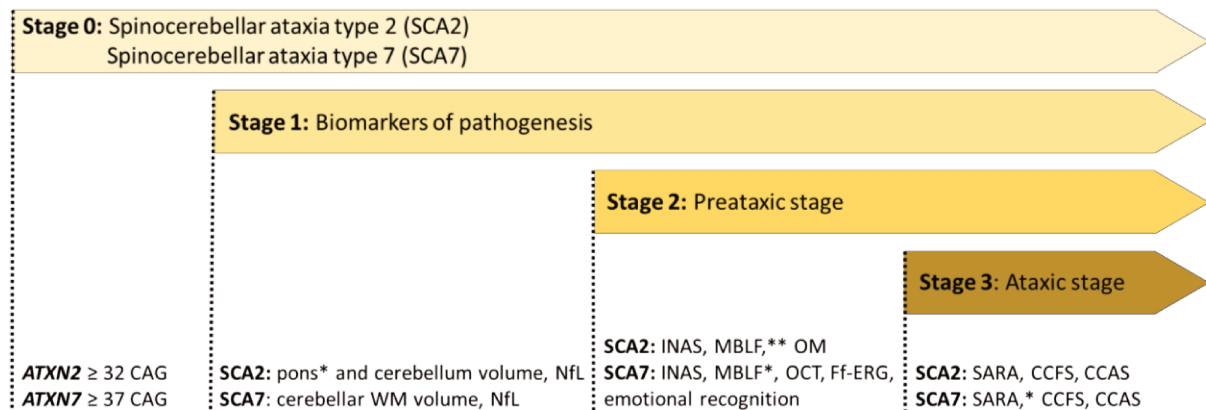


**Figure 7. Correlations between baseline SARA score and ophthalmological exams for SCA7 carriers.**

Scatterplots showing the significant correlations between the scale for the assessment and rating of ataxia (SARA) and best corrected visual acuity (BCVA; left), retinal sensitivity on microperimetry (middle), and outer nuclear layer (ONL) thickness on optical coherence tomography (right).

## Discussion

In the present study, we conducted a multimodal assessment in SCA2 and SCA7 carriers at preataxic and early ataxic stages of the disease ( $SARA \leq 15$  out of 40), over one year. We identified significant changes, already at six months of follow-up, which could be useful endpoints in future clinical trials (Figure 8).



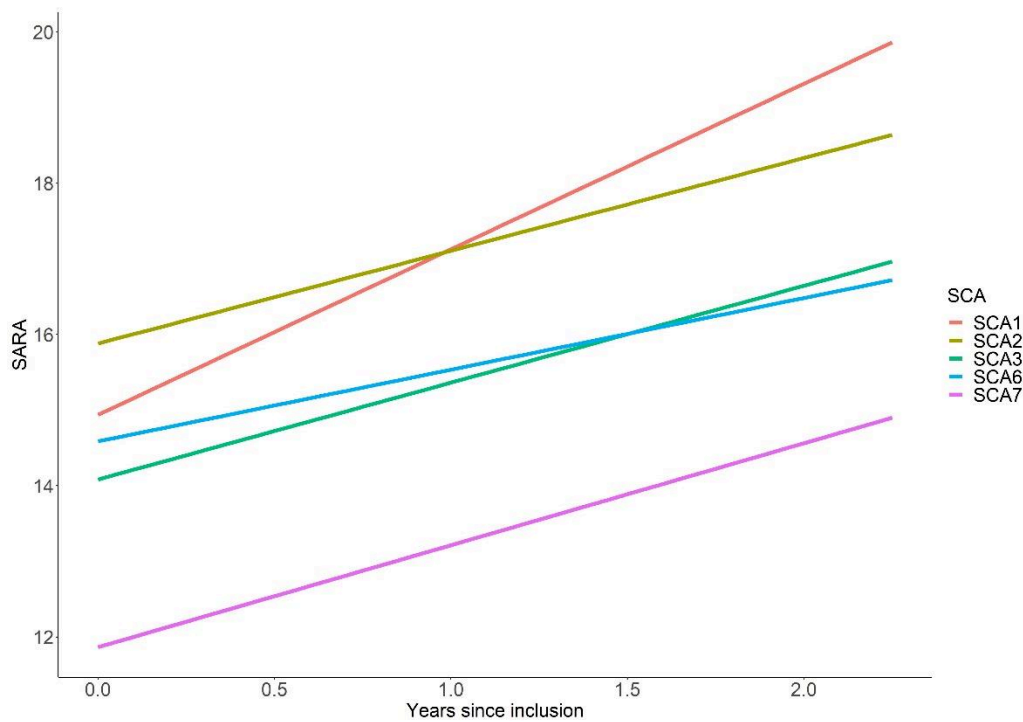
**Figure 8. Staging of Spinocerebellar ataxia type 2 (SCA2) and type 7 (SCA7).**

Based on CERMOI study results, this is a staging proposal for SCA2 and SCA7 disease courses (imaging, oculomotor, and ophthalmological analyses are ongoing) adapted from Tabrizi et al., *Lancet Neurol* 2022.<sup>86</sup>

Abbreviations: CCAS: Cerebellar cognitive affective syndrome; CCFS: Composite Cerebellar Functional Score; Ff-ERG: full-field electroretinography; INAS: Inventory of Non-Ataxia Signs; MBLF: Oral-Lingual-Facial Motility; NfL: Neurofilament light chain; OCT: optical coherence tomography OM: oculomotor recording; SARA: Scale for the Assessment and Rating of Ataxia; WM: white matter. \*Progression detected at month-6 and month-12 follow-up (visit 2 and visit 3). \*\*Progression detected at month-12 follow-up (visit 3).

Among clinical scores assessed by neurological examination, baseline SARA, CCFS, and INAS showed significant differences in SCA carriers compared with controls. SARA score is known to show intraindividual variability<sup>87</sup> and this could explain the fact that two SCA2 carriers around the threshold of SARA score of 3 showed a 1.5-point decrease. SARA score was the most reliable score to track disease progression in SCA carriers pooled together, since it was the only one to significantly increase over one year, and already at month 6. When analyzing SARA progression in SCA subgroups, this trend was confirmed only for SCA7. The SCA7 subgroup included more preataxic (n=9) than ataxic (n=6) carriers and two out of nine preataxic carriers converted to the symptomatic stage of the disease after one year, which did not happen in the five preataxic SCA2 carriers. This might suggest a faster disease progression

for SCA7 than SCA2, translated in the significant increase in SARA score over one year. SCA7 natural history is not well elucidated, except for infantile and juvenile forms,<sup>88</sup> since large SCA consortia such as EUROSCA did not include this specific genotype.<sup>32</sup> In our SPATAX cohort, even if the SCA7 sample size is limited compared with the other groups, the annual SARA score progression between these two groups is similar ( $1.24 \pm 0.26$  for SCA7 cohort  $n=58$  and  $1.22 \pm 0.11$  for SCA2  $n=297$ ) (Figure 9).



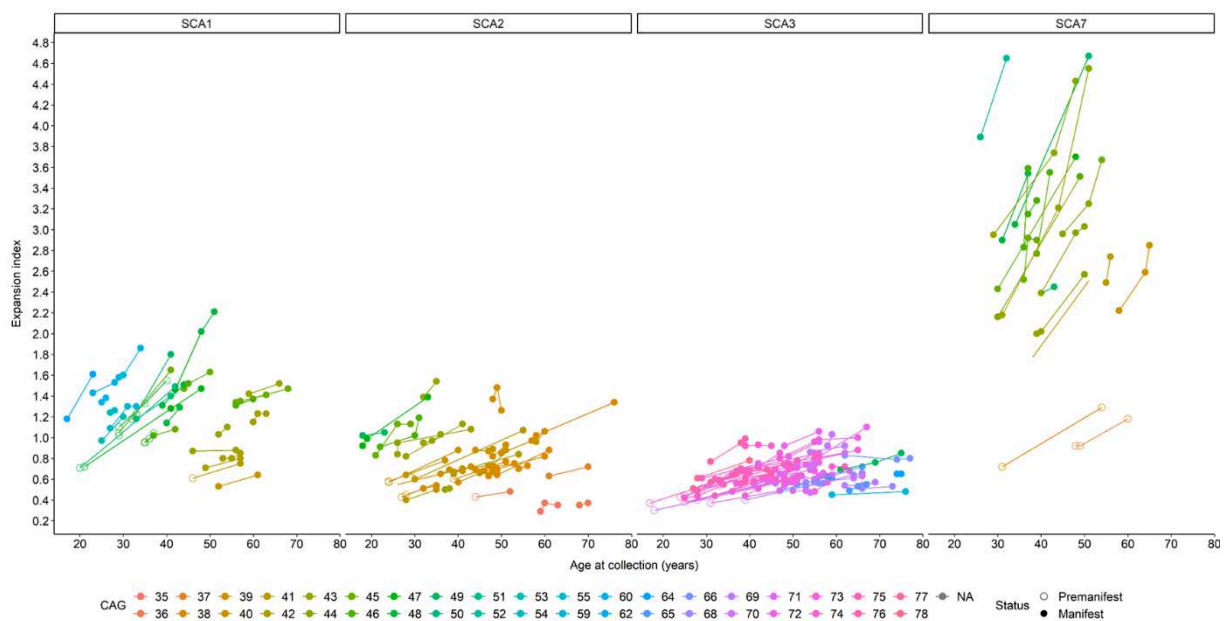
**Figure 9. SARA score progression of polyglutamine SCAs from SPATAX cohort.**

The fastest annual progression is found for SCA1 group ( $n=221$ ) of  $2.19 \pm 0.16$  points/year, followed by SCA3 ( $n=400$ )  $1.28 \pm 0.11$ , SCA7 ( $n=58$ )  $1.24 \pm 0.26$ , SCA2 ( $n=297$ )  $1.22 \pm 0.11$ , and SCA6 ( $n=192$ )  $0.94 \pm 0.26$ . These results are in line with previous data reported by Jacobi et al., 2015<sup>32</sup> for SCA1, SCA2, SCA3, and SCA6.

Nonetheless, the somatic instability of the pathological CAG repeat expansion during life among polyglutamine SCAs is the greatest for SCA7 carriers, (Figure 10, Kacher et al., in preparation). Moreover, SCA7 shows the strongest correlation between increased expansion index and the CAG repeat length ( $\rho: 0.82$ ,  $p < 0.0001$ , Kacher et al., in preparation). Gene modifiers and somatic instability play a role to modulate the disease onset and progression. DNA repair genes modify the age at onset in HD and polyglutamine SCAs.<sup>89,90</sup> For HD, these results have been replicated in different genome-wide association studies.<sup>91,92</sup> To conduct GWAS for the rare polyglutamine ataxias, collaborative, international efforts are required.

Moreover, dysregulation of DNA repair genes also increases the somatic instability that influences disease progression.<sup>93</sup>

The difference with the control participants in INAS score was more marked for SCA7 carriers. Significant differences were detected for upper motor neuron signs, specifically for hyperreflexia in the SCA7 group. Urinary dysfunction was more frequent in SCA7, possibly because of pyramidal syndrome and detrusor overactivity.<sup>94</sup> The majority of SCA7 carriers were at a preataxic stage (SARA < 3 out of 40) but still presented pyramidal signs at examination, which can hence precede the cerebellar ataxia. Dysmetric saccades were another sign significantly observed in SCA carriers rather than controls, testifying of cerebellar involvement. The presence of pyramidal and oculomotor signs in individuals with SARA scores below 3, and the spontaneous report of walking difficulties age at onset by three preataxic SCA7 carriers, may question the definition of presymptomatic carriers. The definition of presymptomatic carrier is challenging and requires more attention especially considering that preataxic individuals are currently excluded from clinical trials.



**Figure 10. Somatic instability of the CAG repeat increases during the life of SCA1, SCA2, SCA3, and SCA7 patients.**

Changes in expansion index (EI) for SCA1, SCA2, SCA3, and SCA7 patients, across two or three visits (when available) over multiple years. Different colors indicate different reference (CAG)*n* at diagnosis. For each value, the disease status is indicated with an empty circle (preataxic) or filled circle (ataxic). The measurement of the inherited allele is not always stable across visits, especially for SCA7 patients, which was taken into account for the EI. For the four groups, the EI increases with age, with the most striking increase for SCA7 carriers, and the slowest increase for SCA3 carriers.

At baseline, quality of life assessment showed impairment in the activities of daily living assessed by FA-ADL in both SCA2 and SCA7 individuals, when compared with controls. The other questionnaires exploring health status, depression, and fatigue (EQ-5D, PHQ-9, and FSS, respectively) reported similar scores among the three groups. This might be explained by the very early stage of the disease of enrolled individuals. However, these questionnaires might also not be appropriate for SCA individuals, since they focus on general well-being. For future studies, it will be more suitable to assess the recently validated Patient-Reported Outcome Measure of Ataxia (PROM-Ataxia).<sup>95</sup> The PROM-Ataxia was developed in adult ataxia patients based on their experience of symptoms and the activities those affected. This scale consists of 70 questions organized within three domains (physical, activities of daily living, mental health), and correlates with other scales already used in ataxia, such as SARA, Brief Ataxia Rating Scale (BARS), and Friedreich Ataxia Rating Scale Functional Staging (FARS). PROM-Ataxia could serve as a pragmatic biomarker to quantify treatment efficacy better than other clinical scales since it is the patient who assesses himself and scores his improvement or worsening in daily activities. Indeed, patient-reported outcome measures are particularly important for FDA approval.

Gait and postural assessment using APDM wearable sensors showed a trend for reduced cadence and speed in SCA carriers associated to longer stance and a reduced swing phase compared with healthy controls. However, no significant difference in parameters' progression was detected after correction for multiple comparisons. Many studies have compared the parameters characterizing locomotion between cerebellar patients and healthy controls. High variability of spatiotemporal gait parameters, wide-base support, reduced cycle duration, and stride length have been shown to be characteristic of ataxic locomotion due to poor dynamic balance and stability.<sup>96-99</sup> Regarding the postural assessment, patients with cerebral ataxia have an increased sway area compared with controls.<sup>100</sup> Our findings are consistent with previous studies. The greater sway area found in our SCA patients reflects their postural instability while standing, especially with the closed eyes condition, which underlines the important role of the sensory system in postural stability.<sup>101</sup> In our study, only preataxic and very early ataxic carriers were able to successfully complete the most difficult tasks, such as tandem gait or eyes closed static positions, further decreasing our already small sample size. We can also speculate that this technology is more reliable in patients at a more advanced stage and it is not sensible to detect subtle abnormalities in preataxic individuals. In what is to date the largest study exploring the use of APDM in SCA carriers, and including 163 SCA patients (SCA1, 2, 3, and 6) and 42

preataxic SCA carriers, gait variability resulted being the discriminative feature of SCA carriers and correlated with disease severity.<sup>102</sup> Some measures such as toe-out angle, double support time, and elevation of feet allowed to discriminate preataxic from control participants, even though with less power than for ataxic SCA patients.<sup>102</sup> We could also suppose that compensatory mechanisms possibly play a role in minimizing gait abnormalities for prodromal carriers far from disease onset. A study on SCA1 preataxic carriers, exploring postural balance, also showed similar performance than controls from baseline to 4-year follow-up.<sup>103</sup> Moreover, day-to-day and within-day fluctuations exist in ataxia patients, resulting in differences in clinical scales' scores. Digital technologies such as SARA<sup>home</sup> can help to evidence these fluctuations and measure ataxia at home.<sup>87</sup>

Dysphagia and dysarthria are two cerebellar elements strongly affecting SCA patients' quality of life. Moreover, dysphagia is a predictor of poor SCA1 survival.<sup>104</sup> We assessed the oro-facial mobility using MBLF<sup>74</sup> and found a significant progression of oro-facial impairment in SCA groups over one year of follow-up. The MBLF score as well as the eyes, lips, cheeks, and tongue subscores worsened at 6-month and 12-month follow-up. This progression was markedly evident for tongue motility. This finding was furthermore supported by the deterioration of hypoglossal (XII) nerve score which progressed at 6-month and 12-month follow-up, both in SCA carriers pooled together or taken separately. The hypoglossal score variation over one year correlated with the SARA score variation. This nerve has an exclusively motor function for the four tongue muscles. It also innervates three of the four extrinsic muscles, the genioglossus, hyoglossus, and stylo-glossus muscles.<sup>105</sup> In SCA2 only, the stylo-glossus muscle damage was reflected in the "disapproval click" task. Conversely, the "rhythm of galloping horse" praxis impairment was exclusively found in SCA7. These two praxes involve cooperation of the VII, IX, and XII cranial nerves. We could assume that the VII and the XII nerves both deteriorate but that a different nervous compensation exists, at least in the early phase of the disease, between the two groups, helping to perform these movements. As expected by the progression of the MBLF score, the facial nerve score also worsened in both groups after 12 months, and correlated with SARA score variation. The impairment of hypoglossal and facial nerves is linked to brainstem degeneration. Severe brainstem dysfunction due to motor neuron degeneration, particularly in the hypoglossal nucleus, has been reported in SCA1 mice.<sup>106</sup> In advanced SCA1 patients, massive neuronal loss exists in the tegmentum of medulla oblongata, particularly for the inferior olive and the hypoglossal motor nucleus<sup>2</sup> (Coarelli et al. 2022, in revision, Annex 1). Electrophysiological and neuropathological data suggest that

neurodegeneration in the medulla tegmentum, and in particular in the motor hypoglossal nucleus, may threaten survival in SCA1 patients (Coarelli et al. 2022, in revision, Annex 1). We could hypothesize that hypoglossal score could help to distinguish carriers with faster progression and to propose early swallowing management. In SCA7, we detected preliminary evidence potentially suggesting the existence of correlations between oro-facial mobility scores and brainstem volumes: MBLF with pons, tongue domain with medulla oblongata, facial nerve score with pons and superior cerebellar peduncle, hypoglossal nerve score with pons. These results are puzzling, especially since the majority of SCA7 carriers were still preataxic after one year of follow-up. In SCA2, speech and swallowing difficulties are already reported in preataxic and early-stages, correlating with time to disease onset and severity.<sup>107</sup> Until now, only few studies investigated oro-facial mobility in SCAs and none performed longitudinal follow-up. The MBLF progression over one year, in particular the tongue involvement, had already been reported in 40 advanced Friedreich's ataxia patients.<sup>74</sup> MBLF thus seems to be useful to track progression in the early and advanced stages of ataxia. This assessment is fast, easy to complete, and it can be used independently of disability stage, language, and age.<sup>74</sup>

We explored a large battery of tests for neuropsychological assessment. The CCAS scale, which is the gold standard to examine cognitive functions in ataxia patients,<sup>75</sup> demonstrated a trend towards lower scores in SCA2 and SCA7 carriers compared with controls. Dynamic emotional recognition assessed by the FACES Battery showed poorer performance in SCA7 carriers, with the lowest scores for sadness and anger expressions. The recognition of facial emotions, an important component of social cognition, is affected in Friedreich's Ataxia patients<sup>108</sup> and SCA patients without correlation with clinical features, possibly relating from a defect in the corticocerebellar network.<sup>109-111</sup> Moreover, anger recognition deficit is associated with atrophy of vermis and lateral cerebellar regions in HD patients.<sup>112</sup> In SCA2 patients, the anger score is reported to correlate with posterior cerebellum lobules volume (lobule VIIIIB, Crus II, and IX) as well as with DTI alterations in the middle cerebellar peduncle.<sup>111</sup> In our SCA7 cohort, cerebellar atrophy was not yet detected, explaining perhaps the lack of correlations between emotional recognition and MRI results. Semantic fluency was affected in both SCA groups, but not significantly after multiple comparisons correction. In both SCA2 and SCA7 patients, impairment of semantic fluency and verbal memory have been reported, correlating with grey matter volumes of association cortices.<sup>113,114</sup> Word fluency is also compromised in SCA1<sup>115</sup> and SCA3 patients.<sup>116</sup> Language impairment has also been described in SCA36, with decreased phonological verbal fluency in preataxic carriers, and impaired



semantic fluency in symptomatic patients.<sup>117</sup> The absence of impairment in neuropsychological assessment after one-year follow-up and the lack of correlations with volumes of cerebral region of interest might be due to the limited sample size and the predominant inclusion of preataxic and early ataxic carriers.

In our cohort, the oculomotor recordings analyzed to date show that relationships between amplitude, duration, and velocity of saccades were altered in SCA2 and SCA7 patients as well as in preataxic SCA2 individuals. Oculomotor parameters, such as saccade peak velocity, saccade latency, saccade accuracy, and antisaccadic task, show abnormalities in SCA2 and SCA7 early disease courses.<sup>118–122</sup> Moreover, oculomotor alterations strongly correlate with pathological CAG repeat expansion length and pontine atrophy,<sup>26,119,123</sup> and worsened in longitudinal follow-up.<sup>119,123</sup> These data reinforces the potential role of electrooculographical measures of saccades as biomarkers of disease progression in clinical trials and natural history studies.

We explored the ophthalmological features of SCA7 patients through a multimodal functional and imaging approach. As previously reported, retinal abnormalities may precede ataxia as they can be present in premanifest stage.<sup>124,125</sup> The retinal phenotype has been initially described as a macular dystrophy; it then was better defined as a cone-rod dystrophy.<sup>7,126</sup> Interestingly, in our cohort, most of the patients presented with cone dystrophy, demonstrating a preserved rod function. This finding is not related to the age of patients as the two subjects with cone-rod dystrophy were younger than the others (Figure 2); it is rather correlated with the CAG repeat size and the severity of cerebellar ataxia scored by SARA (Figure 2). Previous reports converged in agreeing that age and disease duration were not different among various stages of retinal impairment (independently from the used classifications),<sup>127,128</sup> thus suggesting that the pathological allele is the most relevant in determining the retinal phenotype. However, in our cohort the comparison between ICM-034-DC (28-year-old, cone dystrophy) and ICM-003-OA (38-year-old, cone-rod dystrophy) showed a better phenotype for the younger patient even though CAG repeats expansion was longer (fig. 2). The disease has proved to be progressive over time<sup>128,129</sup> and this may explain why we did not find any significant correlation between the number of CAG repeats and the ocular parameters. However, it is not clear whether cone dystrophy inevitably evolves to cone-rod dystrophy, or if rods may be indefinitely preserved in certain conditions. This remarkable observation may shed further light on the pathogenesis of SCA7-related retinal dystrophy, still largely unknown. In this context, one of the proposed mechanisms is linked to the interaction of ataxin-7 with CRX, a nuclear

transcription factor mostly expressed in photoreceptors,<sup>130</sup> and whose variants are associated with an autosomal dominant cone-rod dystrophy.<sup>131,132</sup> Other suggested mechanisms could include interactions with NRL (neural retina leucine zipper protein) and Nr2E3 (Nuclear Receptor Subfamily 2, Group E, Member 3) which alters the photoreceptors differentiation.<sup>133</sup> Understanding the molecular mechanisms of SCA7 would be crucial to enhance the discovery of new therapeutic approaches. Recently, RNA interference-based therapy and antisense oligonucleotides showed encouraging results in SCA mice models.<sup>19,134</sup> In this regards, natural history studies with genotype-phenotype correlations and deep-phenotyping are required to reveal novel biomarkers for systemic assessment and disease progression. Specifically, ocular biomarkers may be particularly useful as they can be monitored through non-invasive in vivo examinations. The correlation between clinical scores and ophthalmological findings has only been partially explored. Recently, Marianelli et al. proposed a novel classification of the retinal degeneration based on fundus examination and OCT imaging.<sup>127</sup> Briefly, the authors defined four stages of the disease, from no abnormalities to generalized dystrophy with nummular confluent atrophic lesions. SARA score correlated significantly with the ophthalmological findings of this classification.<sup>127</sup> While this classification may be useful for clinicians in assessing the disease, it may be less suitable to evaluate the short-term progression of the disease (i.e., 1- or 2-year), which is required in most therapeutic clinical trials. Our study attempted to find more precise correlations between neurological scores and retinal dystrophy through a thorough multimodal examination. Specifically, we found a significant correlation between the SARA score and both functional (i.e., BCVA and microperimetry) and imaging parameters (ONL thickness). Moreover, ONL thickness correlated with NfL levels, a valid biomarker in SCAs allowing to discriminate preataxic from both controls and ataxic carriers<sup>22,23,25</sup> and to predict clinical and radiological progression.<sup>52</sup> Previous studies on SCA7-associated retinal dystrophy defined some biomarkers of disease progression, including the OCT macular thickness, the automated perimetry, or electrophysiology responses.<sup>128,135</sup> Compared with automated perimetry, microperimetry has the advantage of stimulating specific areas of the retina through an eye-tracking system that guarantees precision and replicability.<sup>136</sup> For OCT parameters, given the initial alterations at the photoreceptors level (i.e., central ellipsoid zone integrity and ONL thickness), ONL thickness may be more sensitive than retinal thickness in assessing the disease, however further longitudinal and comparison studies are warranted to confirm this hypothesis. In conclusion, SCA7-related retinal dystrophy is characterized by a cone or a cone-rod dystrophy phenotype whose functional and imaging parameters correlate with neurological findings. The longitudinal assessment of these

parameters with prospective natural history studies may confirm their potential value as biomarkers to track the disease progression and to monitor therapeutic interventions in clinical trials.

At baseline, cerebellar hemispheres and cerebellar grey matter volumes were decreased in SCA2 compared with controls and SCA7 carriers, while cerebellum white matter was reduced in both SCA groups compared with control individuals. In SCA7, the cerebellum whole volume and grey matter volumes were preserved. These results suggest that white matter loss may be happening earlier in the disease course. In a recent study including 14 SCA7 patients with a mean SARA score of about 14/40, microstructural abnormalities were detected brain-wide in the white and grey matter, while volume loss was restricted to the cerebellum, brainstem, thalamus, and corticospinal tracts.<sup>137</sup> It is still unknown whether thalamus and corticospinal tracts atrophies are secondary to the loss of cerebellar efferent pathways, or primarily involved in SCA7 disease. However, pyramidal signs are characteristic of SCA7 and were often found in our presymptomatic carriers. White matter alterations are also extensively reported in SCA2, in association with pontocerebellar degeneration and allow to track disease progression.<sup>138–141</sup> In our study, brainstem volumes were not significantly altered after Holm correction. However, in SCA2 carriers, the pons was the only region to show a significant volume loss over both six-months and one year follow-up. This result replicates our previous report of longitudinal pons volume loss in SCA2 patients,<sup>59</sup> confirming this region volume as a valid biomarker in early and moderate disease phases. Pons atrophy is evident already in SCA2 and SCA3 preataxic carriers<sup>26–28,62</sup> and showed a very large effect size compared with clinical scores.<sup>51,142</sup> For the other cortical and subcortical regions, we did not find any significant differences from controls, possibly because of the early disease stage. Diffusion tensor imaging and spectroscopy analyses might provide us other useful biomarkers.

Among fluid biomarkers, as previously published, plasma NfL concentrations were significantly higher in SCA carriers than in controls.<sup>23,25,52</sup> This result confirms NfL as a valid biomarker, already for early disease stages. However, as already reported in our longitudinal study with two-year follow-up,<sup>52</sup> NfL levels did not increase over time in SCA carriers, but only showed the expected age-dependent increase in controls.<sup>45</sup> We could suppose that, as reported for ALS and other neurodegenerative diseases, NfL levels may have already reached a plateau that masks the age-dependent increase.<sup>45</sup> Some preataxic carriers of CERMOI study who presented neurological signs as pyramidal involvement showed NfL levels close to the pathological cut-off reported in our previous SCA cohort.<sup>52</sup> Moreover, since NfL levels can

predict the age at onset of cerebellar symptoms,<sup>23</sup> they can be considered a reliable fluid biomarker that allows stratifying preataxic carriers in order to possibly include them in clinical trials. The other biomarkers tested in plasma and CSF ( $\alpha$ -synuclein, total Tau, pTau 181, A $\beta$ 40, and A $\beta$ 42) did not differ between SCA and control individuals. One study reported higher CSF total Tau levels in SCA2 patients than in controls as well as a positive trend for  $\alpha$ -synuclein.<sup>143</sup> However, only six SCA2 patients were included in this study. In another cohort including 27 SCA3 patients, the levels of total Tau and pTau181 were similar to our results, not allowing for differentiating carriers from controls.<sup>144</sup> However, in this study A $\beta$ 42 CSF concentrations were higher in SCA3 than in controls and Alzheimer's disease patients.<sup>144</sup> Similarly to SCA3 patients, HD and ALS patients presented higher A $\beta$ 42 levels, which could be explained by the enhanced apoptosis mechanisms in these diseases, leading to an increased activity of caspase-3 which cleaves amyloid precursor protein in A $\beta$ 42. Moreover, ataxins have shown links with amyloid pathways, since ATXN1 reduction causes increased activity of protease  $\beta$ -secretase 1 (BACE1) implicated in the cleavage of amyloid precursor protein.<sup>145</sup> We might not have reproduced these results for A $\beta$ 42 analysis because of the early or preataxic disease stage of our carriers. Further validation of these fluid biomarkers leveraging larger cohorts will be crucial to conclude on their reliability.

One of the biggest limitations of our study is the small sample size. SCA2 and SCA7 however are rare diseases, and the inclusion criteria of SARA score below 15 limited the enrolment possibilities even more. Moreover, since we tested a really high number of parameters, we had to exert drastic correction for multiple comparisons, which lowered the threshold of significance for each individual variable. The strengths of the study however are the exhaustive assessment of carriers via our multimodal approach, and the inclusion of preataxic and early ataxic patients, who will be the target of future gene therapies.

In conclusion, in our cohort of preataxic and early ataxic SCA2 and SCA7 carriers, we identified several significant changes, through a comprehensive multimodal assessment (Figure 8). These could be useful endpoints or biomarkers in future clinical trials. For SCA2, at baseline, we detected differences in clinical scores (SARA, INAS, CCFS), saccade main sequence, oro-facial scores, NfL levels, and cerebellum volumes (white and grey matter). Already after 6-months follow-up, pons atrophy and MBLF score together with hypoglossal and facial nerve scores showed significant progression. In the SCA7 group, for which more than half of the carriers were at preataxic stage, we found differences in clinical scores (SARA, INAS, CCFS), saccade main sequence, oro-facial scores, NfL levels, and cerebellum white

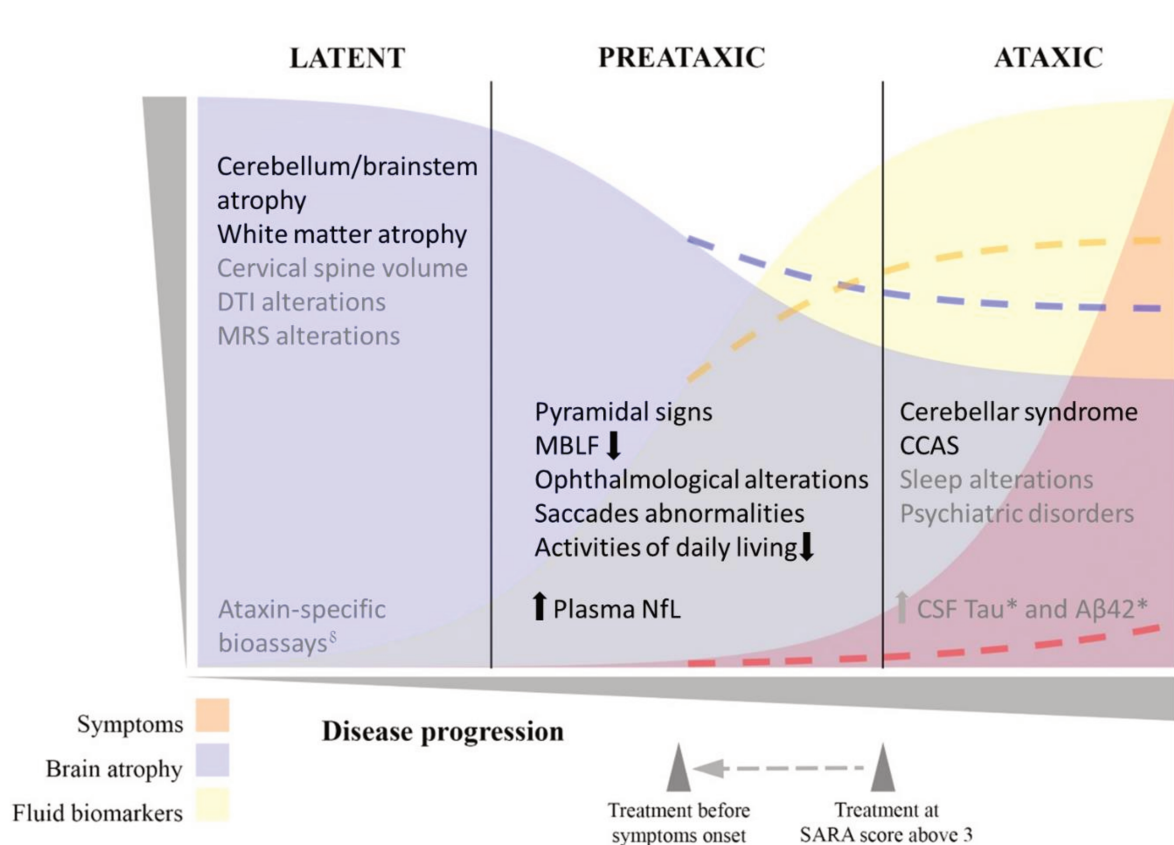
matter volume. Ophthalmological assessments showed cone dystrophy in SCA7 preataxic carriers. After 6 months, SARA score, MBLF score, hypoglossal and facial nerve scores progressed.

## Conclusions and perspectives

To date, clinical trials for spinocerebellar ataxias are targeted to individuals with overt ataxia, and their primary outcome is the improvement of the SARA score. The sample size calculation based on the SARA score progression for SCA1, 2, 3, and 6 showed that hundreds of patients should be enrolled in a one-year clinical trial to detect significant changes due to treatment.<sup>32,146</sup> In rare diseases, achieving the statistical power required is extremely challenging and strongly limits trials' feasibility. Moreover, SARA score presents high intraindividual variability<sup>87</sup> and it thus is an additional source of bias. Modified versions of SARA have been proposed, such as the Modified Functional SARA (mSARA), used in a trial to compare the efficacy of Troriluzole versus placebo in SCAs patients. Their higher sensitivity is however still debated.

The first phase 1 clinical trial with a non-allele-specific ASO, targeting SCA3 patients with SARA score between 3 and 15, started in early 2022 (NCT05160558). The ASOs administration in SCAs is based on promising results reported on SCA mice models.<sup>17-20</sup> However, the early termination of the phase 3 study, GENERATION HD1 (NCT03761849), using Tominersen in patients with Huntington's disease (HD), dampened the enthusiasm for ASO treatment. This non-selective ASO was initially administered every four or eight weeks. The huntingtin reduction was greater than expected, associated with the increase of adverse events in the group receiving Tominersen every four weeks. For these reasons, the interval of administration was extended to eight and 12 weeks. Unfortunately, the trial was halted since the group receiving the treatment every eight weeks performed worse than the placebo, had more serious adverse events, and showed increase in CSF NfL levels.<sup>147</sup> The long-term effects of wild-type and mutant huntingtin reduction are not completely elucidated.<sup>148</sup> Allele-specific ASOs might allow to avoid these pitfalls, since they do not target the wild-type protein, which might help reducing adverse events. Their use is however limited to patients carrying specific single nucleotide polymorphism on the expanded allele. Despite that, in HD, both allele-selective trials WVE-120101 (NCT03225833) and WVE-120102 (NCT03225846) were also stopped since failing to decrease the mutant protein.<sup>149</sup> Interestingly, the latest allele-selective trial WVE-003 (NCT05032196) is showing encouraging results, lowering mutant huntingtin by 22% (Wave Life Sciences USA, Inc.). Building upon all these findings, the safety and pharmacokinetic results of phase 1 non-allele-specific ASO trial are greatly awaited in SCA3.

In the perspective of gene therapies in SCAs, it is crucial to validate new biomarkers, sensitive over short time windows allowing to reduce sample sizes and monitor a potential treatment in clinical trials in these rare diseases. Until now, imaging biomarkers have shown the largest effect size.<sup>51</sup> Volumetry, diffusion tensor imaging analyses, and MR spectroscopy have shown alterations in the preataxic stage already.<sup>26–29,66,138</sup> In ATRIL and CERMOI studies, pons atrophy progressed over one year in moderate SCA2 patients and preataxic/early ataxic SCA2 carriers, respectively. In CERMOI this progression was even detected at 6-month follow-up, a remarkable result since one-third of SCA2 carriers was at the preataxic stage.



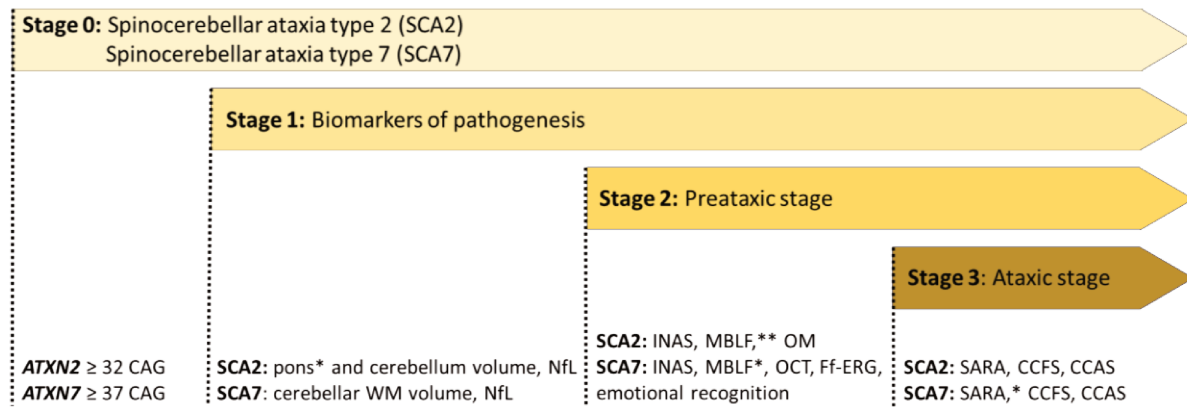
**Figure 1. Schematic representation of polyglutamine spinocerebellar ataxias natural history adapted from Coarelli et al. 2022, in revision.**

The natural history of polyglutamine SCAs can be divided into three main phases: the latent phase, where no signs or symptoms are present; the pre ataxic phase, where clinical signs and symptoms unrelated to ataxia can be detected; then the ataxic phase, with clear cerebellar manifestations (red shaded area). The treatment administration before the onset of symptoms could allow to limit or avoid their occurrence and lessen the brain atrophy (projections in dashed lines). Abbreviations: CCAS: Cerebellar cognitive affective syndrome; CSF: cerebrospinal fluid; MBLF: Oral-Lingual-Facial Motility; NfL: Neurofilament light chain. In black, results from CERMOI study for SCA2 and SCA7 carriers, in grey results from literature for polyglutamine SCAs. \*Only one study, to be replicated. §To date, available only for ATXN3 protein in cerebrospinal fluid, plasma, and urine.

The results collected in the present work highlight that additional abnormalities can be detected in combination with radiological findings before ataxia onset (Figure 1). Oro-facial motility, assessed by the MBLF evaluation, was significantly impaired in SCA2 and SCA7 carriers. MBLF score progressed during the CERMOI study, already after six months in the SCA7 group and 12 months in the SCA2 group. As previously reported, MBLF significantly changed over one year in advanced Friedreich's ataxia patients.<sup>74</sup> The CERMOI study confirms the usefulness of this assessment to reflect disease progression. In addition, in SCA7 carriers involved in this study, cone dystrophy was found at the preataxic stage already. The outer nuclear layer thickness inversely correlated with both NfL levels and SARA score. NfL levels increase was reported in SCA1, SCA2, SCA3, and SCA7 preataxic and ataxic carriers,<sup>22,23,25,52</sup> even though, as shown in the CERMOI study and previously reported,<sup>52</sup> it does not progress over time. However, plasma NfL levels can predict the ataxia onset several years before<sup>23</sup> and the disease severity.<sup>52</sup> Digital assessments such as oculomotor recording<sup>118,120</sup> and gait analysis with wearable sensors<sup>102</sup> are also altered in preataxic carriers, providing useful additional biomarkers. New clinical trials leveraging these novel and reliable biomarkers as primary outcomes, including preataxic individuals, are thus greatly warranted.<sup>61</sup> In other neurodegenerative diseases, using a machine learning approach, the combination of different biomarkers has helped to stratify patients<sup>150</sup> and delineate individual disease trajectories.<sup>151</sup> In the CERMOI study, some correlations between baseline clinical scores and other parameters have been identified. Clinical scores such as SARA, CCAS, and MBLF, as well as blood NfL levels, are easy to assess and could be used to evaluate inclusion of SCA carriers in clinical trials.

To refine inclusion criteria, validation of the disease staging for polyglutamine SCAs, as recently proposed in HD,<sup>86</sup> would be the ideal first step. In these regards, CERMOI results can help to provide a similar staging of the disease course in SCA2 and SCA7 (Figure 2): Stage 0: identification of pathological CAG expansion without any pathological alteration; Stage 1: detectable pathological changes without carrier's complaint; Stage 2: preataxic stage with detectable clinical alterations; Stage 3: manifest ataxic stage.





**Figure 2. Staging of Spinocerebellar ataxia type 2 (SCA2) and type 7 (SCA7).**

Based on CERMOI study results, this is a staging proposal for SCA2 and SCA7 disease courses (imaging, oculomotor, and ophthalmological analyses are ongoing) adapted from Tabrizi et al., *Lancet Neurol* 2022.<sup>86</sup>

Abbreviations: CCAS: Cerebellar cognitive affective syndrome; CCFS: Composite Cerebellar Functional Score; Ff-ERG: full-field electroretinography; INAS: Inventory of Non-Ataxia Signs; MBLF: Oral-Lingual-Facial Motility; NfL: Neurofilament light chain; OCT: optical coherence tomography OM: oculomotor recording; SARA: Scale for the Assessment and Rating of Ataxia; WM: white matter. \*Progression detected at month-6 and month-12 follow-up (visit 2 and visit 3). \*\*Progression detected at month-12 follow-up (visit 3).

This novel disease staging could allow the identification of the ideal time point to propose a preventive treatment, resulting in the delay of the disease onset and reducing cerebral volume loss (Figure 1). In a HD mouse model, early neonatal treatment with an ampakine enhanced the glutamatergic transmission, rescued neural circuit abnormalities, and preserved cognitive and sensorimotor functions as well as brain volume.<sup>152</sup> These results suggest that treating several years before ataxic onset might be the better option to prevent the occurrence of symptoms. In this context, one of our projects (SCAKIDS), in collaboration with the Neuropediatric Department of the Trousseau Hospital in Paris, will focus on following at-risk individuals during their childhood and teenage years, in order to investigate the first stages of the disease and to identify possible compensatory mechanisms.

The mystery of being born with a major genetic defect but developing neurological signs in mid-life or even later is not yet resolved. The search of indicators and modifiers should be continued to better characterize the preataxic phase and the compensation mechanisms at play. Therapeutic options could be to enhance compensation, to decrease the toxicity of expanded alleles with ASOs, or to increase wild-type protein function through gene therapy.

## References

- 1 Bodranghien F, Bastian A, Casali C, *et al.* Consensus Paper: Revisiting the Symptoms and Signs of Cerebellar Syndrome. *Cerebellum* 2016; **15**: 369–91.
- 2 Seidel K, Siswanto S, Brunt ERP, den Dunnen W, Korf H-W, Rüb U. Brain pathology of spinocerebellar ataxias. *Acta Neuropathol* 2012; **124**: 1–21.
- 3 Rüb U, Bürk K, Timmann D, *et al.* Spinocerebellar ataxia type 1 (SCA1): new pathoanatomical and clinico-pathological insights: Spinocerebellar ataxia type 1. *Neuropathology and Applied Neurobiology* 2012; **38**: 665–80.
- 4 KOEPPEN AH. The neuropathology of the adult cerebellum. *Handb Clin Neurol* 2018; **154**: 129–49.
- 5 Koeppen AH, Morral JA, McComb RD, Feustel PJ. The neuropathology of late-onset Friedreich’s ataxia. *Cerebellum* 2011; **10**: 96–103.
- 6 Ruano L, Melo C, Silva MC, Coutinho P. The Global Epidemiology of Hereditary Ataxia and Spastic Paraplegia: A Systematic Review of Prevalence Studies. *Neuroepidemiology* 2014; **42**: 174–83.
- 7 Harding AE. Classification of the hereditary ataxias and paraplegias. *Lancet* 1983; **1**: 1151–5.
- 8 Synofzik M, Puccio H, Mochel F, Schöls L. Autosomal Recessive Cerebellar Ataxias: Paving the Way toward Targeted Molecular Therapies. *Neuron* 2019; **101**: 560–83.
- 9 Klockgether T, Mariotti C, Paulson HL. Spinocerebellar ataxia. *Nat Rev Dis Primers* 2019; **5**: 24.
- 10 Rossi M, Anheim M, Durr A, *et al.* The genetic nomenclature of recessive cerebellar ataxias: Genetic Nomenclature of Recessive Ataxias. *Mov Disord* 2018; **33**: 1056–76.
- 11 Németh AH, Kwasniewska AC, Lise S, *et al.* Next generation sequencing for molecular diagnosis of neurological disorders using ataxias as a model. *Brain* 2013; **136**: 3106–18.
- 12 Coarelli G, Wirth T, Tranchant C, Koenig M, Durr A, Anheim M. The inherited cerebellar ataxias: an update. *J Neurol* 2022; published online Sept 24. DOI:10.1007/s00415-022-11383-6.
- 13 Durr A. Autosomal dominant cerebellar ataxias: polyglutamine expansions and beyond. *The Lancet Neurology* 2010; **9**: 885–94.
- 14 Schöls L, Bauer P, Schmidt T, Schulte T, Riess O. Autosomal dominant cerebellar ataxias: clinical features, genetics, and pathogenesis. *Lancet Neurol* 2004; **3**: 291–304.
- 15 Zesiewicz TA, Wilmot G, Kuo S-H, *et al.* Comprehensive systematic review summary: Treatment of cerebellar motor dysfunction and ataxia: Report of the Guideline Development, Dissemination, and Implementation Subcommittee of the American Academy of Neurology. *Neurology* 2018; **90**: 464–71.
- 16 Yap KH, Azmin S, Che Hamzah J, Ahmad N, van de Warrenburg B, Mohamed Ibrahim N. Pharmacological and non-pharmacological management of spinocerebellar ataxia: A systematic review. *J Neurol* 2022; **269**: 2315–37.

- 17 Friedrich J, Kordasiewicz HB, O’Callaghan B, *et al.* Antisense oligonucleotide-mediated ataxin-1 reduction prolongs survival in SCA1 mice and reveals disease-associated transcriptome profiles. *JCI insight* 2018; **3**. DOI:10.1172/jci.insight.123193.
- 18 Scoles DR, Meera P, Schneider MD, *et al.* Antisense oligonucleotide therapy for spinocerebellar ataxia type 2. *Nature* 2017; **544**: 362–6.
- 19 Niu C, Prakash TP, Kim A, *et al.* Antisense oligonucleotides targeting mutant Ataxin-7 restore visual function in a mouse model of spinocerebellar ataxia type 7. *Science Translational Medicine* 2018; **10**. DOI:10.1126/scitranslmed.aap8677.
- 20 McLoughlin HS, Moore LR, Chopra R, *et al.* Oligonucleotide therapy mitigates disease in spinocerebellar ataxia type 3 mice. *Annals of Neurology* 2018; **84**: 64–77.
- 21 Biomarkers Definitions Working Group. Biomarkers and surrogate endpoints: preferred definitions and conceptual framework. *Clin Pharmacol Ther* 2001; **69**: 89–95.
- 22 Wilke C, Mengel D, Schöls L, *et al.* Levels of Neurofilament Light at the Preataxic and Ataxic Stages of Spinocerebellar Ataxia Type 1. *Neurology* 2022; : 10.1212/WNL.0000000000200257.
- 23 Wilke C, Haas E, Reetz K, *et al.* Neurofilaments in spinocerebellar ataxia type 3: blood biomarkers at the preataxic and ataxic stage in humans and mice. *EMBO Mol Med* 2020; **12**: e11803.
- 24 Peng Y, Zhang Y, Chen Z, *et al.* Association of serum neurofilament light (sNfL) and disease severity in patients with spinocerebellar ataxia type 3. *Neurology* 2020; published online Aug 14. DOI:10.1212/WNL.0000000000010671.
- 25 Li Q-F, Dong Y, Yang L, *et al.* Neurofilament light chain is a promising serum biomarker in spinocerebellar ataxia type 3. *Mol Neurodegener* 2019; **14**: 39.
- 26 Reetz K, Rodríguez-Labrada R, Dogan I, *et al.* Brain atrophy measures in preclinical and manifest spinocerebellar ataxia type 2. *Ann Clin Transl Neurol* 2018; **5**: 128–37.
- 27 Faber J, Schaprian T, Berkan K, *et al.* Regional Brain and Spinal Cord Volume Loss in Spinocerebellar Ataxia Type 3. *Mov Disord* 2021; **36**: 2273–81.
- 28 Nigri A, Sarro L, Mongelli A, *et al.* Progression of Cerebellar Atrophy in Spinocerebellar Ataxia Type 2 Gene Carriers: A Longitudinal MRI Study in Preclinical and Early Disease Stages. *Front Neurol* 2020; **11**: 616419.
- 29 Nigri A, Sarro L, Mongelli A, *et al.* Spinocerebellar Ataxia Type 1: One-Year Longitudinal Study to Identify Clinical and MRI Measures of Disease Progression in Patients and Presymptomatic Carriers. *Cerebellum* 2021; published online June 9. DOI:10.1007/s12311-021-01285-0.
- 30 Schmitz-Hübsch T, du Montcel ST, Baliko L, *et al.* Scale for the assessment and rating of ataxia: development of a new clinical scale. *Neurology* 2006; **66**: 1717–20.
- 31 Jacobi H, du Montcel ST, Romanzetti S, *et al.* Conversion of individuals at risk for spinocerebellar ataxia types 1, 2, 3, and 6 to manifest ataxia (RISCA): a longitudinal cohort study. *Lancet Neurol* 2020; **19**: 738–47.
- 32 Jacobi H, du Montcel ST, Bauer P, *et al.* Long-term disease progression in spinocerebellar ataxia types 1, 2, 3, and 6: a longitudinal cohort study. *The Lancet Neurology* 2015; **14**: 1101–8.

- 33 Coarelli G, Brice A, Durr A. Recent advances in understanding dominant spinocerebellar ataxias from clinical and genetic points of view. *F1000Res* 2018; **7**: F1000 Faculty Rev-1781.
- 34 Lu C-H, Macdonald-Wallis C, Gray E, *et al.* Neurofilament light chain: A prognostic biomarker in amyotrophic lateral sclerosis. *Neurology* 2015; **84**: 2247–57.
- 35 Benatar M, Wu J, Andersen PM, Lombardi V, Malaspina A. Neurofilament light: A candidate biomarker of presymptomatic amyotrophic lateral sclerosis and phenoconversion. *Ann Neurol* 2018; **84**: 130–9.
- 36 Mattsson N, Cullen NC, Andreasson U, Zetterberg H, Blennow K. Association Between Longitudinal Plasma Neurofilament Light and Neurodegeneration in Patients With Alzheimer Disease. *JAMA Neurol* 2019; **76**: 791–9.
- 37 Benedet AL, Leuzy A, Pascoal TA, *et al.* Stage-specific links between plasma neurofilament light and imaging biomarkers of Alzheimer’s disease. *Brain* 2020; published online Nov 19. DOI:10.1093/brain/awaa342.
- 38 Preische O, Schultz SA, Apel A, *et al.* Serum neurofilament dynamics predicts neurodegeneration and clinical progression in presymptomatic Alzheimer’s disease. *Nat Med* 2019; **25**: 277–83.
- 39 Byrne LM, Rodrigues FB, Blennow K, *et al.* Neurofilament light protein in blood as a potential biomarker of neurodegeneration in Huntington’s disease: a retrospective cohort analysis. *Lancet Neurol* 2017; **16**: 601–9.
- 40 Johnson EB, Byrne LM, Gregory S, *et al.* Neurofilament light protein in blood predicts regional atrophy in Huntington disease. *Neurology* 2018; **90**: e717–23.
- 41 Scahill RI, Zeun P, Osborne-Crowley K, *et al.* Biological and clinical characteristics of gene carriers far from predicted onset in the Huntington’s disease Young Adult Study (HD-YAS): a cross-sectional analysis. *Lancet Neurol* 2020; **19**: 502–12.
- 42 Pilotto A, Imarisio A, Conforti F, *et al.* Plasma NfL, clinical subtypes and motor progression in Parkinson’s disease. *Parkinsonism Relat Disord* 2021; **87**: 41–7.
- 43 Bjornevik K, Munger KL, Cortese M, *et al.* Serum Neurofilament Light Chain Levels in Patients With Presymptomatic Multiple Sclerosis. *JAMA Neurol* 2020; **77**: 58–64.
- 44 Kuhle J, Kropshofer H, Haering DA, *et al.* Blood neurofilament light chain as a biomarker of MS disease activity and treatment response. *Neurology* 2019; **92**: e1007–15.
- 45 Gaetani L, Blennow K, Calabresi P, Di Filippo M, Parnetti L, Zetterberg H. Neurofilament light chain as a biomarker in neurological disorders. *J Neurol Neurosurg Psychiatry* 2019; **90**: 870–81.
- 46 Khalil M. Neurofilaments as biomarkers in neurological disorders. *Nat Rev Neurol* 2018; **14**. DOI:10.1038/s41582-018-0058-z.
- 47 Hansson O, Janelidze S, Hall S, *et al.* Blood-based NfL: A biomarker for differential diagnosis of parkinsonian disorder. *Neurology* 2017; **88**: 930–7.
- 48 Bridel C, van Wieringen WN, Zetterberg H, *et al.* Diagnostic Value of Cerebrospinal Fluid Neurofilament Light Protein in Neurology: A Systematic Review and Meta-analysis. *JAMA Neurol* 2019; published online June 17. DOI:10.1001/jamaneurol.2019.1534.
- 49 Olsson B, Alberg L, Cullen NC, *et al.* NFL is a marker of treatment response in children with SMA treated with nusinersen. *J Neurol* 2019; **266**: 2129–36.

- 50 Garali I, Adanyeguh IM, Ichou F, *et al.* A strategy for multimodal data integration: application to biomarkers identification in spinocerebellar ataxia. *Briefings in Bioinformatics* 2018; **19**: 1356–69.
- 51 Adanyeguh IM, Perlberg V, Henry P-G, *et al.* Autosomal dominant cerebellar ataxias: Imaging biomarkers with high effect sizes. *Neuroimage Clin* 2018; **19**: 858–67.
- 52 Coarelli G, Darios F, Petit E, *et al.* Plasma neurofilament light chain predicts cerebellar atrophy and clinical progression in spinocerebellar ataxia. *Neurobiol Dis* 2021; **153**: 105311.
- 53 Ristori G, Romano S, Visconti A, *et al.* Riluzole in cerebellar ataxia: a randomized, double-blind, placebo-controlled pilot trial. *Neurology* 2010; **74**: 839–45.
- 54 Romano S, Coarelli G, Marcotulli C, *et al.* Riluzole in patients with hereditary cerebellar ataxia: a randomised, double-blind, placebo-controlled trial. *The Lancet Neurology* 2015; **14**: 985–91.
- 55 Bellingham MC. A Review of the Neural Mechanisms of Action and Clinical Efficiency of Riluzole in Treating Amyotrophic Lateral Sclerosis: What have we Learned in the Last Decade? *CNS Neuroscience & Therapeutics* 2011; **17**: 4–31.
- 56 Abeti R, Parkinson MH, Hargreaves IP, *et al.* ‘Mitochondrial energy imbalance and lipid peroxidation cause cell death in Friedreich’s ataxia’. *Cell Death Dis* 2016; **7**: e2237–e2237.
- 57 Elden AC, Kim H-J, Hart MP, *et al.* Ataxin-2 intermediate-length polyglutamine expansions are associated with increased risk for ALS. *Nature* 2010; **466**: 1069–75.
- 58 Borghero G, Pugliatti M, Marrosu F, *et al.* ATXN2 is a modifier of phenotype in ALS patients of Sardinian ancestry. *Neurobiol Aging* 2015; **36**: 2906.e1-5.
- 59 Coarelli G, Heinzmann A, Ewencyk C, *et al.* Safety and efficacy of riluzole in spinocerebellar ataxia type 2 in France (ATRIL): a multicentre, randomised, double-blind, placebo-controlled trial. *Lancet Neurol* 2022; **21**: 225–33.
- 60 Ashizawa T, Öz G, Paulson HL. Spinocerebellar ataxias: prospects and challenges for therapy development. *Nat Rev Neurol* 2018; **14**: 590–605.
- 61 Rubinsztein DC, Orr HT. Diminishing return for mechanistic therapeutics with neurodegenerative disease duration?: There may be a point in the course of a neurodegenerative condition where therapeutics targeting disease-causing mechanisms are futile. *Bioessays* 2016; **38**: 977–80.
- 62 Jacobi H, Reetz K, du Montcel ST, *et al.* Biological and clinical characteristics of individuals at risk for spinocerebellar ataxia types 1, 2, 3, and 6 in the longitudinal RISCA study: analysis of baseline data. *Lancet Neurol* 2013; **12**: 650–8.
- 63 Rezende TJR, de Paiva JLR, Martinez ARM, *et al.* Structural signature of SCA3: From presymptomatic to late disease stages. *Ann Neurol* 2018; **84**: 401–8.
- 64 Inada BSY, Rezende TJR, Pereira FV, *et al.* Corticospinal tract involvement in spinocerebellar ataxia type 3: a diffusion tensor imaging study. *Neuroradiology* 2021; **63**: 217–24.
- 65 Park YW, Joers JM, Guo B, *et al.* Assessment of Cerebral and Cerebellar White Matter Microstructure in Spinocerebellar Ataxias 1, 2, 3, and 6 Using Diffusion MRI. *Front Neurol* 2020; **11**: 411.

- 66 Deelchand DK, Joers JM, Ravishankar A, *et al.* Sensitivity of Volumetric Magnetic Resonance Imaging and Magnetic Resonance Spectroscopy to Progression of Spinocerebellar Ataxia Type 1. *Mov Disord Clin Pract* 2019; **6**: 549–58.
- 67 Oz G, Hutter D, Tkác I, *et al.* Neurochemical alterations in spinocerebellar ataxia type 1 and their correlations with clinical status. *Mov Disord* 2010; **25**: 1253–61.
- 68 du Montcel ST, Charles P, Ribai P, *et al.* Composite cerebellar functional severity score: validation of a quantitative score of cerebellar impairment. *Brain* 2008; **131**: 1352–61.
- 69 Jacobi H, Rakowicz M, Rola R, *et al.* Inventory of Non-Ataxia Signs (INAS): Validation of a New Clinical Assessment Instrument. *Cerebellum* 2013; **12**: 418–28.
- 70 Brooks R. EuroQol: the current state of play. *Health Policy* 1996; **37**: 53–72.
- 71 Kroenke K, Spitzer RL, Williams JBW. The PHQ-9. *J Gen Intern Med* 2001; **16**: 606–13.
- 72 Krupp LB, LaRocca NG, Muir-Nash J, Steinberg AD. The fatigue severity scale. Application to patients with multiple sclerosis and systemic lupus erythematosus. *Arch Neurol* 1989; **46**: 1121–3.
- 73 Fahey MC, Corben L, Collins V, Churchyard AJ, Delatycki MB. How is disease progress in Friedreich’s ataxia best measured? A study of four rating scales. *J Neurol Neurosurg Psychiatry* 2007; **78**: 411–3.
- 74 Borel S, Gatignol P, Smail M, *et al.* Oral mobility reflects rate of progression in advanced Friedreich’s ataxia. *Ann Clin Transl Neurol* 2019; **6**: 1888–92.
- 75 Hoche F, Guell X, Vangel MG, Sherman JC, Schmahmann JD. The cerebellar cognitive affective/Schmahmann syndrome scale. *Brain* 2018; **141**: 248–70.
- 76 Bilker WB, Hansen JA, Brensinger CM, Richard J, Gur RE, Gur RC. Development of abbreviated nine-item forms of the Raven’s standard progressive matrices test. *Assessment* 2012; **19**: 354–69.
- 77 Tombaugh TN. A comprehensive review of the Paced Auditory Serial Addition Test (PASAT). *Arch Clin Neuropsychol* 2006; **21**: 53–76.
- 78 Godefroy O, Azouvi P, Robert P, *et al.* Dysexecutive syndrome: diagnostic criteria and validation study. *Ann Neurol* 2010; **68**: 855–64.
- 79 Bertoux M, Delavest M, de Souza LC, *et al.* Social Cognition and Emotional Assessment differentiates frontotemporal dementia from depression. *J Neurol Neurosurg Psychiatry* 2012; **83**: 411–6.
- 80 Holland CAC, Ebner NC, Lin T, Samanez-Larkin GR. Emotion identification across adulthood using the Dynamic FACES database of emotional expressions in younger, middle aged, and older adults. *Cogn Emot* 2019; **33**: 245–57.
- 81 Starkstein SE, Mayberg HS, Preziosi TJ, Andrezejewski P, Leiguarda R, Robinson RG. Reliability, validity, and clinical correlates of apathy in Parkinson’s disease. *J Neuropsychiatry Clin Neurosci* 1992; **4**: 134–9.
- 82 Quental NBM, Brucki SMD, Bueno OFA. Visuospatial Function in Early Alzheimer’s Disease—The Use of the Visual Object and Space Perception (VOSP) Battery. *PLoS One* 2013; **8**: e68398.
- 83 Merck C, Charnallet A, Auriacombe S, *et al.* The GRECO neuropsychological semantic battery (BECS GRECO): Validation and normative data. *Revue de neuropsychologie* 2011; **3**: 235–55.

- 84 Romero JE, Coupé P, Giraud R, *et al.* CERES: A new cerebellum lobule segmentation method. *NeuroImage* 2017; **147**: 916–24.
- 85 Kuhle J, Barro C, Andreasson U, *et al.* Comparison of three analytical platforms for quantification of the neurofilament light chain in blood samples: ELISA, electrochemiluminescence immunoassay and Simoa. *Clin Chem Lab Med* 2016; **54**: 1655–61.
- 86 Tabrizi SJ, Schobel S, Gantman EC, *et al.* A biological classification of Huntington’s disease: the Integrated Staging System. *The Lancet Neurology* 2022; **21**: 632–44.
- 87 Grobe-Einsler M, Taheri Amin A, Faber J, *et al.* Development of SARAtome , a New Video-Based Tool for the Assessment of Ataxia at Home. *Mov Disord* 2021; **36**: 1242–6.
- 88 Bah MG, Rodriguez D, Cazeneuve C, *et al.* Deciphering the natural history of SCA7 in children. *Eur J Neurol* 2020; **27**: 2267–76.
- 89 Bettencourt C, Hensman-Moss D, Flower M, *et al.* DNA repair pathways underlie a common genetic mechanism modulating onset in polyglutamine diseases. *Ann Neurol* 2016; **79**: 983–90.
- 90 Martins S, Pearson CE, Coutinho P, *et al.* Modifiers of (CAG)(n) instability in Machado-Joseph disease (MJD/SCA3) transmissions: an association study with DNA replication, repair and recombination genes. *Hum Genet* 2014; **133**: 1311–8.
- 91 Genetic Modifiers of Huntington’s Disease (GeM-HD) Consortium. Electronic address: gusella@helix.mgh.harvard.edu, Genetic Modifiers of Huntington’s Disease (GeM-HD) Consortium. CAG Repeat Not Polyglutamine Length Determines Timing of Huntington’s Disease Onset. *Cell* 2019; **178**: 887-900.e14.
- 92 Lee J-M, Huang Y, Orth M, *et al.* Genetic modifiers of Huntington disease differentially influence motor and cognitive domains. *Am J Hum Genet* 2022; **109**: 885–99.
- 93 Kacher R, Lejeune F-X, Noël S, *et al.* Propensity for somatic expansion increases over the course of life in Huntington disease. *Elife* 2021; **10**: e64674.
- 94 Jang M, Kim H-J, Kim A, Jeon B. Urinary Symptoms and Urodynamic Findings in Patients with Spinocerebellar Ataxia. *Cerebellum* 2020; **19**: 483–6.
- 95 Schmahmann JD, Pierce S, MacMore J, L’Italien GJ. Development and Validation of a Patient-Reported Outcome Measure of Ataxia. *Mov Disord* 2021; **36**: 2367–77.
- 96 Serrao M, Pierelli F, Ranavolo A, *et al.* Gait pattern in inherited cerebellar ataxias. *Cerebellum* 2012; **11**: 194–211.
- 97 Ilg W, Seemann J, Giese M, *et al.* Real-life gait assessment in degenerative cerebellar ataxia: Toward ecologically valid biomarkers. *Neurology* 2020; **95**: e1199–210.
- 98 Palliyath S, Hallett M, Thomas SL, Lebedowska MK. Gait in patients with cerebellar ataxia. *Mov Disord* 1998; **13**: 958–64.
- 99 Buckley E, Mazzà C, McNeill A. A systematic review of the gait characteristics associated with Cerebellar Ataxia. *Gait & Posture* 2018; **60**: 154–63.
- 100 Paquette C, Franzén E, Horak FB. More Falls in Cerebellar Ataxia When Standing on a Slow Up-Moving Tilt of the Support Surface. *Cerebellum* 2016; **15**: 336–42.

- 101 Warmerdam E, Schumacher M, Beyer T, *et al.* Postural Sway in Parkinson's Disease and Multiple Sclerosis Patients During Tasks With Different Complexity. *Front Neurol* 2022; **13**: 857406.
- 102 Shah VV, Rodriguez-Labrada R, Horak FB, *et al.* Gait Variability in Spinocerebellar Ataxia Assessed Using Wearable Inertial Sensors. *Mov Disord* 2021; **36**: 2922–31.
- 103 Nanetti L, Alpini D, Mattei V, *et al.* Stance instability in preclinical SCA1 mutation carriers: A 4-year prospective posturography study. *Gait Posture* 2017; **57**: 11–4.
- 104 Diallo A, Jacobi H, Cook A, *et al.* Survival in patients with spinocerebellar ataxia types 1, 2, 3, and 6 (EUROSCA): a longitudinal cohort study. *The Lancet Neurology* 2018; **17**: 327–34.
- 105 Iaconetta G, Solari D, Villa A, *et al.* The Hypoglossal Nerve: Anatomical Study of Its Entire Course. *World Neurosurg* 2018; **109**: e486–92.
- 106 Orengo JP, van der Heijden ME, Hao S, Tang J, Orr HT, Zoghbi HY. Motor neuron degeneration correlates with respiratory dysfunction in SCA1. *Disease Models & Mechanisms* 2018; : dmm.032623.
- 107 Vogel AP, Magee M, Torres-Vega R, *et al.* Features of speech and swallowing dysfunction in pre-ataxic spinocerebellar ataxia type 2. *Neurology* 2020; **95**: e194–205.
- 108 Costabile T, Capretti V, Abate F, *et al.* Emotion Recognition and Psychological Comorbidity in Friedreich's Ataxia. *Cerebellum* 2018; **17**: 336–45.
- 109 Sokolovsky N, Cook A, Hunt H, Giunti P, Cipolotti L. A preliminary characterisation of cognition and social cognition in spinocerebellar ataxia types 2, 1, and 7. *Behavioural Neurology* 2010; **23**: 17–29.
- 110 D'Agata F, Caroppo P, Baudino B, *et al.* The recognition of facial emotions in spinocerebellar ataxia patients. *Cerebellum* 2011; **10**: 600–10.
- 111 Clausi S, Olivito G, Siciliano L, *et al.* The neurobiological underpinning of the social cognition impairments in patients with spinocerebellar ataxia type 2. *Cortex* 2021; **138**: 101–12.
- 112 Scharmüller W, Ille R, Schienle A. Cerebellar Contribution to Anger Recognition Deficits in Huntington's Disease. *Cerebellum* 2013; **12**: 819–25.
- 113 Stezin A, Bhardwaj S, Hegde S, *et al.* Cognitive impairment and its neuroimaging correlates in spinocerebellar ataxia 2. *Parkinsonism Relat Disord* 2021; **85**: 78–83.
- 114 Chirino A, Hernandez-Castillo CR, Galvez V, *et al.* Motor and cognitive impairments in spinocerebellar ataxia type 7 and its correlations with cortical volumes. *Eur J Neurosci* 2018; **48**: 3199–211.
- 115 Fancellu R, Paridi D, Tomasello C, *et al.* Longitudinal study of cognitive and psychiatric functions in spinocerebellar ataxia types 1 and 2. *J Neurol* 2013; **260**: 3134–43.
- 116 Thieme A, Faber J, Sulzer P, *et al.* The CCAS-scale in hereditary ataxias: helpful on the group level, particularly in SCA3, but limited in individual patients. *J Neurol* 2022; **269**: 4363–74.
- 117 Martínez-Regueiro R, Arias M, Cruz R, *et al.* Cerebellar Cognitive Affective Syndrome in Costa da Morte Ataxia (SCA36). *Cerebellum* 2020; **19**: 501–9.
- 118 Moscovich M, Okun MS, Favilla C, *et al.* Clinical Evaluation of Eye Movements in Spinocerebellar Ataxias: A Prospective Multicenter Study. *J Neuroophthalmol* 2015; **35**: 16–21.



- 119 Rodríguez-Labrada R, Velázquez-Pérez L, Auburger G, *et al.* Spinocerebellar ataxia type 2: Measures of saccade changes improve power for clinical trials. *Mov Disord* 2016; **31**: 570–8.
- 120 Velázquez-Pérez L, Rodríguez-Labrada R, Cruz-Rivas EM, *et al.* Comprehensive study of early features in spinocerebellar ataxia 2: delineating the prodromal stage of the disease. *Cerebellum* 2014; **13**: 568–79.
- 121 Stephen CD, Schmahmann JD. Eye Movement Abnormalities Are Ubiquitous in the Spinocerebellar Ataxias. *Cerebellum* 2019; **18**: 1130–6.
- 122 Park JY, Joo K, Woo SJ. Ophthalmic Manifestations and Genetics of the Polyglutamine Autosomal Dominant Spinocerebellar Ataxias: A Review. *Front Neurosci* 2020; **14**: 892.
- 123 Seifried C, Velázquez-Pérez L, Santos-Falcón N, *et al.* Saccade velocity as a surrogate disease marker in spinocerebellar ataxia type 2. *Ann N Y Acad Sci* 2005; **1039**: 524–7.
- 124 Park JY, Wy SY, Joo K, Woo SJ. Spinocerebellar ataxia type 7 with RP1L1-negative occult macular dystrophy as retinal manifestation. *Ophthalmic Genet* 2019; **40**: 282–5.
- 125 Aleman TS, Cideciyan AV, Volpe NJ, Stevanin G, Brice A, Jacobson SG. Spinocerebellar ataxia type 7 (SCA7) shows a cone-rod dystrophy phenotype. *Exp Eye Res* 2002; **74**: 737–45.
- 126 David G, Dürr A, Stevanin G, *et al.* Molecular and clinical correlations in autosomal dominant cerebellar ataxia with progressive macular dystrophy (SCA7). *Hum Mol Genet* 1998; **7**: 165–70.
- 127 Marianelli BF, Filho FMR, Salles MV, *et al.* A Proposal for Classification of Retinal Degeneration in Spinocerebellar Ataxia Type 7. *Cerebellum* 2021; **20**: 384–91.
- 128 Horton LC, Frosch MP, Vangel MG, Weigel-DiFranco C, Berson EL, Schmahmann JD. Spinocerebellar ataxia type 7: clinical course, phenotype-genotype correlations, and neuropathology. *Cerebellum* 2013; **12**: 176–93.
- 129 Zou X, Yao F, Li F, *et al.* Clinical characterization and the improved molecular diagnosis of autosomal dominant cone-rod dystrophy in patients with SCA7. *Mol Vis* 2021; **27**: 221–32.
- 130 Chen S, Peng G-H, Wang X, *et al.* Interference of Crx-dependent transcription by ataxin-7 involves interaction between the glutamine regions and requires the ataxin-7 carboxy-terminal region for nuclear localization. *Hum Mol Genet* 2004; **13**: 53–67.
- 131 Evans K, Fryer A, Inglehearn C, *et al.* Genetic linkage of cone-rod retinal dystrophy to chromosome 19q and evidence for segregation distortion. *Nat Genet* 1994; **6**: 210–3.
- 132 Freund CL, Gregory-Evans CY, Furukawa T, *et al.* Cone-rod dystrophy due to mutations in a novel photoreceptor-specific homeobox gene (CRX) essential for maintenance of the photoreceptor. *Cell* 1997; **91**: 543–53.
- 133 Karam A, Trottier Y. Molecular Mechanisms and Therapeutic Strategies in Spinocerebellar Ataxia Type 7. *Adv Exp Med Biol* 2018; **1049**: 197–218.
- 134 Ramachandran PS, Bhattarai S, Singh P, *et al.* RNA Interference-Based Therapy for Spinocerebellar Ataxia Type 7 Retinal Degeneration. *PLOS ONE* 2014; **9**: e95362.
- 135 Azevedo PB, Rocha AG, Keim LMN, *et al.* Ophthalmological and Neurologic Manifestations in Pre-clinical and Clinical Phases of Spinocerebellar Ataxia Type 7. *Cerebellum* 2019; **18**: 388–96.

- 136 Yang Y, Dunbar H. Clinical Perspectives and Trends: Microperimetry as a Trial Endpoint in Retinal Disease. *Ophthalmologica* 2021; **244**: 418–50.
- 137 Parker JA, Merchant SH, Attaripour-Isfahani S, *et al.* In vivo assessment of neurodegeneration in Spinocerebellar Ataxia type 7. *Neuroimage Clin* 2021; **29**: 102561.
- 138 Hernandez-Castillo CR, Diaz R, Rezende TJR, *et al.* Cervical Spinal Cord Degeneration in Spinocerebellar Ataxia Type 7. *AJNR Am J Neuroradiol* 2021; **42**: 1735–9.
- 139 Mascalchi M, Marzi C, Giannelli M, *et al.* Histogram analysis of DTI-derived indices reveals pontocerebellar degeneration and its progression in SCA2. *PLOS ONE* 2018; **13**: e0200258.
- 140 Olivito G, Lupo M, Iacobacci C, *et al.* Microstructural MRI Basis of the Cognitive Functions in Patients with Spinocerebellar Ataxia Type 2. *Neuroscience* 2017; **366**: 44–53.
- 141 Stezin A, Bhardwaj S, Khokhar S, *et al.* In vivo microstructural white matter changes in early spinocerebellar ataxia 2. *Acta Neurol Scand* 2021; **143**: 326–32.
- 142 Contreras A, Ramirez-Garcia G, Chirino A, *et al.* Longitudinal Analysis of the Relation Between Clinical Impairment and Gray Matter Degeneration in Spinocerebellar Ataxia Type 7 Patients. *Cerebellum* 2021; **20**: 346–60.
- 143 Brouillette AM, Öz G, Gomez CM. Cerebrospinal Fluid Biomarkers in Spinocerebellar Ataxia: A Pilot Study. *Dis Markers* 2015; **2015**: 413098.
- 144 Ye L-Q, Li X-Y, Zhang Y-B, *et al.* The discriminative capacity of CSF  $\beta$ -amyloid 42 and Tau in neurodegenerative diseases in the Chinese population. *J Neurol Sci* 2020; **412**: 116756.
- 145 O’Callaghan B, Hofstra B, Handler HP, *et al.* Antisense Oligonucleotide Therapeutic Approach for Suppression of Ataxin-1 Expression: A Safety Assessment. *Mol Ther Nucleic Acids* 2020; **21**: 1006–16.
- 146 Diallo A, Jacobi H, Tezenas du Montcel S, Klockgether T. Natural history of most common spinocerebellar ataxia: a systematic review and meta-analysis. *J Neurol* 2021; **268**: 2749–56.
- 147 Tabrizi SJ, Estevez-Fraga C, van Roon-Mom WMC, *et al.* Potential disease-modifying therapies for Huntington’s disease: lessons learned and future opportunities. *The Lancet Neurology* 2022; **21**: 645–58.
- 148 Tabrizi SJ, Leavitt BR, Landwehmer GB, *et al.* Targeting Huntingtin Expression in Patients with Huntington’s Disease. *N Engl J Med* 2019; **380**: 2307–16.
- 149 Kingwell K. Double setback for ASO trials in Huntington disease. *Nat Rev Drug Discov* 2021; **20**: 412–3.
- 150 Gaubert S, Houot M, Raimondo F, *et al.* A machine learning approach to screen for preclinical Alzheimer’s disease. *Neurobiol Aging* 2021; **105**: 205–16.
- 151 Koval I, Bône A, Louis M, *et al.* AD Course Map charts Alzheimer’s disease progression. *Sci Rep* 2021; **11**: 8020.
- 152 Braz BY, Wennagel D, Ratié L, *et al.* Treating early postnatal circuit defect delays Huntington’s disease onset and pathology in mice. *Science* 2022; **377**: eabq5011.

## **Annex 1**

*Manuscript submitted to Neuropathology and Applied in Neurobiology in august 2022*

### **Motor neuron involvement threatens survival in spinocerebellar ataxia type 1**

Giulia Coarelli<sup>1,2</sup>, Maya Tchikviladzé<sup>2</sup>, Pauline Dodet<sup>3</sup>, Isabelle Arnulf<sup>3</sup>, Perrine Charles<sup>2</sup>, Frederic Tankeré<sup>4</sup>, Thomas Similowski<sup>5</sup>, Alexis Brice<sup>1</sup>, Charles Duyckaerts<sup>1,6</sup>, Alexandra Durr<sup>1,2</sup>

<sup>1</sup>Sorbonne Université, Paris Brain Institute (ICM Institut du Cerveau), INSERM, CNRS, Assistance Publique-Hôpitaux de Paris (AP-HP), Paris, France.

<sup>2</sup>Department of Genetics, Pitié-Salpêtrière Charles-Foix University Hospital, Assistance Publique – Hôpitaux de Paris (AP-HP), 75013, Paris, France

<sup>3</sup>Sleep Disorders Unit, Pitié-Salpêtrière University Hospital, AP-HP, Paris, France; ICM, Sorbonne Université, Inserm U 1127, CNRS UMR 7225, Paris, France

<sup>4</sup>Department of Otolaryngology-Head and Neck Surgery, Pitié-Salpêtrière Charles-Foix University Hospital, Assistance Publique – Hôpitaux de Paris (AP-HP), Sorbonne Université, 75013, Paris, France

<sup>5</sup>Sorbonne Université, INSERM, UMRS1158 *Neurophysiologie Respiratoire Expérimentale et Clinique*; AP-HP, Groupe Hospitalier Universitaire APHP-Sorbonne Université, site Pitié-Salpêtrière, Département R3S (*Respiration, Réanimation, Réhabilitation respiratoire, Sommeil*), F-75013 Paris, France

<sup>6</sup>Laboratoire de Neuropathologie R. Escourolle, Pitié-Salpêtrière Charles-Foix University Hospital, Assistance Publique – Hôpitaux de Paris (AP-HP), Sorbonne Université, 75013, Paris, France

Corresponding author: Pr Alexandra Durr, Paris Brain Institute, Pitié-Salpêtrière Paris CS21414, 75646 PARIS Cedex 13, France, alexandra.durr@icm-institute.org, tel. +33 1 57 27 46 82, fax +33 1 57 27 47 26.

Character count for the title: 76; Character count for the running title: 26

Total word count of the manuscript: 1485; Total word count of the abstract: 250

Total number of figures and tables: 2; Number of supplemental figures: 1

Keywords: spinocerebellar ataxia, SCA1, dysphagia, hypoglossal nucleus, motor neuron

## **Abbreviations**

ALS: Amyotrophic Lateral Sclerosis

INAS: Inventory of Non-Ataxia Symptoms

OSA: Obstructive Sleep Apnea

PolyQ: Polyglutamine

REM: Rapid Eye Movement

SARA: Scale for the Assessment and Rating of Ataxia

SCAs: Spinocerebellar ataxias

## **Key points**

1. This study aimed to explore life-threatening conditions in spinocerebellar ataxia type 1.
2. Laryngeal dysfunction was severe in all patients resulting as the most life threatening condition, causing swallowing and respiratory alterations and death by aspiratory pneumonia.
3. Sleep alterations may be caused by progressive loss of pontine REM-on neurons.
4. Diaphragmatic exploration suggested impairment in upper motor neuron pathway.
5. Quantified neuronal loss was severe in the medulla tegmentum, especially for massive neuronal loss in inferior olive and in the hypoglossal motor nucleus.
6. Brainstem involvement with severe motor neuron depletion may explain the life-threatening conditions of SCA1 patients.

## **Introduction**

Spinocerebellar ataxias (SCAs) are progressive and fatal neurodegenerative diseases. The most frequent forms are polyglutamine SCAs due to expansions of coding CAG repeats: *ATXN1/SCA1*, *ATXN2/SCA2*, *ATXN3/SCA3*, *CACNA1A/SCA6*, *ATXN7/SCA7*, *TBP/SCA17* and *ATN/DRPLA*. These SCAs show faster disease progression than SCAs due to conventional mutations or intronic expansions.[1] Among polyQ SCAs, SCA1 has the shortest survival[2] and the strongest risk factors for death are the presence of dysphagia and higher scores of the Scale for the Assessment and Rating of Ataxia (SARA).[3] The aim of this study was to explore how the neurodegenerative process explained a shorter survival time in SCA1 patients. Neuropathological studies indicate that brainstem involvement is major in SCA1,[4] including the structures responsible for the swallowing process.[5] Motor neurons of the brainstem and cervical spinal cord degenerate in SCA1 knock-in (*Atxn1*<sup>154Q/+</sup>) mice, in particular for hypoglossal nucleus, (nucleus of cranial nerve XII).[6] The XII cranial nerve impairment is involved in dysphagia and dysarthria. The different phases (lingual, pharyngeal or esophageal) of swallowing are altered in almost all SCAs patients with consequent dysphagia. Dysphagia represents a risk factor for aspiration pneumonia, weight loss, and malnutrition and it is usually alleviated by a nasogastric tube, parenteral nutrition, or percutaneous endoscopic gastrostomy. In this study, patients underwent multimodal explorations and post mortem analysis to understand how the neurodegenerative process threatened life in SCA1 patients.

## **Methods**

We included ten SCA1 patients (from 10 distinct families) with respiratory distress, all followed in the national reference center for rare diseases at Pitié-Salpêtrière University Hospital in Paris starting in 2010; the last patient (399-818) died in 2021. They underwent i) laryngofibroscope and electromyography of larynx muscles to explore laryngeal functions; ii) overnight polysomnography with measure of the apnea-hypopnea index (number of apnea and hypopnea

per hour slept, an index higher than 30 defines severe sleep apnea). The percentage of REM sleep without atonia, whether phasic or tonic, was measured on chin EMG[7] iii) assessment of diaphragm function; the diagnosis of diaphragmatic dysfunction was based on previously defined criteria.[8]

Each participant consented according to the French legislation with approval from local ethic committee (Necker Enfant-Malades on 19/12/1990, 10/11/1992, followed by the Ethics committee Ile de France II on 30/9/2004 and 18/2/2010 to AD). Details for neuropathological methods are in Supplementary materials.

## **Results**

Mean age at onset was  $32.1 \pm 17$  years (17-67), mean disease duration at examination  $14.7 \pm 6.1$  years (8-25) and SARA score  $26.8/40 \pm 6.75$  (19-34) (Table 1). All patients had severe swallowing difficulties, including one patient with tube feeding. Patients described no REM sleep behavioral sleep disorders. Mean age at death was  $51.0 \pm 23.2$  (29-88), after a mean of disease duration of  $18.9 \pm 8.0$  (10-34). The cause of death was aspiration pneumonia (n=5), gastroscopy complications (n=1), and unknown (n=4). The CAG repeat size was inversely correlated with the age of death ( $r=-0.87$ ,  $p<0.001$ ).

Laryngoscopy, performed after a mean disease duration of  $15.7 \pm 6.3$  years with a mean SARA score of  $26.3 \pm 6.4$  (n=7), showed failure to abduct the vocal cords in all, with a resulting narrowing of the glottic airway (n=3) and inspiratory stridor (n=2). Electromyography confirmed laryngeal dystonia (n=3), motor neuron denervation (n=3) and laryngeal diplegia (n=1). Dystonia resulted of increased activity of thyroarytenoid and/or posterior cricoarytenoid muscles. Botulinum toxin injection into the involved muscle provided a transitory improvement in dysphonia and dyspnea. Posterior cordotomy in one patient and autologous fat graft in the vocal cord in two additional patients were performed and improved the symptoms.

Overnight polysomnography was performed after a mean disease duration of  $12.5 \pm 4.8$  years with a mean SARA score of  $28.4 \pm 5.5$  and body mass index of  $23.8 \pm 3.2$  kg/m<sup>2</sup> (n=6). Total

sleep time, duration of wakefulness after sleep onset, and sleep efficiency were within normal ranges, except for one patient (326-79) who slept less than 70% of the night. The percentage of sleep stages N1, N2 and N3 were within normal ranges but REM sleep percentage was decreased (<15% of total sleep time) in 4/6 patients (Table 1). The percentage of enhanced tonic plus phasic muscle chin activity during REM sleep was increased (18 to 59%) in 6/6. The mean arousal index was  $31 \pm 16$ . The apnea-hypopnea index was below 5 in two patients, between 5 and 15 in three patients, between 15 and 30 in one patient (369-20). Diaphragmatic exploration (n=6) revealed diaphragm dysfunction in three (326-79, 361-31, and 465-13), with a lower esophageal pressure (<11 cm H<sub>2</sub>O) in response to bilateral phrenic stimulation. The first had phasic respiratory accessory cervical muscles activation. All had delayed central motor conduction (i.e. prolonged latency of diaphragmatic motor evoked potentials in response to transcranial magnetic stimulation of 24.7, 27.7, and 16 ms, respectively), suggesting impairment in upper motor neuron pathway. There was neither a neuropathy on the electromyogram, nor abnormal phrenic nerve conduction. In two, REM sleep percentages were decreased (4.8% and 4%, respectively). The minimal oxyhemoglobin saturation during REM sleep was between 89% and 91%. Both died of acute respiratory failure.

### Neuropathology

We analyzed the medulla oblongata in three SCA1 patients (detailed neuropathological examinations in supplementary data) to investigate motor neurons density, especially for hypoglossal nucleus. The ages **at death** were 29, 51 and 68 years after a disease duration of 9, 21, and 25 years and a pathological *ATXN1* CAG repeat size of 63, 49, and 48, respectively. We compared the findings with those obtained in three control cases (ages at death dead 54, 58, 60 without neurological diseases).

Compared to controls, motor neurons degeneration was evident in SCA1 brainstems with smaller medulla oblongata surface area and motor neurons depletion, especially for the



hypoglossal nucleus (Figure 1, Supplementary Figure 1).

## **Discussion**

This study aimed to explore life-threatening conditions in spinocerebellar ataxia type 1. We only enrolled SCA1 patients with respiratory distress. Dysphagia was the most common alteration, found in all patients, followed by dyspnea and dysphonia. Laryngeal dysfunction was present in all patients, as glottis leak, vocal cords paralysis, laryngeal hypotonia, vocal cords spasm in adduction, inspiratory stridor, and vocal cord abduction weakness. We showed that laryngeal dysfunction in SCA1 was the most life threatening condition, causing swallowing and respiratory alterations and death by aspiratory pneumonia. These data should help clinical management: early detection of dysphagia, dysphonia and dyspnea should be anticipated and explained. Avoiding aspiration pneumonia and consequently recurrent hospital admissions could improve quality of life of these patients. Detection of vocal cord abnormalities is essential to propose symptomatic treatments as botulinum toxin, posterior cordotomy, autologous fat graft in the vocal cord and eventually tracheotomy. For respiratory and sleep alterations, the nocturnal ventilator assistance should be considered, based on polysomnographic studies.

These alterations are similar to other polyglutamine SCAs and multiple system atrophy patients.[9, 10] Loss of bulbospinal motor neurons were thought to be responsible for neurogenic atrophy of laryngeal muscles.[9] In particular, the hypoglossal nucleus extends the length of medulla and innerves intrinsic and extrinsic muscles of the tongue (except for palatoglossus), essential for mastication, speech, swallowing and upper airway airflow during sleep.[11]

A notable exception of bulbar motor neuron loss is SCA6[4] that present a less severe phenotype. In SCAs, clinical signs, found by the different explorations, are well correlated to neuropathology: atrophy of brainstem, neuronal loss in cranial nerve nuclei, overall ambiguous and hypoglossal nuclei, pyramidal tract reduction, loss of neurons in the substantia nigra, spinocerebellar tracts thinning, moderate depletion of Purkinje cells, neuronal loss in dentate

nucleus, neuronal rarefaction in the anterior horn of spinal cord. Post-mortem examination of the three SCA1 patients in our study match the characteristics found in previous neuropathological studies.[12, 13]

Some specific sleep alterations, including reduced REM sleep percentage, increased arousals and REM sleep without atonia may be caused by progressive loss of pontine REM-on neurons (non-motor neurons) since the locus coeruleus appeared normal. In addition, deficiency in genioglossus muscle (innervated by hypoglossal nerve), a muscle that usually prevents airflow decrease and pharyngeal collapse, may increase the risk of obstructive sleep apnea syndrome, but this occurrence was however rare here. This is the case in SCA1 since apnea-hypopnea events was associated with increased disease severity despite the lack of typical risk factors like age or obesity.[14] Diaphragm is the single inspiratory muscle active during REM sleep, as it is not inhibited during REM atonia. It was dysfunctional in three patients, resulting in decreased REM sleep percentages in two. This deficit was not related to the presence of neuropathy but probably due to degeneration of upper and lower motor neurons as in amyotrophic lateral sclerosis. Small number of patients limits our conclusions. However, SCA patients are rare and the inclusion criteria of respiratory distress was difficult to attain, since they are severely functionally impaired at this stage of disease.

In conclusion, laryngeal dysfunction was evident in our patients causing respiratory and swallowing failure. This was confirmed by neuropathological findings showing significant brainstem involvement in SCA1 with severe motor neuron depletion, which explains the life-threatening conditions of these patients.

Contributors: Giulia Coarelli: Data curation, Formal analysis, Writing – original draft, Maya Tchikviladzé: Investigation, Data curation, Formal analysis, Writing – review and editing, Pauline Dodet: Investigation, Data curation, Writing – review and editing, Isabelle Arnulf: Investigation, Writing – review and editing, Myriam Cohen: Investigation, Writing – review and editing, Perrine Charles: Investigation, Writing – review and editing, Frederic Tankeré: Investigation, Writing – review and editing, Thomas Similowski: Investigation, Writing – review and editing, Alexis Brice: Writing – review and editing, Charles Duyckaerts: Conceptualization, Methodology, Writing – review and editing, Alexandra Durr: Conceptualization, Methodology, Investigation, Writing – review and editing

Data availability: The data that support the findings of this study are available from the corresponding author ([alexandra.durr@icm-institute.org](mailto:alexandra.durr@icm-institute.org)) upon reasonable request.

Declaration of interests: The authors report no competing interests.

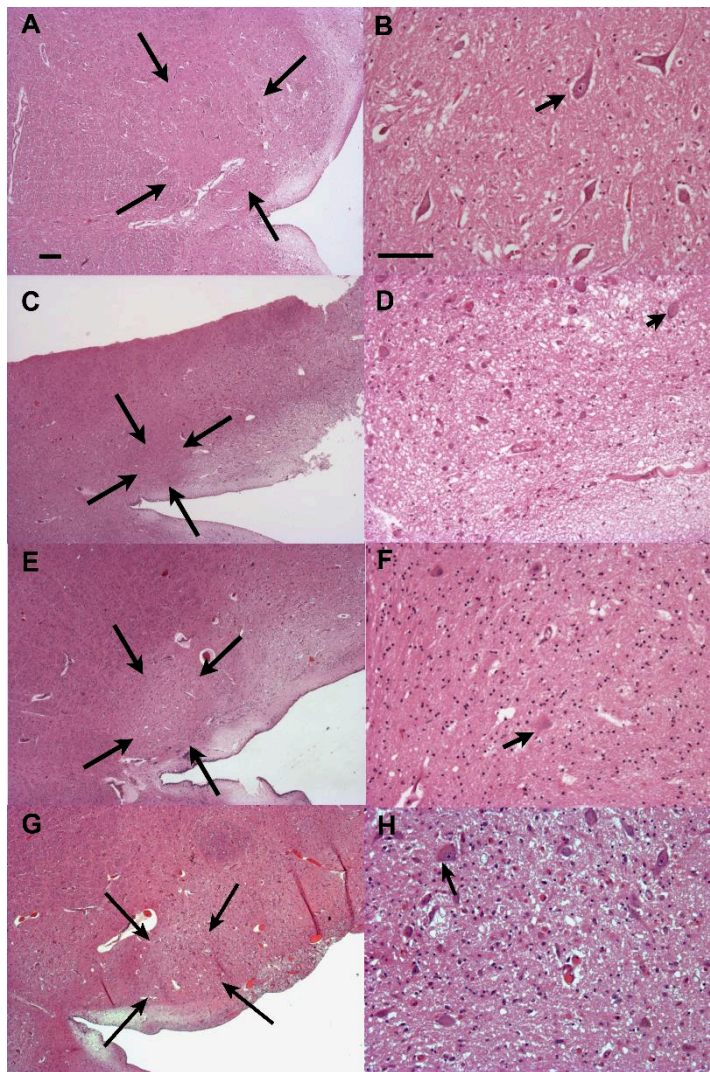
Acknowledgements: We would like to thank the patients for their participation in this study.

## References

1. Durr A (2010) Autosomal dominant cerebellar ataxias: polyglutamine expansions and beyond. *The Lancet Neurology* 9:885–894. [https://doi.org/10.1016/S1474-4422\(10\)70183-6](https://doi.org/10.1016/S1474-4422(10)70183-6)
2. Monin M, Tezenas du Montcel S, Marelli C, et al (2015) Survival and severity in dominant cerebellar ataxias. *Ann Clin Transl Neurol* 2:202–207. <https://doi.org/10.1002/acn3.156>
3. Diallo A, Jacobi H, Cook A, et al (2018) Survival in patients with spinocerebellar ataxia types 1, 2, 3, and 6 (EUROSCA): a longitudinal cohort study. *The Lancet Neurology* 17:327–334. [https://doi.org/10.1016/S1474-4422\(18\)30042-5](https://doi.org/10.1016/S1474-4422(18)30042-5)
4. Seidel K, Siswanto S, Brunt ERP, et al (2012) Brain pathology of spinocerebellar ataxias. *Acta Neuropathol* 124:1–21. <https://doi.org/10.1007/s00401-012-1000-x>
5. Rüb U, Brunt ER, Del Turco D, et al (2003) Guidelines for the pathoanatomical examination of the lower brain stem in ingestive and swallowing disorders and its application to a dysphagic spinocerebellar ataxia type 3 patient: Pathoanatomical examination of ingestion-related brain stem nuclei. *Neuropathology and Applied Neurobiology* 29:1–13. <https://doi.org/10.1046/j.1365-2990.2003.00437.x>
6. Orengo JP, van der Heijden ME, Hao S, et al (2018) Motor neuron degeneration correlates with respiratory dysfunction in SCA1. *Disease Models & Mechanisms* dmm.032623. <https://doi.org/10.1242/dmm.032623>
7. Arnulf I, Merino-Andreu M, Bloch F, et al (2005) REM sleep behavior disorder and REM sleep without atonia in patients with progressive supranuclear palsy. *Sleep* 28:349–354
8. Laveneziana P, Albuquerque A, Aliverti A, et al (2019) ERS statement on respiratory muscle testing at rest and during exercise. *Eur Respir J* 53:1801214. <https://doi.org/10.1183/13993003.01214-2018>
9. Isozaki E, Naito R, Kanda T, et al (2002) Different mechanism of vocal cord paralysis between spinocerebellar ataxia (SCA 1 and SCA 3) and multiple system atrophy. *J Neurol Sci* 197:37–43. [https://doi.org/10.1016/s0022-510x\(02\)00046-1](https://doi.org/10.1016/s0022-510x(02)00046-1)
10. Shiojiri T, Tsunemi T, Matsunaga T, et al (1999) Vocal cord abductor paralysis in spinocerebellar ataxia type 1. *J Neurol Neurosurg Psychiatry* 67:695. <https://doi.org/10.1136/jnnp.67.5.695>
11. Hicks A, Cori JM, Jordan AS, et al (2017) Mechanisms of the deep, slow-wave, sleep-related increase of upper airway muscle tone in healthy humans. *J Appl Physiol* (1985) 122:1304–1312. <https://doi.org/10.1152/jappphysiol.00872.2016>
12. Robitaille Y, Schut L, Kish SJ (1995) Structural and immunocytochemical features of olivopontocerebellar atrophy caused by the spinocerebellar ataxia type 1 (SCA-1) mutation define a unique phenotype. *Acta Neuropathol* 90:572–581. <https://doi.org/10.1007/BF00318569>
13. Rüb U, Bürk K, Timmann D, et al (2012) Spinocerebellar ataxia type 1 (SCA1): new pathoanatomical and clinico-pathological insights: Spinocerebellar ataxia type 1. *Neuropathology and Applied Neurobiology* 38:665–680. <https://doi.org/10.1111/j.1365-2990.2012.01259.x>

14. Anttalainen U, Tenhunen M, Rimpilä V, et al (2016) Prolonged partial upper airway obstruction during sleep - an underdiagnosed phenotype of sleep-disordered breathing. *Eur Clin Respir J* 3:31806. <https://doi.org/10.3402/ecrj.v3.31806>

**Figure 1. Comparison of the hypoglossal nucleus in SCA1 patients and control.**



Haematein-eosin staining. A, C, E, G: x2 objective, scale bar: 200 $\mu$ m. B, D, F, H: x10 objective; scale bar: 100  $\mu$ m.

A-B: control case, 60 years at death. A: the black arrows delineate the limits of the hypoglossal nucleus. At higher per view (B), normal motor neurons.

C-D: Patient 369-20, 51 years at death, *ATXNI* pathological expansion of 49 CAG repeats (normal allele 29). In C, the surface area of the hypoglossal nucleus (black arrows) appears smaller. In D, neurons are smaller.

E-F: Patient 326-79, 29 years at death. *ATXNI* pathological expansion of 63 CAG repeats (normal allele 30). In E, the nucleus appears atrophic (black arrows) and pale. The number of neurons is reduced (F), one of which (arrow) is chromatolytic.

G-H: Patient 860-17, 68 years at death, *ATXNI* pathological expansion of 48 CAG repeats (normal allele 29). In G, hypoglossal nucleus smaller and pale. Chromatolytic motor neurons are present (arrow).

**Table 1. Clinical and multimodal explorations of SCA1 patients with respiratory distress.**

ID	395-5	326-79*	721-10	302-15	347-11	369-20*	860-17*	361-31	399-818	465-13
ATXN1 CAG repeats (pathological/normal)	66/29	63/30	57/30	56/31	50/29	49/29	48/29	45/29	39/32	39/22
Sex	W	W	M	W	M	M	W	M	M	W
Age at onset (years)	17	18	20	20	25	30	43	27	54	67
Age at death (years)	30	29	32	30	52	51	68	42	88	88
Disease duration (years)	8	8	8	10	25	19	19	13	20	17
SARA score (max value 40)	32	31	19	24	34	34	29.5	29.5	19	21
Pyramidal signs	+	+++	++	++	++	+++	++	++	++	++
Extrapyramidal signs	-	+++	++	+	-	+	++	-	-	-
Lingual fasciculation	++	++	++	++	++	-	++	++	-	-
Cognitive impairment	-	++	-	-	+	-	+	+	-	+
Dysphonia	+	-	-	-	+	-	+	-	+	-
Dysphagia	+++	++	++	++	++	++	++	+	++	++
Dyspnea	+	+	+	+	++	+	++	++	++	++

Laryngo-fibroscope	Laryngeal hypotonia and spasms	nd	Glottic leak	nd	Failure to abduct the vocal cords, IS	nd	VP, glottic leak	NGA, laryngeal diplegia	Failure to abduct the vocal cords, NGA, IS	NGA
Larynx EMG	nd	nd	LD	nd	MN	nd	MN	LD	MN	LD
Apnea-hypopnea index	1	8	nd	13	nd	29	nd	3	nd	12
Apnea hypopnea index in REM sleep	9	13	nd	4	nd	5	nd	11	nd	32
Periodic leg movements during sleep, N/h	32	19	nd	3	nd	39	nd	84	nd	33
Arousal index, N/h	13	32	nd	34	nd	50	nd	13	nd	46
REM sleep, % of total sleep time	13	4	nd	21	nd	13	nd	20	nd	4
REM sleep without atonia, % of REM sleep	59	24	nd	26	nd	36	nd	37	nd	18
Cortico-diaphragmatic CT (from transcranial magnetic stimulation), msec	nd	24.7	nd	nd	nd	nd	nd	27.7	nd	16
Phrenic nerve CT (from	7.75	6.4	nd	6.25	nd	6.65	nd	6.3	nd	6



cervical magnetic stimulation), msec										
--------------------------------------	--	--	--	--	--	--	--	--	--	--

Abbreviations: CT: conduction time; DD: disease duration; EMG: electromyography; IS: inspiratory stridor; LD: laryngeal dystonia; MN: motor neuronal denervation; NGA: Narrowing of the glottic airway; REM: rapid eye movement; VP: Vocal cords paralysis; nd: not done. + mild, ++ moderate, +++ severe.

\* Patients came to autopsy.

## **Supplementary materials**

### **Methods of neuropathological examination**

Autopsy was performed within 48 hours. The brain was removed: one half, randomly left or right, was fixed by immersion in 4 % formaldehyde (10 % formalin); systematic samples from the other hemisphere were frozen at -80°C. After at least two months formalin fixation, a systematic sampling protocol was applied including the whole brainstem, the vermis and the hemisphere of the cerebellum. The samples were embedded in paraffin and cut at a thickness of 5 µm. The sections were deparaffinized in graded alcohol and stained with haematein-eosin and haematein-eosin luxol fast blue. Selected samples were immunostained with the following antibodies: ubiquitin, p62, 1C2 for polyglutamin, and tau (AT8). Double labeling for myelin basic protein and neurofilament was also performed. All the immunostainings were performed on a BenchMark ULTRA automated immunohistochemistry slide staining system (Roche) according to manufacturer instructions. The neuronal density in medulla tegmentum was evaluated by manually drawing the borders of the region and pointing the neuronal profiles within these borders with a specially devised system including a video-camera, a computerized moving stage and an ad hoc mapping program (BrainMap, Biocom). The density was evaluated by Voronoi polygons as previously described [1].

### **Results of neuropathological examination**

Patient 326-79. This woman, carrying 63 CAG repeats in *ATXN1*, died at age 29 at the hospital after 9 years of disease duration. She had severe swallowing difficulties leading to tube feeding at age 28. Frequent aspiration pneumonia occurred; dyspnea required oxygen therapy. In addition, there was diaphragm dysfunction.

The right hemisphere weighted 571g and the cerebellum with brainstem 58g. There was no atrophy of the neocortex and hippocampus and no enlargement of the lateral ventricles. Putamen and pallidum were macroscopically normal. There was severe atrophy of the subthalamic nucleus. The substantia nigra was mildly depleted. There was a severe decrease in

the number of neurons in the pontine nuclei. The locus coeruleus appeared normal. The neuronal loss was severe in the inferior olives, hypoglossal and ambiguous nuclei. The folia of the cerebellum appeared normal. The number of Purkinje cells was slightly reduced; Bergmann glia were abnormally visible. The neuronal loss was massive in the dentate nucleus; the superior cerebellar peduncle was atrophic. The spinal posterior column and the spinocerebellar tracts were thin particularly in the dorsal part of spinal cord. The direct pyramidal tract was pale. The numerical density of motor neurons was low in the anterior horn; 1C2 positive intranuclear inclusions were found only 2% of the motor cortex, 1% of insular cortex, 9% of the striatum, 8-10% in pontine neurons, but none in Purkinje cells. Optic nerve showed macular degeneration.

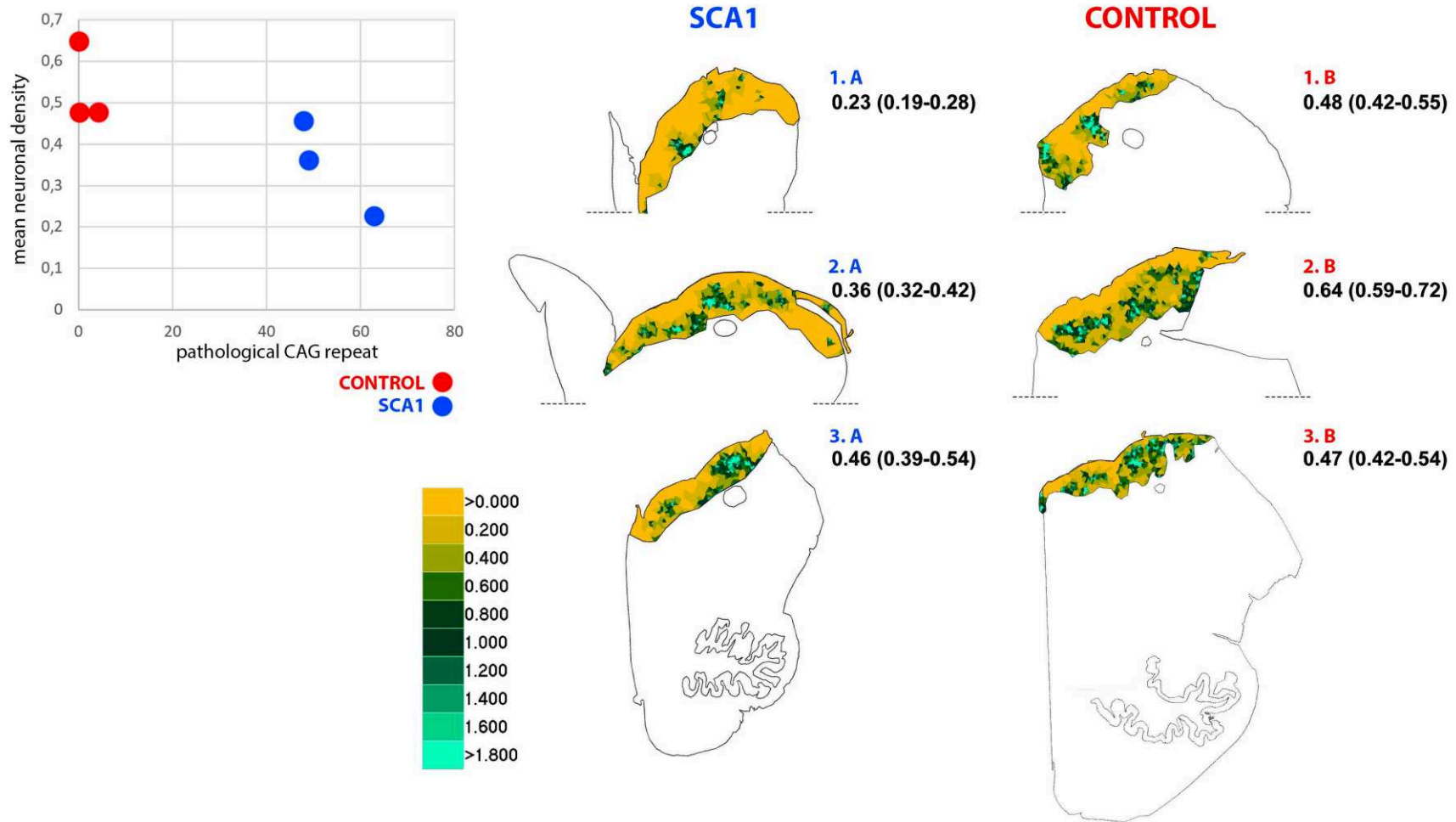
Patient 369-20. This man died of SCA1 (CAG repeats 49/29) at age 51 after 21 years disease duration for pneumonia. He had severe swallowing difficulties leading to frequent aspiration pneumonia and gastrostomy after 20 years disease duration. For dyspnea aggravation, tracheotomy was done after 20 years disease duration. The left hemisphere weighted 561g. There was no atrophy of the cerebral cortex, lenticular nucleus, thalamus, subthalamic nucleus, pallidum, or putamen. The brainstem and cerebellum was small – because of atrophy or developmental hypoplasia. In the mesencephalon, there was a mild loss of neurons in the substantia nigra. The pontine nuclei were small and contained a reduced number of neurons. In the medulla, the pyramidal tracts were small. There was massive neuronal loss in the inferior olive. The hypoglossal and ambiguous nuclei were small and the number of motor neurons was reduced. In the cerebellum, the numerical density of the Purkinje cells was abnormally low and Bergmann glia were abnormally prominent. The neuronal loss was severe in the dentate nucleus. The superior cerebellar peduncle was atrophic. Ubiquitin-positive intranuclear inclusions were observed in the cortex and the remaining substantia nigra neurons.

Patient 860-17. This woman, carrying 48 CAG repeats in *ATXN1*, died after 25 years of disease duration, at age 68. She had severe dysphagia, vocal cord paralysis and dyspnea requiring

oxygen therapy. The right hemi-brain weighted 528 g. The cerebral cortex was slightly atrophic. The volume of the brainstem was small as well as the cerebellum. The lateral ventricles were mildly dilated (2/10). The amygdala was small but the hippocampus was of normal size. Putamen, pallidum and subthalamic nucleus were macroscopically normal. The substantia nigra and the locus coeruleus were normally pigmented. The pons was small in height, width and along the antero-posterior direction; the pes pontis was particularly small. In the medulla, there was some neuronal loss in the hypoglossal and ambiguous nuclei. The inferior olivary nucleus was gliotic; the neuronal packing density was massively reduced. The hilus of the dentate nucleus was severely atrophic as well as the superior cerebellar peduncle, its efferent pathway. The number of Purkinje cells was mildly reduced. Empty baskets and torpedoes were however seen. In the granule cell layer, the density of glomeruli was reduced. In the spinal cord, the posterior column was pale as well as the spino-cerebellar tracts. The packing density of motor neurones appeared slightly decreased in the anterior horn of the upper cervical cord. Immunohistochemistry of tau protein and Abeta peptide revealed numerous tangles and plaques in the neocortex and hippocampus; amyloid deposits were seen in the neocortex, hippocampus, basal ganglia and mesencephalon (Braak neurofibrillary stage V; Thal amyloid phase 4). p62 antibody labelled not only some neurofibrillary tangles but also a large number of typical neuronal intranuclear inclusions in the cortex.

## **References**

1. Duyckaerts, C, G Godefroy, and J J Hauw. 1994. "Evaluation of Neuronal Numerical Density by Dirichlet Tessellation." *J Neurosci Methods* 51 (1): 47–69.



**Supplemental Figure.1 Comparison of medulla tegmentum motor neurons density in SCA1 patients and controls.**

1.A, 2.A, 3.A (blue): SCA1 patients (326-79 age at death 29, 369-20 age at death 51, and 860-17 age at death 68, respectively); 1.B, 2.B, 3.B (red): controls, ages at death 58, 54,

60, respectively, without neurological diseases. For each patient is reported the mean motor neurons density and related range. Regions are colored based on neuronal density, following color scale in the bottom left corner. In the upper left corner, negative correlation trend is shown between mean motor neurons density and pathological CAG expansion in ATXN1.

## **Annex 2**

### **List of publications during the PhD**

#### **1. The inherited cerebellar ataxias: an update.**

**Coarelli G**, Wirth T, Tranchant C, Koenig M, Durr A, Anheim M.

J Neurol. 2022 Sep 24:1-15.

#### **2. The mitochondrial seryl-tRNA synthetase SARS2 modifies onset in spastic paraplegia type 4.**

Parodi L, Barbier M, Jacoupy M, Pujol C, Lejeune FX, Lallemand-Dudek P, Esteves T, Pennings M, Kamsteeg EJ, Guillaud-Bataille M, Banneau G, **Coarelli G**, Oumoussa BM, Fraidakis MJ, Stevanin G, Depienne C, van de Warrenburg B, Brice A, Durr A.

Genet Med. 2022 Sep 3:S1098-3600(22)00875-9.

#### **3. De Novo and Dominantly Inherited SPTAN1 Mutations Cause Spastic Paraplegia and Cerebellar Ataxia.**

Van de Vondel L, De Winter J, Beijer D, **Coarelli G**, Wayand M, Palvadeau R, Pauly MG, Klein K, Rautenberg M, Guillot-Noël L, Deconinck T, Vural A, Ertan S, Dogu O, Uysal H, Brankovic V, Herzog R, Brice A, Durr A, Klebe S, Stock F, Bischoff AT, Rattay TW, Sobrido MJ, De Michele G, De Jonghe P, Klopstock T, Lohmann K, Zanni G, Santorelli FM, Timmerman V, Haack TB, Züchner S; PREPARE Consortium, Schüle R, Stevanin G, Synofzik M, Basak AN, Baets J.

Mov Disord. 2022 Feb 12.

#### **4. Safety and efficacy of riluzole in spinocerebellar ataxia type 2 in France (ATRIL): a multicentre, randomised, double-blind, placebo-controlled trial.**

**Coarelli G**, Heinzmann A, Ewencyk C, Fischer C, Chupin M, Monin ML, Hurmic H, Calvas F, Calvas P, Goizet C, Thobois S, Anheim M, Nguyen K, Devos D, Verny C, Ricigliano VAG, Mangin JF, Brice A, Tezenas du Montcel S, Durr A.

Lancet Neurol. 2022 Mar;21(3):225-233.

#### **5. Genetics in hereditary spastic paraplegias: Essential but not enough.**

Darios F, **Coarelli G**, Durr A.

Curr Opin Neurobiol. 2022 Feb;72:8-14.

#### **6. Clinical and genetic spectra of 1550 index patients with hereditary spastic paraplegia.**

Méreaux JL, Banneau G, Papin M, **Coarelli G**, Valter R, Raymond L, Kol B, Ariste O, Parodi L, Tissier L, Mairey M, Ait Said S, Gautier C, Guillaud-Bataille M; French SPATAX network, Forlani S, de la Grange P, Brice A, Vazza G, Durr A, Leguern E, Stevanin G.

Brain. 2022 Jan 4:awab386.

### **7. Motor neuron pathology in CANVAS due to RFC1 expansions.**

Huin V,\* **Coarelli G**,\* Guemy C, Boluda S, Debs R, Mochel F, Stojkovic T, Grabli D, Maisonobe T, Gaymard B, Lenglet T, Tard C, Davion JB, Sablonnière B, Monin ML, Ewencyk C, Viala K, Charles P, Le Ber I, Reilly MM, Houlden H, Cortese A, Seilhean D, Brice A, Durr A.

Brain. 2021 Dec 20:awab449.

### **8. Implication of folate deficiency in CYP2U1 loss of function.**

Pujol C, Legrand A, Parodi L, Thomas P, Mochel F, Saracino D, **Coarelli G**, Croon M, Popovic M, Valet M, Villain N, Elshafie S, Issa M, Zuily S, Renaud M, Marelli-Tosi C, Legendre M, Trimouille A, Kemlin I, Mathieu S, Gleeson JG, Lamari F, Galatolo D, Alkouri R, Tse C, Rodriguez D, Ewencyk C, Fellmann F, Kuntzer T, Blond E, El Hachimi KH, Darios F, Seyer A, Gazi AD, Giavalisco P, Perin S, Boucher JL, Le Corre L, Santorelli FM, Goizet C, Zaki MS, Picaud S, Mourier A, Steculorum SM, Mignot C, Durr A, Trifunovic A, Stevanin G.

J Exp Med. 2021 Nov 1;218(11):e20210846.

### **9. Questioning the causality of HTT CAG-repeat expansions in FTD/ALS.**

Thomas Q, **Coarelli G**, Heinzmann A, Le Ber I, Amador MDM, Durr A.

Neuron. 2021 Jun 16;109(12):1945-1946.

### **10. Biallelic loss-of-function variations in PRDX3 cause cerebellar ataxia.**

Rebelo AP, Eidhof I, Cintra VP, Guillot-Noel L, Pereira CV, Timmann D, Traschütz A, Schöls L, **Coarelli G**, Durr A, Anheim M, Tranchant C, van de Warrenburg B, Guissart C, Koenig M, Howell J, Moraes CT, Schenck A, Stevanin G, Züchner S, Synofzik M; PREPARE network.

Brain. 2021 Jun 22;144(5):1467-1481.

### **11. Plasma neurofilament light chain predicts cerebellar atrophy and clinical progression in spinocerebellar ataxia.**

**Coarelli G**, Darios F, Petit E, Dorgham K, Adanyeguh I, Petit E, Brice A, Mochel F, Durr A. Neurobiology of disease 2021 Feb 23;153:105311.

### **12. Increasing involvement of CAPN1 variants in spastic ataxias and phenotype-genotype correlations.**

Méreaux JL, Firanescu C, **Coarelli G**, Kvarnung M, Rodrigues R, Pegoraro E, Tazir M, Taithe F, Valter R, Huin V, Lidström K, Banneau G, Morais S, Parodi L, Coutelier M, Papin M, Svenningsson P, Azulay JP, Alonso I, Nilsson D, Brice A, Le Guern E, Press R, Vazza G, Loureiro JL, Goizet C, Durr A, Paucar M, Stevanin G.

Neurogenetics 2021 Jan 23. doi: 10.1007/s10048-020-00633-2.

### **13. Clinical, neuropathological and genetic characterization of STUB1 variants in cerebellar ataxias: a frequent cause of predominant cognitive impairment.**



Roux T, Barbier M, Papin M, Davoine CS, Sayah S, **Coarelli G**, Charles P, Marelli C, Parodi L, Tranchant C, Goizet C, Klebe S, Lohmann E, Van Maldergem L, van Broeckhoven C, Coutelier M, Tesson C, Stevanin G, Duyckaerts C, Brice A, Durr A.

Genetics in Medicine 2020 Nov;22(11):1851-1862.

**14. Informing about genetic risk in families with Huntington disease: comparison of attitudes across two decades.**

Pierron L, Hennessy J, Tezenas du Montcel S, **Coarelli G**, Heinzmann A, Schaerer E, Herson A, Petit E, Gargiulo M, Durr A.

Eur J Hum Genet. 2021 Apr;29(4):672-679.

**15. Loss of paraplegin drives spasticity rather than ataxia in a cohort of 241 patients with SPG7.**

**Coarelli G**, Schule R, van de Warrenburg BPC, De Jonghe P, Ewenczyk C, Martinuzzi A, Synofzik M, Hamer EG, Baets J, Anheim M, Schöls L, Deconinck T, Masrori P, Fontaine B, Klockgether T, D'Angelo MG, Monin ML, De Bleecker J, Migeotte I, Charles P, Bassi MT, Klopstock T, Mochel F, Ollagnon-Roman E, D'Hooghe M, Kamm C, Kurzwelly D, Papin M, Davoine CS, Banneau G, Tezenas du Montcel S, Seilhean D, Brice A, Duyckaerts C, Stevanin G, Durr A.

Neurology 2019 Jun 4;92(23):e2679-e2690.

**16. Recent advances in understanding dominant spinocerebellar ataxias from clinical and genetic points of view.**

**Coarelli G**, Brice A, Durr A.

F1000Res. 2018 Nov 12;7.